Synthesis and Characterization of Polymers with Phosphorus Side Chains

Zur Erlangung des akademischen Grades eines
DOKTORS DER NATURWISSENSCHAFTEN
(Dr. rer. nat.)

am Institut für Technische Chemie und Polymerchemie
der Fakultät für Chemie und Biowissenschaften
am Karlsruher Institut für Technologie (KIT) - Universitätsbereich

genehmigte
DISSERTATION
von

Jördis Eisenblätter

aus
Berlin, Deutschland

Dekan:	Prof. Dr. M. Bastmeyer
Referent:	Prof. Dr. C. Barner-Kowollik
Korreferent:	Prof. Dr. M. Wilhelm
Tag der mündlichen Prüfung:	19.07.2013

Die vorliegende Arbeit wurde von April 2009 bis Mai 2013 unter Anleitung von Herrn Prof. Dr. C. Barner-Kowollik, Frau Dr. L. Barner und Herrn Dr. U. Fehrenbacher am Fraunhofer Institut für Chemische Technologie (ICT) angefertigt.

Ich erkläre hiermit, dass ich die vorliegende Arbeit selbständig verfasst und keine anderen als die angegebenen Quellen und Hilfsmittel verwendet habe. Des Weiteren erkläre ich, dass ich mich derzeit in keinem laufenden Promotionsverfahren befinde und auch keine vorausgegangenen Promotionsversuche unternommen habe.

Karlsruhe, den 04.06.2013

Zusammenfassung

Polymere sind aufgrund ihres Kohlenstoffgerüsts brennbar und müssen mit Flammschutzmitteln (FSM) ausgestattet werden, bevor sie in Anwendungen wie dem Transportbereich, Bausektor oder elektronischen Geräten verwendet werden können. In den letzten Jahren hat das Interesse an phosphorhaltigen FSM deutlich zugenommen, da diese eine umweltfreundliche Alternative zu häufig verwendeten halogenierten FSM repräsentieren. Heute sind phosphorhaltige FSM meist niedermolekulare Verbindungen, welche dem zu schützenden Polymer als Additive zugegeben werden, mit dem Nachteil, dass diese FSM über die Zeit aus dem Polymer migrieren können. Darüer hinaus ist es schwierig, die Agglomeration des FSM im Polymer zu verhindern, was zu inhomogenen Verteilungen führt. In phosphorhaltigen Polymeren, welche bereits als FSM verwendet werden, ist der Phosphor in der Regel in das Polymerrückgrat eingebaut, so dass die Hauptkette zersetzt werden muss, um die phosphorhaltige Flammschutzkomponente freizusetzen.
In der aktuellen Arbeit sind die Entwicklung neuer (Co-)Polymere mit phosphorylierten Seitenketten über zwei kontrollierte/lebende Polymerisationsansätze und deren Evaluation im Hinblick auf ihr mögliches Flammschutzpotential aufgezeigt.
Zum Einen wird eine kontrollierte/lebende radikalische Polymerisation (RAFT) von funktionalisierten Styrol-*co*-Polymeren, welche anschließend über eine modulare Ligation in phosphorylierte Polymere umgewandelt werden, untersucht. In diesem Kontext werden verschiedene alkinierte Phosphorsäureester über eine neuartige Syntheseroute entwickelt. Die Anbindung von Phosphorsäureestern durch modulare Ligation bietet die Möglichkeit, individuell Typ und Konzentration der phosphorhaltigen Gruppen in der Seitenkette von Polymeren über ein Baukastenprinzip zu steuern.
Zum Anderen werden neue phosphorylierte Epoxymonomere synthetisiert, welche in einer anionische ROP unter Verwendung eines Ammonium/Aluminium-Komplexes direkt zu phosphorylierten (Co)-Polymeren umgesetzt werden. Die Monomere und Polymere werden durch spektroskopische (IR, NMR, XPS, EGA, SEM/EDX), chromatographische Methoden (SEC) und Thermogravimetrie (TGA, TG-MS, DSC) charakterisiert. Basierend auf den Analyseergebnissen, werden Modelle für die Anbindung des Aluminium-Katalysators an die P=O-Doppelbindung des phosphorylierten Monomers in der anionischen Polymerisation postuliert.
Um das Flammschutzpotential der gebundenen Phosphorsäureester bewerten zu können, wird ein ausgewähltes polymeres FSM durch Extrusion/Spritzguss als auch Rühren in verschiedene Polymersysteme eingearbeitet. Die flammhemmende Wirkung wird mit Hilfe von FSM-Tests im Labormaßstab (LOI, TGA) untersucht, wobei Polymersysteme für die Einarbeitung der in dieser Arbeit synthetisierten polymeren FSM ermittelt werden.

Abstract

Polymers are flammable due to their carbon skeleton and must be equiped with flame-retardants (FRs) before they can be used in applications, such as transport, building construction or electronic devices. In recent years, interest in phosphorus-containing FRs has increased significantly since they represent an environmentally friendly alternative to commonly used halogenated FRs. Today, phosphorus-containing FRs are mostly low molecular compounds added to the polymer to be protected as additives, with the disadvantage that the FRs can migrate and be released from the polymer over time. In addition, it is difficult to prevent agglomeration of the FRs in the polymer, resulting in non-homogeneous distributions. In phosphorus-containing polymers, which have already been used as FRs, the phosphorus is usually incorporated into the polymer backbone, so the main chain has to decompose in order to release the FR phosphorus compound.

In the current work, the development of novel (co)polymers with phosphorylated side chains via two different controlled/living polymerization approaches and their evaluation in terms of their FR potential are reported.
Firstly, controlled/living radical polymerization (RAFT) of functionalized styrene-*co*-polymers, which are subsequently transformed via modular ligation into phosphorylated polymers, is studied. In this context, various alkyne phosphoric esters are developed via a novel synthetic route. The connection of phosphoric esters via modular ligation offers the opportunity to individually adjust type and concentration of the phosphorus-containing groups in the side chain of polymers via a building block principle.
Secondly, novel phosphorylated epoxy monomers are prepared and employed in the direct polymerization of phosphorylated (co)polymers via anionic ROP using an ammonium/aluminium initiator/catalyst complex. By varying the comonomer ratios, individually adjustable polymers are accessible. The monomers and polymers are characterized by spectroscopic (IR, NMR, XPS, EGA, SEM/EDX), chromatographic (SEC) and thermogravimetric (TGA, TG-MS, DSC) methods. Based on the analytical results, models for the ligation of aluminium catalyst onto the P=O double bond of phosphorylated monomers in anionic polymerization are postulated.

To evaluate the FR potential of phosphoric esters bound to a polymer backbone, a selected polymeric FR is integrated via extrusion/molding and stirring into various polymer systems. The flame retardancy is determined using flame retardant tests on the laboratory scale (LOI, TGA). Polymer systems for the incorporation of the phosphorylated FR compound synthesized in the current work are determined.

Contents

Chapter 1

Introduction and Outline

1.1 Introduction

Applications of natural and synthetic polymers have gained ground in many fields. The main classes of polymers used for example in the construction industry, in electrical engineering, transport as well as in furniture and textiles are polymers with unfunctionalized side chains such as polyethylene (PE), polypropylene (PP), polyethyleneterephthalate (PET) and polystyrene (PS).[1, 2] Due to the increasing demand for polymeric materials, polymers with specific and, in addition, tuneable properties led the gradually development of polymers with functionalized side chains. Such functionalized polymers can be obtained by post-modification of already defined polymers or by direct polymerization of functionalized monomers.[3, 4]
However, a major problem for the industrial application of polymers is their high flammability due to their carbon skeleton. Depending on the application, harsh fire safety requirements are imposed. Untreated polymers, e.g. without functionalization or combination with inorganic materials, often not fulfill these requirements. Hence, the decoration of polymers with flame retardants represents a necessary step to reduce fire hazards. Flame retardants prevent or at least slow down ignition of polymers or may also interrupt the spread of fire. Most of the flame retardants used up till now, however, show two main problems:
Firstly, mainly halogenated materials are used as flame retardants due to their good performance. However, an increasing concern about their persistence in the environment and the potential negative health effects of these materials as well as the banning of halogenated flame retardants in the coming years, encouraged the flame retardant community to develop environmentally friendlier alternatives such as phosphorus compounds. In addition, phosphorus compounds, in particular organo phosphorus compounds, show high flame retardancy.[5, 6] In the flame retardancy process phosphorus flame retardants mainly act in the condensed phase, e.g. by enhancing

charring.[7, 8] The formed char layer can limit the volatization of flammable gases and isolate the polymer from further heat and oxygen diffusion. In addition, phosphorus compounds can also act in the gaseous phase via the release of PO_x radicals. These radicals disrupt the radical chain mechanism by the replacement of highly reactive $H^{\bullet}$ and $OH^{\bullet}$ radicals with the less reactive phosphorus radicals, whereby the combustion rate decreases.[9] Even though phosphorus flame retardants can act in both phases, commercial exploitation of such systems is still in its infancy and halogenated systems still dominate the market due to their exeptional performance. Secondly, until now most of the flame retardants are incorporated into the polymer as additives to achieve the protection of organic material. A drawback of this method is the emission of potentially environmentally harmful substances from the polymer over time. In addition, preceeding studies have shown that a ratio of flame retardant to polymer of up to 60 % is necessary if the flame retardant is not homogeneously distributed within the polymer. If the flame retardant is distributed uniformly in the polymer, loadings of only 3 % can be sufficient to cause a significant reduction in heat release.[10] In addition to increasing cost (flame retardants mostly determine the price of the protected polymer), these two characteristic of low molecular additive flame retardants can lead to an alteration of the properties of the material, both by changing the mechanical properties at a high content of flame retardant as well as by migrating from the material. Especially for highly strained construction materials (e.g. polyamides) these issues constitute a major drawback. By direct synthesis of phosphorylated polymers, e.g. phosphorylated polyols, or by binding organo phosphorus compounds covalently to a functionalized polymer backbone, e.g. via modular ligation reactions, polymeric flame retardants can be synthesized, where no emission of flame retardant from the protected polymer over time, can occur. In addition, the covalently bound phosphorus compounds are homogeneously distributed within the synthesized polymers, whereby an agglomeration of the flame retardant component is prevented. Subsequently, the polymeric flame retardants can be further incorporated into the polymer to be protected via an additive or reactive approach. In the reactive approach, individually adjustable end group functionalities of the polymeric flame retardant can react with the polymer to be protected, e.g. via urethane binding.

In recent years, several attemps have been made to synthesize phosphorus-containing polymers in the field of polymer science. Polyphosphates and polyphosphonates (Figure 1.1) are the predominantly synthesized polymers, which can contain H or carbon/heterogeneous chains or rings at three positions (R^1, R^2, R^3).

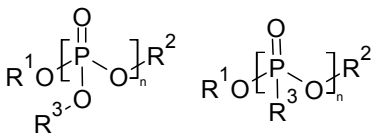

Figure 1.1: Chemical structures of polyphosphates (left) and polyphosphonates (right).

Especially when the application as fire retardant is envisaged, these polymers have various disadvantages in terms of release and variability of the flame retardant component in form of the phosphoric ester themselves as well as the PO_x radicals. Firstly, the phosphorus is part of the backbone and therefore the main chain has to decompose in order to release the phosphorus component. Secondly, a variation of the phosphorus component is very difficult, since two valencies of the phosphorus component are involved in the formation of the polymer chain. Thus, the two valancies of the introduced phosphorus component cannot act as active groups.
A new approach is therefore the connection of the phosphorus component to the side chain of a polymer backbone (Figure 1.2), wherein only one valency is involved in the linkage to the polymer. Since the phosphorus group is not directly involved in the polymerization process, a much larger variability of the polymerizable group (e.g. vinyl, epoxy) and also of the phosphorus group (e.g. phosphonates, phosphates, phosphites) is possible compared to the polymers described before. Further more, no combustion of the polymer backbone is necessary to release the flame retardant components (phosphoric esters, PO_x radicals).

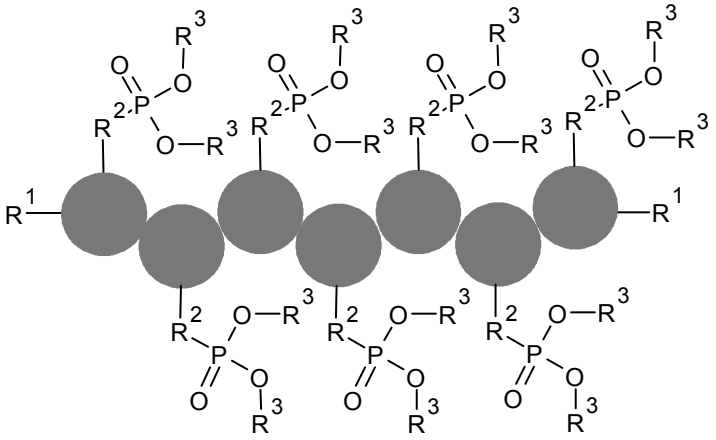

Figure 1.2: Schematic view of polymers with phosphorus side chains with R^1, R^2, R^3 = carbon, heteroatom.

In order to obtain well-defined potential flame retardants, the generated polymers have to exhibit narrow polydispersities and either phosphorus groups or other functional groups in the side chains which can be converted to phosphorus groups. On the one hand, using a phosphorylated monomer containing an oxirane ring, living ionic ring opening polymerization can be applied to synthezize a polymer with phosphorylated side chains directly. On the other hand, living/controlled radical polymerization techniques give access to excellent control over molecular weight of the polymers as well. In addition, particulary the reversible addition-fragmentation chain transfer (RAFT) polymerization is tolerant to a wide range of functional groups.[11, 12] Therefore, it is possible to prepare well-defined polymers containing functional groups in the side chains that can subsequently be modified. Several functional groups (e.g. azide, alkyne) can be used for modular ligations which sometimes fullfill the "*click*" criteria (refers to Chapter 2.2.1.) and can therefore be employed as modular ligation points for functional substances such as phosphorylated compounds.[13] The synthesis of copolymers with a variable concentration of functional groups in the side chains opens the possibility to tailor the content of the phosphorus component in the polymer. Moreover, it is possible to connect a range of various phosphoric esters to one polymer, which thereby shows flame retardancy at different temperatures. Hence, a wider temperature range of the generated polymeric flame retardant is individually adjustable.

1.2 Outline

In the current work, phosphorylated polymers are synthezized via different living/controlled polymerization techniques, either directly or via well-defined functionalized copolymers and subsequently modular ligation. The synthesized phosphorus compounds and polymers are characterized with respect to their molecular structures as well as their thermal behavior in view of a potential flame retardancy. In addition, a selected phosphorylated polymeric flame retardant has to be integrated into various polymer systems, to determine its flame retardant potential using flame retardant tests on the laboratory scale. In the scope of the present work the following approaches will be examined:

Polymer-analogous reaction of radically pre-polymerized copolymers via modular ligation reactions with functionalized phosphoric esters:

A controlled radical polymerization approach is envisaged to synthesize phosphorylated copolymers with various contents of functionalities and various phosphoric ester groups. Therefore, functionalized copolymers synthesized via a controlled radical polymerization reaction will be linked with alkyne phosphoric esters using a modular ligation reaction (copper catalyzed 1,3-dipolar cycloaddition by Huisgen). Firstly, polystyrene-based copolymers with various content of chloride functionalities will be synthesized by RAFT copolymerization of styrene and 4-vinylbenzyl chloride (VBC) (left structure Figure 1.3). Secondly, these copolymers will be azidized. In parallel, through various approaches alkyne phosphoric compounds (right structure Figure 1.3) will be synthesized and subsequently attached to the previously azidized copolymers via alkyne/azide chemistry. Influences of the phosphorus content and type of phosphoric ester group (R^1) on the conversion behavior in the polymer-analogous reaction and thermal behavior of the generated phosphorylated copolymers will be examined.

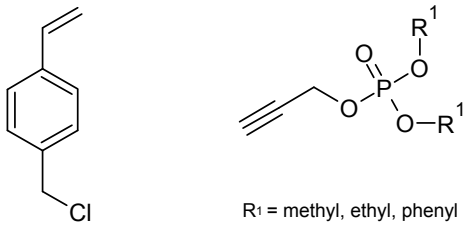

Figure 1.3: Chemical structure of 4-vinylbenzyl chloride (left) and general structure of alkyne phosphoric esters prepared in the present work (right).

Direct polymerization of phosphorylated polymers via living anionic polymerization of phosphorylated monomers

In this chapter, phosphorus-containing monomers are to be synthesized, which can be polymerized via a ring-opening anionic polymerization process. Fosfomycin (Figure 1.4) and derivatives thereof will be used as epoxy- and phosphorus-containing monomers. Fosfomycin has, in addition to an epoxy ring, a phosphonic acid group, which must first be converted quantitatively to different ester groups. These fosfomycin diesters and derivatives are envisaged to be polymerized directly by a living anionic ring-opening polymerization to phosphorus-containing polymers. Influences of catalyst to initiator ratio as well as temperature and reaction time on the poly-

merization behavior have to be examined. In addition, the phosphorus-containing monomers should be reacted with other monomers leading to partially phosphorylated copolymers to compare them with the homopolymers.

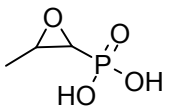

Figure 1.4: Chemical structure of fosfomycin (1,2-epoxypropylphosphonic acid).

The successful conversion to phosphorylated low molecular compounds and polymers will be confirmed by a combination of different analytic methods such as nuclear magnetic resonance (NMR), size exclusion chromotography (SEC), infrared (IR) / raman spectroscopy, X-ray photoelectron spectroscopy (XPS), elemental analysis (EA) and scanning electron microscopy in combination with energy dispersive X-ray analysis (SEM/EDX). Thermogravimetry (TGA) and differential scanning calorimetry (DSC) measurements will be used to determine the influence of different phosphorus esters and polymer backbones on the thermal properties of the polymers.

Chapter 2

Fundamentals

2.1 Polymerization Techniques

Polymer science is concerned with the generation, understanding and tailoring of macromolecular structures. In a polymerization process, monomer molecules react with each other covalently in a chemical reaction to form polymer chains or three-dimensional networks. Due to their high molar masses, polymers show particular properties, which cannot be observed for low molecular compounds, such as high tensile strength, the ability to form fibres or high thermal resistance.
In general, polymerization reactions are characterized by their process conditions, variety of different types of monomers, kinetic and thermodynamic features and formation of various polymer structures. In the present chapter, the fundamentals and most common methods of free and controlled/living polymerizations are described.

2.1.1 Free Radical Polymerization

The conventional free radical polymerization (FRP) is suitable for a variety of monomers (e.g. styrenes, vinyl acetate, vinyl chloride, acrylonitrile and (methyl) methacrylates) and is relative insensitive to the reaction conditions. Therefore, it is the most important industrial method for the preparation of synthetic polymers.[14]
The overall free radical polymerization process consists of five fundamental steps: initiator fragmentation (1), initiation of the reaction (2), propagation (3), termination reactions (4) and transfer reactions (5). The general polymerization mechanism of FRP is depicted in Figure 2.1 and is described in detail in the following.

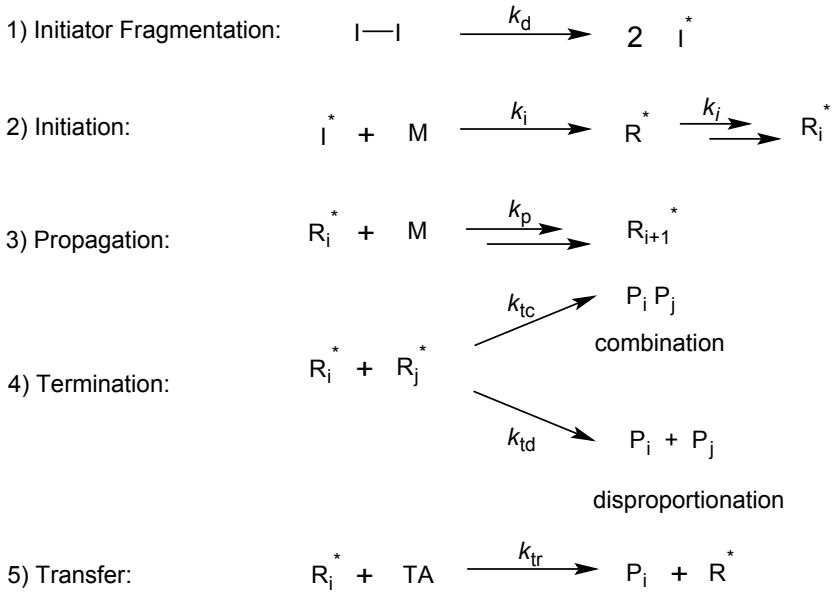

Figure 2.1: General polymerization steps of free radical polymerization (FRP). I-I = initiator; M = monomer; $R_{i/j}$* = radical of chain length i/j; TA = transfer agent; P = polymer.

The FRP is initiated by radicals, which are formed by e.g. thermal decomposition or photolysis of a free radical initiator (1). Typically, azo- or peroxo-initiators are used which have dissociation rate coefficients k_d in the range of 10^{-5} to 10^{-1} s^{-1}. Further reaction of the initiator radical with a monomer occurs at initiation rate cofficients k_i of approximately 10^4 L $\cdot$ (mol $\cdot$ s)$^{-1}$. However, this value can vary significantly in the range of seven orders of magnitude.[15] Generally, the formation of primary radicals represents the rate-limiting step. Further monomers add to the radical, until a so-called macro-radical is formed. At this stage, no influence of the starting initiator radical coefficient on the chain propagation rate coefficient k_p occurs. Further addition of monomer units is termed as propagation (3) with e.g. propagation rates around 10^3 L $\cdot$ (mol $\cdot$ s)$^{-1}$ at 60-80 °C for styrene.[16] Due to the high reactivity of the radical chain ends, a fast chain growth is ensured. However, termination reactions can occur by combining two radical chains or via disproportionation (4), which lead to a decrease of radical concentration and inactive, so-called "dead", polymer chains. As a result, the molecular weight distribution broadens. The rate of termination depends on the time that radicals take to interact with each other. Therefore, termination reactions are diffusion-controlled. The termination rate coefficients k_{tc} and k_{td} depend on conversion, temperature, pressure, chain length and the resulting viscosity in the reaction mixture. Values in solution are in the range of 10^6 to 10^8 L $\cdot$ (mol $\cdot$ s)$^{-1}$.[17, 18, 19] A process which also affects the molecular

weight distribution of the resulting polymer, yet without changing the overall radical concentration, are transfer reactions between the active radical chains and a transfer agent (5). Solvents, additives, monomers or polymer chains can act as transfer agents. Transfer of the reactive group via an intramolecular transfer (backbiting) leads to short chain branches. If the transfer takes place intermolecular, long chain branches are formed. Both transfer reactions lead to an increased polydispersity. The transfer rate coefficient k_{tr} is related to k_{p} [20], resulting in the so-called transfer constant C (see Equation 2.1).

$$C = \frac{k_{\mathrm{tr}}}{k_{\mathrm{p}}} \tag{2.1}$$

A high transfer constant to monomer or solvent, combined with a rapid reinitiation by the transfered radical, leads to no change in the polymerization rate, yet to a reduction in the degree of polymerization. To determine the values for k_{tr}, the Mayo method [21] or the chain length distribution method [22] can be used. Both are theoretically equivalent.[23] Termination and transfer reactions can occur at every stage of the described polymerization process, yet become more dominant at higher conversions.
The occurring transfer and irreversible termination reactions are decisive disadvantages of FRP, leading to broad molecular weight distributions and limited control over the synthesis of defined structures and compositions. Therefore, the FRP is not suitable for the generation of well-defined structures with controlled ratio of functionalities.

In recent years, several methods have been developed for radical as well as ionic polymerizations, which drastically reduce the proportion of termination and transfer reactions. A distinction is made between so-called "living" polymerizations, in which the polymer chain remains active and can be re-started at a later time (e.g. for the synthesis of block copolymers), and "controlled" polymerizations, where a narrow molecular weight distribution and predictable molecular weights can be achieved.
In general, controlled/living polymerizations fulfill the following conditions:

1. Linear increase of molecular weight with conversion.
2. Chain ends that can be reactivated, i.e. the generated polymer posses the ability to be chain extended.
3. Narrow polydispersities.

The simultaneous start of chain growth and the absence of chain transfer and termination steps in the polymerization are the basic statistical differences from conventional free radical polymerization, leading to a considerably narrower molecular weight distribution, the so-called Poisson distribution. The polydispersity index PDI is then given by Equation 2.2, which results from the ratio of the weight average M_w and number average M_n molecular weight of the generated polymer.[24] The degree of polymerization P_n increases linearly with the conversion of the monomer in a controlled/living polymerization, in contrast to the free radical polymerization.

$$PDI = \frac{M_w}{M_n} = 1 + \frac{1}{P_n} \tag{2.2}$$

P_n is than given by the ratio of the initiator concentration $[I]_0$ to the change in concentration of the monomer $[M]_0$-$[M]$ at a given conversion by:

$$P_n = \frac{[M]_0 - [M]}{[I]_0} \tag{2.3}$$

In practice, PDI > 1 (Equation 2.2) and non-linear growth of the degree of polymerization (Equation 2.3) can be found. Possible causes are the incomplete exclusion of termination and transfer reactions, apparatus imperfections (impurities, too slow mixing of initiator and monomer) or kinetic reasons. In radical polymerizations, it is virtually impossible at higher conversions to exclude termination reactions completely (see explanation above). Therefore, radical polymerizations with living features are often referred to as "controlled/living" radical polymerizations. In the case of ionic, especially of anionic polymerization, the term "living" ionic polymerization is used, since termination reactions can largely be excluded, due to the charged chain ends. Both controlled/living polymerization methods will be described in detail in the following chapters.

2.1.2 Living Ionic Polymerization

In general, ionic polymerizations are initiated by compounds which readily split off either a proton (e.g. perchloro acid, trifluoromethanesulfonic acid) or forming a carbanion (e.g. butyllithium). Depending on the nature of the initiator, a differentiation between cationic and anionic polymerization is made. Similar to free radical polymerization, both types of ionic polymerization can be divided into initiator decomposition (1), initiation (2), propagation (3), termination (4) and transfer (5) reactions.[25] The general steps are shown on the example of cationic polymerization in the Figure 2.2.

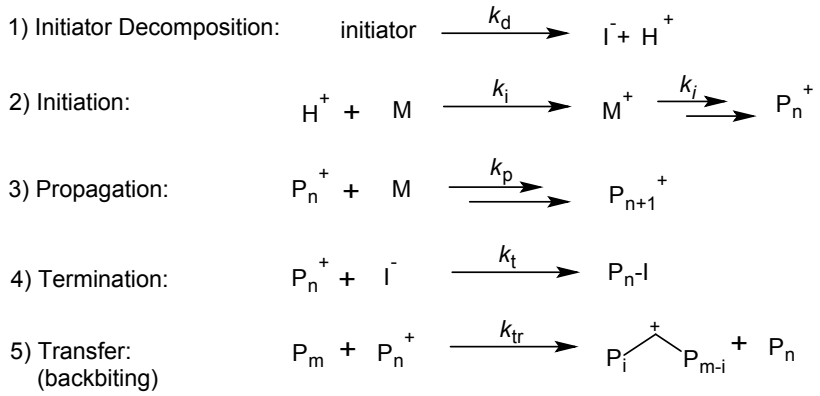

Figure 2.2: General steps of cationic polymerizations. I = counter ion; M = monomer; $P_{n/m}$ = polymer of chain length n/m.

As shown in Figure 2.2, yet in cationic polymerizations, termination and transfer reactions can occur, leading to broad molecular weight distrubutions. In general, transfer reactions did not occur in anionic polymerizations, yet terminations. The general steps of anionic polymerizations are shown in Figure 2.3.

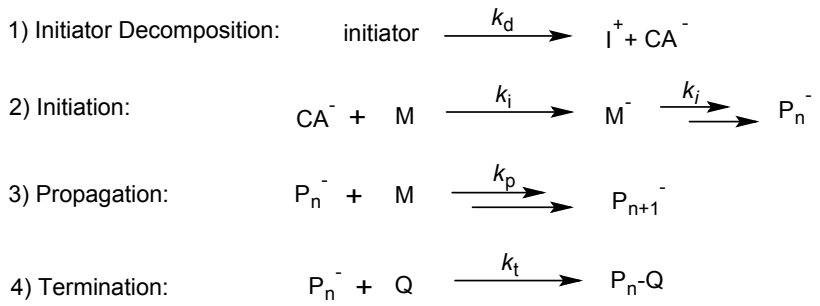

Figure 2.3: General steps of anionic polymerizations. I = counter ion; M = monomer; CA^- = carbanion; Q = termination compound; P_n = polymer of chain length n.

In 1968, Szwarc developed the so called "living" anionic polymerization for vinyl and diene monomers.[26] As mentioned above, the term "living" refers to the absence of chain termination and transfer reactions during the polymerization. To prevent termination reactions in anionic polymerization, high purity of solvents and monomers and moreover absolute exclusion of moisture must be guaranteed. Major termination reactions specific for the anionic polymerization are shown in Figure 2.4. The living anionic polymerization method is mainly used in the current work.
As seen in Figure 2.4, water (H_2O) terminates the propargating chain via proton transfer. The formed hydroxy-counter ion is mostly not sufficiently nucleophilic to reinitiate macromolecular growth. Reaction with carbon dioxide (CO_2) leads to carboxy end groups, which are not reactive enough to propagate further. In addition,

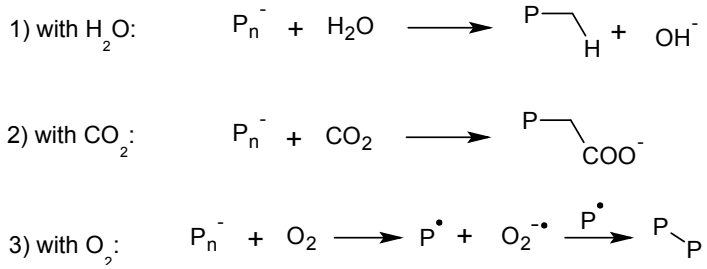

Figure 2.4: Overview of the main termination reactions in anionic polymerizations.[27] P = polymer chain.

imperfections in the polymer backbone and an increase in the molecular weight distribution occur. It is thus possible to terminate the polymerization via the controlled addition of carbon dioxide in combination with e.g. water or methane. Thereby, polymers with carboxylic acids or esters at the chain end can be obtained. The reaction of growing polymer chains with oxygen (O_2) involves a radical mechanism leading to a dimerization. Due to the described termination reactions, living anionic polymerizations have to be performed under inert gas and with high purity solvents and monomers.

In addition to increased demands on the reaction conditions and purities of the employed chemicals, a limiting point for the application of ionic polymerizations, is the fact that there are only applicable to a relatively small number of monomers and a limited choice of suitable reactive initiators can be used. For example acrylic acid and its esters (except tertbutyl acrylate), monomers with abstractable protons (OH, NH or NH_2 groups) and olefins are not polymerizable via ionic polymerization techniques or broad distributed products are obtained.

In the case of cationic polymerization only monomers with electron-donating substituents such as vinyl, phenyl or alkoxy can be used. As catalysts, Lewis acids such as $BF_3{\cdot}Et_2O$, oxocarbenium salts, esters and anhydrides are suitable. Because cations are very reactive and can hardly be stabilized, several side reactions such as backbiting (as in FRP) can take place.
Anionic polymerization is preferably carried out with monomers having electron-withdrawing substituents such as acrylic compounds, aldehydes, ketones or carboxy groups. Furthermore, anionic ring opening polymerization of e.g. epoxides, lactams and lactones is possible. Under very controlled reaction conditions and via the employment of highly pure chemicals and solvents, anionic polymerizations exhibit no termination reactions. Therefore, this approach was used in the current work as ionic polymerization method.

After exclusion of termination reactions in anionic polymerizations, the initiation of the polymerization has to be considered in more detail. To achieve polymers with narrow molecular weight distribution, the initiation (2) must occur much faster than the propagation (3). This has the result that all chains start at approximately the same time. The initiation (2) and propagation (3) rates depend on the type of solvent, due to aggregation of the organometallic compounds, which are used for initiation, and the propagating chains. Polar solvents (e.g. tetrahydrofuran) can coordinate with the evolving cations from the initiator, leading to a break up of the polymer-counter ion aggregates. Due to less aggregated active chains, higher initiation and propagation rates are achieved. Using a non-polar solvent (e.g. toluene) the polymerization rates decrease compared to reactions in polar solvents. At the beginning of the initiation process only slow initiation of the monomers occurs. At a later point of initiation, it is assumed that by direct insertation of the monomer in an aggregated initiator species, self-acceleration takes place leading to an increase in propagation.[28, 29] For the acceleration of the initiation step, Lewis bases, like *N,N,N´,N´*-tetramethylethylenediamine (TMEDA), tetraetyleneglycoledimethylether (tetraglyme) and crown ethers (e.g. 18-crown-6) can be used. When termination and transfer reactions can be excluded, all chains grow at the same rate and the concentration of active chains remains constant. Therefore, the propagation (3) in living ionic polymerizations leads to a linear correlation between polymerization degree P_n and conversion. Thus the propagation rate v_p is obtained as:

$$v_p = -\frac{[M]}{dt} = k_p[M][I]_0 \tag{2.4}$$

with the propagation rate coefficient k_p. At ideal reaction conditions, the monomer concentration [M] (see Equation 2.3) is zero at the end of the polymerization, leading to:

$$P_n = \frac{[M]_0 - [M]}{[I]} = \frac{[M]_0}{[I]_0} \tag{2.5}$$

Therefore, the polymerization degree P_n, respectively the molar mass (Equation 2.2.) can be adjusted by the initial monomer to initiator ratio. In addition, due to the remaining active chain ends at the end of the polymerization, further addition of monomers is possible, which can be used for the synthesis of well-defined block copolymers. Thus, anionic polymerization is very well suited for the synthesis of polymers having a narrow molecular weight distribution and will be explained in detail.

As mentioned before, the chain growth of anionic polymerizations is initiated by the nucleophilic attack of a negatively charged initiator to the monomer and then by further addition of monomer units with respective successive acquisition of the negative charge. Suitable initiators are Lewis bases, such as the organometallic compound 2-butyllithium. During living anionic polymerizations, the negatively charged chain ends repel each other and are stabilized by their counter ions. Bimolecular termination reactions are therefore eliminated. Furthermore, the active centers in living anionic polymerizations, in contrast to free radical polymerizations, are generated not only by a decomposition reaction, but rather they are already existing due to the ionic nature of the initiator, which is the precondition for a quasi-simultaneous initiation of all chains. After reaching the desired conversion, a chain termination is usually accomplished by the addition of proton donors such as methanol or degassed water. By using electrophilic compounds with the proton donor bound to a (hetero)carbon chain or ring, also target (functional) end groups can be introduced into the macromolecule.[30]

In the present study, an ammonium/aluminum complex was used as initiator/catalyst complex to polymerize phosphorylated polymers via an anionic ring-opening polymerization, as it is described by Carlotti *et al.* for the polymerization of epichlorohydrin.[31] The mechanism of the living anionic ring-opening polymerization postulated by Carlotti is shown in Figure 2.5. Previously described methods to polymerize epichlorohydrin are mainly based on cationic strategies, due to a predominant reaction between the chloromethyl group of the epichlorohydrin and the most highly nucleophilic propagating species.[32] Unlike previously described in the literature, a weak nucleophilic initiating system obtained by the combination of triisobutylaluminium ($Al(^{i}Bu)_3$) and tetraoctylammonium bromide ($NOct_4Br$) was used to achieve living anionic polymerization of epichlorohydrin. The combination of the initiation complex with the epoxy monomer forms a strongly activated initiator-monomer-complex. Under these conditions, the reactivity of epichlorohydrin toward nucleophiles is strongly enhanced and the ring-opening polymerization proceeds in the presence of weak nucleophiles. It is thus possible to synthesize poly(epichlorohydrin) with non-reacted chloromethyl functionalities in the side chain with molar masses (M_n) in the range of 9 400 to 83 500 $g \cdot mol^{-1}$ and PDI of 1.08 to 1.23.[31] On the basis of these conditions, the living anionic ring-opening polymerization should also be well suited for the targeted polymerization of polymers with phosphorylated side groups and narrow molecular weight distribution.

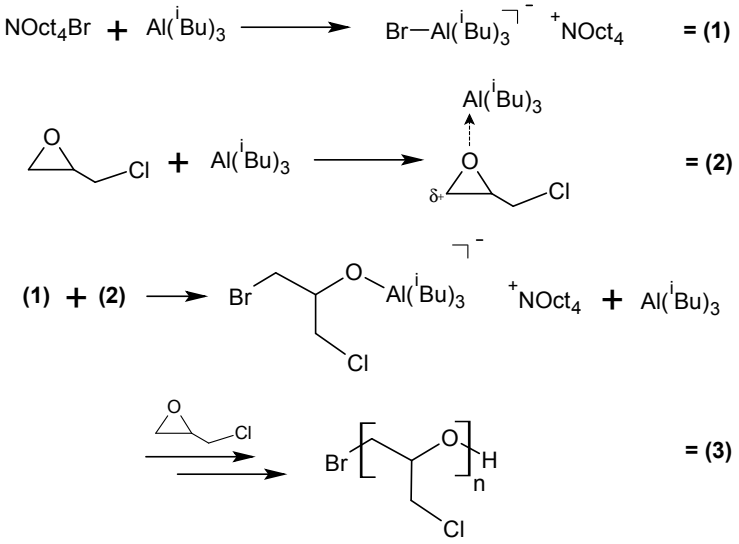

Figure 2.5: Adapted reaction scheme of the anionic ring-opening polymerization mechanism described by Carlotti *et al.*[31] 1) Formation of initiation complex; 2) Activation of monomer; 3) Initiation, propagation and termination of the polymerization.

2.1.3 Controlled/Living Radical Polymerization

As described in Chapter 2.1.1., the free radical polymerization (FRP) is a very attractive method for industrial applications as many monomers are easily polymerizable via this technique. These advantages faced a long time the described disadvantages (Chapter 2.1.1.) of irreversible termination reactions and the consequently poor control over the molecular weights. Different concepts for well-defined radical polymerizations have been developed since 1980, which introduce the living characteristics of ionic polymerization methods (Chapter 2.1.2.) also in radical polymerization systems.[33] With the first experiments using the nitroxide mediated polymerization (NMP) in 1979 [34], the first controlled/living radical polymerization was developed. However, only with the development of the atom transfer radical polymerization (ATRP) in 1995 [35, 36], respectively the reversible addition-fragmentation chain transfer (RAFT) polymerization in 1998 [37], the rapid development in this field began.

Controlled/living radical polymerizations are an attempt to combine the advantage of technically simple to perform radical polymerizations with the kinetic characteristics of anionic polymerizations. NMP and ATRP include an equilibrium reaction between a reversibly terminated, the so-called dormant species, and the active species. RAFT processes, in contrast, are governed by reversible chain transfer reactions. In all approaches, the reversible equilibrium controlling the polymerization is on the

polymerization inactive side. By this means, the concentration of active centers compared to a free radical polymerization is at a level that the possibility of irreversible chain terminations is minimized, but the chain growth still can take place. The formation and cleavage of the reversible binding must take place at a reasonable speed, so for all chains the same growth probability is given. For the same reason all potential active sites may be present at the beginning of the polymerization or may be formed in a short initiation period. The most prominent methods (NMP, ATRP and RAFT) will be briefly discussed:

NMP (Nitroxide Mediated Polymerization)

The synthesis of polymers having a narrow molecular weight distribution under controlled radical conditions in the context of the nitroxide mediated polymerization (NMP) is based on the reversible trapping of alkyl radicals with linear or cyclic nitroxides (e.g. 2,2,6,6-tetramethyl-1-oxide = TEMPO). It was first described by Solomon and Rizzardo in 1979 for the polymerization of acrylates.[34] A general reaction mechanism is depicted in Figure 2.6.

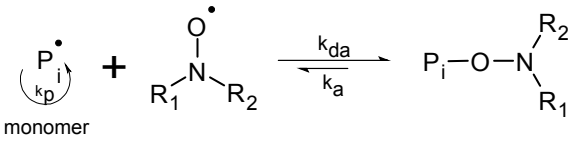

Figure 2.6: General polymerization mechanism of NMP. P_i = polymer with chain length i; O-N-R_x = nitroxide; R_1, R_2 = carbon chain/ring.

The used alkoxyamines, e.g. TEMPO, are heat labil, forming a reactive and a stable radical (Figure 2.7), which offer the possibility of controlling the propagation. The reactive radical initiates polymerization while the growing polymer chain is reversibly deactivated by the nitroxide (stable radical), resulting in a reduction of the free radical concentration of growing chains.

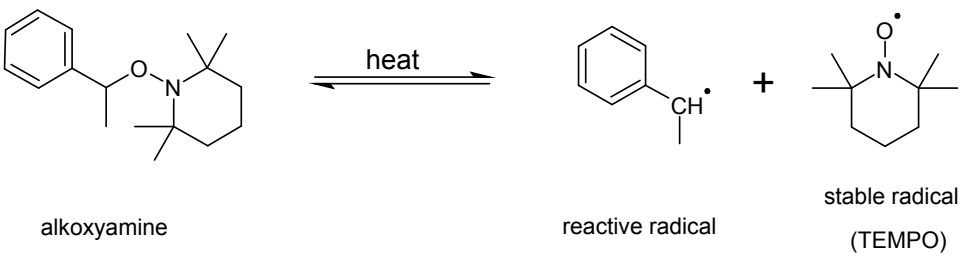

Figure 2.7: Thermal decomposition of an alkoxyamine generating "TEMPO".

There is a differentiation in NMP between uni- and bimolecular initiation. In the bimolecular initiated polymerization, a mixture of a conventional radical initiator (eg. 2,2‘-azobis(2-methylpropionitrile) = AIBN) and a stable nitroxide is involved. The advantage of this method is the simple feasibility. The initiation with conventional radical initiators in excess of the nitroxide, however, leads to a high proportion of termination reactions at the beginning of polymerization. Therefore, the adjustment of the desired molar masses is difficult. The unimolecularly initiated polymerization involves the thermal decomposition of an alkoxyamine into reactive and stable radicals (see Figure 2.7). Since TEMPO derivatives form relatively stable alkoxyamines (activation rate constant for styrene/TEMPO at 125 °C: $K_a = k_a/k_{da} = 2.1 \cdot 10^{-11}$), high reaction temperatures are required and they are only suitable for styrene derivatives. In recent years, other nitroxides (Figure 2.8) have been synthesized, enabeling the polymerization of monomers such as acrylamides and acrylonitrile at lower temperatures.

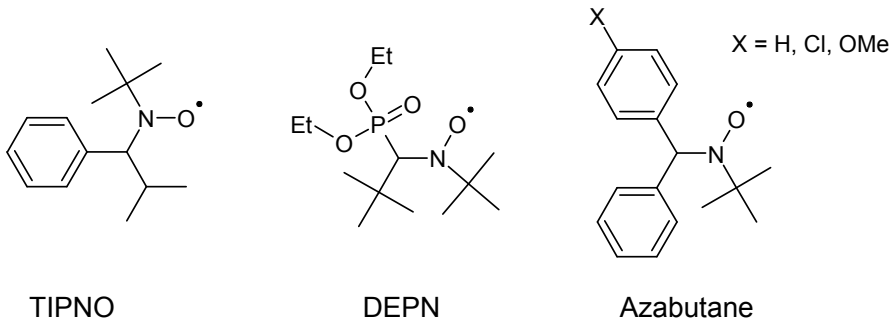

Figure 2.8: Nitroxides usable for polymerization of acrylamides and acrylonitrile at lower temperatures.

The advantage of the NMP is the easy applicability, due to its insensitivity to the purity of monomers and solvents. In addition, the nitroxide radicals are sufficiently stable so that they can be stored at ambient temperatures without change. A disadvantage of NMP are the few initiators commercially available. Therefore, they have to be synthesized. Additional drawbacks are the high initial reaction temperature, long reaction times (24 to 72 h) and the possible reaction of the nitroxide with the β-hydrogen atom of the alkyl radical to hydroxylamine, resulting in terminated vinylidene ended polymer chains. This side reaction complicates particularly the controlled polymerization of methacrylates.

ATRP (Atom Transfer Radical Polymerization)

Radical generation in ATRP involves an organic halide undergoing a reversible redox process catalyzed by a transition metal compound (Figure 2.9). It was described in 1995 by K. Matyjaszewski for copper and iron complexes [35] and by M. Sawamoto for ruthenium and iron complexes [36]. Further examined and used transition metals are nickel, rhenium, rhodium and palladium. However, especially copper, yet also ruthenium or nickel complexes are used today.

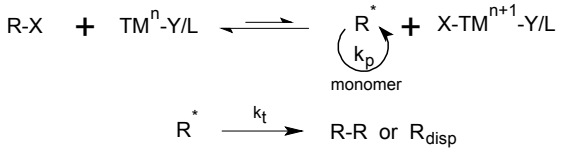

Figure 2.9: General polymerization mechanism of ATRP. TM^n = transition metal; X = halogen; Y = ligand or counter ion; L = ligand.

ATRP is based on a reversible activation/deactivation mechanism. The starting radicals are generated by homolytic cleavage of a carbon-halogen bond. The cleavage is catalyzed by a transition metal complex. The complex themselves is transformed to a higher oxidation state by an oxidative addition of the halogen atom. The initiator radical ($R^\bullet$) starts the polymerization, while the oxidized metal complex reversibly disables the active chain for further polymerization. For this reason, the complex is also referred to as deactivator or dormant species. The equilibrium between the active and the dormant species is the key reaction in the ATRP, imparting the living characteristics. To provide a reasonable polymerization rate, the equilibrium constant $K_e = k_a / k_{da}$ must be sufficiently small to supress termination reactions, but at the same time sufficiently high to keep the propagation at an acceptable rate. Typical K values are in the range of 10^{-9} to 10^{-4} [38], depending on the ligand, initiator, monomer and reaction conditions (temperature, solvent, pressure). The rate of termination reactions is very low at appropiate conditions. Ideally, more than 90 % of the polymer chains contain a halide at the end of the polymerization, which can be substituted further. However, the halide-end functionality decreases with increasing conversion, often leading to broad molecular weight distributions at high conversions.

ATRP is tolerant to many functional groups, such as epoxy and hydroxy groups, present in either the monomer or the initiator. Monomers such as styrene, (meth)-acrylates and (meth)acrylamides can be polymerized. Due to a unique set of rate coefficients for every monomer, the ATRP system of initiator and catalyst have to be tuned individually for every system. In recent years, modifications have been made to improve the versability of the ATRP process. The most promising ones are:

1. **"Reverse" ATRP**:
   The ATRP is generated in-situ by the decomposition of conventional free radical initiators, which are less sensitive against air.
   Disadvantage: Only linear polymers can be synthesized with lower end-group functionalities compared to the use of a conventional initiator.

2. **Activator Generated by Electron Transfer (AGET) ATRP**:
   The catalyst is continously regenerated by a reducing agent (e.g. Cu^0 or tin(II)-2-ethyl hexanoate), so that only small amounts of catalyst are needed. The main advantage is the possible use in aqueous and miniemulsion systems.
   Disadvantage: The amount of copper catalyst is still in the range of conventional ATRP.

3. **Activator Re-Generated by Electron Transfer (ARGET) ATRP**:
   A much lower concentration of active metal catalyst is used, due to a large exess of a reducing agent (see AGET).
   Disadvantage: Limited functionalities at higher polymerization rates.

Finally, ATRP methods are advantageous due to the ease of preparation and commercially available and inexpensive catalysts (copper complexes). Thus, ATRP is presently the most effective and most idely used method of controlled radical polymerizations next to RAFT. Nevertheless, one drawback is that the polymerization rate decreases significantly at high conversion ($\approx 90\%$) since termination reactions are not sufficiently suppressed. In addition, the removal of the metal complex after the reaction include a tedious work-up.

RAFT-Polymerization (Reversible Addition-Fragmentation Chain Transfer Polymerization)

The latest development in the field of controlled/living radical polymerization is the RAFT polymerization. This process was first described in 1998 by a group from the Commonwealth Scientific and Industrial Research Organisation (CSIRO).[37] In this controlled radical polymerization technique, the controlled chain growth is achieved not as in ATRP and NMP via reversible termination, but by reversible chain transfer. The polymerization is carried out with a conventional initiator, such as peroxide or AIBN, in the presence of a chain-transfer reagent. One of the main advantages of the RAFT process is the absence of a transition metal complex. As a so-called RAFT agent, various carbonyl thio compounds are used as chain transfer agents. Four classes are distinguished - dithioesters, trithiocarbonates, dithiocarbamates and xanthates - which are shown in Figure 2.10. Parallel to the development of the RAFT process, Corpart and co-workers proposed an approach using only xanthates. This

polymerization, which adheres to the RAFT mechanism is called "macromolecular design by interchange of xanthates" (MADIX), which can be utilized only for high reactivity monomers.[39]

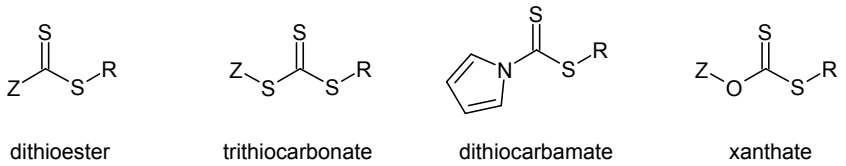

Figure 2.10: General structures of RAFT agents.

The RAFT/MADIX agent consists basically of three parts: the stabilizing Z group, a dithio-unit and a leaving group R. The Z group is intended to stabilize the radical intermediate, without forming a unreactive species. The R group should be cleaved easily from the reagent, thus form a stable radical, however, the radical must be able to reinitiate macromolecular growth. Typical Z groups are phenyl, benzyl, as well as nitrogen, oxygen, and sulfur derivatives. Typical R groups are higher branched carbon structures than the monomer (e.g. the trisubstituted cumyl residue), as they form more stable radicals than the monomer. Thus, they preferably cleaved from the RAFT agent. However, the radical formed may not be too stable, as it needs to initiate a further polymerization chain.
The reaction starts identical to the free-radical polymerization with the decomposition of the initiator and further reaction of the radical with monomer units (refers to initiation in Figure 2.11). In the so-called reversible pre-equilibrium, the radically activated short polymer chain reacts with the RAFT agent to a radical RAFT intermediate. By cleavage of the R group, the intermediate is converted to the corresponding polymeric form, the so-called macro-RAFT (refers to pre-equilibrium in Figure 2.11). Next, the cleaved radical initiates propagation via the formation of new radically activated short polymer chains (refers to re-initiation in Figure 2.11). The main equilibrium is achieved, as soon as the macro-RAFT agent is in equilibrium with the growing radical chains. A polymeric radical intermediate is formed that can fragment in a new propagating chain and a new macro-RAFT agent. The propagating chain polymerizes further until it is reversibly deactivated by the macro-RAFT, releasing a new active polymer chain. Since the concentration of macro-RAFT compared to the free radical chain is very high (usually 1:10 radical chain to RAFT), the free radical chains are only briefly released before being re-attached to the macro-RAFT. Thereby, the termination with another free radical chain is minimized. As a result, the propagation rate should not be reduced. However, deviations from the ideal conditions can be observed. This observation

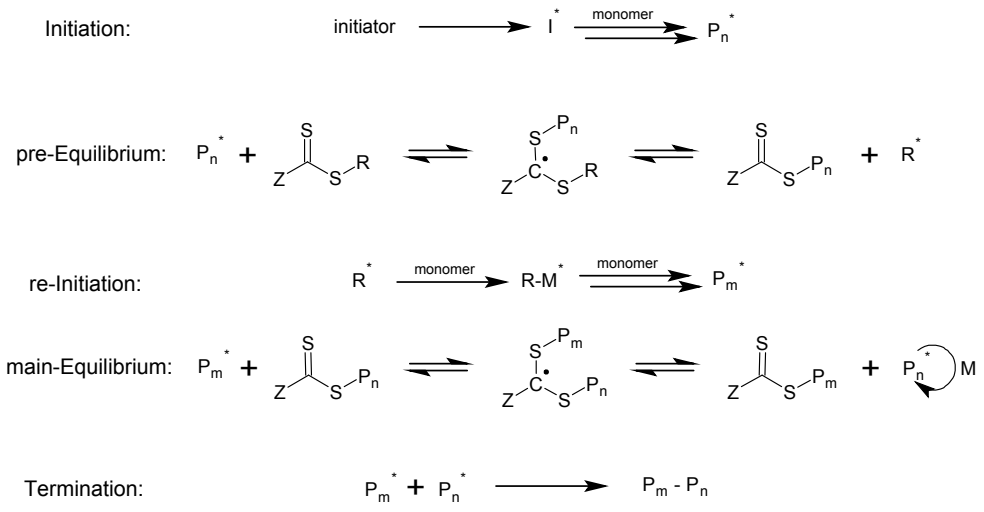

Figure 2.11: General polymerization mechanism of RAFT polymerization.

can e.g. be attributed to the so-called retardation, refering to reduced conversions with increasing RAFT agent concentration. Retardation can occur when the RAFT intermediate is too stable, so that the release of the radical chain is delayed, which may be caused by the wrong choice of the Z group, since it is responsible for the stability of the intermediate.[40] Retardation may also be caused when two RAFT intermediates react with each other and thus form a reversible termination product, leading to the effect that the release of the radical chain is delayed, and the reaction is slowed down. Irreversible termination of RAFT intermediate radicals with propagating chains has also been discussed as a cause of rate retardation effects.
For RAFT polymerizations, usually all monomers and also the same conditions (solvent, temperature, initiator, monomer) can be used as in free-radical polymerizations. The application spectrum of RAFT polymerization is therefore very wide and an important advantage over the other controlled radical polymerization techniques. Unlike in the other methods, the radical concentration is not reduced in the RAFT polymerization, so that many radical chains can grow simultaneously. In addition, it is possible to convert the RAFT end-groups to other functional groups such as unsaturated groups or hydroxy groups, solving the problem that the coloration of the polymers due to the sulfur content may be a hindrance in industrial processes. Due to the fact that the end-group conversion is not used in the present work, such processes are not considered here in more depth. The main drawback of the RAFT synthesis represents the RAFT agents. Each agent can be used only for a few monomers and must be produced by time-consuming syntheses. Up till now, only a few RAFT agents are commercially available. Moreover, some are not stable over long periods.

However, due to their high tolerance for functional groups, the RAFT polymerization is suitable for the synthesis of the desired functional polymers in the current work. Therefore, RAFT is used in the current work as the selected controlled/living radical polymerization for the synthesis of functionalized copolymers, which then will be further substituted by phosphoric ester groups using a modular ligation approach as described in Chapter 2.2.1.

2.2 Polymer-Analogous Reactions

Due to functionality and reactivity issues, just a few functionalized polymers can be synthesized directly via living ionic or controlled/living radical polymerization methods (see Chapter 2.1.). By using so called polymer-analogous reactions, novel uniformly tailored polymers with low polydispersities can be formed using pre-synthesized functional polymers. Such polymer-analogous reactions are chemical reactions between macromolecules, such as polymers, and low-molecular compounds (Figure 2.12).[41]

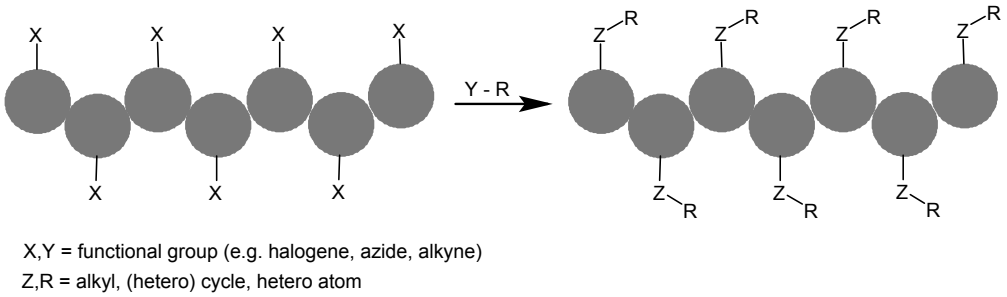

Figure 2.12: Reaction scheme of a polymer-analogous conversion between a polymer with functionalized side chains and low-molecular compounds.

Characteristic values such as the number of monomer units, hence the degree of polymerization, will remain unchanged. Only if decomposition and incomplete conversions can be excluded, the reaction is refered as "true" polymer-analogous reaction. A variety of different factors determine the scale of conversion. The two most important factors are shown in the following part on some examples:

1. Intramolecular reactions

For example, in the case of acetalization of polyvinylalcohol (Figure 2.13), the intramolecular acetalization is strongly favored compared to the intermolecular acetalization through local high concentrations of OH groups. Due to the irreversible nature of this reaction, no complete conversion can be achieved.

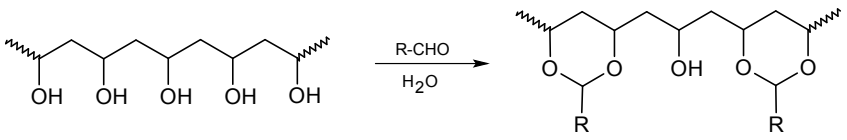

Figure 2.13: Reaction scheme of the favored intramolecular acetalization reaction of polyvinylalcohol (PVC) in polymer-analogous reactions.

2. Reaction delay

Due to electrostatic effects to neighboring groups, polymer-analogous reactions may be delayed, as occurs during saponification of polyacrylamide (Figure 2.14).

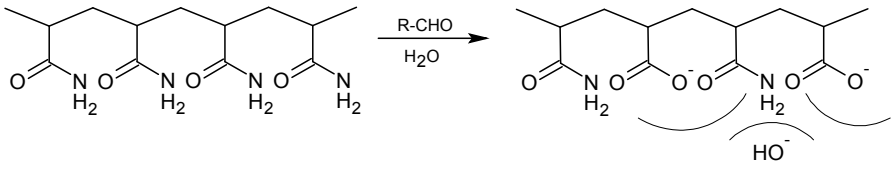

Figure 2.14: Reaction scheme depicting the reaction delay in polymer-analogous reactions due to electrostatic effects of neighboring groups.

With increasing conversion, the rate of hydrolysis decreases sharply, because the further formed carboxylate groups complicate the integration of additional hydroxyl ions. Therefore, complete reactions are very rare. Almost always a small percentage of non-converted units remains.

The separation of incomplete converted products is not possible, since both the converted and the non-converted units are incorporated into one macromolecule. In polymer-analogous reactions, steric effects play a significant role in incomplete conversions, since the polymers are usually entangled in shape and so the access is disabled, despite of the mostly low-molecular reaction partners. The above points have to take in careful consideration, when selecting appropriate reaction conditions and reactants for a polymer-analogous reaction.

Despite these complications, there are numerous reasons why chemical reactions on macromolecular substances are interesting and important. Already in the pioneering work of Staudinger [42], they were used to evidence the macromolecular structure of substances with high molecular weight. By using polymer-analogous reactions, the distinguish whether a substance is of high molecular weight, or is only part of a loosely held together structure, such as in soaps due to their micellar structure, can be made.

In addition to the structure elucidation of macromolecular substances, polymer-analogous reactions can also be employed for the synthesis of polymers, which are not accessible via classic polymerization techniques. Nowadays, polymer-analogous reactions are used, for example, for the preparation of polyvinylalcohol using saponification of pre-polymerized polyvinylacetate (Figure 2.15). Direct polymerization using vinylalcohol is not possible due to the hydroxy groups, which prevent most of the controlled/living polymerization approaches (see Chapter 2.2. and 2.3).

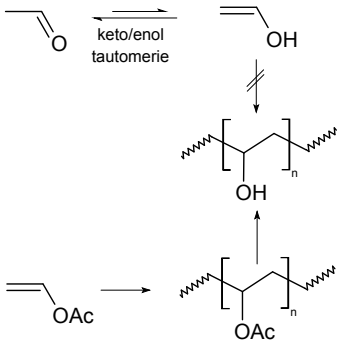

Figure 2.15: Polymer-analogous reaction for the preparation of polyvinylalcohol.

In addition, for the preparation of ion exchange resins, polymer-analogous reactions can be used. For instance, styrene-divinylbenzene copolymers can be converted with concentrated sulfuric acid (H_2SO_4) to a cation exchange resin (Figure 2.16).

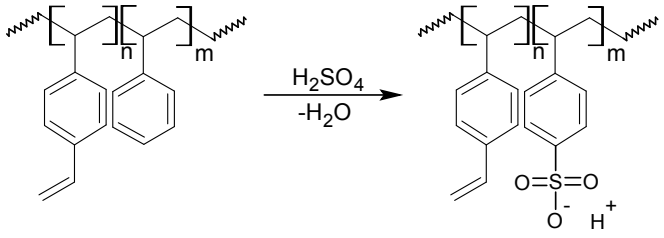

Figure 2.16: Polymer-analogous reaction for the preparation of ion exchange resins by the reaction of H_2SO_4 with a styrene-divinylbenzene copolymer.

Polymer-analogous reactions can also be used for intramolecular cyclizations, as for polyacrylonitrile leading to graphite fibers (Figure 2.17).

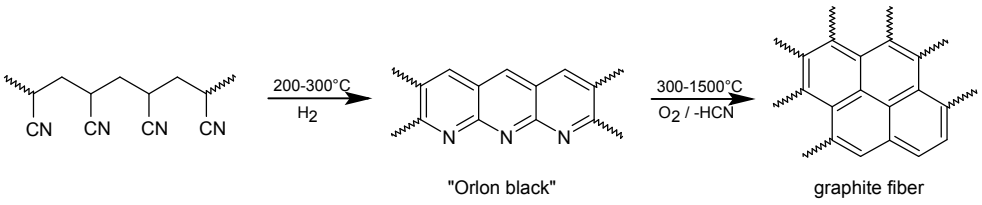

Figure 2.17: Polymer-analogous reaction for the preparation of graphite fibers.

Besides the described methods, transformations of functionalized side chains to other functionalities are possible via polymer-analogous reactions. Such an approach is followed in the current work. Pre-polymerized chloride functionalized copolymers can be converted to azide functionalized copolymers, as shown in Figure 2.18. By using modular ligation reactions, different alkyne phosphoric esters can subsequently be attached to these copolymers. In this context, the reaction conditions of the conversion and effects on the resulting polymers will be examined. In the following subchapter the covalent binding via modular ligation as a special type of polymer-analogous reactions is described in detail.

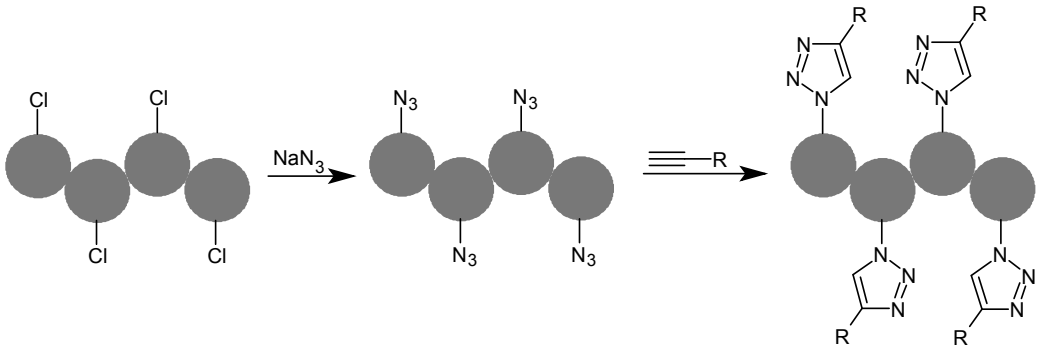

Figure 2.18: Schematic representation of the polymer-analogous reaction for the transformation of chloride functionalized copolymers to azide functionalized copolymers as modular ligation points for further connection of phosphorylated compounds.

2.2.1 *"Click"* Chemistry

In 2001, a concept was described by Sharpless and colleagues, by which target molecules can be synthezized much faster and more focused from smaller units.[43] This group of reactions are described as "*click*" chemistry, which must meet the following conditions [44]:

- quantitative yield
- high tolerance of functional groups
- no or safe/not harmful by-products
- stereospecificy
- modular design and wide range of applications
- simple reaction conditions
- solvents, that allow easy product isolation (preferably water)

- simple work-up and isolation of the product
- high thermal driving force
- high atom efficiency

Chemical reactions that meet these criteria can include:

- cycloaddition reactions (especially Cu(I) catalyzed cycloaddition by Huisgen and Diels-Alder reactions)
- nucleophilic substitution reactions (especially of small strained rings such as epoxides or aziridines)
- carbonyl-like formations of ureas and amides (not aldol)
- addition reactions of carbon-carbon double bonds (eg. epoxidation)

As mentioned above, cycloadditions, in particular the 1,3 dipolar azide/alkyne cycloaddition (Figure 2.19), provide a straight forward way to functionalized compounds, due to the fact that alkynes and azides are simple to synthesize.

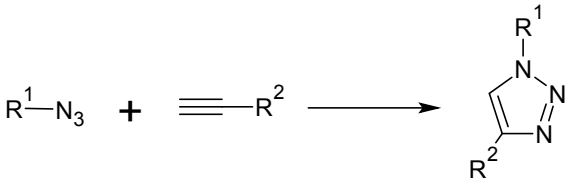

Figure 2.19: Reaction scheme of azide/alkyne 1,3-dipolar cycloaddition.

In addition, especially azides allow, despite their high reactivity, only the chemoselective ligation with a very limited group of reactants (e.g. in cycloadditions or Staudinger ligation) and are therefore tolerant (i.e. orthogonal) to other functional groups. The azide/alkyne 1,3-dipolar cycloaddition can be performed only with activated alkynes, since the activation energy for the cycloaddition reaction is very high. The high activation barrier is responsible for a very low conversion rate even at high temperatures. Another disadvantage is the formation of two regioisomers (1,4 - and 1,5-disubstituted 1,2,3-triazoles), since the two possible HOMO-LUMO interactions between the reactants are energetically similar. The classical 1,3-dipolar cycloaddition is therefore not referred to as *click* reaction.
Using a copper-catalyzed variant of the 1,3-dipolar cycloaddition by Huisgen, however, selectively 1,4-disubstituted 1,2,3-triazoles can be synthesized. 1,5-disubstituted 1,2,3-triazoles can be selectively obtained by a ruthenium-catalyzed reaction. These reactions meet the requirements of *click* reactions and have led to a great interest

in the azide/alkyne 1,3-dipolar cycloaddition as a prototype of the *click* reaction. A catalytic cycle (Figure 2.20) including a binuclear reaction mechanism via a concerted mechanism was proposed, which proceeds at ambient temperature.[45] Most methods use Cu(I) salts directly. Other methods generate the copper(I) species using copper(II) sulfate and the reducing agents sodium ascorbate or even metallic copper for the in-situ generation of the required reactive Cu(I) species.

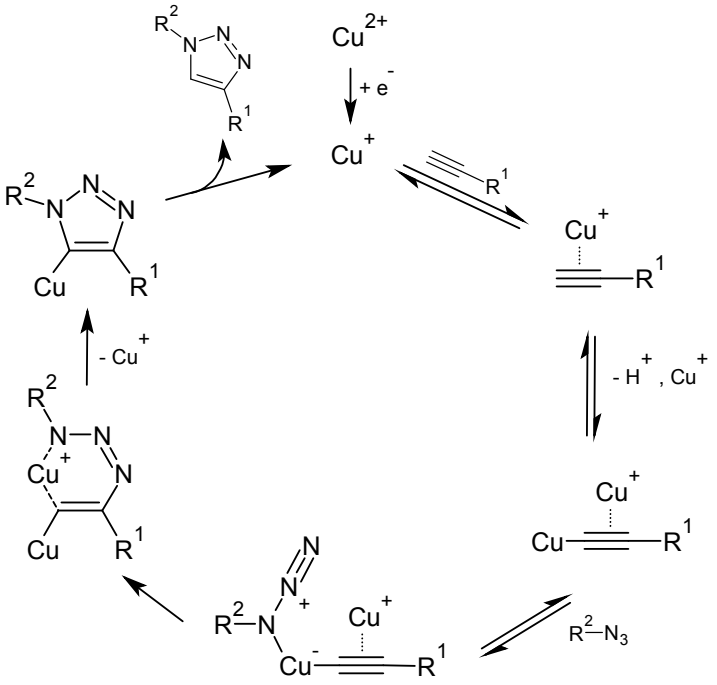

Figure 2.20: Mechanism of copper-catalyzed azide/alkyne cycloaddition. Adapted from [45].

The first application of the 1,3-dipolar cycloaddition by Huisgen in polymer and material science was decribed in 2004 by several groups.[46, 47, 48] For the use in polymer and material science, additional specific criteria for the *click* reactions need to be determined.[13] Since facile purification methods of small compounds (e.g. destillation, crystallization) are not feasible for polymer-polymer *click* reactions, the starting materials have to be used in strictly equimolar amounts. Only if a polymer building block is easily seperable from the system, e.g. rinse of polyethylene glycol (PEG), an excess of this component can be used. In the case of *click* reactions between polymer end-groups or side chains and low-molecular compounds (see Figure 2.21 for the side chain approach), the ratio of low molecular compound compared to the *clickable* groups in the polymer do not have to be equimolar. An excess of the *clickable* small organic molecules can sometimes be employed to overcome the mentioned reaction delays or incomplete transformations (refers to Chapter 2.2.).

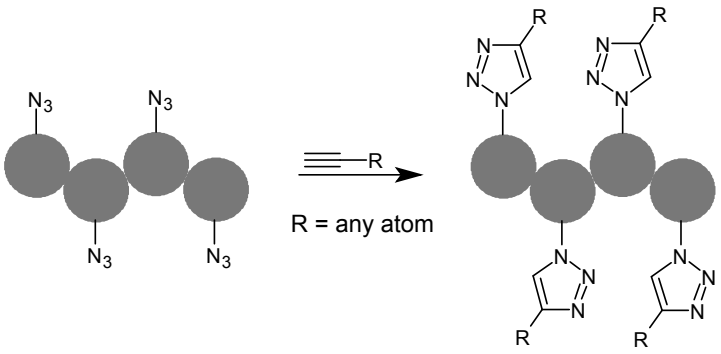

Figure 2.21: General reaction scheme of the azide/alkyne 1,3-dipolar cycloaddition of low-molecular alkyne compounds and a polymer with azide functionalities in the side chains.

In summary, it can be said that the metal catalyzed Huisgen 1,3-dipolar cycloaddition reaction between azides and terminal acetylenes, the so-called azide/alkyne *click* reaction, represents a versatile polymer modification approach. It combines high efficiency (usually above 95 %) with a high tolerance of functional groups and solvents as well as moderate reaction temperatures (25–70 °C). Therefore, it is very suitable for the ligation of alkyne phosphorus esters to functionalized polymers and has been chosen as the method of choice for polymer-analogous conversions in the current work.

2.3 Phosphorus-Containing Polymers

In recent years, phosphorus-containing monomers and polymers have been subject to extensive research.[49, 50, 51, 52] The range of phosphorus-containing compounds is extremely wide, since phosphorus can exist in several oxidation states (+I to +V). These oxidation states lead to different chemical environments and therefore interesting properties. In previous studies, phosphorylated materials have shown - among other characteristics - higher chemical and thermal stability than sulfonic acid materials, which makes them suitable for the use in material engineering e.g. as flame retardants or proton-conducting fuel-cell membranes. In addition, phosphorylated polymers, such as polyphosphonates and phosphonated poly(meth)acrylates, were shown to be biodegradable, blood compatible and lead to strong interactions with biomaterials such as bones and proteins, which makes them appropriate for the biomedical field in terms of tissue engineering [49] or drug delivery [52]. Due to the aptitude of phosphorus-containing materials, such as poly(vinylphosphonic acid), to complex metals [53], they can also be used for dispersants, corrosion inhibiting agents and for preventing deposit formation.[53]. The variable applications of phosphory-

lated (co)polymers are described in Chapter 2.3.1. in more detail and on the basis of some examples. Chapter 2.3.2. gives an overview about the polymerization techniques used up till now, for both the direct (co)polymerization of phosphorylated monomers and the post-phosphorylation of functionalized (co)polymers.

2.3.1 Applications of Phosphorus Polymers

1. In biomedical applications

Phosphorylated polymer surfaces were shown to be of great interest in tissue engineering due to their capability to interact with biomaterials such as bone cells and proteins.[49] Hence, phosphorylated polymers with phosphorylated side chains are increasingly coming into focus as materials for the biomedical sector.
Important solid biomaterials such as bones and teeth containing both mineralic and organic components such as hydroxyapatite ($Ca_5(PO_4)_3(OH)$) and collagen. In order to obtain functional materials, it is necessary to combine the properties of mineral and polymeric constituents. The PO_4^{-3} ions of hydroxyapatit (HAp) crystals are readily exchangeable with other phosphate ions e.g. by phosphorylated polymers. With increasing ratio of phosphate groups in the polymer, adhesion of a restorative material with enhanced physiochemical properties to a defective stiff biological material can be increased.[54] Thus, for example, poly(vinylphosphonic acid) copolymers can be used in bone-tissue-engineering scaffolds design.[49, 55] In addition, copolymers of vinylphosphonic acid and acrylamide can be employed as thin sheets of anionic hydrogels, which support cell adhesion and proliferation.[56] In addition, these copolymers show a high swelling ratio and they respond to changes in pH and ionic strength, which makes them also suitable for drug delivery.
A further approach are the structural similarities of polyphosphates to naturally occurring nucleic (DNA) and teichoic acids (polysaccharides of glycerol phosphate linked via phosphodiester bonds (Figure 2.22)).

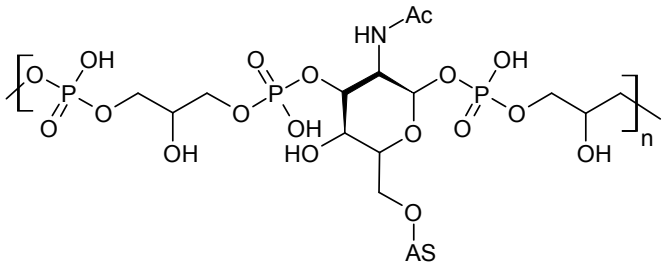

Figure 2.22: Exemplary chemical structure of a techoic acid.

Teichoic acids are known to be responsible for ion transport through bacteria cell walls or binding of Mg^{2+} on the external surface of the cytoplasmic membrane. Therefore, polyphosphates and polyphosphonates also exihibit interesting properties such as biocompatibility, low toxicity and biodegradability through hydrolysis. In addition, enzymatic digestion of phosphate linkages is possible under physiological conditions.[57] Especially derivatives of 2-methacryloyloxyethyl phosphorylcholine (MPC) (Figure 2.23) copolymerized with different monomers, such as alkyl methacrylates and vinylalcohol, are used for biomedical purposes. Due to the phospholipid group, these MPC copolymers exhibit comparable biometric structures, leading to blood compatibility and protein adsorption resistance, which makes them suitable for tissue engineering.[58]

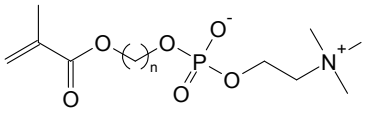

Figure 2.23: General chemical structure of derivatives of 2-methyacryloyloxyethyl phosphorylcholine (MPC).

2. As metal complexing material

A wide range of complexing groups enable the ligation of metal cations onto a polymer. In recent years, the focus is increasingly on phosphonate groups since some authors have pointed out their good complexation properties for metal cations, such as Ca^{2+}, Ni^{2+} and Cu^{2+}.[59, 60, 61] By combining a temperature-responsive polymer, such as poly(*N*-isopropylacrylamide) = P(N^iPAAM), with a monomer containing phosphorus moieties, copolymers can be prepared, which can complex metals and precipitate from solution (e.g. water) at higher temperatures. Nonaka *et al.* copolymerized acryloyloxypropyl phosphinic acid (APPA) and N^iPAAM (Figure 2.24) and studied the thermo-responsibility and metal-complexing behavior of the resulting polymers.[62] They could show that the ratio of APPA not only had an influence on the metal complexing behavior, but also increase the lower critical solution temperature (LCST) in comparison to pure P(N^iPAAM). For example, copolymers with approximately 11% APPA ratio show a LCST of 45 °C compared to 32 °C of pure P(N^iPAAM). At APPA ratios higher than 21%, the LCST was above 55 °C. In addition, Nonaka *et al.* could show that such APPA-N^iPAAM-copolymers exhibit different adsorption capacities for several metal cations. The APPA–N^iPAAM (1:9) copolymer complexed with Sm^{3+}, Nd^{3+} and La^{3+} became water-insoluble above 45 °C at pH 6-7, whereas the copolymer complexed with Cu^{2+}, Ni^{2+} and Co^{2+}

remain water-soluble in the examined temperature range of 25 to 55 °C under otherwise identical conditions. Such copolymers are therefore capable to seperate metal cations in a solution depending on the temperature.

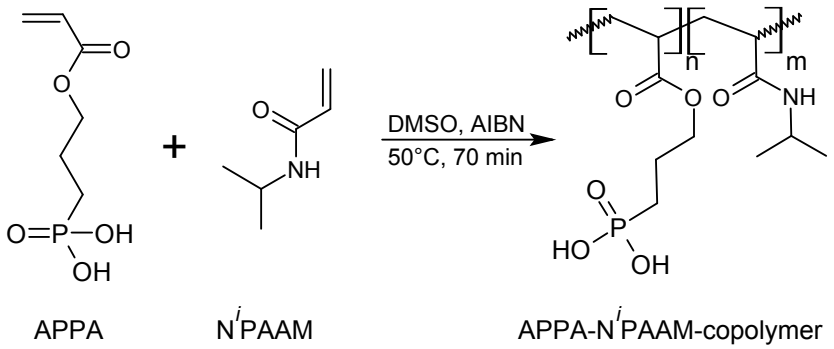

Figure 2.24: Reaction scheme of the copolymerization of acryloyloxypropyl phosphinic acid (APPA) and the thermal sensitive *N*-isopropylacrylamide (N^iPAAM).

3. As proton-conducting fuel-cell membranes

The key properties of a fuel cell are provided by the electrolyte in form of low-molecular or polymeric electrolyts. In the case of a polymeric electrolyte membrane, the charged groups are attached to a polymer backbone. This linkage of charged groups is the main advantage of a polymeric electrolyte. Not only can such polymeric electrolyts exhibit high charges due to a high number of ionizable groups in every single polyelectrolyte molecule, but such ions can also seperate only to a certain extent, because they are connected to each other by the polymer backbone. In contrast to low-molecular electrolytes, the ionic charge interaction of polymeric electrolyts therefore do not vanish in a diluted system, due to interaction of charges in every single molecule. Nevertheless, the ionic strength of a polymeric electrolyte differs in the overall system. The ionic strength is high, in and near by the polyelectrolyte chains, but lower in the bulk phase.
In recent years, especially perfluorinated ionomers, such as perfluorosulfonic membrans are used in low-temperature fuel-cell applications due to their high proton conductivity.[50, 63] These sulfonic membranes are designed to operate at temperatures as low as 80 °C, which represent a major drawback due to carbon monoxide (CO) poisoning of the platinum anode catalysts in this temperature range.
Functional polymers based on vinylphosphonic acid and derivatives therof show superior conducting properties and high chemical as well as thermal stability, which make them suitable as polymer electrolyte membranes in fuel cells, without anode poisoning due to higher operating temperatures.[64] In addition, they exhibit less

emission of CO_2 under anhydrous conditions in the range between ambient temperature and 160 °C. Therefore, phosphorylated polymers feature a high potential as efficient energy conversion devices for proton-conducting materials and also good environmental features. However, it is not possible to use pure poly(vinylphosphonic acid) (PVPA) due to the high ratio of phosphonic acid groups, which are bonded to each other by hydrogen bridges, which makes PVPA to a rigid polymer. Nevertheless, it is possible to adjust the stiffness individually, by copolymerization with other monomers, such as (meth)acrylates.

4. As flame retardant

Different kinds of phosphorus-containing (co)polymers such as polyphosphates are increasingly successful as halogen-free alternatives for various flame retardant applications, due to their high thermal stability.[65] Phosphorus may be either act in the condensed phase and/or in the gas phase (see Chapter 2.4.1. subchapter "phosphorylated flame retardants").
Flame retardancy is among others, a major problem in lithium batteries. Under heavy load, it may come to a thermal instability of the electrolyte material, which results in a high temperature increase. The temperature increase can subsequently lead to a battery explosion or fire. Therefore, fire-retardant polymer electrolytes are key materials for the safer operation of batteries. Therefore, phosphorylated polymers have the potential to act both as polymeric electrolyte and as flame retardant. Novel safe and non-flammable phosphorus-based poly(ethylene glycol) electrolytes, linked via a phosphate group could be synthesized (Figure 2.25).[66, 67, 68]

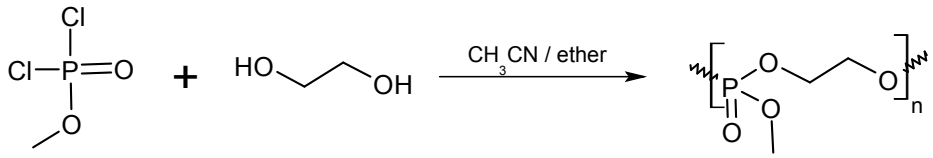

Figure 2.25: Synthetic pathway of copolymers of methyl phosphorodichloridate and 1,2-ethanediol, implementable in flame retardancy applications.

By combining phosphorus moieties with nitrogen or aromatic groups, a further increase in flame retardancy can be expected (see Chapter 2.4.1. "phosphorylated flame retardants"). Kannan synthesized arylazophosphate polymers (Figure 2.26) with good mechanical and thermal properties due to high cristallinity and at the same time good solubility.[69] Via the incorporation of aromatic groups, the thermal stability as well as the flame retardancy could be increased even further.

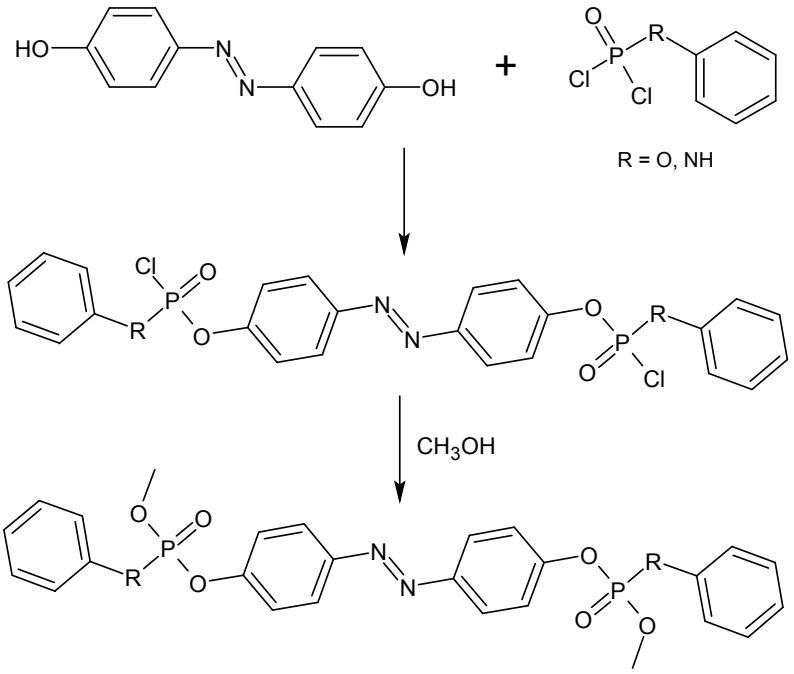

Figure 2.26: Synthesis of arylazophosphate copolymers as flame retardants.

Due to the neccessary decomposition of the backbone using polyphosphates, respectively polyphosphonates, polymers with phosphorylated side chains came more and more into focus for use in the field of flame retardancy.
A widely used phosphorus compound, which can be linked to functionalized (co)polymers, is 9,10-dihydro-9-oxa-phosphaphenthrene-10-oxide (DOPO) (Figure 2.27). DOPO and its derivatives were firstly synthesized by Saito [70] in 1972 and are nowadays widely used as flame retardant in e.g. electronic or aerospace applications.[5, 71, 72]

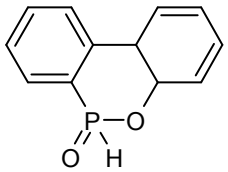

Figure 2.27: Chemical structure of 9,10-dihydro-9-oxa-phosphaphenthrene-10-oxide (DOPO).

An example of phosphorus and nitrogen-containing polymers with phosphorus moieties in the side chains are copolymers of diethylbenzyl phosphonate (DEBP) and acrylonitrile. In this case, the phosphonate moieties act as nucleophilic non-volatile residue and in addition as cross-linking promoter. The poly(acrylonitrile) cyclizes at high temperatures, making it more thermally stable. This cyclization is

promoted by the phosphorus group, as it is depicted in Figure 2.28.[73] In addition, an increase in the limiting oxygen index (LOI) (see Chapter 2.4.2.) and a decrease in the overall heat release could be found. Even a classification as V0 in the UL94 test (see Chapter 2.4.2) could be reached, making it a self-extinguising material.[74]

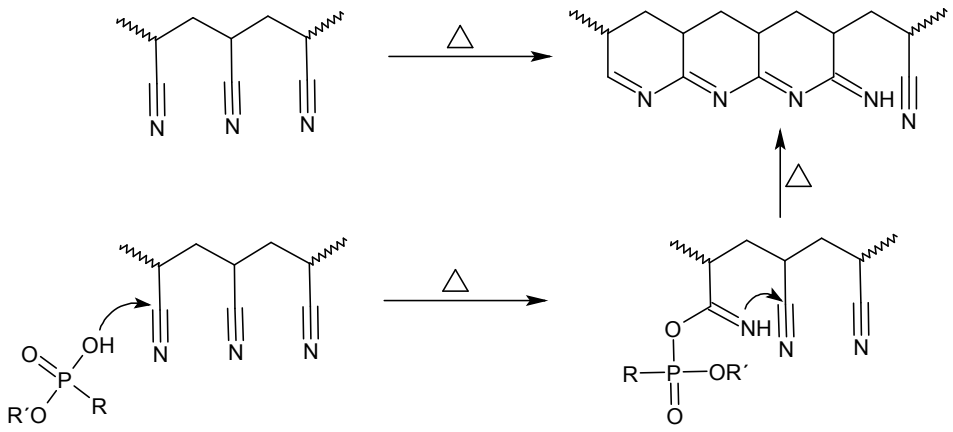

Figure 2.28: Reaction pathway of the thermal cyclization of poly(acrylonitrile) promoted by phosphonate moieties in a diethylbenzyl phosphonate-acrylonitrile copolymer.

2.3.2 Synthesis of Phosphorylated Polymers

The most obvious way to prepare phosphorylated polymers is the direct polymerization of phosphorus-containing monomers. However, there are no significant commercial progress in this area, although a variety of phosphorus-containing polymers have been synthesized on the laboratory scale showing remarkable properties (refer to Chapter 2.3.1.).

On the following pages an overview about the preparation of different types of phosphorus-containing monomers and their (co)polymerization is described.

First, the polymerization of phosphates and phosphonates is considered, leading to (co)polymers having phosphorus moieties incorporated into the polymer backbone. Already in 1962, the synthesis of polyphosphonates by polycondensation using linear phosphonates was described by Gefter, yet without detailed information about the final products.[75] In the late 80s, several improved mechanisms for the synthesis of polyphosphates and -phosphonates via a combined polycondensation and transesterification process were developed.[76, 77] The reaction scheme of the polycondensation (first step) and transesterification (second step) reactions is shown in Figure 2.29. However, the polymerization of phosphates is difficult, because it can easily lead to cross-linking due to the three ester groups.

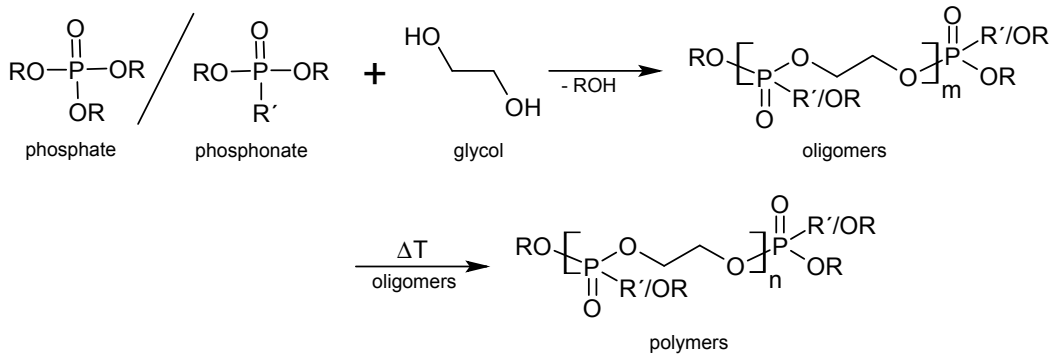

Figure 2.29: General reaction scheme of the polycondensation reaction of small phosphate/phosphonate molecules with glycol and subsequent transesterification to linear polyphosphates/-phosponates.

Iliescu *et al.* could show that polyphosphates and polyphosphonates can be synthesized by polycondensation both in liquid-liquid system [78], gas–liquid system [79] and inverse phase transfer catalysis [80].
In 1976, the synthesis of high-molar-mass linear polyphosphates and copolymers via ring-opening polymerization (ROP) has been described.[81] In 1984, even a controlled anionic ROP mechanism could be found for 2-alkoxy-2-oxo-1,3,2-dioxaphospholanes, leading to polyphosphates as shown in Figure 2.30.[82]

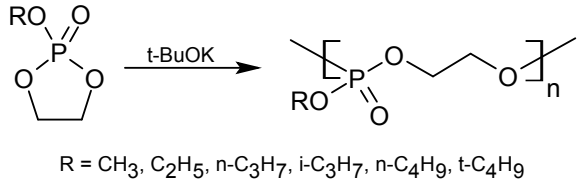

Figure 2.30: General reaction scheme of the anionic ring-opening polymerization of 2-alkoxy-2-oxo-1,3,2-dioxaphospholane leading to linear polyphosphonates.

The ester groups of phosphates and phosphonates can also be copolymerized with e.g. poly(ethylene glycol), poly(ethylene oxide) and poly(propylene oxide). Depending on the monomer ratios, the copolymers can be used as liquid membranes in biomedical applications [83] or as solid polymer electrolytes in fuel-cells [84]. Copolymerized with aromatic- or nitrogen-containing monomers, they can also be employed as flame retardants.[69]
To better utilize the properties of different phosphorus compounds, phosphorylated moieties can be linked onto polymers by either (co)polymerization of phosphorylated monomers or by grafting of phosphorus groups onto functionalized pre-polymerized materials. Thereby, polymers with phosphorylated side chains can be obtained.

In recent years, syntheses of phosphate and phosphonate bearing vinyl, allyl, (meth)-acrylic and styrenic monomers and their direct synthesis to polymers with phosphorylated side chains are emerging. The main problem for the synthesis of these new phosphorus-containing polymers is the fact that up till now only few phosphorus-containing monomers are commercially available and most of them are phosphate-type methacrylate monomers (Figure 2.31 upper line).

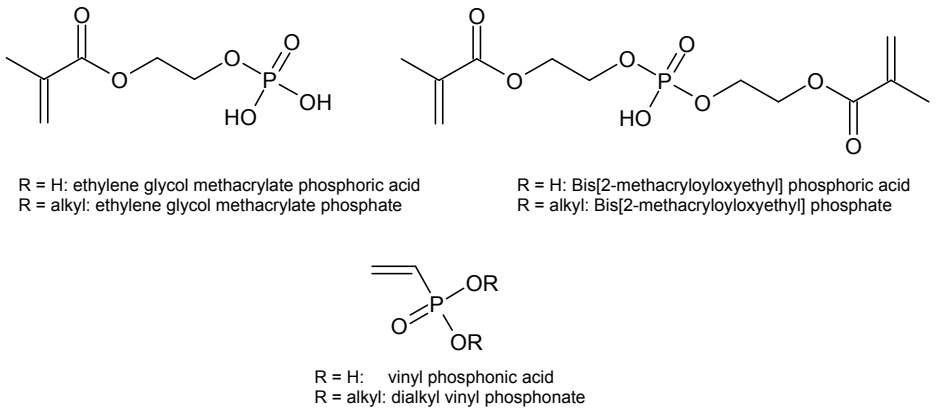

Figure 2.31: Chemical structures of commercially available phosphorylated methacrylic (upper line) = phosphate-type and vinyl (lower line) = phosphonate-type monomers.

Phosphonate-type monomers are recognized as hydrolytically more stable than their phosphate-type homologues [85] due to the C-P bond in phosphonates compared to the C-O-P bond in phosphates, which makes them more usable in applications such as coatings. Despite this, in the current work, both the synthesis of phosphate-type (Chapter 3) and phosphonate-type (Chapter 4) monomers will be discussed. Since almost exclusively methacrylates (Figure 2.31 upper line) and vinylphosphonic acid (VPA) and some derivatives (Figure 2.31 lower line) are the only commercially available phosphate/phosphonate-type monomers, further development of novel phosphorylated monomers and subsequent synthesis of novel phosphorylated polymers is neccessary. In the following sections the synthesis of the main types of phosphorylated monomers and their further polymerization are described.

1. Phosphorylated allyl monomers

Phosphonate bearing allyl monomers were first prepared in the early nineties according to methods described by Arbuzov (nucleophilic substitution of alkyl halides by trialkyl phosphates, see Figure 2.32 reaction Arbuzov) [86], Michaelis and Becker (nucleophilic substitution of alkyl halides by dialkylsodiumphosphonates, see Figure 2.32 reaction Michaelis-Becker), respectively Kinnear and Perren (reaction of

allyl halide with phosphorus trichloride (PCl_3) in the presence of aluminum chloride ($AlCl_3$) and a Lewis acid) [87] followed by a subsequent esterification to the phosphorylated allyl monomers (see Figure 2.32 reaction Kinnear-Perren).

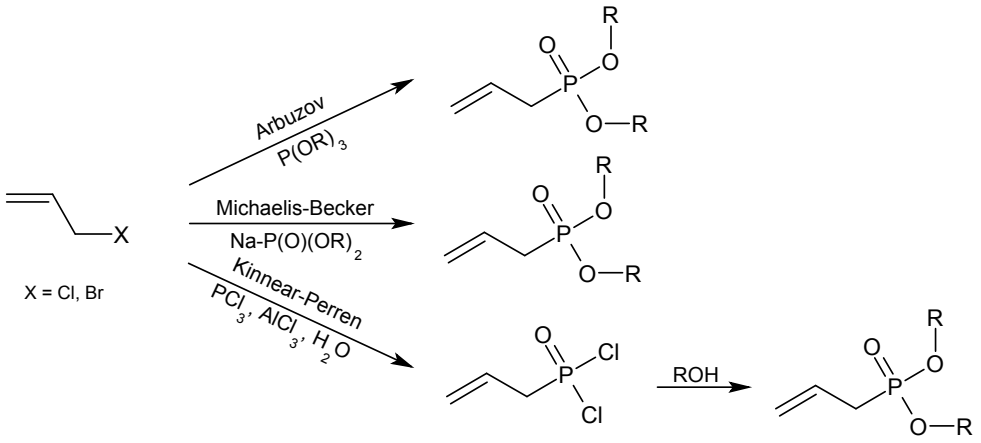

Figure 2.32: Reaction pathways for the synthesis of phosphorylated allyl monomers.

More recently, the synthesis of phosphorylated allyloxy monomers as depicted in Figure 2.33 was described, in which the reaction of an allyl bromide with a phosphorylated primary alcohol was performed.[88, 89]

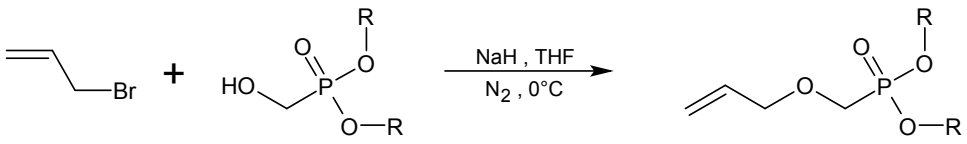

Figure 2.33: Reaction pathways of the synthesis of phosphorylated allyloxy monomers.

A special type of phosphorylated allyloxy monomers represent dioxaphosphorinanes as they show a cyclic structure (Figure 2.34) and the phosphonate group is not directly bound to the allyl unit. These cyclic allyl monomers are synthesized by transesterification of a glycol bearing a double bond and a hydrogenophosphonate (Figure 2.34 upper line). To obtain phosphorinanes with R = butyl or benzyl, a pathway starting from a hydrogenodioxaphosporinane and further alkylation with an alkyl halide must be pursued. This reaction is promoted by cesium carbonate ($CsCO_3$) and tetrabutylammoniumiodide (Figure 2.34 lower line).[90]
The polymerization of the obtained phosphorylated ally(oxy) monomers is quite challenging. Previous free radical polymerizations of (phosphorylated) allyl monomers were mostly unsuccessful, leading only to low molecular weight structures, due to a chain transfer process occurring onto the methylene group of allyl monomers.

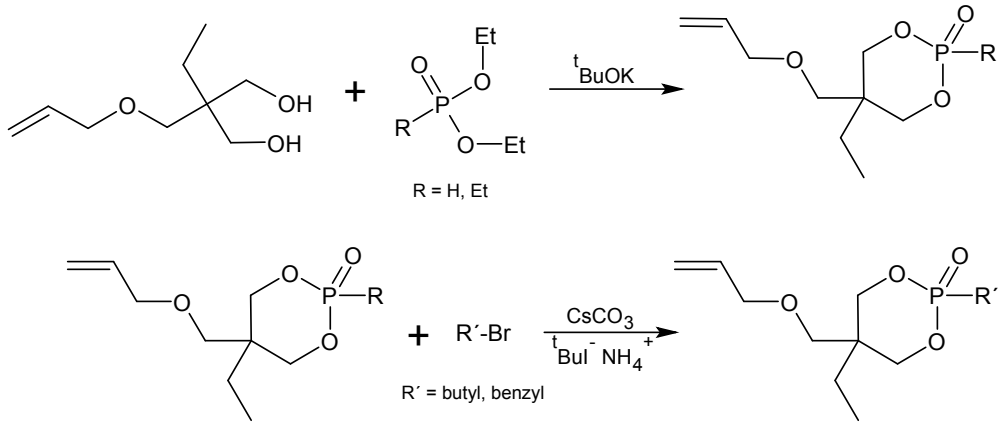

Figure 2.34: Reaction pathway of the synthesis of phosphorinanes.

Only by copolymerization of phosphorylated allyl monomers with electron-accepting monomers, an efficient polymerization is possible. This copolymerization was described e.g. by Negrell-Guirao *et al.* for the copolymerization of diethyl-1-allyl phosphonates with maleic anhydride (Figure 2.35).[89] These copolymers can be used as highly effective flame retardants for the use in textiles.

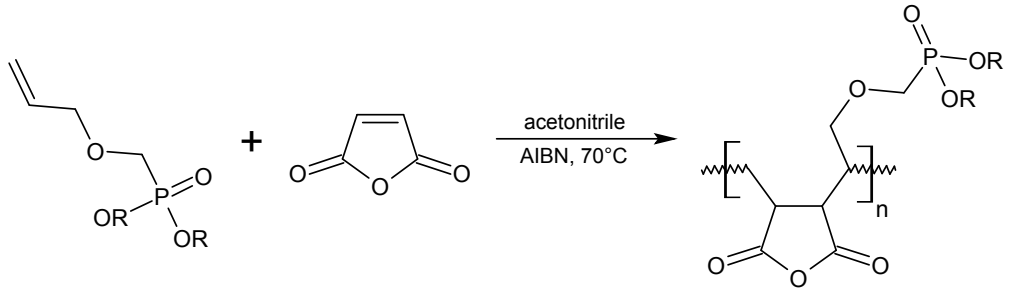

Figure 2.35: Reaction pathway of the synthesis of phosphorylated copolymers using a phosphorylated ally monomer and maleic anhydride.

Unlike non-cyclic allyl monomers, cyclic allyloxy monomers such as dioxaphosphorinanes (see Figure 2.34) with R = H can be polymerized with high degrees of polymerization without the addition of a comonomer. Indeed, a phosphorylated monomer with R = H can also acts as a chain transfer agent, since the P-H bond is active towards allyl bonds, leading to hyperbranched species.[91]

2. Phosphorylated vinyl monomers

In contrast to phosphorylated allyl monomers, the phosphonate group in phosphorylated vinyl monomers is directly attached to the double bond. Due to the electron-

accepting character, an increase of the reactivity in radical polymerizations is expected.

Vinylphosphonic acid (VPA) and derivatives therof were first prepared and characterized by Kabachnik and Medved [92], using the reaction of phosphorus trichloride (PCl_3) with a carbonyl compound, as shown in Figure 2.36.

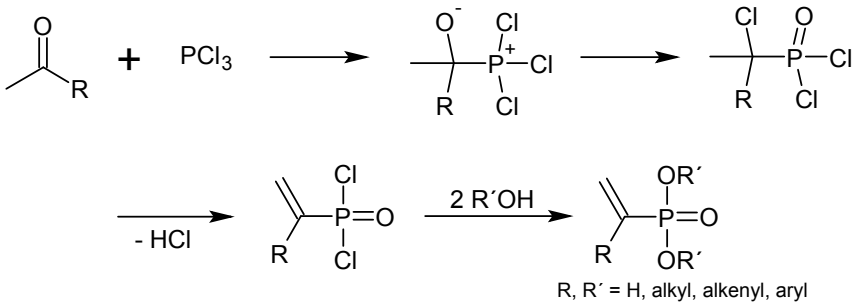

Figure 2.36: Reaction scheme of the reaction of phosphorus trichloride (PCl_3) with a carbonyl compound followed by a rearrangement, dehydrochlorination and hydrolysis respectively esterification to vinylphosphonic acid (VPA) and derivatives thereof.

An alternative approach to vinylphosphonic acid derivatives uses ethylene oxide as carbon source (Figure 2.37).[93] Since the reaction pathway involves 5 steps and the use of thionyl chloride ($SOCl_2$), an industrial process would be too cost consuming, thus the synthesis is used only on the laboratory scale.

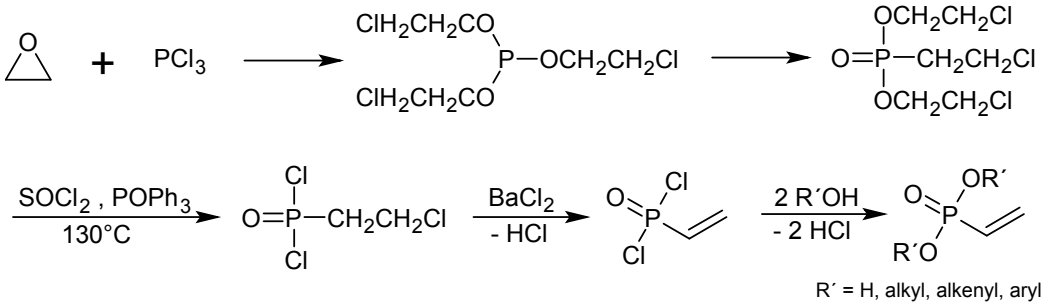

Figure 2.37: Reaction scheme of the reaction of phosphorus trichloride (PCl_3) with ethylene oxide followed by a rearrangement, dehydrochlorination and hydrolysis respectively esterification to vinylphosphonic acid (VPA) and derivatives thereof.

An alternative starting material for the preparation of VPA is 2-chloroethylphosphonic acid (see Figure 2.38 left structure), which is already used as growth regulator for plants and prepared on an industrial scale. By heating 2-chloroethylphosphonic acid of up to 220 °C in the presence of a catalyst and subsequent dehydrochlorination, vinylphosphonic acid can be obtained.[94] Also a halogen-free approach was described using pyrolysis and optionally subsequently hydrolysis of dialkyl 2-acetoxy-

ethanephosphonates (Figure 2.38 right structure), which can be prepared by the reaction of dialkyl phosphite with vinyl acetate.[95]

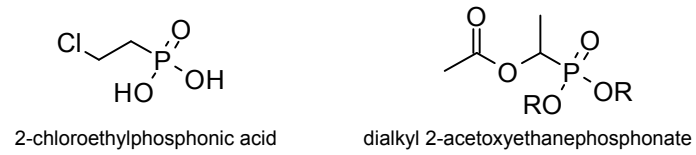

Figure 2.38: Chemical structures of 2-chloroethylphosphonic acid (left structure) and dialkyl 2-acetoxyethanephosphonates (right structure).

As shown in the previous reactions, most syntheses of phosphorylated vinyl monomers involve multi-step pathways. Only few simple to perform syntheses are described in the literature. Until now, the Arbuzov reaction (Figure 2.39 upper line) is the most commonly used method for the synthesis of phosphorylated vinyl monomers. Nevertheless, a drawback of this reaction is the required use of a platinum or nickel catalyst, which can remain in the final product.[96] In addition, a radical approach is described using dialkylphosphites, which can act as chain transfer agent (Figure 2.39 middle line). In this reaction, the dialkylphosphite has to be used in excess to avoid polymerization of the vinylchloride. Another approach uses the esterification reaction between dichlorovinylphosphonic acid and an alcohol, catalyzed by a primary amine (Figure 2.39 lower line). This reaction usually proceeds quantitatively, yet requires the prior synthesis of the chlorinated vinylphosphonic acid.

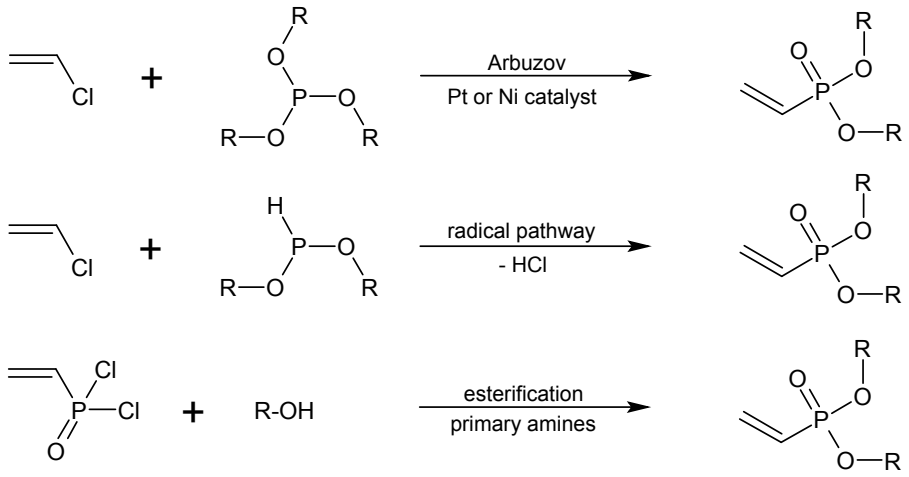

Figure 2.39: Reaction pathways of the synthesis of phosphorylated vinyl monomers.

Until now, relatively few attemps to homopolymerize vinylphosphonates have been reported, due to the fact that most polymerization reactions were unsuccessful. Only via radical polymerization methods, phosphorylated vinyl monomers could be polymerized in low yields, however leading to oligomers and high ratio of by-products.

This observation can be assigned to an intramolecular hydrogen transfer of phosphonate hydrogens, leading to a thermally lable P-O-C bond in the main chain, which subsequently leads to a chain scission reaction.[97] The transfer reaction and scissoring are depicted in Figure 2.40.

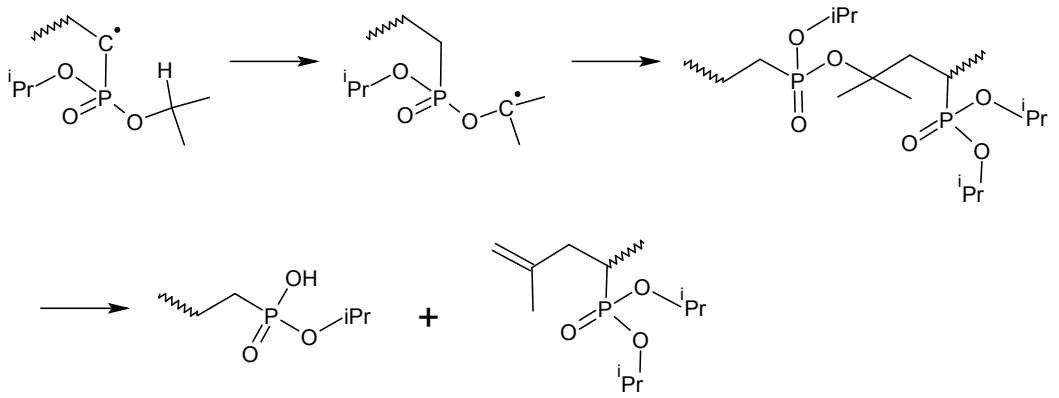

Figure 2.40: Reaction pathway of the intramolecular hydrogen transfer of phosphate ester groups during polymerization exemplified by the chain scission of poly(diisopropylvinyl phosphonate).

Only poly(vinylphosphonic acid) could be obtained in higher yields and low polydispersities.[49] The obtained poly(vinylphosphonic acid) can be used as corrosion inhibition agent in aqueous systems, since it is capable to complex calcium ions.[53] In addition, poly(vinylphosphonic acid) and derivatives therof can be used for polymer electrolyte membranes, which can be used for fuel cells [51], drug delivery (hydrogels) [59] as well as biomimetic mineralization [98].
Syntheses of copolymers of phosphorylated vinyl monomers have been extensively studied. By copolymerization of e.g. diethyl vinyl phosphonate with styrene, copolymers with high molecular weights could be obtained [99], which show lower T_g values compared to pure polystyrene due to steric hinderance of the phosphonate group. Thus, polymers with adjustable T_g values and specific properties can be synthesized.

3. Phosphorylated vinyl ether monomers

The synthesis of phosphorylated vinyl ethers is relatively challenging due to occuring side reactions. First attempts were made through the Arbuzov reaction [86] by the reaction of chloroethylvinylether with triethylphosphite (Figure 2.41). The desired vinyloxyphosphonate was obtained in good yields, however ethyldiethylphosphonate is always obtained in non-negligible amounts, despite drastic reaction conditions.

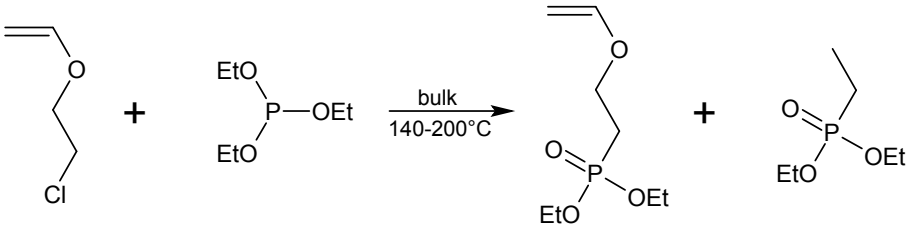

Figure 2.41: Reaction pathway for the synthesis of a phosphorylated vinyl ether via the Arbuzov reaction on the example of diethyl-2-vinyloxyethylphosphonate.

To improve the synthesis of phosphorylated vinyl ethers, an approach using transetherfication between a phosphorylated hydroxy compound and a vinyl ether was accomplished. Using catalytic amounts of a mercury or palladium salt, efficient transetherfication could be observed, however acetals could also be formed, depending on the the efficiency of the reaction and also the stability of the catalyst.[100] With a slightly modified approach described by Iftene *et al.* using 1,10-phenanthroline to avoid the formation of acetals [101], phosphorylated vinyl ethers could be obtained in high yields. The reaction is shown in Figure 2.42.

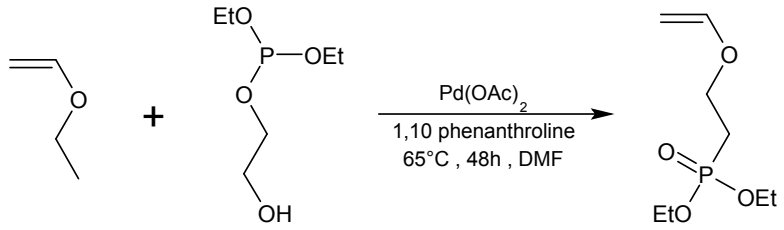

Figure 2.42: Reaction pathway of the synthesis of a phosphorylated vinyl ether via transetherfication on the example of diethyl-2-vinyloxyethylphosphonate.

Previous experiments revealed the electron-donating properties of vinyl ether monomers, which makes them capable to reach high molecular weight polymers either by cationic homopolymerization [102] or by radical copolymerization with an electron-accepting monomer.[103, 104] Using a radical copolymerization method and an electron-accepting monomers, such as maleimides, even alternating polymers can be synthesized.[105, 106]
Based on this knowledge, Kohli and Blanchard described the synthesis of alternating copolymers starting from phosphorylated vinyl ethers and *N*-phenylmaleimide, according to the synthetic route shown in Figure 2.43.[107] These copolymers allow the design and controlled growth of layered polymer assemblies.[107, 108]

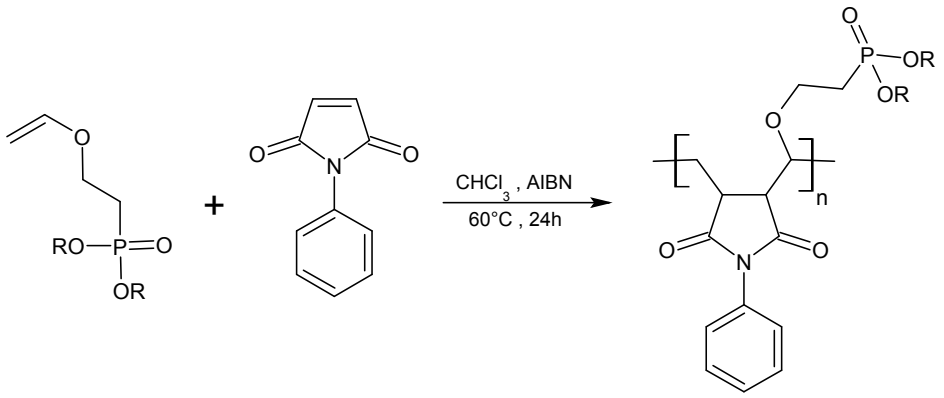

Figure 2.43: Synthesis of alternating copolymers by radical copolymerization of a phosphorylated vinyl ether monomer (electron-donating) and maleimide (electron-accepting).

4. Phosphorylated styrene monomers

Several syntheses of phosphorylated styrene monomers and their radical (co)polymerization are described in the literature.[91] The variety of studies is propably due to the different positions at the ring where the phosphorus-containing group can be bound to. Despite the possibility to prepare and polymerize styrenic monomers with the phosphorus group bound to the α or β position, no investigations have been reported since the seventies. Thus, they will not be discussed in the current work.
The ligation of the phosphorus group directly onto the *para*-position of the phenyl group is difficult. Nevertheless, the reaction can proceed by phosphonation of bromostyrene using a palladium catalyst, however leading to only low yields.[36] By insertion of alkyl spacers between the phenyl ring and the halogen atom, phosphonation can be obtained much easier using the Arbuzov reaction [109] (Figure 2.44 upper line) or the Michaelis-Becker reaction [110] (Figure 2.44 lower line). The Michaelis-

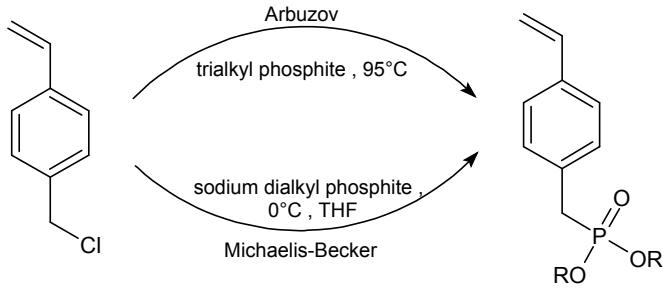

Figure 2.44: Synthesis of phosphorylated styrene monomers via the Arbuzov (upper line) and Michaelis-Becker (lower line) reaction.

Becker reaction has thus the advantage of low reaction temperatures, which avoids the partial polymerization of vinylbenzyl chloride.[111]

Free radical polymerizations of phosphorylated styrene monomers have been reported since 1970.[112] A homopolymerization of *p*-benzylalkylphosphonates using chain transfer agents, was described by Yu *et al.* in 1990, leading to control of both the chain length and chain-end functionality.[113] By copolymerization of *p*-benzylalkylphosphonates with *N*-heterocycle monomers, such as 1-vinylimidazole (Figure 2.45), via an ATRP approach, defined proton-conducting polyelectrolyt membranes can be prepared.[114, 115] Also copolymers of *p*-benzylalkylphosphonates are described, leading to specific properties, such as diethylbenzylphosphonate-acrylonitrile copolymers, which can be used as efficient flame retardants.[73]

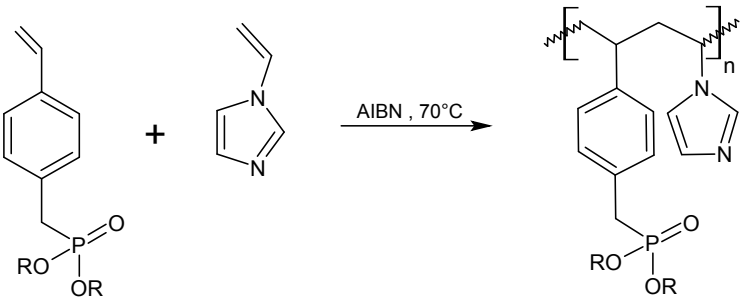

Figure 2.45: Synthesis of phosphorylated styrene copolymers via ATRP of *p*-benzylalkylphosphonates and 1-vinylimidazole.

5. Phosphorylated (meth)acrylic monomers

Among all phosphorylated monomers, (meth)acrylates are the largest group. Due to the activation of the (meth)acrylic double bond by the polar phosphoric substituent, phosphorylated (meth)acrylic monomers exhibit high reactivity in radical polymerizations. Therefore, phosphorylated (meth)acrylic monomers have been studied for a greater extent than other phosphorylated monomers. A multitude of syntheses are described, which allow for a variation of the atom-type between the double bond and the phosphonate (directly bound, via carbon, via nitrogen, via oxygen), as shown in Figure 2.46.[116, 117, 118] Despite the large number of studies, all largely based on similar basic reactions as described by Arbuzov, Kabachnik and Michaelis-Becker.

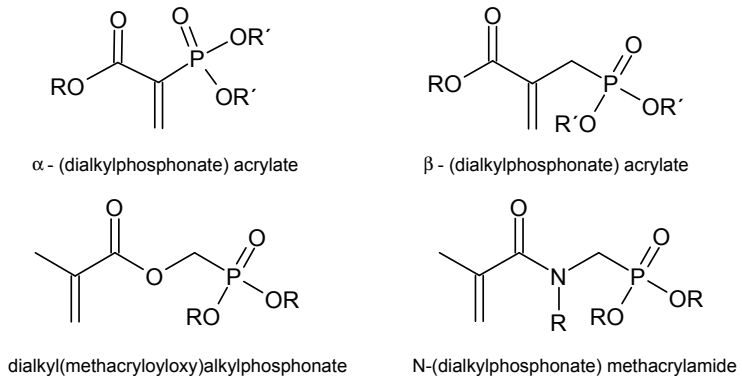

Figure 2.46: Overview of phosphorylated (meth)acrylates with variation of the atom between phosphonate group and double bond.

α-Phosphorylated acrylates, where the phosphonate group is directly bound to the double bond, are synthesized mainly by the Arbuzov reaction [86] of α-bromoacrylate at elevated temperatures. Due to high reaction temperatures, partial polymerization of the α-bromoacrylate occurs.[119] Concerning β-phosphorylated acrylate monomers, an important contribution has been made by Avci *et al.*, who applied several chemical modifications on β-halato acrylate (Figure 2.47).[120, 121, 122, 123]

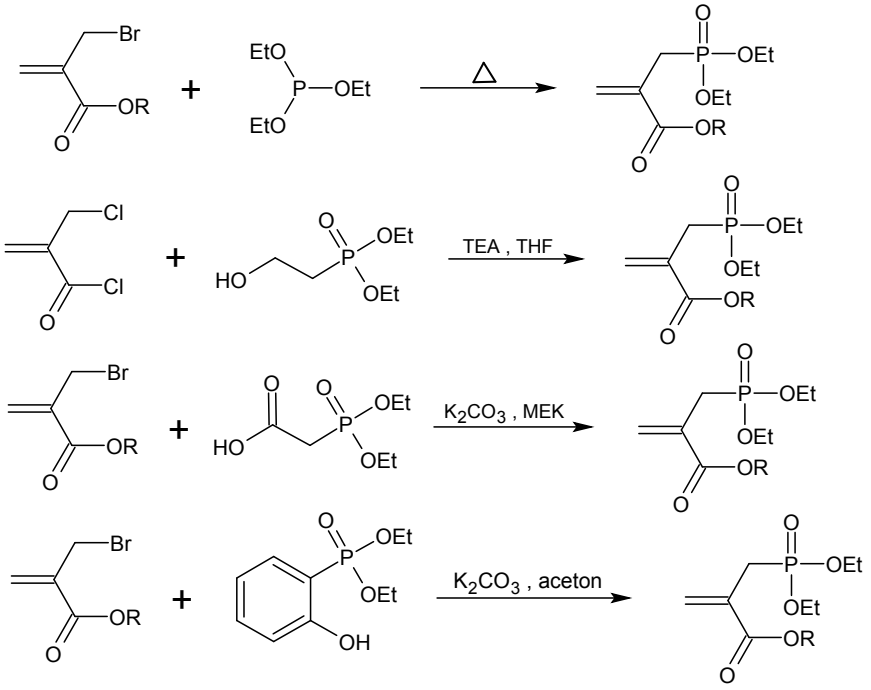

Figure 2.47: Syntheses of phosphorylated acrylate monomers based on β-halato acrylates.

Homopolymerization of β-(dialkylphosphonate) acrylates proceeds very slowly, due to chain transfer processes and slow re-initiating coefficients (e.g. for β-diethylphosphonate acrylate the propagation rate coefficient is $k_p = 3.61 \cdot 10^3$, respectively the chain transfer coefficient $k_{tr} = 2.22 \cdot 10^1 \cdot (\mathrm{M{\cdot}s})^{-1}$ at 85 °C).[121]

Homopolymerization experiments with dimethyl(methacryloyloxy)methylphosphonate showed that the k_p^2/k_t value at 80 °C is just one magnitude lower than that of methylmethacrylate (MMA).[91] Further, the radical copolymerization with MMA revealed a quasi-ideal polymerization behavior, leading to statistical copolymers, which can be used as anti-corrosive coatings for metallic substrates. In addition, phosphorylated (meth)acryl polymers have comparable transparencies as polymethylmethacrylates.
(Meth)acrylamide monomers exhibit an improved hydrolytic stablity in acidic aqueous solutions compared to ester-type monomers. Therefore, phosphorylated (meth)-acrylamides can be used as self-etching adhesives in dentistry. Reacted with a crosslinking comonomer under UV light, polymers with excellent chelating properties and high hydrolytic stability can be obtained.

In recent years, considerable efforts have been made to introduce living radical polymerization techniques such as RAFT (see Chapter 2.1.3.) for the synthesis of phosphorylated polymers. Rixens *et al.* described a terpolymer synthesis using vinylidenechloride, methylacrylate and a phosphonated methacrylate, so called MAUPHOS.[117] The phosphonated methacrylate was synthesized according to the reaction shown in Figure 2.48 using isocyanatoethylmethacrylate (IEM) and dimethylhydroxyethylphosphonate alcohol (DMHP).

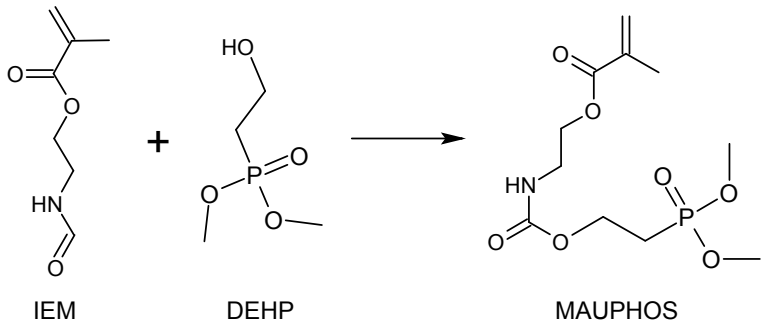

Figure 2.48: Synthesis of 3-methoxy-3-oxido-7-oxo-2,6-dioxa-8-aza-3λ^5-phosphadecan-10-yl 2-methylprop-2-enoate (MAUPHOS).

The polymerization reaction is shown in Figure 2.49.

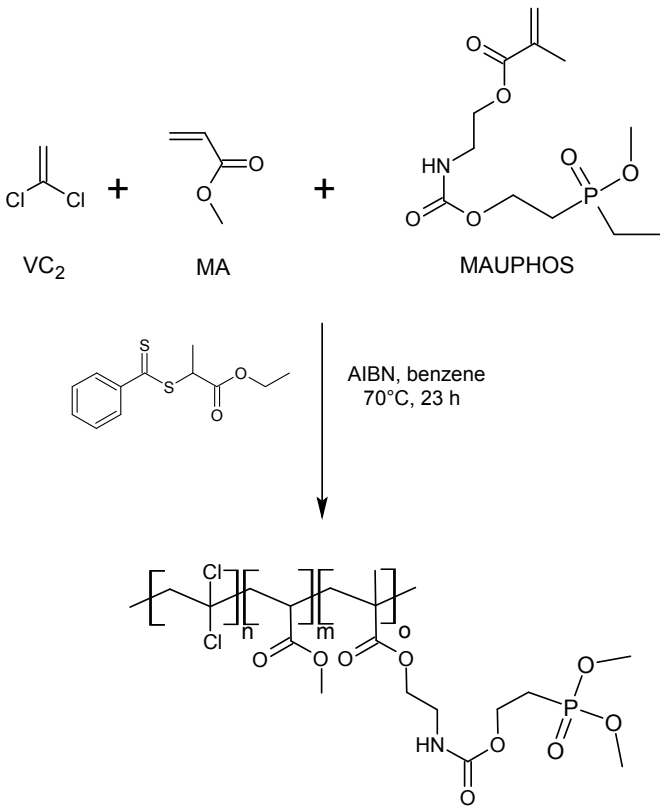

Figure 2.49: Living radical polymerization (RAFT) of a terpolymer consisting of vinylidene chloride (VC_2), methylacrylate (MA) and 3-methoxy-3-oxido-7-oxo-2,6-dioxa-8-aza-3λ^5-phosphadecan-10-yl 2-methylprop-2-enoate (MAUPHOS).

Kinetic studies showed an approximately linear increase of molecular weight with conversion resulting in a polymer with $M_\mathrm{n} = 6900$ g $\cdot$ mol^{-1} and PDI = 1.5 at 83 % conversion. This result was in good agreement with the theoretical expected value. Despite the large number of phosphorylated monomers, which can be polymerized directly using phosphorylated monomers, post-phosphorylation of functionalized (co)polymers represents an interesting tool to prepare phosphorylated (co)polymers. Therefore, attempts have been made to individually phosphorylate polymers, depending on the required application. The advantage of such a synthetic route is, besides the individually adjustable properties of the polymer, the usually simpler synthesis of small phosphorus components. Some of them are even commercially available (e.g. phosphites).

As noted in Chapter 2.3.1. (section "As flame retardant") phosphorus compounds can be attached to functionalized (co)polymers via classical organic reactions. Sun described a post-phosphorylation of styrene polymers via chloromethylation and sub-

sequently phosphorylation.[124] Due to the fact that this method is quite complex and due to steric effects not applicable to long chains, it is not usable in industrial processes. Belfield described a synthesis, in which a styrene-vinylbenzylchloride copolymer is prepared directly in bulk and subsequently post-phosphorylated with a trialkylphosphite leading to phosphorylated copolymers (Figure 2.50) With such a method a nearly quantively conversion of the chloromethyl group to the phosphonate group could be examined and is therefore a good starting point for further developments of novel phosphorus-containing polymers.

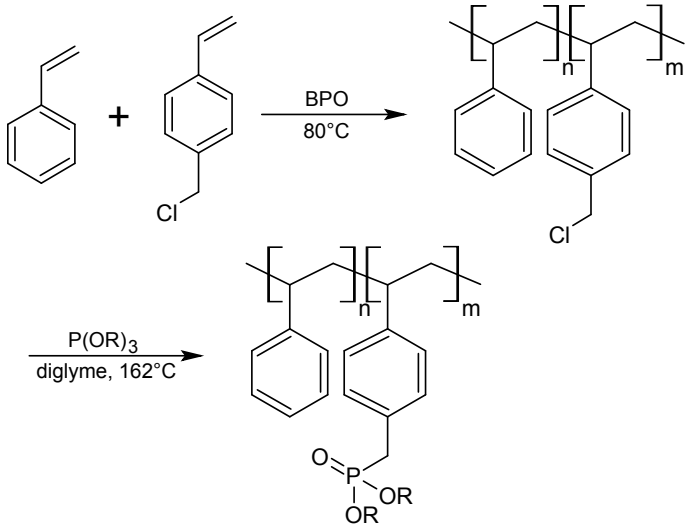

Figure 2.50: Reaction scheme for the copolymerization of styrene and vinyl benzylchloride using divinylbenzoylperoxide (BPO) as initiator and subsequent phosphorylation with a trialkylphosphite leading to phosphorylated copolymers.

In the current work, both the direct polymerization and the post-phosphorylation to phosphorylated (co)polymers via a controlled/living ionic (anionically), respectively, a radical (RAFT) method are examined.

Mainly rings containing the phosphoric moiety have been used to synthesize phosphorus-containing polymers via a ring-opening approach.[125] Using these monomers, the phosphorus will be part of the polymer backbone, which lowers the applicability in terms of flame retardancy (see Chapter 1). As a result, a new approach is pursued in the current work. A three-membered ring, which is directly attached to a phosphonic ester (so called fosfomycin; described in more detail in Chapter 4) is to be polymerized directly via living anionic polymerization to form polymers with phosphorus-containing side chains. To date, no studies can be found in literature, which adress this topic.

In addition, in the field of post-phosphorylation, a new pathway is examined. Up till now, phosphites and other small phosphorus compounds were attached to the pre-funcionalized (co)polymers via classical chemical reactions (e.g. esterification, addition- and elimination reactions).[126, 124] To increase the possibility to individually tune the flame retardancy of these polymers, the phosphorus compound will be linked to the polymer via an 1,3-dipolar cycloaddition (see Chapter 2.2.1). Therefore, novel phosphorus compounds have to be synthesized bearing an alkyne group, which can be used for the modular ligation process. Using such an approach, it should be possible to individually bind various phosphorus esters onto the copolymer, depending on the required temperature range of flame retardancy (see Chapter 2.4).

2.4 Combustion and Flame Retardancy of Polymers

In general, organic polymers decompose under heat to give volatile combustion products. For the development of a fire, in addition to the energy which acts on the material in the form of heat, oxygen is necessary. By the action of heat, a temperature increase is effected in the material, which causes a decomposition reaction (pyrolysis). Thereby, the emerging volatile products and the quantity of decomposition depend on the chemical structure of the polymer. The release of flammable gases, combined with oxygen in the air, can lead to a flammable gas mixture. The oxidation reaction of the pyrolysis gases with oxygen in the air is referred to as combustion. The combustion of polymeric materials is a highly complex process involving related and/or independent stages, which occur as well in the condensed as in the gas phase and also at the interphase between them.[127] After ignition, the burning material releases heat and high-energy $H^{\bullet}$ as well as $OH^{\bullet}$ radicals, causing an additional increase in temperature and combustion in the gas phase. The pyrolysis processes are accelerated and other combustible material is ignited. By strong heat development and large gas release in the course of the fire (particularly in room fires), a gas mixture, which causes an expansion of the fire with very high speed, may occur. This sudden ignition and burning of pyrolysis gases is designated as flash-over. The entire combustible material is involved and only if one of the components (oxygen, polymer, heat) is consumed by the fire, the flame subsides.[128]
Each fire scenario is characterized by the availability and transport of components material, i.e. oxygen and heat. Figure 2.51 schematically shows the combustion cycle of a material with the processes of mass transfer of oxygen and material as well as the heat transport. The reduction or obstruction of material, oxygen or heat transport processes and therefore the interruption of the combustion process at one or more points is the basis of different flame retardant mechanisms and concepts.

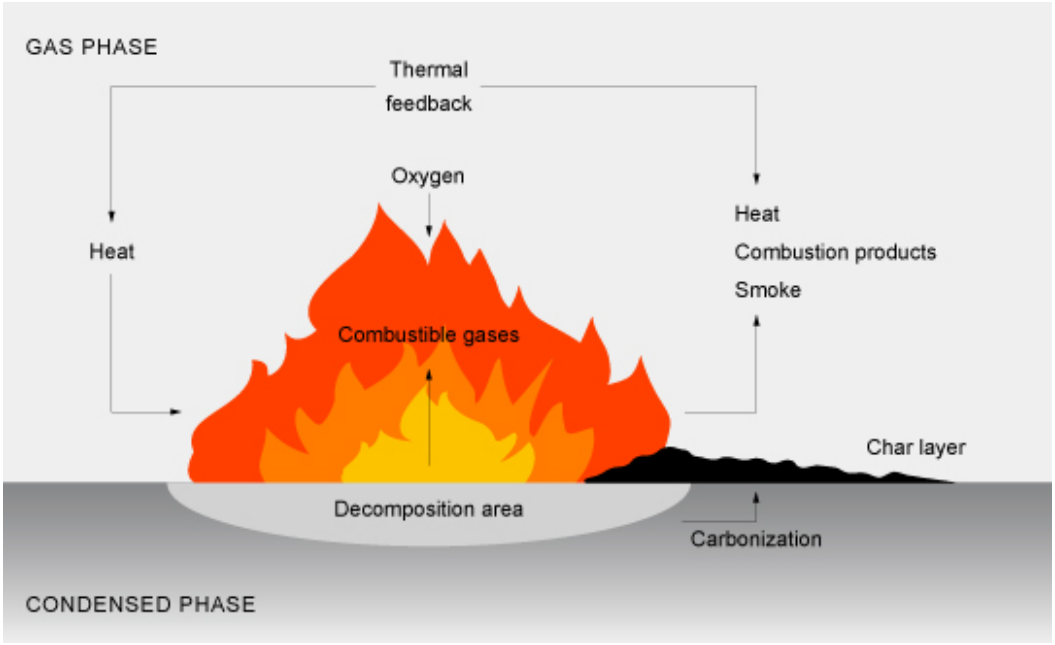

Figure 2.51: Schematical presentation of the combustion cycle, adapted from [129]. Reduction of material, heat or oxygen transport interrupts the cycle.

It has to be noted that the efficiency of flame retardants depends not only on the flame retardant itself, but also on its interactions with the protected polymeric material and employed additives. Therefore, an individual selection of polymer and flame retardant has to be made to reach good flame retardant properties and good mechanical properties at the same time.

2.4.1 Flame Retardants and their Mechanisms of Action

Flame retardants are used for inhibition, ideally to avoid ignition, flame spread and/or fire load. There is a differentiation between different physical and chemical modes of action, wherein a clear distinction between the two effects is not always possible.[130]

Physical Mechanisms:

- Release of water causes a cooling of the flame.
- Endothermic release of non-combustible gases such as H_2O, CO_2 or NH_3 causes a fuel dilution.
- Increase of the enthalpy of vaporization and reduction of the effective heat of combustion.

- Formation of a protective layer shields the combustible condensed phase from the gas phase (reducing of heat input into the material and/or obstruction of the mass transport of the pyrolysis gases from the condensed phase to the gas phase).
- Replacement of combustable material by non-combustable materials (inert fillers) and formation of a diluent.

Chemical Mechanisms:

- Interruption of the radical mechanism by endothermic reactions, whereby the heat of the flame and the heat release are reduced.
- Char layer formation at the interface of condensed and gas phase, thereby reducing of the amount of available combustable materials.

A flame retardant often acts in several ways, and the manner of operation is often depending on the polymer to be protected.
Presently, halogenated and more particularly brominated materials are mainly used as flame retardants due to their good performance. In recents years, an increasing concern about the persistence in the environment and potential negative health effects of these materials has led to the banning of a varity of halogenated flame retardants. This encouraged the flame retardant community to develop environmentally friendlier alternatives which meet the new regulations. In previous studies, organo phosphorus compounds showed high flame retardancy, due to a broad action spectrum.[5, 6] The advantage of phosphorus components as flame retardants is their feasibility to act on the one hand in the condensed phase by enhancing the formation of protecting layers, which act as barrier to inhibit release of volatile gases and shield the polymer surface from heat and oxygen. Types of protecting layers are denoted by charring (carbonaceous layer) [7, 8], by intumescence (porous foamed layer, usually carbonaceous) [131, 132] and inorganic glass formation (glassy inorganic layer).[133] On the other hand, phosphorylated flame retardants can also act in the gas phase through flame inhibition via the release of PO_x radicals.[7, 134]

Until now, most of the flame retardants are incorporated into the polymer as additives to achieve the protection of organic material. Nevertheless, drawbacks of the additive method are the often poor compatibility, leaching and the reduction of mechanical properties at higher flame retardant content. Especially the emission of potential environmentally harmful substances from the polymer as a function of time has to be solved. By direct synthesis of phosphorylated polymers, e.g. phosphorylated polyols, or by binding organophosphorus compounds covalently

to a functionalized polymer backbone, e.g. via a polymeric analogous reaction, polymeric flame retardants can be synthesized, with the advantage that no emission or solvent leaching of flame retardant from the protected polymer over time can occur. In addition, attempts by Wilkie with nanocomposites and fillers as flame retardants have shown that significantly lower levels of flame retardant ($\approx$ 3 %) are needed to cause a remarkable increase in flame retardancy, if the flame retardant is distributed homogeneously within the polymer. Up to 60 % can be necessary if the flame retardant is not homogeneously distributed.[10] The direct synthesized flame retardant polymers and covalently bound flame retardants are prevented from forming a seperate phase within the protected polymer matrix. Using controlled/living polymerization techniques as described in Chapter 2.1.2. and Chapter 2.1.3., polymers with individual amounts of flame retardant groups can be synthesized in which the covalently bound phosphorus compounds are homogeneously distributed within the synthesized polymers. The polymeric flame retardants can be further incorporated into the polymer to be protected via an additive or reactive approach. In the reactive approach, individually adjustable end group functionalities of the polymeric flame retardant can react with the polymer to be protected, e.g. via a urethane linkage. In addition to the associated cost issues, migration and higher flame retardant ratio in the additive approach using low molecular components can lead to the alteration of the properties of the material by changing the mechanical properties. Especially for highly strained construction materials (e.g. polyamides) these issues can constitute a major drawback. The higher production cost of reactive flame retardants can be compensated by the lower ratio of required flame retardant. However, covalent binding of flame retardant groups to polymers can bring the problem with it that modifications of commercially well-established methods for manufacturing unfunctionalized polymers are required to prepare the necessary functionalized polymers. Thus, it is important to realize that every application demands a different formulation of polymer/flame retardant (different polymer backbones, varying flame retardant ratio or even composition of different flame retardants). The next paragraphs will give a brief overview of the four main classes of flame retardants, their flame retardant mechanism, advantages and disadvantages in comparision to phosphorus flame retardants.

1. Mineralic Flame Retardants

The most common mineral flame retardants are metal hydrates and hydroxides such as aluminum trihydrate ($Al_2O_3 \cdot 3\ H_2O$) and magnesium hydroxide ($Mg(OH)_2$). They are relatively inexpensive and environmentally friendly.[135] During a fire, they de-

compose to metal oxide and water in a highly endothermic reaction. The drop in energy leads to the interruption of the decomposition cycle, and thus invalidate the flame. Moreover, the water formed during decomposition evaporates, which also contributes to cooling and dilution of the flammable gases.[136] They are used, for example, in polyvinylchloride (PVC), polypropylene (PP), polyamide (PA), yet also in thermosets, such as epoxy resins and polyacrylates.[135] Because of their relatively low flame retardant efficiency, very high loading rates (30-60%) are required, which negatively affect the physical properties of the treated polymers.

2. Halogenated Flame Retardants

Halogenated compounds, such as tetrabromobisphenol-A (TBBA), decabromodiphenylether (Deca-BDE) as well as hexabromocyclododecane (HBCDD), shown in Figure 2.52, in combination with mineral synergists are usually the most effective

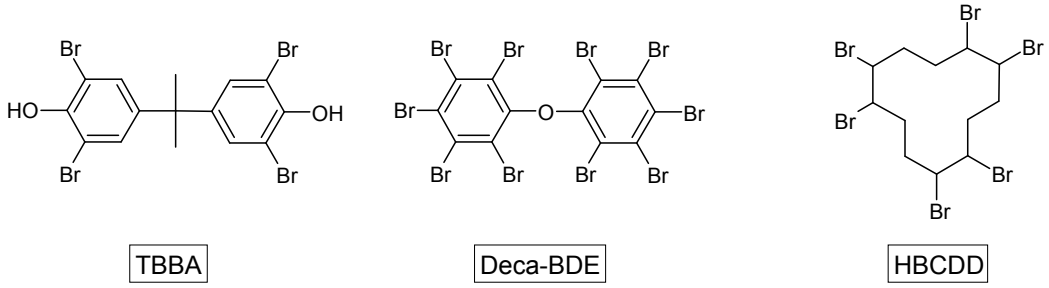

Figure 2.52: Chemical structures of the industrial mainly used brominated flame retardants TBBA, Deca-BDE and HBCDD.

flame retardants. The halogenated flame retardants act mainly in the gas phase via the release of hydrogen halides.[137] Halogen radicals disrupt the radical chain mechanism by replacement of highly reactive $H^{\bullet}$ and $OH^{\bullet}$ radicals by the less reactive halogen radicals, whereby the combustion rate decreases. This process is known as flame poisoning and can be described by the following elemental reactions:

1. Release of halogen radicals
    1. R-X $\rightarrow$ $R^{\bullet}$ + $X^{\bullet}$
2. Formation of hydrogen halide
    1. R-H + $X^{\bullet}$ $\rightarrow$ $R^{\bullet}$ + H-X
3. Binding of oxygen radicalsvia intermediates (endotherm)
    1. $X^{\bullet}$ + $^{\bullet}$O-$O^{\bullet}$ $\rightarrow$ X-$O^{\bullet}$ + $^{\bullet}O^{\bullet}$
    2. $X^{\bullet}$ + $^{\bullet}O^{\bullet}$ $\rightarrow$ X-$O^{\bullet}$

3. H-X + $^{\bullet}O^{\bullet}$ → X$^{\bullet}$ + OH$^{\bullet}$
4. H-X + X-O$^{\bullet}$ → 2 X$^{\bullet}$ + OH$^{\bullet}$

4. Neutralization and recombination
   1. H-X + OH$^{\bullet}$ → H_2O + X$^{\bullet}$
   2. R$^{\bullet}$ + OH$^{\bullet}$ → R-OH
   3. 2 R$^{\bullet}$ → R-R

R-X correspond to the halogenated flame retardant and R-H to the polymer. According to the literature [9], reaction 2 is twice as fast as reaction 3, and thus the deciding factor of the radical mechanism. However, all reaction rates decrease sharply with increasing temperature [138], which is the reason that halogenated flame retardants at high temperatures have lower efficiency. In addition, due to environmental and health concerns, some halogenated flame retardants are already banned or will be banned in the next years. Nevertheless, to date halogenated flame retardants still constitute the largest proportion of flame retardants, because they can be used in thermoplastics, elastomers and thermosets.[135]

3. Nitrogenated Flame Retardants

The most commonly used nitrogen-containing flame retardants are melamine and its derivatives and homologues (Figure 2.53). For example, melamine sublimes at a temperature of about 200 °C from the material into the gas phase, where it decomposes.[129] The release of molecular nitrogen and NH_3 has a dilution effect of the combustible gases. In addition, sublimation and decomposition processes are endothermic, through which combustion energy is withdrawn. Under thermal stress, melamine and its derivatives also form non-flammable network structures, favoring charring, as shown in Figure 2.51. Nitrogenated flame retardants are mainly used for flexible polyurethane foams and polyamide-6 as well as polyamide-66.[135]

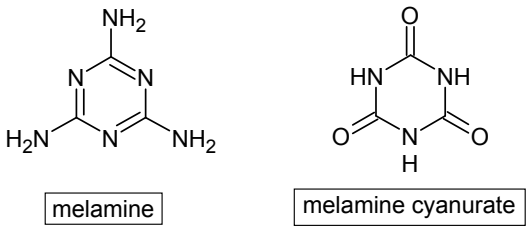

Figure 2.53: Chemical structures of melamine and melamine cyanurate used as nitrogenated flame retardants.

4. Phosphorylated Flame Retardants

The range of phosphorus-containing flame retardants is extremely wide and the materials versatile, since phosphorus exists in several oxidation states (eg. phosphonates, phosphites, phosphates and elemental red phosphorus). This characteristic of phosphorus allows for a wide range of applications in flame retardancy.[139] In addition, non-halogenated organic phosphorus flame retardants were found to have an environmentally friendlier profile compared to halogenated ones.[135] Up till now mostly P(V)-compounds such as 9,10-Dihydro-9-oxa-10-phosphaphenanthrene-10-oxide (DOPO) and derivatives thereof are used next to red phosphorus (Figure 2.54). Phosphorylated flame retardants have the advantage to act either in the

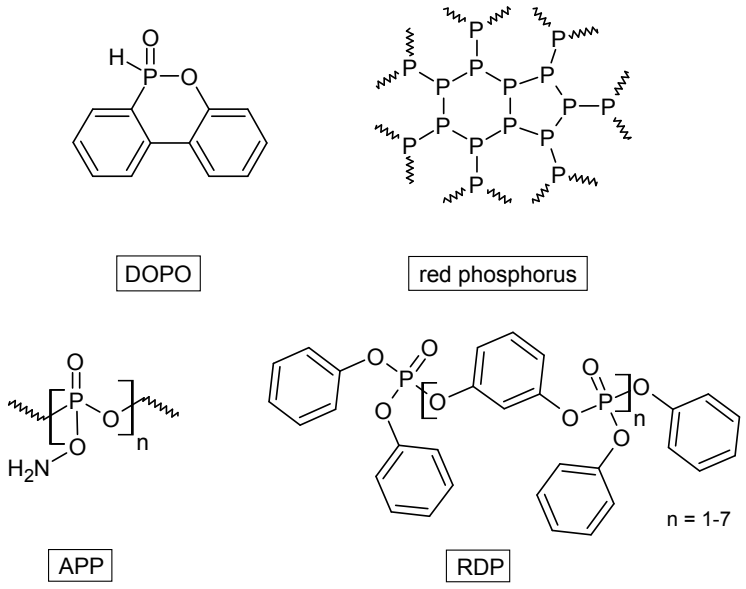

Figure 2.54: Chemical structures of the mainly used phosphorylated flame retardants 9,10-Dihydro-9-oxa-10-phosphaphenanthrene-10-oxide (DOPO), red phosphorus, ammonium polyphosphate (APP) and resorciol bis(diphenylphosphate) (RDP).

condensed or the gas phase or even in both phases.[140] Therefore, it is impossible to describe one single flame retardancy mechanism for phosphorylated flame retardants. In general, both inorganic and organic phosphorus compounds demonstrated good flame retardant efficiency in previous attempts.[141, 142] Previous experiments showed that inorganic phosphorus compounds (e.g. ammonium salts of phosphoric acid oligomers) can be used in intumescent systems [143] and organophosphorus compounds added to a material lead in most cases to an increase in carbonization (char formation) during a fire.[144, 145, 146] The flame retardancy effect caused by carbonization takes place in the condensed phase, which can be seperated in two

processes of charring. Firstly, organophosphorus compounds alter the reaction process during decomposition in the direction of the preferred formation of hydrocarbon structures compared to noxious CO or CO_2. Secondly, they favor the formation of a less flammable carbonaceous protective layer on the surface of the material, formed by a polymeric form of phosphoric acid (polypyrophosphates) through decomposition of the phosphorus compound into water vapor and phosphorus oxides in the presence of heat and oxygen. The phosphorus oxides subsequently react with the polymer matrix and dehydrate it, reforming phosphoric acids, which can further decompose and dehydrate the polymer among the formation of a carbonization layer. The underlying material is protected from oxygen, whereby a further decomposition into flammable gases is prevented. In addition, reactions in the gas phase can be observed. This gas-phase mechanism is comparable to the halogen-containing gas-phase mechanism. During the combustion of phosphorus-containing compounds mainly low molecular radical fragments, such as $P_2^\bullet$, $PO^\bullet$ and $PO_2^\bullet$ are formed.[147] These volatile radical phosphorus fragments can interrupt the radical combustion process by trapping the essential radicals for the combustion ($OH^\bullet$ and $H^\bullet$). Since $PO^\bullet$ radicals are the main fragment evolving during decomposition, the radical mechanism is shown for $PO^\bullet$:

1. $PO^\bullet + H^\bullet \rightarrow HPO$
2. $HPO + H^\bullet \rightarrow H_2 + PO^\bullet$
3. $HPO + OH^\bullet \rightarrow H_2O + PO^\bullet$
4. $PO^\bullet + R\text{-}H \rightarrow R^\bullet + HPO$

Especially oxygen-rich polymers, such as polyurethanes and polyesters, form phosphorus-containing acids by pyrolysis, resulting in the formation of char layers. In olefins, phosphorus-containing flame retardants have thus a poor efficiency, since only the atmospheric oxygen as the oxygen source is available. However, aromatic polymers without oxygen in the polymer matrix, e.g. polyphenylenes, have lower flammabilities than aliphatic polymers. The higher thermal stability of aromatic structures gives rise to greater degree of condensation into aromatic char, leading to lower levels of volatile gase which can maintain the fire. Phenyl-containing polymers, such as styrene, are therefore suitable as polymer backbones for the linkage of flame retardant groups. Due to this fact, polystyrene is used as polymer in the current work for the ligation of phosphoric esters.

Finally it can be said that phosphorus-containing flame retardants exhibit high potential to protect different kinds of polymers, even though the exact mechanistic mode of action is not yet fully known. The predominance of one over the other flame retardancy mechanism depends on the structural features of the polymers as

well as the chemical environment of the phosphorus (valency and nature of chemical surroundings). Nevertheless, the predominant mode of action of phosphorus flame retardants in thermosets and thermoplastics is considered to be in the condensed phase.[148] Most organic phosphorylated flame retardants are converted to phosphoric acid compounds, which further condense with each other, leading to pyrophosphates (char layer) and in addition the release of water vapor. By homogeneous distribution of char forming flame retardants within the polymer, only a few percent of such flame retardants are necessary in order to form a char layer.[149] Once the layer is formed, there is no need for higher flame retardant ratios.

An overview of the characteristics of the various types of flame retardants is shown in Table 2.1.

	mineralic FR	**halogenated FR**	**nitrogenated FR**	**phosphorylated FR**
site of action	condensed/ gaseous phase	gaseous phase	condensed/ gaseous phase	condensed/ gaseous phase
mode of action	physically	chemical	chemical/ physically	chemical/ physically
efficiency	-	+	+	+
polymer compatibility	0	+	0	0
fire side effects	+	-	+	+
price / performance	0	0	0	0

Table 2.1: Performance comparison of the flame retardants. [129]
- = negativ; 0 = neutral; + = positiv

Some of the described flame retardants can be combined with each other and thereby lead to synergistic effects. For example, nitrogen-containing flame retardants can also act synergistically with mineral- and phosphorus-containing flame retardants.[150, 151] A flame retardant which combines phosphorus and nitrogen is ammonium polyphosphate (APP), which is shown in the right hand structure of Figure 2.54. In addition, there are also combinations with compounds, which do not exhibit any flame retardant effect when using alone. An example of such a synergistic effect, is antimony trioxide combined with halogens, particularly chlorine and bromine.[152] Antimony trioxide is almost totally ineffective if used without halogen. Synergism may occur through the reaction: Sb_2O_3 + 6 HBr $\rightarrow$2 $SbBr_3$ + 3 H_2O Antimony tribromide ($SbBr_3$) forms a white smoke that smother the flame. Water formed in the decomposition reaction causes a decrease in temperature.

As can be seen in Table 2.1, phosphorus-containing flame retardants exhibit good flame retardancy behavior. Theoretically, chemical tailoring of the phosphorus derivatives can favor one flame retardant mechanism (e.g. charring, release of radicals) over the other. However, reports on the chemical tailoring of phosphorus derivatives for specific flame retardant mechanisms remain rare. Previous investigations have shown that a combination of nitrogen and phosphorus-containing compounds enhance dehydration of the polymer and also charring, which may result in an increased flame retardancy. The mechanism is not yet fully understood, yet it is believed that intermediates occur including P-N bonds.[150]
Based on the above, in the current work the influence on the thermal behavior of phosphorylated polymers with phosphorus esters directly or via a nitrogen-containing linkage bound to various polymers was examined.

2.4.2 Flame Retardancy Measurements

There exist a number of different methods for examining and testing of flame retardant materials and components, which differ in their methodology and dimensions. In general, eluciation of the molecular mechanism of decompostion can be carried out by thermal analysis, e.g. TGA/DSC or evolved gas analysis (EGA). These methods are used to gain a deeper insight into the chemical composition and fragmentation of the flame retardants. Typical flame retardancy tests to determine the flame retardancy behavior are e.g. the minimum oxygen concentration to maintain a fire (LOI), the burning rate after inflammation (UL94) or studies of fire behavior (Cone Calorimeter) which are performed in gram to kilogram scale. In general, it is difficult to characterize a material with respect to fire according to the current standards if either only small amounts of material or material with a geometry unusual for the targeted application is available.
The general principles of the three mentioned flame retardant test set-ups are described shortly: The UL94 test is a common test for flame retardancy, which measures the ease of ignition. In this test the sample is exposed to a calibrated Bunsen burner flame for 10 s and the time for self-extinguishing is determined. The fire behavior is rated by the classification V0, V1 and V2 (*ISO* 1210). A V2 material requires the lowest demands. Here an extinction by burning drops is allowed. Materials with this classification are not declared as flame-protected. A material is considered non-flammable once it is classified as V0, what requires a self-extinguishing within 10 s without the formation of burning drops. The limiting oxygen index (LOI) test determines the minimum concentration of oxygen in a nitrogen–oxygen mixture that will sustain combustion for 180 s after ignition of a test specimen (*ISO* 4589-2). The

LOI test is simple and reproducible and can be used to guide development work. Conclusions about flame retardancy of a material in an actual fire can not be made unrestricted based on results from the LOI nor UL94. Nevertheless, flame retardant potentials in various materials can be investigated. Every flame retardant has to be evaluate in a larger scale, to determine the real flame retardancy behavior, for example using the cone calorimeter test. The cone calorimeter test measures the heat release and is the most important research tool for fire testing in the pilot scale (*ISO* 5660). The cone calorimeter test simulates the phase of flame spread of a real fire progression. Thereby, a constant radiant heat effect of up to 100 kW $\cdot$ m^{-2} acts on the sample. The heat release rate of the sample material is determined by the oxygen consumption method. It describes the proportional relationship between heat energy released and the amount of oxygen consumed. Regardless of the material examined approximately 13.1 MJ thermal energy per kg of oxygen (Huggett constant) are released.[153] This value allows the determination of the fire load and the flame spread of the examined material. Also fire by-products, such as the release of smoke and CO production can be determined by using the cone calorimeter.
In the current work, the phosphorylated polymers were analyzed via TGA/DSC and EGA. In addition, thermogravimetric measurements in combination with mass spectroscopy (TG-MS) were used to determine the decomposition fragments evolving from the phosphorylated polymers at higher temperatures.
Due to the fact that the experiments were conducted on a laboratory scale and the resulting limited sample volumes, the use of the cone calorimeter test was waived. Since the UL94 test only gives general statements about whether a full flame retardancy is reached or not, the UL94 test was not used in the context of the current work. In the LOI measurements, test specimens in the range of 70-150 x 6-10 x 3 mm (L x W x H) required by the *ISO* 4589-2 norm are utilize. The specimens are analyzed in a test assembly like it is shown in Figure 2.55.

Materials with a high LOI value are considered as less flammable. Materials with LOI under 21 %, which is equal to the concentration of oxygen in air, are considered as flammable. On the other hand, materials with LOI over 26% are considered as self-extinguishing. The LOI value is calculated using the following equation:

$$LOI = \frac{[O_2]}{[O_2] + [N_2]} \tag{2.6}$$

Therefore, the LOI test gives a precise specification of the influence of the flame retardant and was therefore used to elucidate the flame retardancy potential of the prepared phosphorylated polymers. In the current work, the incorporation of phos-

phorylated polymers into various polymer systems (e.g. polystyrene, polyurethanes) via different approaches (e.g. extrusion, incorporation during polymerization) was performed to measure the flame retardancy behavior as a function of the polymer system (Chapter 5).

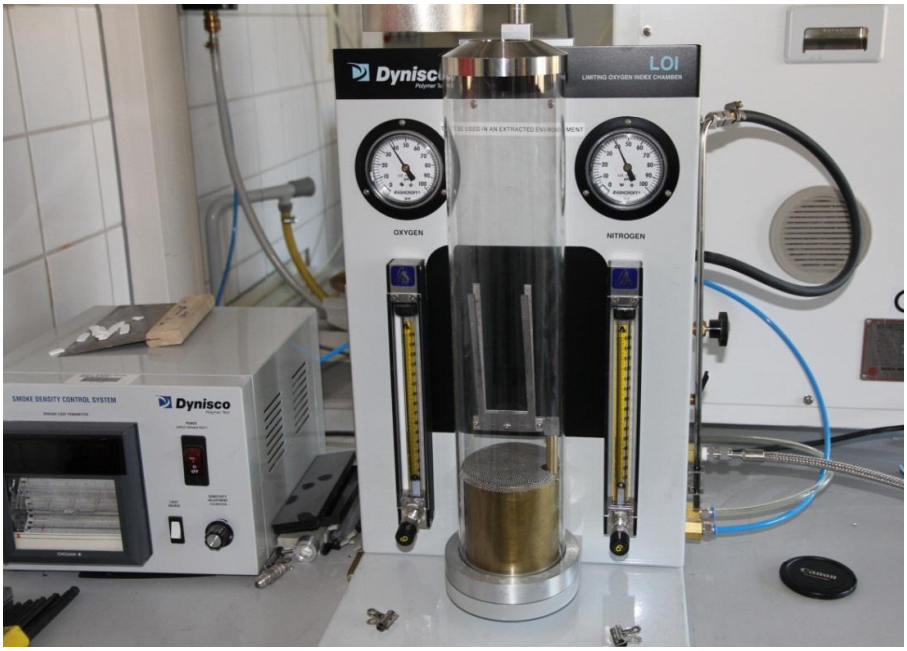

Figure 2.55: Test set-up for the determination of the limiting oxygen index (LOI).

Chapter 3

Phosphorylated Polymers via RAFT Polymerization and Modular Conjugation[1]

The current chapter describes a novel approach for the synthesis of phosphorus-containing polymers via the conjugation of phosphorus components to functional groups in the side chains of precisely designed copolymers via the copper-catalyzed 1,3-dipolar cycloaddition by Huisgen - one of the so-called modular conjugation reactions carrying *"click"* characteristics. An overal reaction scheme of the synthesis is shown in Figure 3.1.

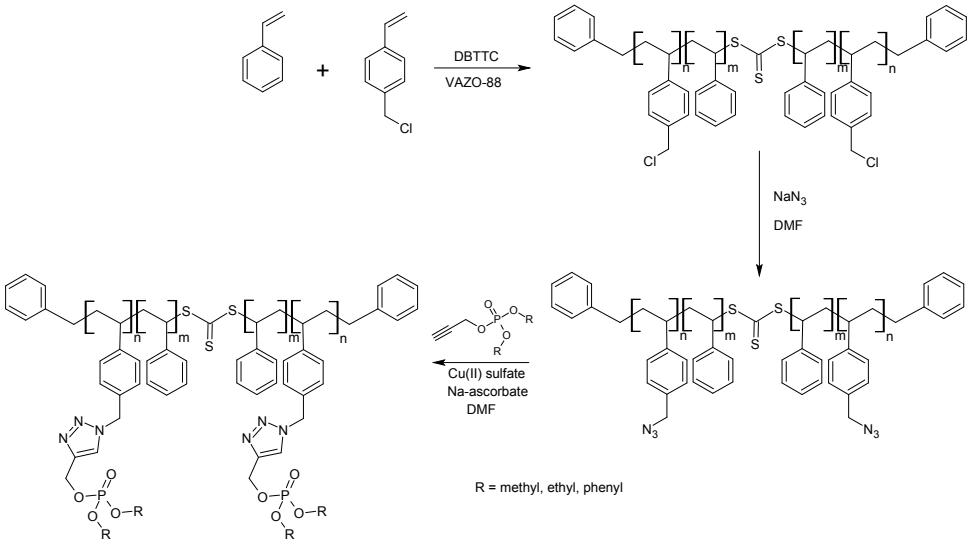

Figure 3.1: Reaction scheme for the synthesis of phosphorylated copolymers.

[1]Adapted with permission from J. Eisenblaetter, M. Bruns, U. Fehrenbacher, L. Barner, C. Barner-Kowollik; Polymer Chemistry; 4:2406; 2013; Copyright 2013 American Chemical Society

In order to obtain well-defined materials, the generated polymers have to exhibit narrow polydispersities and functional groups in their side chains. Controlled/living polymerization techniques such as the reversible addition-fragmentation chain transfer (RAFT) polymerization provide access to excellent control over molecular weight of the polymers while being tolerant to a wide range of functional groups.[11, 12] Therefore, it is possible to prepare well-defined polymers containing functional groups in the side chains that can subsequently be modified to functional groups (e.g. azides) which subsequently are employed as modular ligation points. Thereupon, functional compounds such as alkyne units bearing phosphoric esters can be integrated into these polymers via covalent linkages to the side chains of the polymer.
The synthesis of copolymers with variable concentration of functional groups opens the possibility to tailor the proportion of the phosphorus component within the polymer. Moreover, it is possible to simultaneously conjugate a range of phosphoric esters to one polymer and therefore fine tune the properties of the generated polymers. With the ability to not only connect various phosphoric esters in general, but also to bind them in variable concentrations, it is possible to investigate both the influence of the type as well as the concentration of the phosphoric ester on the thermal behavior of the synthesized polymers.
In the following chapter the various synthetic strategies for preparing *clickable* phosphoric esters (Section 3.1) as well as the corresponding *clickable* polymer systems (Section 3.2) are described. In Section 3.3, the ligation of the previously synthesized phosphoric esters to the prepared *clickable* polymer systems via copper-catalyzed 1,3-dipolar cycloaddition and their effects on the thermal behavior of these polymers are investigated. Parts of this chapter were reproduced from [154] by permission of the Royal Society of Chemistry.

3.1 Synthesis of Alkyne Phosphoric Esters as *Clickable* Synthon

Chlorophosphates (Figure 3.2) are, in addition to P(III) compounds, the most common phosphorylation reagents.[155] Thus, different attemps have been made using chlorophosphates as starting material for the synthesis of alkyne phosphoric esters.

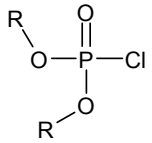

Figure 3.2: General structure of chlorophosphates.

Initially, attempts were made to synthesize alkyne phosphoric esters via various multi-step syntheses employing phosphorus trichloride as starting material. In the first step, chloromethylphosphonic dichloride **(1)** was synthesized from phosphorus trichloride (PCl_3), aluminum chloride ($AlCl_3$) and dichloromethane (CH_2Cl_2) via a Kinnear-Perren reaction.[87] The reaction is shown in Figure 3.3.

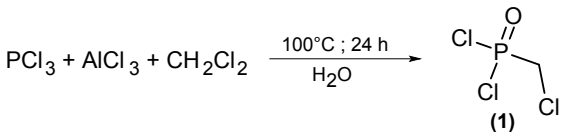

Figure 3.3: Reaction scheme of the chloromethylphosphonic dichloride **(1)** synthesis.

Equimolar concentrations of PCl_3, $AlCl_3$ and CH_2Cl_2 were placed in a high pressure tube and the mixture was heated for 24 h at 100 °C. Towards the end of the reaction time, the reaction mixture consisted of a colorless fluffy solid and a yellowish liquid. Subsequently, the mixture was diluted with dichloromethane and cooled to -20 °C by an isopropanol/N_2 bath. Under prolonged cooling and stirring with a mechanical stirrer, water was slowly added. When the water was added, the temperature increased and a white solid precipitated. The precipitate was seperated from the supernatant solution in the cold. After evaporation of CH_2Cl_2 in vacuo, the product was obtained as an almost colorless liquid in only low yields of ≤ 24 %. The synthesis of chloromethylphosphonic dichloride was evidenced by ^{1}H NMR measurements (see Figure 3.4). A clear shift of the CH_2 resonance at 5.30 ppm (-CH_2Cl_2) to

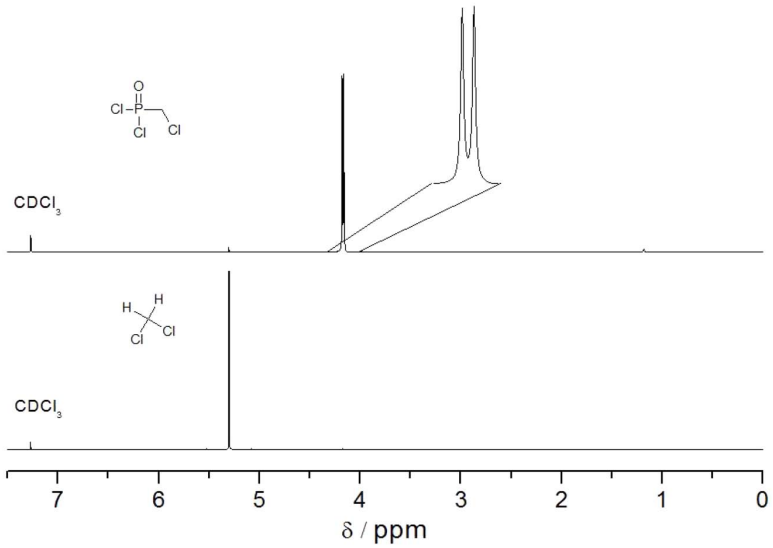

Figure 3.4: ^{1}H NMR spectra of dichloromethane (lower part) and chloromethylphosphonic dichloride **(1)** (upper part) in $CDCl_3$.

4.17 ppm (P-CH_2Cl) reveals the formation of the desired phosphonic dichloride. In addition, the CH_2 resonance is split into a doublet, which is a common phenomenon of carbon-hydrogen-groups next to phosphorus, due to the spin - $^1/_2$ nucleus of the phosphorus and the proton. Therefore, the H-P coupling behavior is analogous to H-H coupling.[156]

The low yields are due to side reactions, which can occur at higher temperatures. The addition of water leads to a strong local temperature increase. The effect is intensified by the synthesis on a laboratory scale, since the proportion of added water in form of a drop is relatively high in relation to the reaction solution. Due to the temperature increase, the very reactive intermediate might anneal two oxygens instead of one leading to the formation of the linear or even cyclic anhydride of the chloromethylphosphate (Figure 3.5), also known as pyrophosphate.

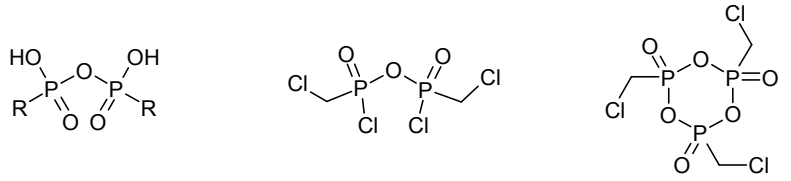

Figure 3.5: Structures of a phosphonic anhydride (left), a possible linear anhydride (middle) and a cyclic anhydride (right) originated from the described reaction.

In addition, the amount of water used for the final formation of the phosphonic dichloride can be a problem. It is absolutely necessary that at least one equimolar amount of water is used to obtain high yields. Excess amounts of water in the work up lead to increasing yields without an increased formation of by-products. Nevertheless, a careful assessment with regard to the water sensitivity of the final product has to be made. During evaporation, an exess of water can lead to side products due to the necessarily higher temperature to remove the water. Finally, by very slow addition of a slight excess of water to a vigorously stirred reaction solution, very pure phosphonic dichlorides were obtained in yields of up to 39 %.
In the second step, esterification of the dichloride was carried out via the reaction shown in Figure 3.6. The dichloride was dissolved in THF under initially slight cool-

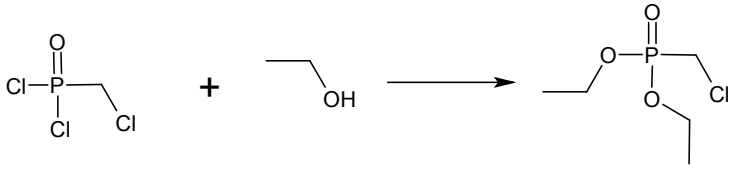

Figure 3.6: Reaction scheme of the synthesis of chloromethylphosphonic diester.

ing with an ice bath. However, it appears that cooling to at least -15 °C using an isopropanol/N_2 bath is necessary to obtain a pure product. To the cold solution, 2.1 equivalents of triethylamine were added dropwise, whereby the mixture turned slightly yellowish. Subsequently 2.1 equivalents of methanol, respectively, ethanol were added to the mixture in a dropwise fashion. At this point it must be ensured that the temperature remains $<$ 10 °C. The mixture was stirred for an additional 30 min at this temperature and then further stirred for 1 h at ambient temperature. The precipitated solid was filtered off. By mixing the filtrate with diethyl ether, a white solid precipitated again and was filtered. The filtrate was washed several times with saturated NH_4Cl solution and finally extracted 3 times with water. The organic phase was dried over Na_2SO_4 and the excess of diethyl ether was removed under vacuum. As a result, a slightly yellowish oil was obtained in 68 % (chloromethylphosphonic dimethylester **(2)**) respectively 74 % (chloromethylphosphonic diethylester **(3)**) yield. Figure 3.7 shows a comparative ^{1}H NMR spectrum

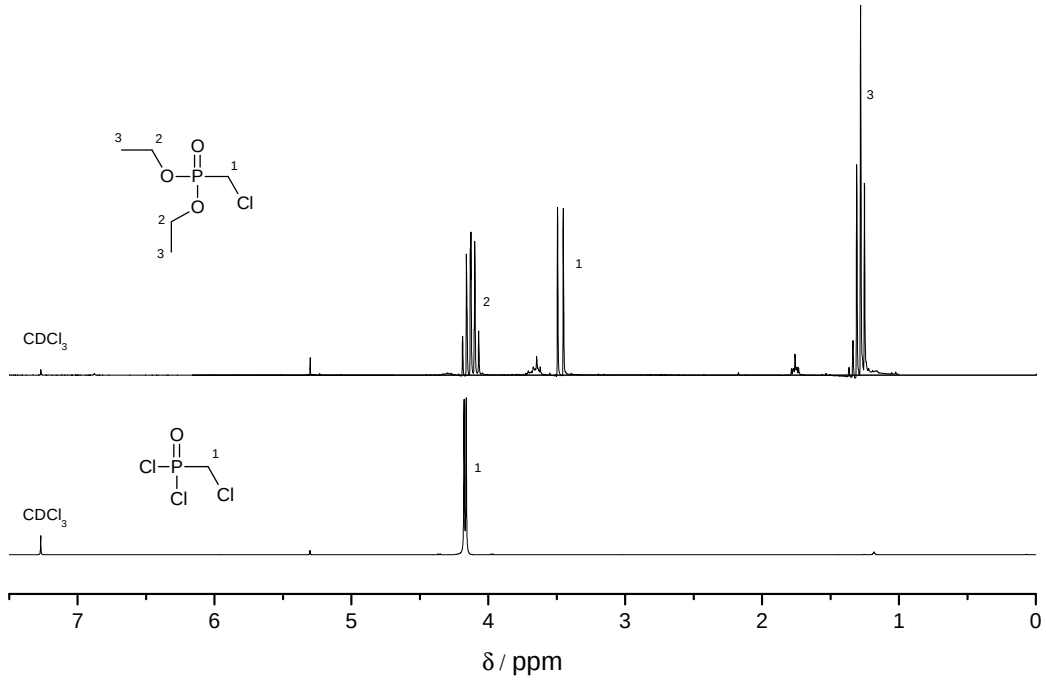

Figure 3.7: ^{1}H NMR spectra of chloromethylphosphonic dichloride **(1)** (lower part) and corresponding diethylester **(3)** (upper part) in $CDCl_3$. The resonances are assigned to the respective structure. **chloromethylphosphonic dichloride**: 4.17 ppm (d, 2H, CH_2 = proton 1) = 2,00; **chloromethylphosphonic diethylester**: 4.19 - 4.07 ppm (m, 4H, CH_2 = proton 2) = 3.98; 3.47 ppm (d, 2H, CH_2 = protons 1) = 2.00; 1.28 ppm (t, 6H, CH_3 = proton 3) = 6.03.

of the chloromethylphosphonic dichloride and the corresponding diethylester **(3)**. A clear shift of the CH_2 group next to the phosphorus from 4.17 to 3.47 ppm and the appearance of a multiplet at 4.13 ppm and a triplet at 1.28 ppm evidences the conversion to the corresponding diethylester.
The diester should subsequently be converted to the alkyne functionalized phosphoric ester using propargyl alcohol. Therefore, several experiments were performed in solvents such as THF **(4a)** and polyethylene glycol (PEG-400) **(4b)** through activation of the propargyl alcohol by deprotonation using sodium hydride (NaH). Quantitative conversions were never observed. Only a maximum conversion of ≈50 % could be achieved. The preparation of alkyne compounds from chloromethylphosphonates was therefore no longer followed.

Due to the higher reactivity of a Cl-P relative to a Cl-C-P bond, chlorophosphonates with the general structure Cl-P(O)-$(OR)_2$ (see Figure 3.8) were used in the following test series, with R = methyl, ethyl or phenyl.

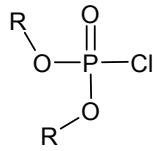

Figure 3.8: General structures of chlorophosphonates used as starting materials in the current work.

Several of these compounds are commercially available and most of them are stable to air and moisture. Due to the high reactivity of the remaining Cl-P bond, even traces of water during the reaction lead to the formation of by-products, such as pyrophosphates. Therefore, working under an inert gas atmosphere (nitrogen or argon) is essential. The main issues associated with such reagents are the conditions under which they will react. Previously, the synthesis of an alkyne synthon bearing phosphoric esters was only possible using catalysts. In previous attempts Ti(^{t}-BuO)$_4$ [157] or $MoOCl_4$ [158] were used as catalyst to synthesize alkyne phosphoric esters such as diphenyl prop-2-ynyl phosphoric ester (DPPP) **(7)**. Chemical structures of the methylated **(5)**, ethylated **(6)** and phenylated **(7)** phosphoric esters are shown in Figure 3.9.

Remaining metal salts may lead to a mixture of regioisomers in the polymer prepared via 1,3-dipolar cycloaddition, as described for ruthenium salts.[159] Moreover, undesirable side reactions at decomposition of the polymer, such as the release of

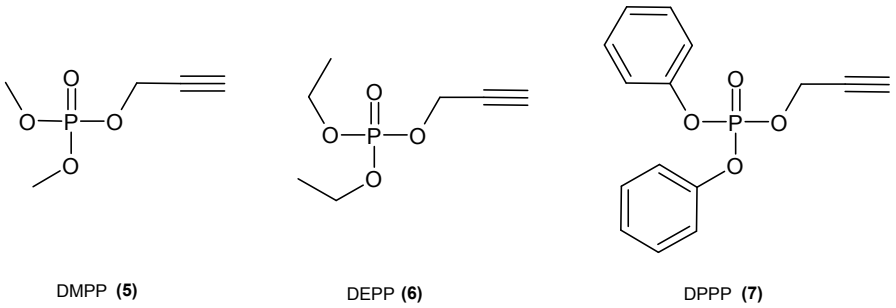

Figure 3.9: Structures of the alkyne phosphoric esters dimethyl prop-2-ynyl phosphoric ester (DMPP) **(5)**, diethyl prop-2-ynyl phosphoric ester (DEPP) **(6)** and diphenyl prop-2-ynyl phosphoric ester (DPPP) **(7)**.

potentially harmful substances from the polymeric flame retardant, can also take place. To avoid remaining titanium or molybdenum salts in the reaction mixture resulting from the 1,3-dipolar cycloaddition, a new metal-free approach had to be developed to synthesize alkyne phosphoric esters.
After several attemps, it could be shown that in contrast to the synthesis described by Jones *et al.*[157], alkyne phosphoric esters can be synthezized without using a catalyst via the pathway shown in Figure 3.10.

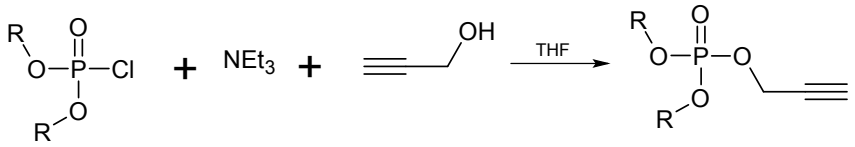

Figure 3.10: Synthetic pathway to alkyne functionalized phosphoric esters starting with dialkyl- respectively diarylchlorophosphates.

The chlorophosphate was first dissolved in THF and subsequently triethylamine and propargyl alcohol were added dropwise to the solution at low temperature. After warming to ambient temperature, the solution was stirred for at least two additional hours. Work-up consisted of filtration and washing with saturated sodium hydrogen sulphate solution. Evaporation results in a slightly yellow oil in good yields (78 % (DMPP), 83 % (DEPP), 86 % (DPPP)). The reaction to alkyne phosphoric ester was confirmed by IR/Raman measurements and NMR spectroscopy in $CDCl_3$ for DMPP **(5)** and DEPP **(6)**, respectively, DMSO-d_6 for DPPP **(7)**. One example is depicted in Figure 3.11, where the ^{1}H NMR spectra of diphenyl prop-2-ynyl phosphoric ester (DPPP) **(7)** and the corresponding chlorophosphate diphenyl phosphoryl chloride (DPPC) are compared with each other.
The NMR spectrum of DPPP **(7)** shows two additional signals at 5.08 and 3.73 ppm, evidencing the conversion of the chlorophosphate to the alkyne containing compound.

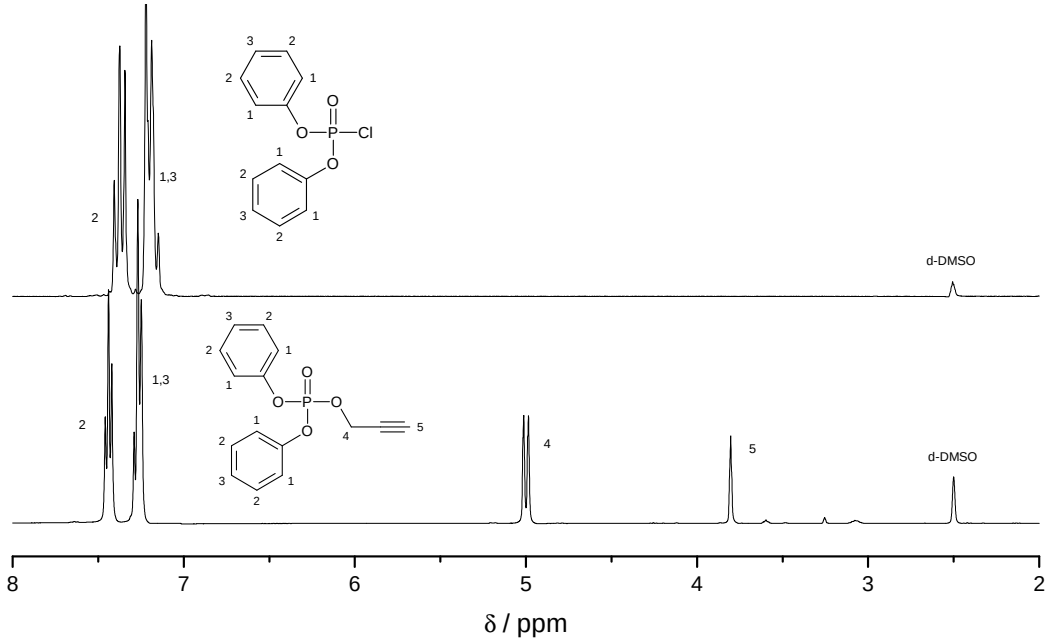

Figure 3.11: ^{1}H NMR spectra of DPPP (lower part) and the corresponding chlorophosphate DPPC (upper part) measured in DMSO-d_6. Peaks are assigned to the respective structure. **DPPC**: 7.41-7.34 ppm (m, 4H, Ph-H = proton 2) = 4,00; 7.22-7.15 ppm (m, 6H, Ph-H = protons 1+3) = 5,98; **DPPP**: 7.42-7.46 ppm (m, 4H, Ph-H = proton 2) = 3,97; 7.28-7.26 ppm (m, 6H, Ph-H = protons 1+3) = 5,97; 5.08 ppm (d, 2H, CH_2 = proton 4) = 2,00; 3.73 ppm (s, 1H, CH = proton 5) = 0,94.

The integrals for the individual peaks of DPPP (Ph-H at 7.42 - 7.46 ppm (proton 2) = 3,97 (expected 4), Ph-H at 7.28 - 7.26 ppm (protons 1+3) = 5,97 (expected 6), CH_2 at 5.08 ppm (proton 4) = 2,00 (expected 2) and CH at 3.73 ppm (proton 5) = 0,94 (expected 1)) are consistent with the expected values. Until further use, the alkyne phosphoric esters were stored in a refrigerator under argon.

3.2 Synthesis of Linear P(St-VBA) Copolymers

For the controlled/living copolymerization of 4-vinylbenzyl chloride (VBC), the RAFT polymerization process shows deciding advantages compared to the two others controlled/living radical polymerizations. Compared to NMP, the RAFT process has the major advantage of lower reaction temperatures. ATRP also suffers from the disadvantage that specifically in the case of VBC, the ATRP technique can not

be applied, because the chloromethyl group can act as an initiator.[160] Therefore, the RAFT process was employed for the controlled/living polymerization of azide functionalized styrene copolymers **(9)** starting from VBC and styrene in a two step process (Figure 3.12).

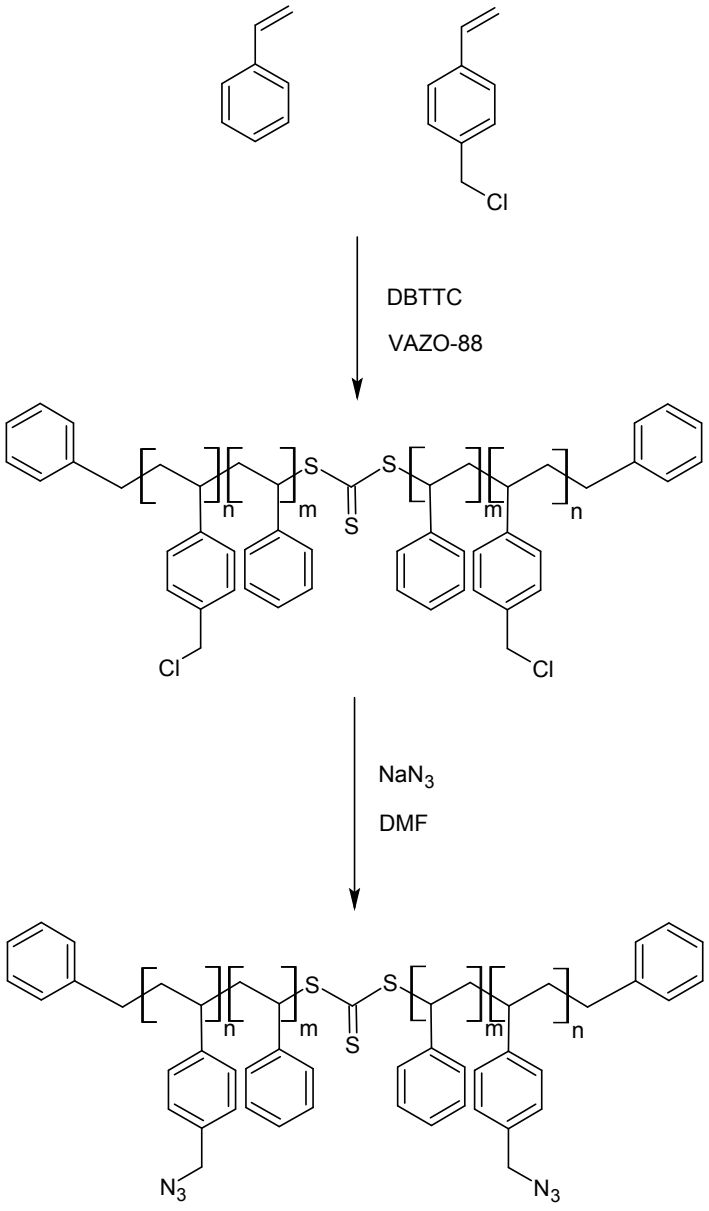

Figure 3.12: Synthesis of linear polystyrene-vinylbenzyl azide copolymers via RAFT polymerization using styrene (St), 4-vinylbenzyl chloride (VBC), dibenzyl trithiocarbonate (DBTTC) and 1,10-azobis-(cyclohexane carbonitrile) (VAZO-88) and subsequent conversion to polystyrene-vinylbenzyl azide copolymers using sodium azide (NaN_3) in dimethylformamide (DMF).

The first step involved the RAFT copolymerization of various ratios of styrene (St) and 4-vinylbenzyl chloride (VBC) in the presence of 1,10-azobis-(cyclohexane carbonitrile) (VAZO-88) as initiator and dibenzyl trithiocarbonate (DBTTC) as chain transfer agent, according to a procedure described by Lang *et al.*[161] The chemical structures of DBTTC and VAZO-88 are depicted in Figure 3.13.

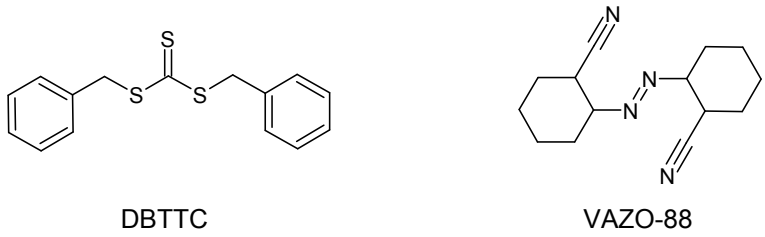

Figure 3.13: Chemical structures of dibenzyl trithiocarbonate (DBTTC) and 1,10-azobis-(cyclohexane carbonitrile) (VAZO-88)

The mixture was cooled in an ice bath and percolated with argon for 1 h. The polymerization proceeded at 80 °C for 20 h. After cooling to 0 °C, the mixture was diluted with THF and precipitated from methanol. The polymer was re-precipitated twice and finally dried in vacuo at 40 °C. Five chloride functionalized styrene copolymers **(8)** were synthesized and analyzed via ^{1}H NMR measurements and SEC (refer to Table 3.1). The ^{1}H NMR spectra of P_{Cl}.33 is shown in Figure 3.14.

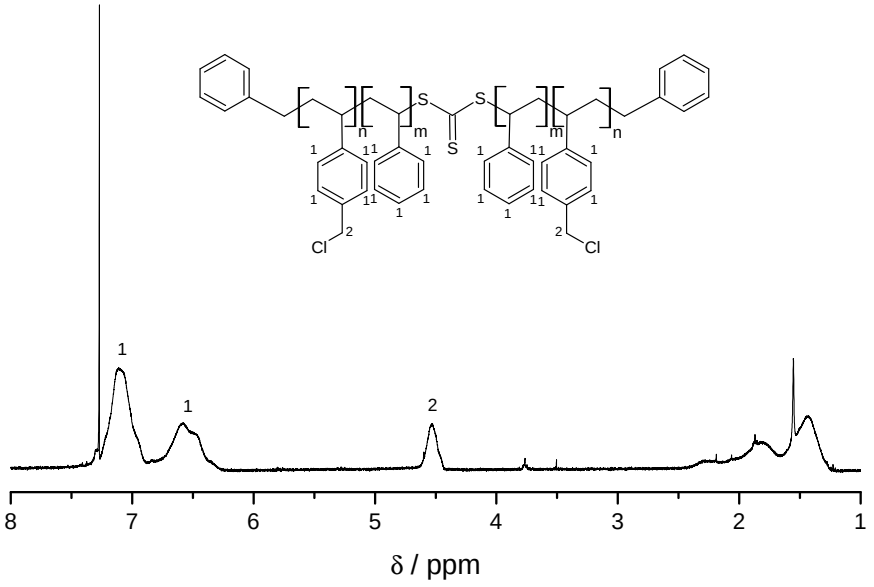

Figure 3.14: ^{1}H NMR measurement of a chloride functionalized copolymer on the example of P_{Cl}.33. The assignment of the CH_2Cl and backbone resonances are depicted within the structure.

For the calculation of the experimentally copolymer composition, the integrals of Ph-H and -CH_2Cl were correlated employing the protons for styrene with 5 Ph-H and without -CH_2Cl per monomer unit and 4-vinylbenzyl chloride with 4 Ph-H and 2 -CH_2Cl per monomer unit (Equation 3.1).

$$\frac{I(Ph-H)}{I(CH_2Cl)} = \frac{5 \cdot F_{\mathtt{m}} + 4 \cdot F_{\mathtt{n}}}{2 \cdot F_{\mathtt{n}}} \tag{3.1}$$

The sum of both fractions (styrene = $F_{\mathtt{m}}$ and VBC = $F_{\mathtt{n}}$) is set to 100 % (Equation 3.2), wherein the end groups formed by the RAFT agent were neglected in the calculation.

$$F_{\mathtt{n}} + F_{\mathtt{m}} = 1 \tag{3.2}$$

By comparison of the value of the integrated signals of the benzylic protons between ρ = 7.47 ppm and 6.24 ppm with the integration of the -CH_2Cl signal at ρ = 4.54 ppm in the respective ^{1}H NMR spectra of P_{Cl}.X, the copolymer compositions could be calculated using Equation 3.3:

$$F_{\mathtt{n}}^{exp} = \frac{5}{2\frac{I(Ph-H)}{I(CH_2Cl)} + 1} \tag{3.3}$$

The X in the sample description (e.g. P_{Cl}.X) specifies the proportion of experimentally determined VBC ratio in the copolymer rounded to whole numbers. The experimentally determined VBC ratios were in the range between 0.9 % and 73.1 % in good agreement with the theoretically expected content calculated by Equation 3.4, considering the reactivity ratios of styrene ($r_{\mathtt{m}}$ = 0.72) and VBC ($r_{\mathtt{n}}$ = 1.31) [162] and the monomer compositions ($f_{\mathtt{n}}$,$f_{\mathtt{m}}$).

$$F_{\mathtt{n}}^{theo} = \frac{r_{\mathtt{n}} \cdot f_{\mathtt{n}}^2 + f_{\mathtt{n}} \cdot f_{\mathtt{m}}}{r_{\mathtt{n}} \cdot f_{\mathtt{n}}^2 + r_{\mathtt{m}} \cdot f_{\mathtt{m}}^2 + 2 \cdot f_{\mathtt{n}} \cdot f_{\mathtt{m}}} \tag{3.4}$$

Molecular weights ($M_{\mathtt{n}}$) of the chloride functionalized copolymers **(8)** determined by SEC were in the range of 5 400 to 9 900 g $\cdot$ mol^{-1}.
In the second step, the obtained chloride functionalized copolymers **(8)** were converted with sodium azide in DMF under ambient conditions for 60 h. After precipitation from water, the azide functionalized copolymers **(9)** were re-precipitated from methanol and dried in vacuo at 40 °C. Quantitative conversion was determined by the complete disappearance of the -CH_2Cl ^{1}H NMR signal at ρ = 4.54 ppm. Instead, a signal at ρ = 4.24 ppm appears, which can be assigned to -CH_2N_3 (Figure 3.15).

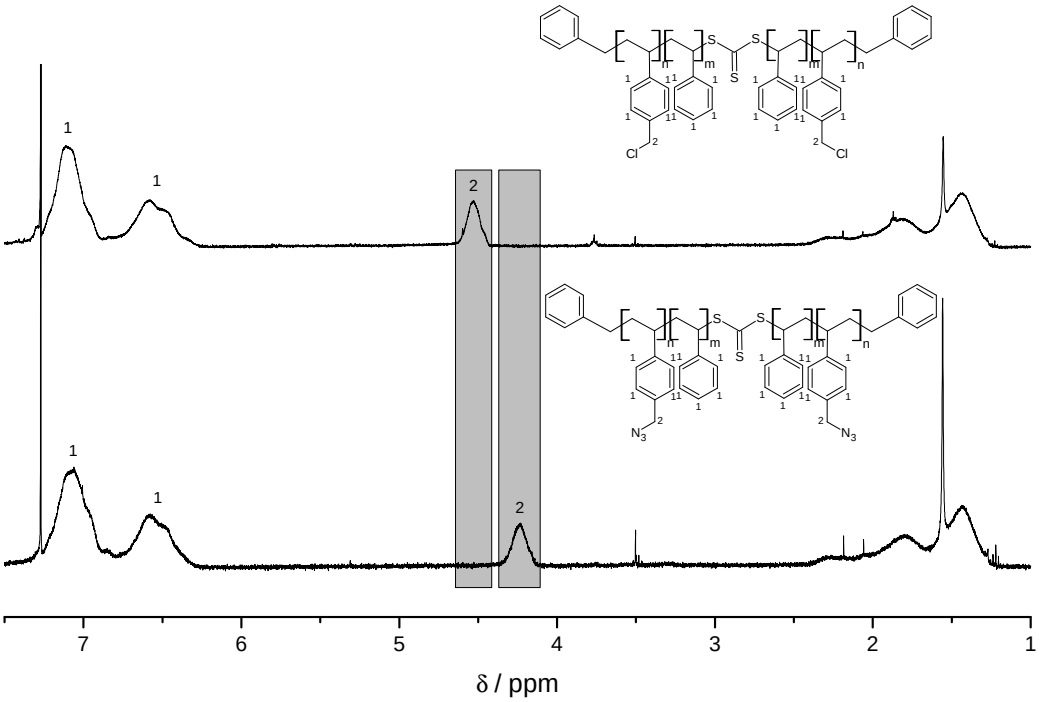

Figure 3.15: ^{1}H NMR spectra of a chloride (upper part) and azide (lower part) functionalized copolymer on the example of $P_{Cl}.33/P_{N3}.33$. The assignment of the resonances is depicted within the structures. The complete disappearance of the -CH_2Cl ^{1}H NMR signal at $\delta = 4.54$ ppm and the appearance of the signal at $\delta = 4.24$ ppm indicates full conversion to -CH_2N_3. The intensity ratios of the characteristic integrals of Ph-H and -CH_2Cl, respectively -CH_2N_3, are maintained during the reaction.

The compositions of the azide functionalized copolymers **(9)** were calculated by replacing I(CH_2Cl) by I(CH_2N_3) in Equation 3.3. The values of the azide content in the respective ^{1}H NMR spectra of P_{N3}.X are generally slightly lower than the experimentally calculated chloride contents of P_{Cl}.X ranging from 0.8 % to 71.8 % (refer to Table 3.1).

No significant change in molecular weight between the chloride **(8)** and azide **(9)** functionalized copolymers was expected since the molecular weights of the chloride and azide functionalized monomer units are similar. The molar masses of the monomers are $M = 104.15$ g $\cdot$ mol^{-1} (styrene), $M = 152.62$ g $\cdot$ mol^{-1} (VBC), $M = 159.19$ g $\cdot$ mol^{-1} (4-vinylbenzyl azide) respectively, and $M = 290.40$ g $\cdot$ mol^{-1} for the chain transfer agent. However, a general shift of the azide functionalized copolymers **(9)** to smaller molecular weights in the SEC is evidenced, which is probably due to a different hydrodynamic radius of the azide functionalized copolymers in comparison to the chloride functionalized copolymers **(8)** and polystyrene standards employed for the SEC calibration. However, as shown in Table 3.1, the

molecular weights of the obtained azide functionalized polymers P_{N3}.X **(9)** and the chloride **(8)** functionalized polymers are identical within the error range of the SEC (ca. 10 %).

Polymer	$M_n^{theo,a}$ **[g/mol]**	$M_n^{exp,b}$ **[g/mol]**	**PDI**^{b}	$F_n^{theo,c}$	$F_n^{exp,d}$	**XPS [eV]**
P_{Cl}.1	9700	9900	1.42		0.009	200.5/201.9
P_{N3}.1	9700	8900	1.57		0.009	n.d.
P_P.1-DMPP	n.d.	n.d.	n.d.	0.018	n.d.	not measured
P_P.1-DEPP	n.d.	n.d.	n.d.		n.d.	not measured
P_P.1-DPPP	n.d.	n.d.	n.d.		n.d.	134.6/400.3/402.1
P_{Cl}.7	7900	8100	1.47		0.069	200.4/201.8
P_{N3}.7	7900	7600	1.53		0.057	399.3/401.1/404.7
P_P.7-DMPP	n.d.	n.d.	n.d.	0.068	n.d.	134.5/400.5/401.9
P_P.7-DEPP	n.d.	n.d.	n.d.		n.d.	134.6/400.4/401.8
P_P.7-DPPP	n.d.	n.d.	n.d.		n.d.	134.8/400.4/402.3
P_{Cl}.24	6600	6500	1.21		0.240	200.4/201.8
P_{N3}.24	6600	6400	1.37		0.235	399.3/401.0/404.7
P_P.24-DMPP	n.d.	n.d.	n.d.	0.225	n.d.	not measured
P_P.24-DEPP	n.d.	n.d.	n.d.		n.d.	not measured
P_P.24-DPPP	n.d.	n.d.	n.d.		n.d.	134.4/400.4/402.6
P_{Cl}.33	5500	5400	1.24		0.328	200.4/201.9
P_{N3}.33	5500	5100	1.34		0.307	399.2/401.1/404.7
P_P.33-DMPP	n.d.	n.d.	n.d.	0.0313	n.d.	134.4/400.7/402.4
P_P.33-DEPP	n.d.	n.d.	n.d.		n.d.	134.5/400.4/401.7
P_P.33-DPPP	n.d.	n.d.	n.d.		n.d.	134.6/400.4/402.2
P_{Cl}.73	6600	6700	1.28		0.731	200.4/201.9
P_{N3}.73	6600	6000	1.30		0.708	399.1/401.0/404.6
P_P.73-DMPP	n.d.	n.d.	n.d.	0.712	n.d.	134.4/401.0/402.4
P_P.73-DEPP	n.d.	n.d.	n.d.		n.d.	134.5/400.4/401.8
P_P.73-DPPP	n.d.	n.d.	n.d.		n.d.	134.2/400.4/402.3

Table 3.1: Overview of theoretically and experimentally determined molecular weights, *PDI*, functionality ratio and XPS data of P_{Cl}, P_{N3} and P_P. Not detectable values are specified as "n.d.", which are due to insolubility issues. Values of additional not measured data are specified as "not measured".

During the conversion of chloride functionalized copolymers **(8)** with sodium azide a color change from bright yellow to colorless polymers occurs. Sun *et al.* proposed that the RAFT end group is transformed to a thiol end group during the azidation.[163] In the current study, a symmetrical RAFT agent (DBTTC) was used. Hence, a bisection of the molecular weight of the corresponding azide functionalized copolymers **(9)** was expected. However, SEC measurements did not support such a cleavage. Since the transformation process to the azide containing polymer is fully evidenced via NMR spectroscopy, the implementation of the above indicated azide functionalized copolymers with alkyne phosphoric esters was continued.

3.3 Modular Ligation Reactions

The azide functionalized styrene copolymers (P_{N3}.X) **(9)** dissolved in dry DMF were seperately reacted with each of the three previously prepared alkyne phosphoric esters **(5)**, **(6)**, **(7)** in a 1,3-dipolar cycloaddition (Figure 3.16) at ambient temperature using copper(II) sulfate and the reducing agent sodium ascorbate for the in-situ generation of the required reactive Cu(I) species.

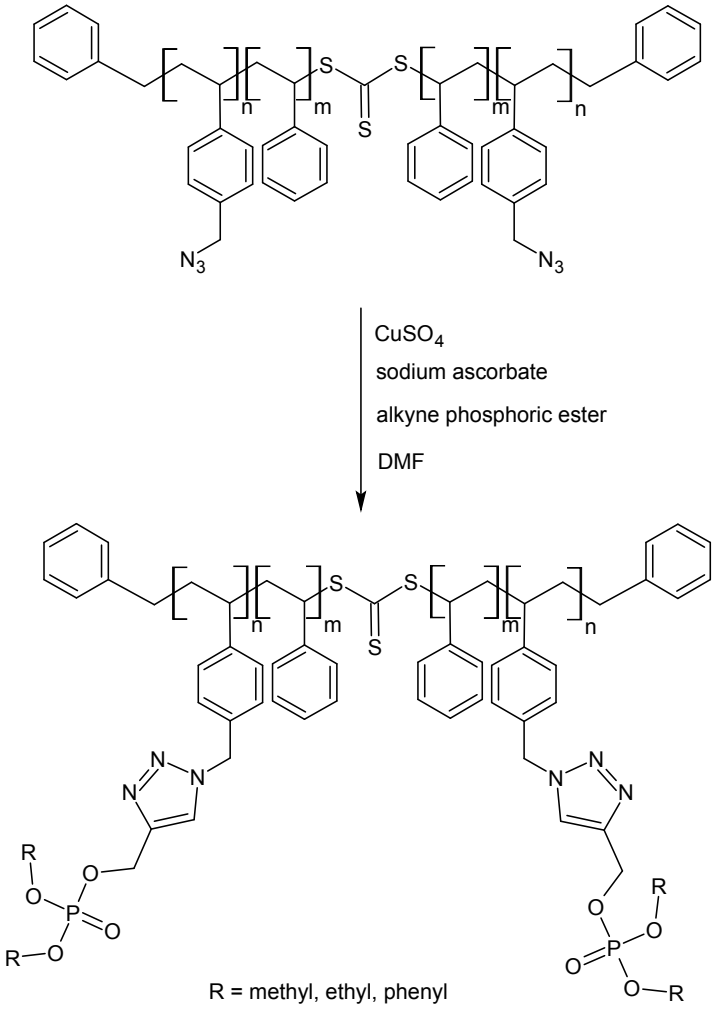

Figure 3.16: Synthesis of phosphorylated copolymers via a modular ligation reaction.

After precipitation from water, the phosphorylated copolymer **(10)** was suspended in DMF and precipitated from methanol and dried in vacuo at 40 °C. The final phosphorylated polymers have an ocher color and were found to be insoluble in most of the common organic solvents, disallowing any SEC analysis.

Table 3.1 in the previous Section 3.2 shows a summary of the prepared chloride (P_{Cl}.X) **(8)**, azide (P_{N3}.X) **(9)** and phosphorylated (P_P.X) **(10)** functionalized styrene copolymers and their characteristics. SEC data of phosphorylated polymers (P_P.X) could not be obtained due to their insolubility in all evaluated SEC solvents. Firstly, it should be determined whether a complete conversion to azide and finally phosphorylated copolymers was achieved by using various analytical methods. It should also be examined whether the type of phosphoric ester and the proportion of functional groups in the copolymer have an influence on the quantive implementation within the modular ligation reaction. For the sake of clarity, in the following explanations and graphics only the results of a 33 % functionalized copolymer reacted with DPPP (P_P.33-DPPP) are discussed as a representative example. The values of the other copolymers are summarized in Table 3.1. Secondly, the influence of the phosphorus content and type of phosphoric ester group on the thermal behavior of the phosphorylated copolymers should be determined. General considerations are again demonstrated on the example of P_P.33-DPPP.
To preclude cross-linking as the reason for the insolubility of the phosphorylated copolymers, solid state NMR measurements were performed with the phosphorylated copolymer samples. The ^{31}P spectrum of P_P.33-DPPP as a representative sample showed only one peak at -11 ppm (Figure 3.17). If cross-linking would occur to any significant extent, an additional peak from the P-O-P bond would appear in the ^{31}P spectrum.

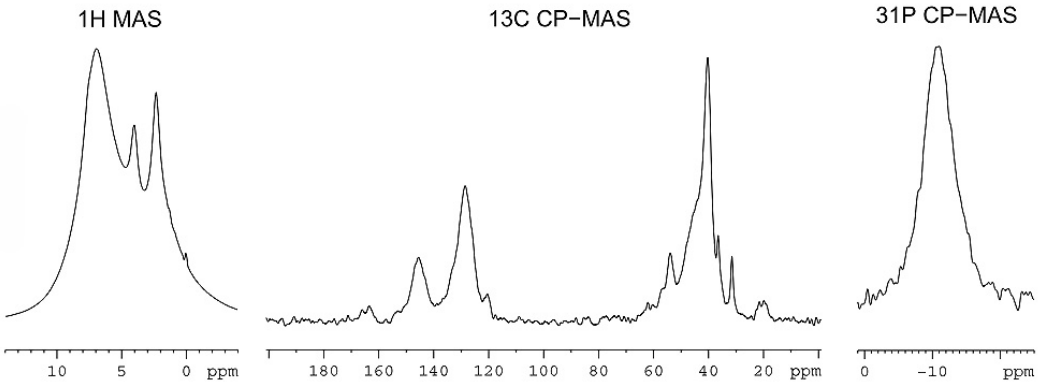

Figure 3.17: Solid state NMR measurements of a phosphorylated copolymer (P_P.33-DPPP). All measurements were performed at 25 kHz MAS with 100 kHz RF field strength on all channels.

FT-IR measurements were performed to investigate the covalent ligation of the alkyne phosphoric esters onto the lateral chains by conversion of the azide to the triazole ring. The FT-IR spectral evolution of P_P.33-DPPP is displayed in Figure 3.18, where a clear disappearance of the characteristic azide peak is shown.

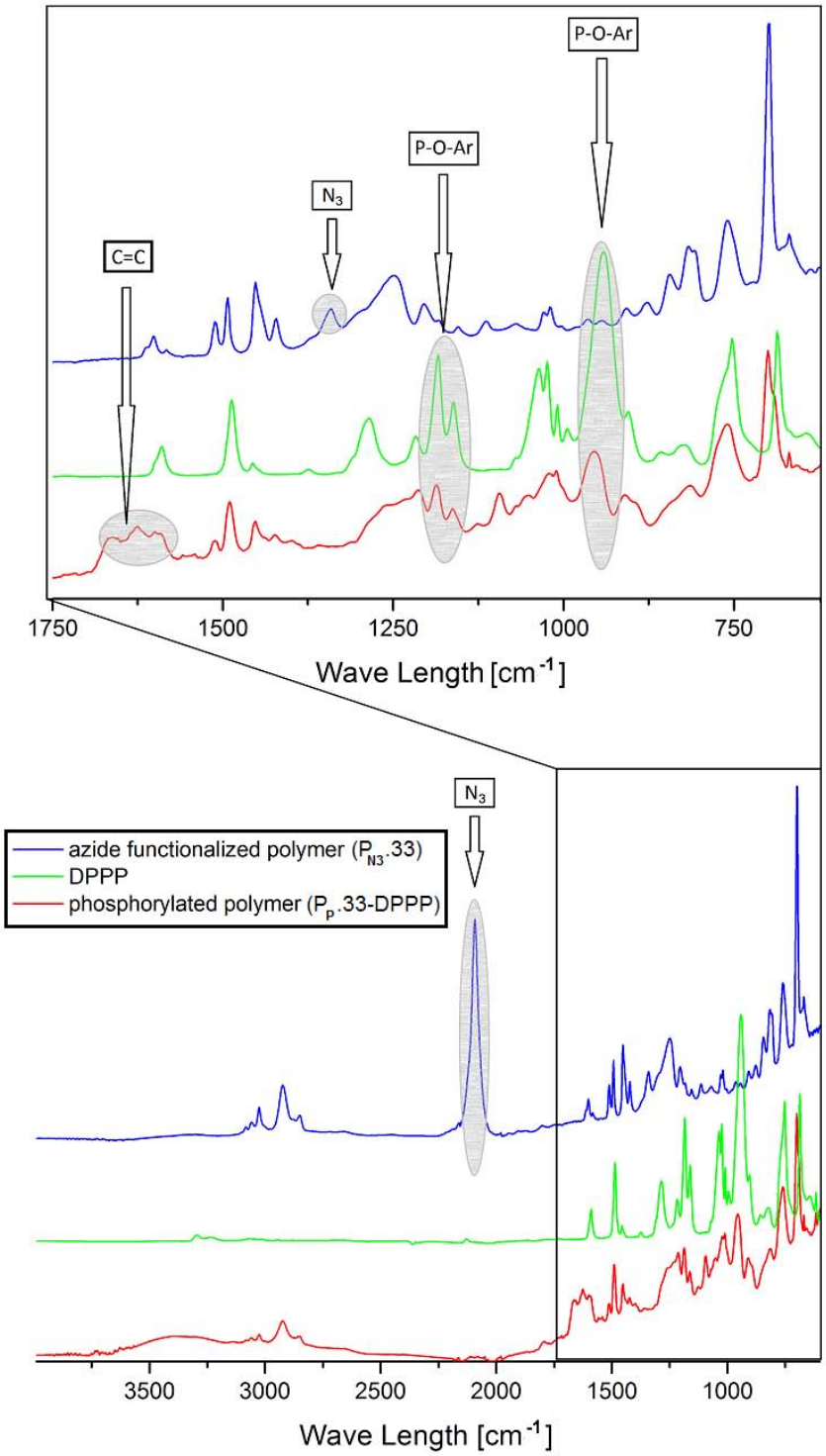

Figure 3.18: FT-IR spectra of an aromatic alkyne phosphoric ester (DPPP) and an azide functionalized copolymer (P_{N3}.33) in comparison to the corresponding phosphorylated copolymer (P_P.33-DPPP)

The detailed spectrum (wave length region of 700 to 1750 cm^{-1}) shows in addition to the characteristic peaks of the aromatic phosphoric ester, the appearance of peaks in the range of 1670 cm^{-1}, which point to an aromatic system, such as the one found in triazole rings.[164]
In addition to FT-IR measurements, X-ray photoelectron spectroscopy (XPS) measurements were carried out to obtain quantitative information about the elemental composition and conversion of the polymer side chains during the transformation of the chloride to azide functionalities and finally to phosphorylated polymers (refer to Figure 3.19 for the synthesis of P_P.33-DPPP). Full conversion of the chloride to azide functionalized copolymers was confirmed by the complete disappearance of the Cl 2p doublet at Cl 2p 3/2 = 200.4 eV and Cl 2p 1/2 = 202.0 eV and in addition by the appearance of the three characteristic N 1s azide peaks at 399.3 eV, 401.0 eV and 404.7 eV. Comparison of the N 1s signals before (P_{N3}) and after modular ligation (P_P) evidences the clear transformation of the azide peaks to 400.3 eV and 402.6 eV, which distinguish nitrogen in a triazole ring.[165] Furthermore, a peak at P 2p 3/2 = 134.3 eV (P_P) occurs, which can be associated with the phosphoric ester group.[166]

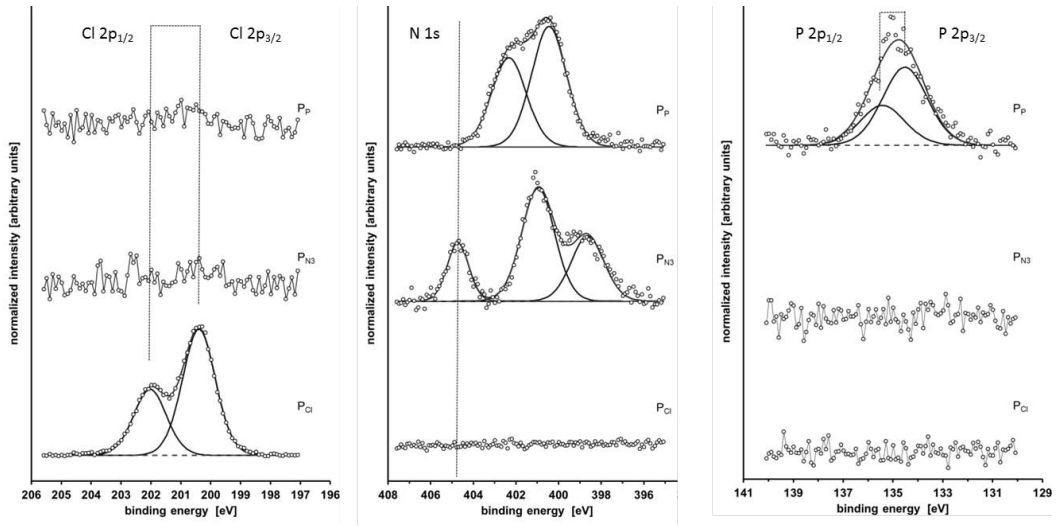

Figure 3.19: XPS analysis of the transformation of a chloride (P_{Cl}.33) to an azide (P_{N3}.33) and finally to a phosphorylated (P_P.33-DPPP) copolymer.

Comprehensive thermal analysis (TGA and DSC) was conducted to gain insight into the decomposition characteristics of the phosphorylated copolymers. Figure 3.20 shows the thermal profiles of the DSC and TGA measurements of a polystyrene prepared via RAFT polymerization (RAFT-PS), the pure aromatic alkyne phosphoric ester (DPPP) and the corresponding phosphorylated copolymer P_P.33-DPPP.

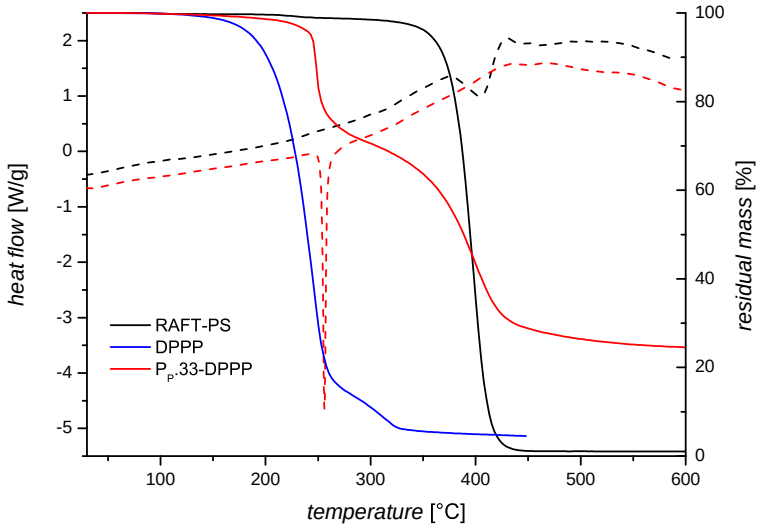

Figure 3.20: DSC (dotted lines) and TGA (full lines) measurements of polystyrene prepared by RAFT polymerization (RAFT-PS), aromatic alkyne phosphoric ester (DPPP) and corresponding phosphorylated copolymer (P$_P$.33-DPPP).

DSC measurements exhibit one endothermic decomposition stage at 405 °C for the polystyrene synthesized via RAFT polymerization. Compared to commercially available polystyrenes which, depending on its structural composition, show softening at 80-100 °C, polystyrene prepared via RAFT polymerization shows no softening or melting.[1] Only an endothermic decomposition at very high temperature (405 °C) was observed. The phosphorylated copolymers exhibit similar heat flows independent of the phosphoric ester content, with a strong endothermic decomposition at 254 °C followed by a subsequent slow increase of the heat flow. For the sake of clarity, Figure 3.20 only shows the thermal profiles of the DSC measurements of polystyrene (RAFT-PS) and P$_P$.33-DPPP. Inspection of Figure 3.20 shows that the endothermic DSC peak of the phosphorylated copolymer close to 250 °C corresponds to the first decomposition step of the phosphorylated copolymer associated with a release of the phosphoric group (based on the below noted TG-MS experiments, i.e. release of phosphorus moieties at 245 to 247 °C). The endothermic peak close to 405 °C of the polystyrene prepared via RAFT (RAFT-PS) corresponds to the decomposition of the polymer backbone. Thus, the second decomposition step of the phosphorylated polymer in the same temperature regime corresponds as well to the degradation of the polymer backbone. The two decomposition steps of the phosphorylated polymer are thus clearly identified. The decomposition of pure DPPP sets in at a somewhat lower temperature than in its polymer bound state. Such an observation is not en-

tirely surprising given that in the polymer it is attached via a triazole ring, altering its chemical environment.

TG-MS measurements should provide deeper insight into the thermal decomposition behavior of the phosphorylated styrene copolymers. The possible decomposition products of the various substances are shown in Figure 3.21. TGA measurements (refer to Figure 3.20) of DPPP **(7)** displayed a weight loss of 85.6 % around 245 °C associated with the release of decomposition products with masses of $m = 39\ Da$ ($HC{\equiv}C\text{-}CH_2$), 55 *Da* ($HC{\equiv}C\text{-}CH_2\text{-}O$) and 77 *Da* ($C_6H_5$) detected via TG-MS measurements. The phosphite group $(C_6H_5\text{-}O)_2\text{-}P{=}O$ with a mass of $m = 233\ Da$ could not be detected with the employed setup due to a long capillary between oven and detector, which disallowed its detection. However, an increase of the baseline indicated a non-detectable, but still present substance in the system. Moreover, a second weight loss of 8.2 % at 310 °C was observed with the release of a compound with $m = 93\ Da$. Such an observation points to a further decomposition of the released phosphite group ($m = 233\ Da$) into $C_6H_5\text{-}O$ ($m = 93\ Da$) and $P{=}O$ ($m = 47\ Da$).

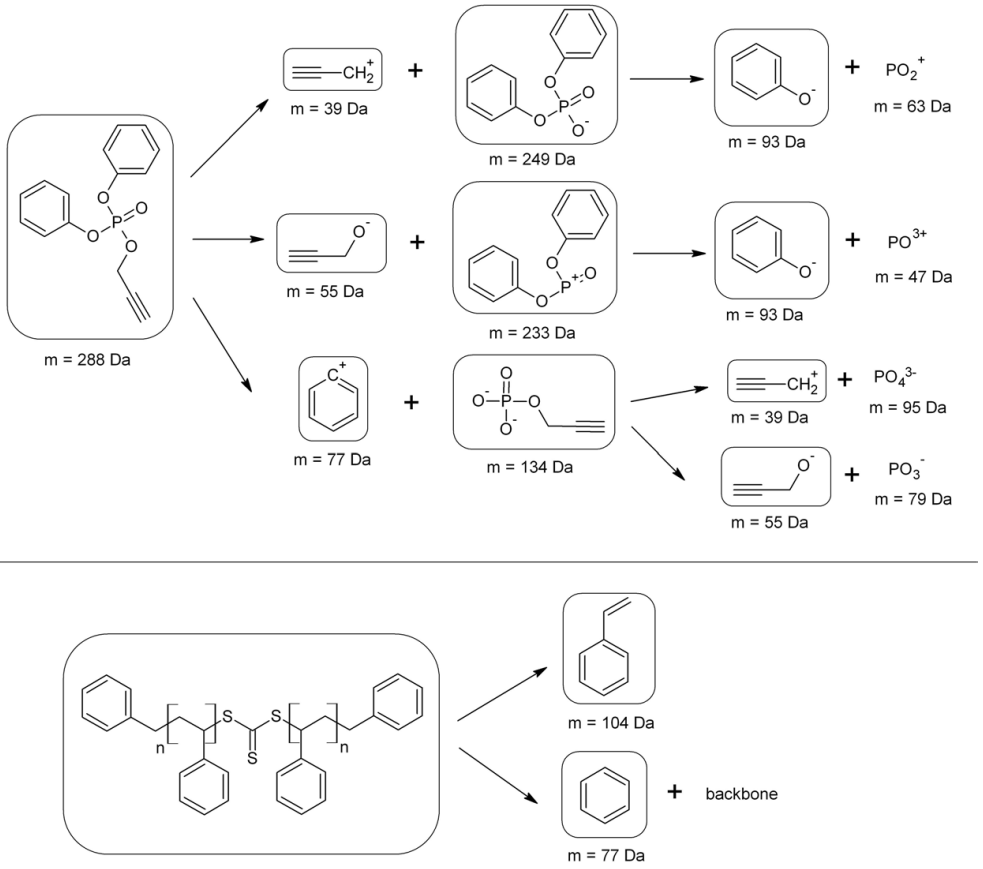

Figure 3.21: Fragmentation behavior of DPPP and polystyrene polymerized via RAFT polymerization with $M_n = 26\ 400\ g \cdot mol^{-1}$ and $PDI = 1.31$.

The PO_x components were not detectable via TG-MS. Polystyrene synthesized via RAFT polymerization showed a one-step degradation behavior with the release of $m = 104\ Da$ (styrene) and an immediately following release of $m = 77\ Da$ (C_6H_5). The TG-MS analysis of the phosphorylated copolymers revealed the characteristic masses, which are released during the decomposition of DPPP and polystyrene. The elimination of the phosphite group occured at 247 °C for DPPP **(7)**. As can be seen in Figure 3.20, the polystyrene backbone of the phosphorylated copolymer decomposes within the same temperature region as polystyrene (405 °C), yet in a somewhat broader temperature range. In addition, a residual mass of more than 40 % of the phosphorylated copolymer could be detected at temperatures exceeding 600 °C, which may be due to carbonization of the copolymer. A possible explanation for the high char residue might be the dehydration of the polymer backbone by the formation of phosphorus-containing acids due to the release of phosphorus fragments (refer to Figure 3.21).[167]

After evaluation of the complete conversion to phosphorylated copolymers, the influence of the concentration and nature of the phosphoric ester was studied. To determine the influence of the concentration of the respective phosphoric esters, the azide functionalized copolymers synthesized in Section 3.2, were reacted with the three phosphoric esters **(5)**, **(6)**, **(7)** and their thermal decomposition behavior were examined. Figures 3.22 to 3.24 show the TGA measurements of the various phosphorylated copolymers.

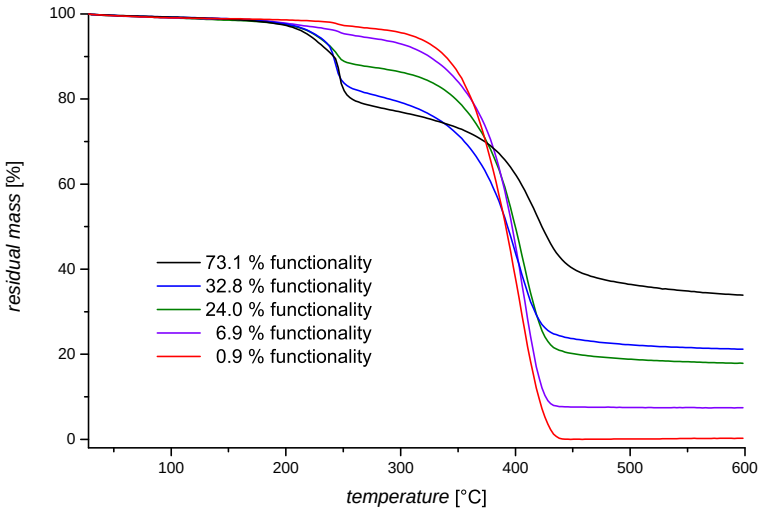

Figure 3.22: Influence on the decomposition behavior of the phosphoric ester content of phosphorylated copolymers reacted with methylated alkyne phosphoric ester (DMPP) **(5)**. TGA measurements were carried out under a nitrogen atmosphere in the temperature range between 40 and 600 °C at a temperature increase of $5K{\cdot}min^{-1}$.

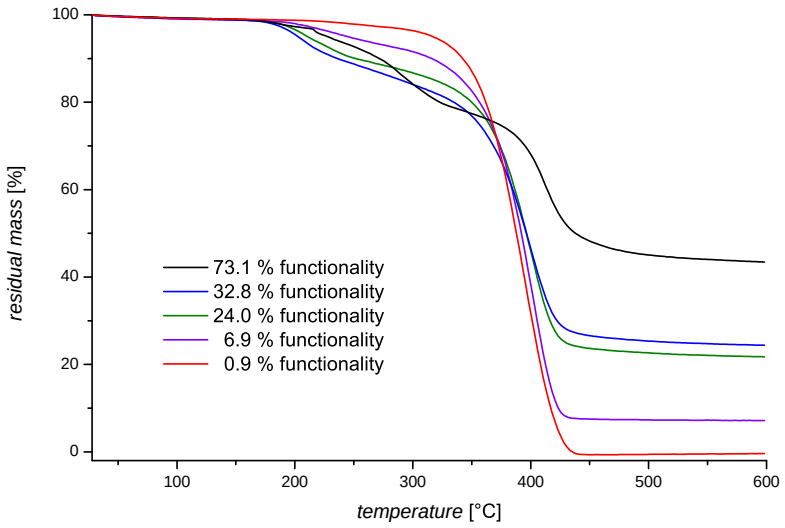

Figure 3.23: Influence on the decomposition behavior of the phosphoric ester content of phosphorylated copolymers reacted with ethylated alkyne phosphoric ester (DEPP) **(6)**. TGA measurements were carried out under a nitrogen atmosphere in the temperature range between 40 and 600 °C at a temperature increase of $5\text{K}\cdot\text{min}^{-1}$.

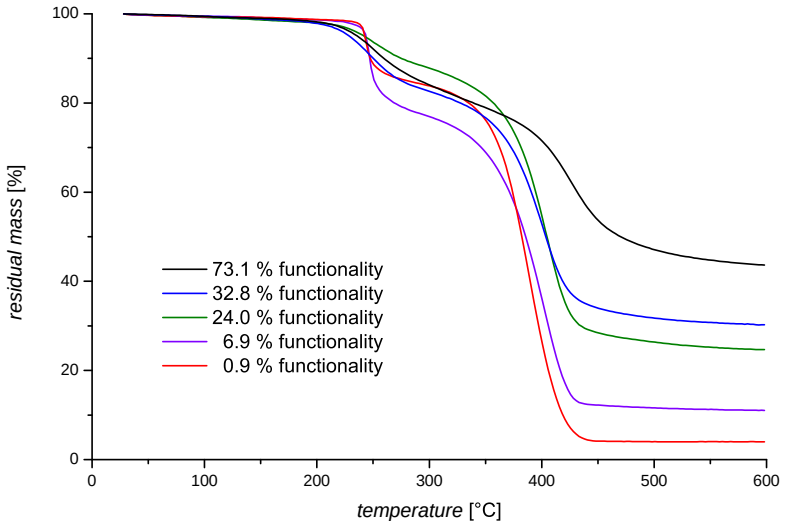

Figure 3.24: Influence on the decomposition behavior of the phosphoric ester content of phosphorylated copolymers reacted with phenylated alkyne phosphoric ester (DPPP) **(7)**. TGA measurements were carried out under a nitrogen atmosphere in the temperature range between 40 and 600 °C at a temperature increase of $5\text{K}\cdot\text{min}^{-1}$.

An inspection of Figure 3.22 to 3.24 shows that the proportion of residual mass increases proportional with increasing phosphorus content. To compare the influence of the different phosphoric esters with each other, the phosphorus content, degradation temperatures, mass losses and residual mass are shown in Table 3.2 for the different phosphorylated copolymers.

Polymer	**P-content** [%]	**degradation T** [°C]	**mass loss** [%]	**residual mass** [%]
P_P.1-DMPP	0.09	244.6 / 404.3	1.52 / 96.72	0.27
P_P.7-DMPP	0.66	250.4 / 382.4	2.24 / 87.01	7.24
P_P.24-DMPP	2.28	246.4 / 405.0	12.86 / 65.94	17.87
P_P.33-DMPP	3.12	241.2 / 396.8	19.35 / 55.99	21.17
P_P.73-DMPP	6.96	245.0 / 416.1	22.09 / 39.89	33.87
P_P.1-DEPP	0.08	—— / 393.7	0.00 / 97.92	0
P_P.7-DEPP	0.61	234.7 / 401.6	6.19 / 84.99	7.17
P_P.24-DEPP	2.10	208.0 / 402.0	12.12 / 63.67	21.74
P_P.33-DEPP	2.88	208.2 / 403.0	12.78 / 60.07	24.40
P_P.73-DEPP	6.41	288.7 / 412.3	21.00 / 31.99	43.44
P_P.1-DPPP	0.06	244.3 / 398.3	14.40 / 80.10	4.01
P_P.7-DPPP	0.48	247.0 / 401.2	21.09 / 65.62	11.04
P_P.24-DPPP	1.65	249.4 / 406.6	11.74 / 59.98	24.66
P_P.33-DPPP	2.26	247.0 / 401.8	17.86 / 48.03	30.23
P_P.73-DPPP	5.04	251.1 / 428.8	17.66 / 35.96	43.62

Table 3.2: Overview of the phosphorus content, degradation temperatures, mass losses and residual mass of the different phosphorylated copolymers.

By plotting the content of phosphorus in the polymer to the residual mass (Figure 3.25) after TGA measurements of up to 600 °C, the influence of the phosphorus content on the degree of carbonization is clearly shown. In addition, a clear increase in the char formation at comparable phosphorus content of DMPP over DEPP to DPPP is shown. These observations reveal a clear correlation between the employed esters and charring. On the one hand, the observed increase in char formation with increasing chain length of the phosphoric ester groups is surprising since the phosphorus content in the polymer is inversely proportional to the chain length of the phosporic ester groups, and therefore a less pronounced char formation is expected. On the other hand, former experiments using halogenated flame retardants have shown that particularly ring systems such as diphenyl ether and bisphenol derivatives exhibit excellent flame retardancy.[168] Therefore, the use of increasing chain

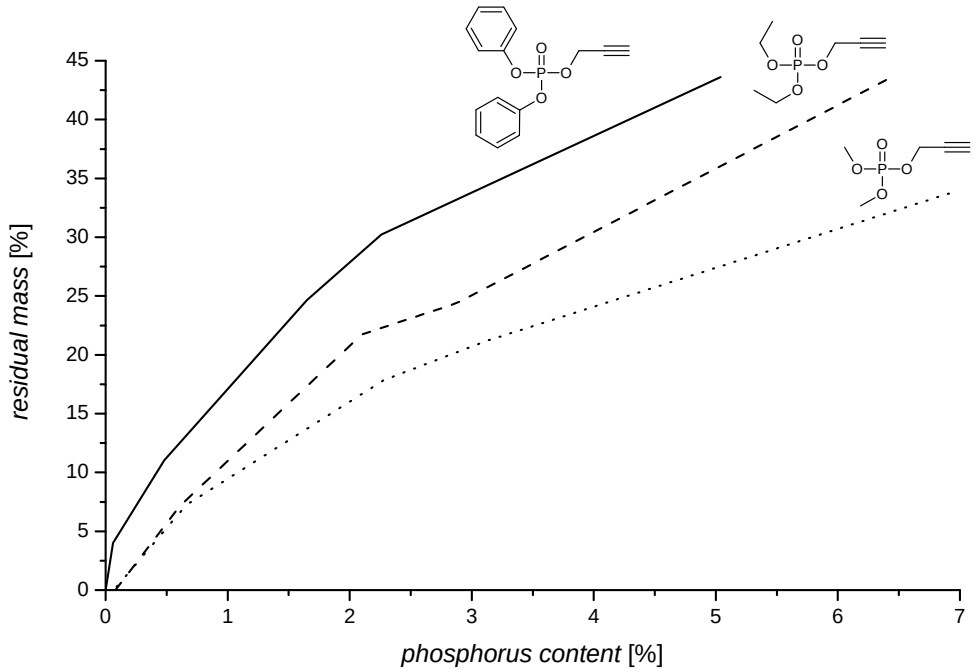

Figure 3.25: Influence of the phosphorus content and type of phosphoric ester group on the carbonization.

length and maybe even branched chains as phosphorus ester groups, in particular by using phenolic rings seems to have a positive influence on the flame retardancy. Moreover, it could be shown by scanning electron microscopy combined with energy dispersive X-ray analysis (SEM/EDX) measurements and a mapping of characteristic elements (see Figure 3.26) that the phosphoric esters are randomly distributed throughout the prepared copolymers.

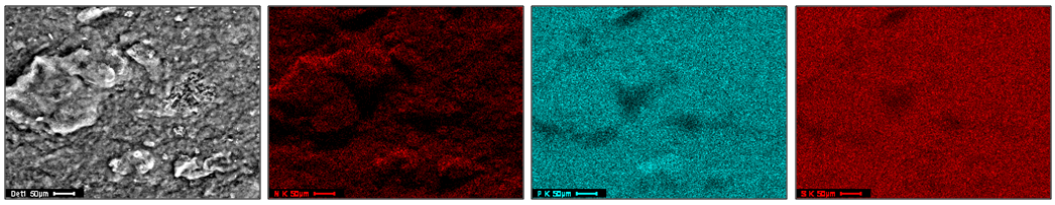

Figure 3.26: Mapping of the characteristic elements N (dark red), P (blue) and S (light red) in the phosphorylated polymer P_p.33-DPPP.

As noted in Chapter 2.4., significantly lower levels of flame retardant are needed to cause a significant increase in flame retardancy, if the flame retardant is distributed homogeneously within the polymer.[10] In the case of the examined copolymers, this may explain the low levels of flame retardant necessary to achieve a potentially high flame retardancy in form of charring in TGA measurements. Furthermore, the high

degree of carbonization indicates a synergistic effect with the nitrogen of the triazole ring. Comparable carbonization results were already described by Einsele for phosphorus-containing flame retardants combined with nitrogen compounds incorporated in cellulose.[150] The carbonization is due to a dehydration mechanism that is catalyzed by phosphorus compounds, in particular phosphoric acids. The phosphorus compounds influence the direction of the pyrolysis of the protected material in such a way that less-flammable compounds are generated. Thus, the energy released during combustion is reduced. Such a controlled pyrolysis must take place at a lower temperature, so that the normal pyrolysis does not even come into play. For all investigated phosphorus-containing flame retardants, decreased decomposition temperatures were measured by Einsele for the protected cellulose samples. The directed pyrolysis can thus occur up to 100 °C earlier with the formation of water and highly increased charring. The phosphorus-containing copolymers examined in the current work showed as well a strong peak in the TG-MS at the mass $m = 18\ Da$, which can be attributed to water. As a reason for the strong charring, a dehydration by phosphorus-containing compounds, which is amplified by a synergetic effect with the nitrogen of the triazole, can be assumed.

3.4 Summary of Chapter 3

The phosphorus-containing polymers described in the current chapter may be suitable as flame retardants, as they in addition to the releasable phosphorus component, which showed high flame retardant potential in previous experiments feature additional advantages. Firstly, with the synthetic route described here, well-defined materials with narrow polydispersities and individually adjustable concentration and type of phosphorus-containing groups in the side chains can be obtained. Secondly, phosphorylated copolymers can not migrate from the protected polymer, due to the polymeric structure. In addition, due to the covalent binding of the phosphoric esters onto the copolymer, an agglomeration of the flame retardant component in the polymer matrix is prevented. Beyond that, the homogeneously distributed flame retardant has the effect that less flame retardant is required to reach comparable results in comparison to the addition of additives. In addition, the thermal stability of the aromatic polymer backbone brings an advantage since phenolic rings may have an additional positive influence on the flame retardancy.[169] Furthermore, the release of the phosphoric esters around 250 °C indicates a potential use as flame retardant, since in previous experiments a release of flame retardant substances in the range of 200 to 400 °C has been shown to be very effective.[8, 131] In addition, a high residual mass at temperatures > 600 °C points to carbonization of the copolymers

which can additionally increase the flame retardancy potential of these polymers in the form of char, thereby forming a protective layer on the protected polymer.[131] The limited solubility of the prepared phosphorylated polymers is not necessarily a drawback with respect to its use as a flame retardant in a polymer processing step. The fact that the flame retardants developed in the current work exhibit no melting point, must be considered differentiated. A non-existing melting point has the advantage that the flame retardant will not melt from the polymer, yet makes it difficult to incorporate the powderous flame retardant into polymer systems in particular by extrusion/molding processes, but also by stirring processes. As typical polymer processing occurs via extrusion, the prepared polymers can be readily added to an extrusion process. Typical polystyrene extrusion is conducted at 180 °C. TGA and DSC measurements evidenced that the phosphorylated polymers commence degradation above 200 °C, thus making their incorporation via extrusion a viable option. Thus, their limited solubility in organic solvents while complicating its molecular analysis is not a critical drawback for its employment as a flame retardant additive during a polymer processing step. Thus, the herein presented synthetic methodology towards phosphorus-containing polymers holds significant potential for the use as next generation flame retardant.

Chapter 4

Phosphorylated Polymers via Living Ionic Polymerization

In the current chapter, a novel approach of the direct polymerization of phosphorylated epoxy monomers via living ionic ring-opening polymerization (ROP) is described. The structural features (epoxy ring and phosphonic acid group) of 1,2-epoxypropyl phosphonic acid, so-called fosfomycin (Fos) and its disodium salt (Na-Fos), suggest the possibility of using them as starting materials for the synthesis of phosphorylated polyols via ring-opening polymerization. The chemical structure of fosfomycin is depicted in Figure 4.1.

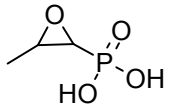

Figure 4.1: Chemical structure of fosfomycin (1,2-epoxypropyl phosphonic acid).

On the one hand, the epoxy ring can act as an electrophilic site which offers the possibility to synthesize polyols via an anionic, cationic or even a coordinative ring-opening polymerization approach. On the other hand, fosfomycin has a high phosphorus content of 22,4 % (Fos), respectively 17,0 % (Na-Fos); therefore a decisive influence of the phosphonate group on the resulting polymer is expected. A significant improvement in flame retardancy is described for post-phosphorylated poly(vinyl alcohol) compared to unmodified poly(vinyl alcohol).[170] The increased flame retardancy in this system arises primarily from a condensed phase mechanism involving dehydration, cross-linking and char formation.
As mentioned in Chapter 2.1.2, the monomer should not contain abstractable protons, if it should be polymerized in a living ionic process. As a result, fosfomycin respectively the disodium salt thereof, had to be quantitatively esterified to a diester

first. In the framework of the current work, different synthetic strategies were pursued for the preparation of dimethyl- and diethyl 1,2-epoxypropyl phosphonate by esterification starting from the fosfomycin disodium salt. The aim was to develop a synthetic route in which the corresponding diesters are selectively formed, without opening of the epoxy ring. The development of a novel synthetic strategy and purification steps are described in Chapter 4.2. The polymerization experiments of the fosfomycin diesters and derivatives thereof via anionic ring-opening polymerization to homo- and copolymers are described in Chapter 4.3. In addition, the reaction conditions and limitations of living ionic ring opening polymerization for the direct synthesis of phosphorus-containing polymers were studied. A general pathway of the synthesis to diesters of fosfomycin and their polymerization is depicted in Figure 4.2.

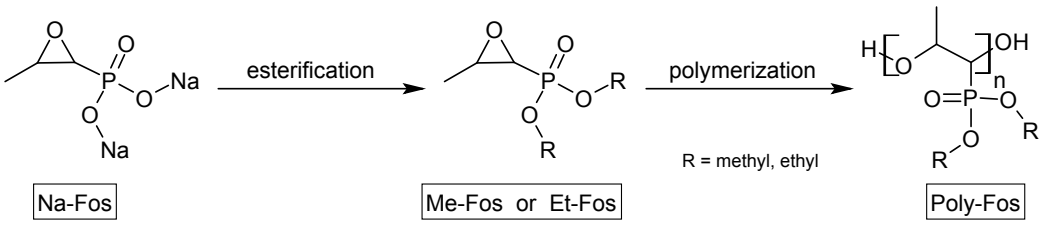

Figure 4.2: General synthetic strategy to diesters of fosfomycin and polymerization of these starting from fosfomycin disodium salt.

4.1 Overview of Previous Synthesis and Applications of Fosfomycin and Derivatives thereof

Fosfomycin (1,2-epoxypropyl phosphonic acid) is a naturally occurring antibiotic which is produced by strains of *Streptomyces*. It was first described under its former name phosphonomycin by Hendlin *et al.* in 1969.[171] Fosfomycin (CAS: 23155-02-4) is a small, water-soluble molecule that combines two unusual features: an epoxy ring and a phosphonic acid group.

The epoxy ring is responsible for its antibacterial activity. Through its unique chemical structure, fosfomycin is the only representative of the epoxy group of antibiotics. Resistance and allergies, as they are usually seen with other antibiotics, have not been described, and are not to be expected due to the different structure and mode of action. The antibiotic effect of fosfomycin is based on a disturbance of the cell wall construction, respectively peptidoglycan (also known as murein) in growing bacteria by inhibiting an early precursor of the peptidoglycan synthesis by irreversible alkylation of a thiol group in the active site of phosphoenolpyruvate-transferase.[172] The

peptidoglycan themselves consists of cross-linked chains of the alternating amino sugars *N*-acetylglucosamic acid (NAM) and *N*-acetylmuramic acid (NAG). Since peptidoglycan is a component of the cell wall of gram-positive and gram-negative bacteria only, fosfomycin therefore acts specifically on bacterial walls and does not interfere with the cell wall construction of human cells.
Fosfomycin is mainly formed fermentatively. The synthesis of fermentatively formed fosfomycin is shown in Figure 4.3 and described in detail in the following section.

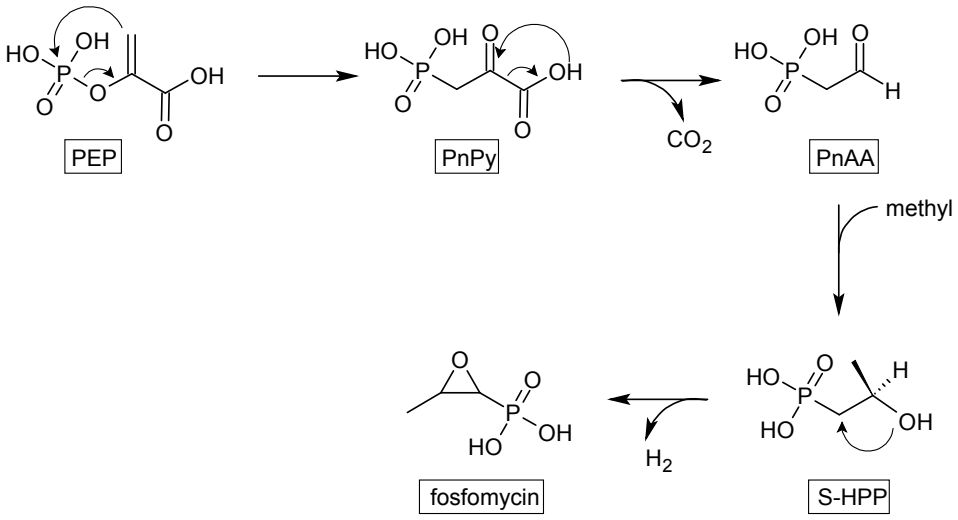

Figure 4.3: Synthetic pathway of fermentatively formed fosfomycin.[173]

Through intramolecular rearrangement of phosphoenolpyruvate (PEP), phosphonopyruvat (PnPy) is generated, which is subsequently transformed into phosphonoacetaldehyd (PnAA) via decarboxylation. By methylation, using a PnAA methylase, 2-hydroxypropyl phosphonic acid (S-HPP) is formed, which finally forms the desired fosfomycin by an oxidative cyclization.[173]
In the literature, various methods for the chemical preparation of fosfomycin and its salts are reported.[174] All have in common that they are based on different phosphonic acid- or ester compounds as starting material and the subsequent introduction of the epoxy ring using variable synthetic strategies. To reach enantiomeric pure fosfomycin and derivatives thereof, most syntheses have been accomplished by stereospecific *cis*-epoxidation of (*Z*)-1-propenylphosphonic acid (refer to line 1 in Figure 4.4), followed by optical resolution of the racemic epoxide with optically active amines.[175] A further possibility for achieving enantiomeric pure fosfomycin or its salts, is the use of chiral auxiliaries [176] or chiral catalysts [177]. All three methods are depicted in Figure 4.4.

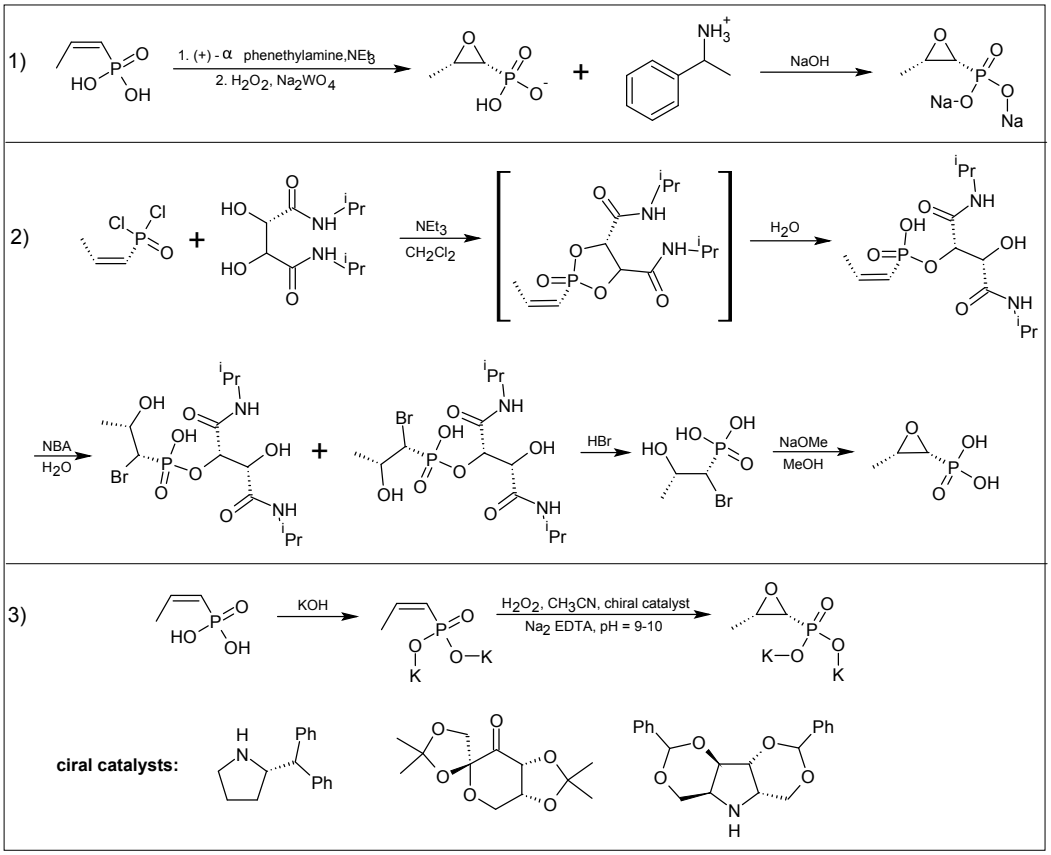

Figure 4.4: Chemical pathways to enantiomeric pure fosfomycin, respectively its salts. 1) Using optical active amines [175]; 2) Using chiral auxiliaries [176]; 3) Using chiral catalysts [177].

In order to achieve an enlarged application profile beyond the biological spectrum, in addition to pure fosfomycin, esters thereof can be synthesized. The main methods are the reaction via dialkyl chloromethylphosphonates via Darzens reaction (A), the synthesis via dialkyl halohydrinphosphonates with bases (B) and the oxidation of 1,2-unsaturated phosphonates with a peroxide (C). All of the mentioned reaction methods lead to compounds with the general structure shown in Figure 4.5 and are described in detail in the following sections.

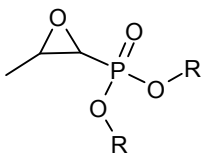

Figure 4.5: General structure of fosfomycin diesters relevant to the current work.

(A) Reaction via α-halophosphonates with carbonyl compounds (Darzens reaction)

In general, the Darzens reaction allows for the synthesis of α,β-epoxy esters by condensation of a carbonyl compound and an α-halo ester in the presence of a base, according to Figure 4.6.[178]

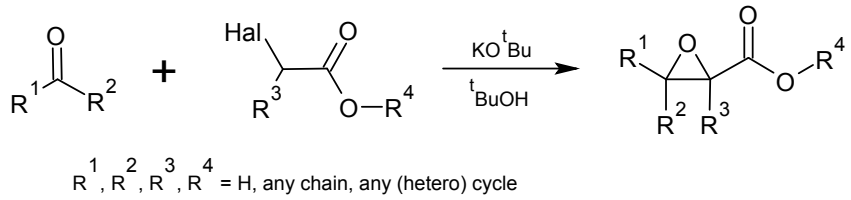

Figure 4.6: Epoxidation via the reaction of α-halo esters wih a carbonyl compound in the presence of a base (Darzens Reaction).[178]

Therefore, the Darzens reaction is the most general and perhaps most widely employed method for the synthesis of dialkyl fosfomycins involving the reaction of dialkyl halomethylphosphonates with carbonyl compounds (Figure 4.7).[179]

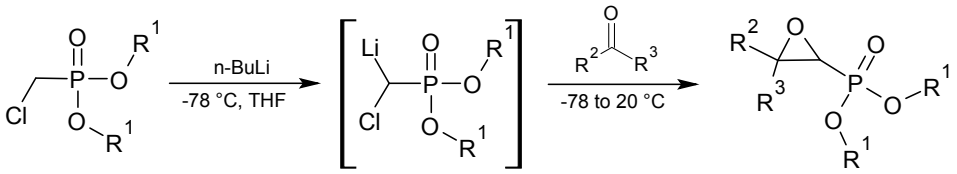

Figure 4.7: Reaction scheme of the reaction of dialkyl chloromethylphosphonates with carbonyl compounds to fosfomycin diesters via the Darzens Reaction.[179]

In general, every halomethylphosphonate can be used in the Darzens reaction. The reaction to iodine phosphonates from trialkyl phosphites was already described in 1936 by Arbuzov and Kushkova.[86] However, this reaction results in low yields, due to the so-called Arbuzov-Michaelis rearrangement between trialkyl phosphite and methyl iodide. The methyl iodide is formed by the transformation of dichloromethane to triiodomethyl and methyliodide. The rearrangement leads to dialkyl methylphosphonates, which cannot be used in the Darzens reaction, making the pathway inefficient for industrial scale. The Arbuzov reaction and the Arbuzov-Michaelis-rearrangement are shown in Figure 4.8.

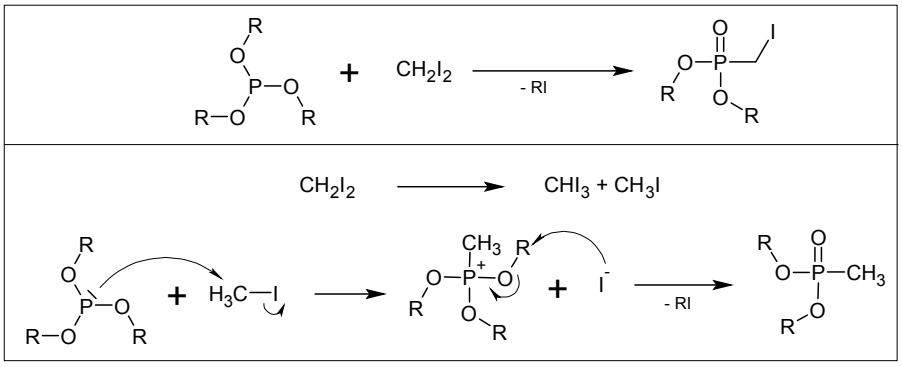

Figure 4.8: Reaction scheme of the Arbuzov reaction (upper part) and Arbuzov-Michaelis rearrangement (lower part).

Attempts to synthesize fluoromethylphosphonates via the Michaelis-Becker reaction (Figure 4.9) provided only moderate yields of close to 40 %. In addition, the employed fluoromethane is no longer commercially available, due to its mutagenic properties. Therefore, almost exclusively dialkyl chloromethylphosphonates are used for the synthesis of epoxyphosphonates via the Darzens reaction.

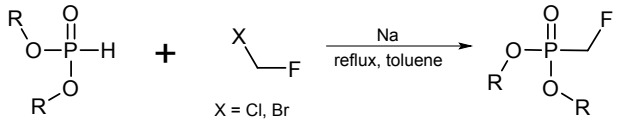

Figure 4.9: Reaction scheme of the Michaelis-Becker reaction.

To obtain dialkyl chloromethylphosphonate, the key ingredient of the Darzens reaction, two synthetic strategies can be followed. Both strategies employ phosphorus trichloride (PCl_3) as starting material. The reaction with dihalomethane in combination with aluminum chloride ($AlCl_3$) (Kinnear-Perren reaction) or with paraformaldehyde at higer temperature (Kabachnik reaction) gives the intermediate halomethylphosphoryl dichloride, which subsequently can be converted to the dialkyl under anhydrous conditions. Both reaction schemes are shown in Figure 4.10.

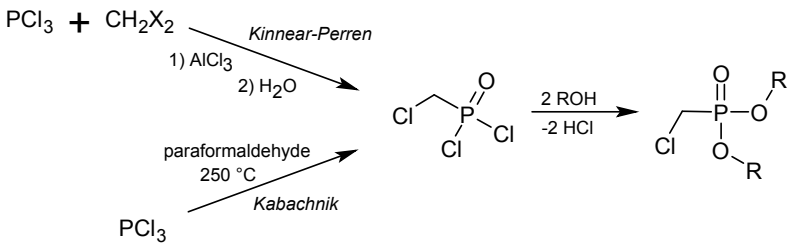

Figure 4.10: Kinnear-Perren and Kabachnik reaction to chloromethylphosphonates.

As shown in Figure 4.7, the reaction to dialkyl fosfomycin proceeds via an α-metallated dialkyl chloromethylphosphonate. Due to its instability, the synthesis conditions of the intermediate state are critical. Best yields are obtained using butyllithium (BuLi) in tetrahydrofuran (THF) at low temperatures.[179] The resulting carbanions (intermediate stage) undergo facile addition with carbonyl compounds giving chlorohydrins, which form the desired dialkylfosfomycin under warming without traces of side products.
An additional reaction of the dialkyl chloromethylphosphonate with dimethyl sulfide via a sulfonium salt was described by Christensen.[180] The sulfonium salt is further converted with the sodium salt of dimethyl sulfoxide (DMSO-Na) to its stable ylide, which can be finally converted with acetaldehyde to the epoxyphosphonate (Figure 4.11). This reaction avoids the problems associated with the stability of chloromethyl carbanions.

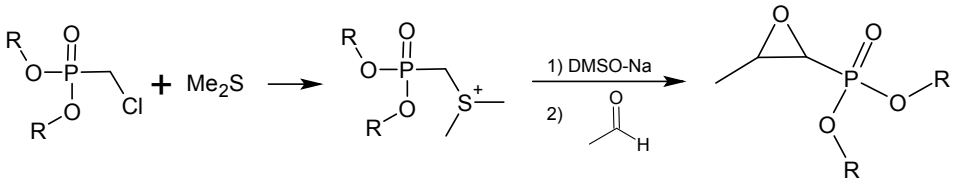

Figure 4.11: Reaction of a dialkyl chloromethylphosphonate with the sodium salt of dimethyl sulfide (DMSO-Na) and acetaldehyde leading to epoxyphosphonates.

The Darzens reaction is applicable to a wide range of carbonyl compounds. In addition to aliphatic and aromatic aldehyds, aliphatic, cyclic and aromatic ketones can be introduced into the compound. However, this reaction is not stereoselective, thus the obtained products cannot be used in most biological applications.

(B) Reaction via dialkyl halohydrinphosphonates with bases

The reaction of halohydrins with bases, such as NaOH and KOH, is a well-known method for the formation of epoxides. The halohydrin is initially formed via the reaction of an alkene with a halogen (Br_2 or Cl_2) and water. During the reaction of the halohydrin with the base, the alcohol group is deprotonated, followed by an intramolecular nucleophilic substitution, which leads to an epoxide (Figure 4.12).

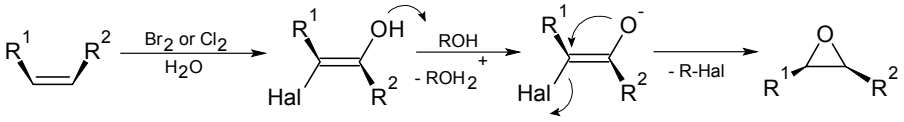

Figure 4.12: Reaction scheme of the epoxide formation via halohydrin-base reaction.

The halohydrin-base reaction can also be exploited in the synthesis of epoxy phosphonates. Therefore, the halohydrin is formed by the treatment of *cis*-1-propylphosphonic acid with *tert*-butyl- or sodium hypochlorite.[181] By subsequent reaction with aqueous sodium hydroxide solution, the desired dialkyl fosfomycin is formed (Figure 4.13).

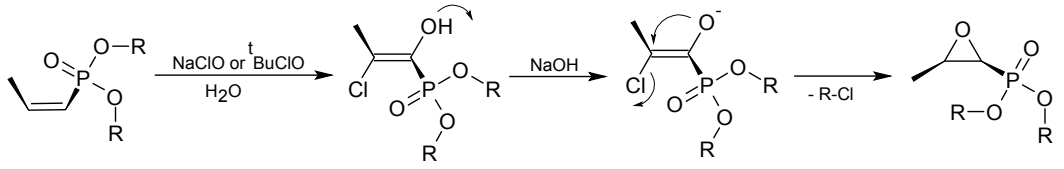

Figure 4.13: Reaction scheme of the reaction of dialkyl halohydrinphosphonates with sodium hydroxide to dialkyl fosfomycin.

The preparation of the halohydrin is generally accompanied by the formation of undesired double halogenated dialkyl 1,2-dihalohosphonates (Figure 4.14), which do not react further to epoxyphosphonates. The dihalophosphonates can indeed be very well separated from the product, but lower the yields noticeably.

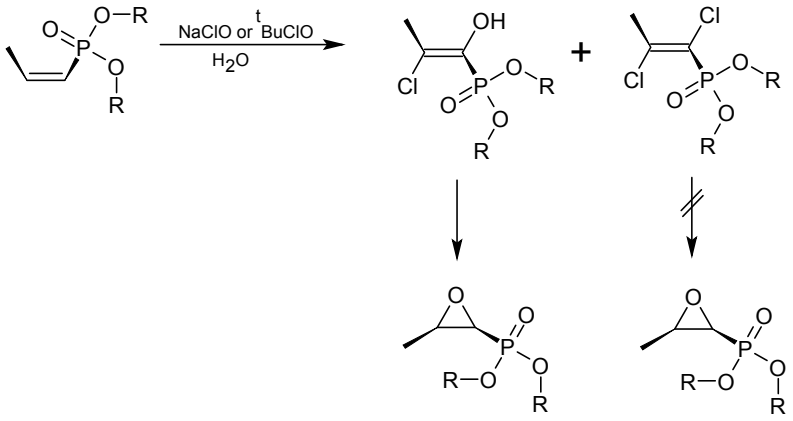

Figure 4.14: Side reaction of the halohydrin synthesis leading to dihalophosphonates, which do not react further to epoxyphosphonates.

(C) Oxidation of 1,2-unsaturated phosphonates with a peroxide

The most attractive and potentially most general route for the synthesis of dialkyl fosfomycin appears to be the the direct epoxidation of the corresponding dialkyl vinylphosphonate (Figure 4.15).

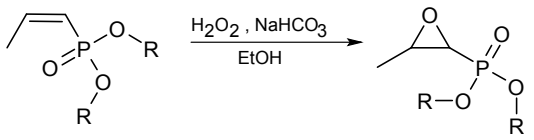

Figure 4.15: Reaction scheme of the oxidation of 1,2-unsaturated phosphonates with a peroxide to dialkyl fosfomycin.

Vinylphosphonates can be synthesized via different approaches. The most important reaction is the reaction of a triphenyl phosphoranylidenemethyl phosphonate with an aldehyde via a Wittig reaction under *E*-selectivity. Such an approach was first described by Jones *et al.* [182] and is depicted in Figure 4.16.

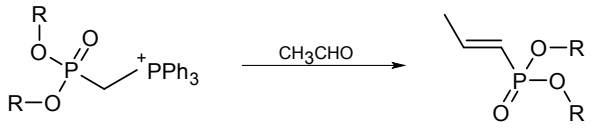

Figure 4.16: Synthesis of vinylphosphonates via the Wittig reaction.

The use of vinylphosphonates offers considerable advantages. On the one hand, the two isomeric unsaturated phosphonates are readily separable prior to *cis*- or *trans*-epoxidation of the appropriate isomer. On the other hand, the use of these unsaturated intermediates permits an acid-catalyzed hydrolysis of the ester functions prior to epoxidation. The double bond of vinylphosphonates exhibit a relatively weak electrophilicity and the vinylphosphonates have the tendency to undergo nucleophilic additions (Michael addition). For these reasons, epoxidations with either strong electrophilic peracids or nucleophilic oxidants are attempted. The competing side reaction (Michael addition) occurs due to the nucleophilic addition at the double bond (e.g. by carbanions) or ring-opening of the epoxide. These disadvantages can be overcome by using an alkaline hydrogene peroxide solution (30 % solution) in alcohol.[181] Therefore, alkaline hydroperoxide is recognized as the most common and perhaps most generally useful reagent for epoxidation of double bonds conjugated with electron-withdrawing groups.

A detailed literature research reveals that most applications of the diesters of fosfomycin and its analogues are based on ring-opening reactions with nucleophiles and rearrangements through thermal ring-opening.[183, 184, 185, 186]
The opening of the epoxy ring is specific at the C2 carbon due to both steric and electronic factors at the α-position to the phosphoryl group. The formation of α,β-difunctionalized alkylphosphonates can be achieved by both acid-catalyzed and

non-catalyzed ring-opening. Preferred nucleophiles are alcohols, water, aqueous ammonia, amines and phosphites. It is thus possible to prepare 1,2-dihydroxyalkyl phosphonates by the reaction of 1,2-alkylphosphonates with aqueous H_2SO_4 under reflux (refer to first line in Figure 4.17 with R´ = H).[185] By addition of H_2SO_4 in combination with a carbon alcohol, it is further possible to obtain 1-hydroxy-2-alkoxy-alkylphosphonates (refers to first line in Figure 4.17 with R´= carbon chain or ring). An alternative attractive approach is the ring-opening with amines or aqueous ammonia, leading to phosphorylated amino alcohols (refers to second line in Figure 4.17).[187, 188] The functionalized phosphornic esters obtained from the ring-opening reactions can further be employed to phosphorylate various materials.

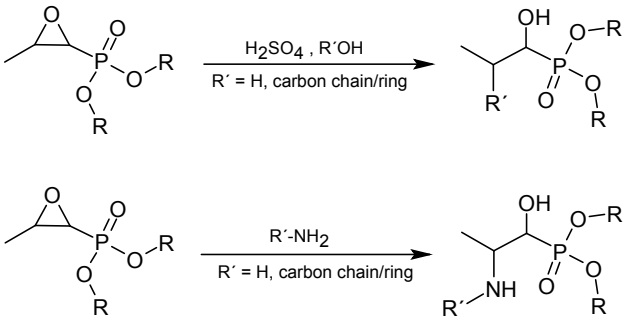

Figure 4.17: Overview of ring-opening reactions of fosfomycin esters.[185, 187, 188]

Rearrangements of epoxy phosphonates were first reported in 1966 by Churi [183], who described a thermal and acid-catalyzed phosphoryl shift from carbon to carbon as it is shown in Figure 4.18.

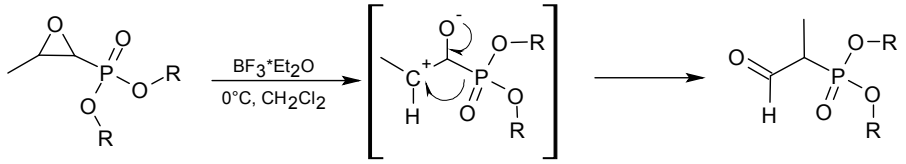

Figure 4.18: Rearrangement through phosphoryl shift during ring-opening reaction of fosfomycin esters.

Besides the ring-opening reactions, α-metallated 1,2-epoxyalkylphosphonates can serve as precursor to higher homologues (Figure 4.19).

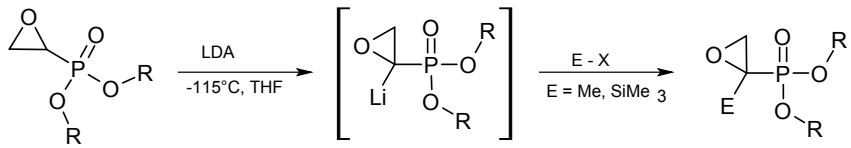

Figure 4.19: 1,2-Epoxyalkylphosphonates as precursors to higher homologues.

The structure of epoxyalkylphosphonates and homologues suggests that it is possible to synthesize polyols via ionic ring-opening polymerization. The anionic, especially the living anionic ring-opening polymerization (see Chapter 2.1.2) seems to be the most promising synthesis method to achieve polyols with narrow polydispersity and phosphorus side chains starting from epoxyalkylphosphonates. However, a literature search reveals no approaches to polymerize fosfomycin or derivatives thereof.
As noted in Chapter 2.1.2, it is absolutely neccessary to use monomers without any abstractable protons in a living anionic polymerization. Contrary to the previous syntheses of esterified fosfomycin described above, in the current work, a new pathway was investigated, which uses the fosfomycin salt as starting material. Parallel to the described chemical syntheses in the present work, attemps where made at the Fraunhofer Institute for Interfacial Engineering and Biotechnology (IGB) to convert fosfomycin respectively its disodium salt quantitively to fosfomycin diesters via an enzymatic or fermentative approach. It was found that via an enzymatic or fermentative pathway only monoesters can be achieved. A detailed description of the experiments can be found in the report of the BMBF project: "Neue Polyurethane auf Basis flammgeschützter Polyole" (support code: 03FPF00021). In the following chapter, the chemical syntheses of fosfomycin dimethyl- and diethylesters starting from the disodium salt are described.

4.2 A Novel Approach for the Synthesis of Fosfomycin Esters as Polymerizable Phosphonic Compound

Initially, the conversion of the fosfomycin disodium salt (Na-Fos) to the corresponding dimethylester (1,2-DiMe-Fos) via the free acid (Fos) (refer to Figure 4.20) was examined. In a first approach, Na-Fos was converted in methanol (MeOH) with methane sulfonic acid (MSA) at low temperature (0 °C) to the free acid and subsequently reacted at ambient temperature with trimethylsilyl diazomethane (TMS-diazomethane) **(11)**. In an alternative approach, a methylated polymer-bound triazene (loading: 0.001 mol $\cdot$ g^{-1}) was used instead of TMS-diazomethane **(12)**, which led to esterification of phosphites in previous attemps.[189] Both approaches are displayed in Figure 4.20. In both cases, a white solid precipitated after addition of MSA, which could be assigned to the sodium salt of MSA. Such an observation suggested that there was a conversion to the free acid (Fos). Nevertheless, in both cases, no conversion to the expected 1,2-DiMe-Fos could be observed under the chosen conditions after work-up via NMR measurements. The pure fosfomycin does not seem to be transformable directly to the diester under the employed conditions.

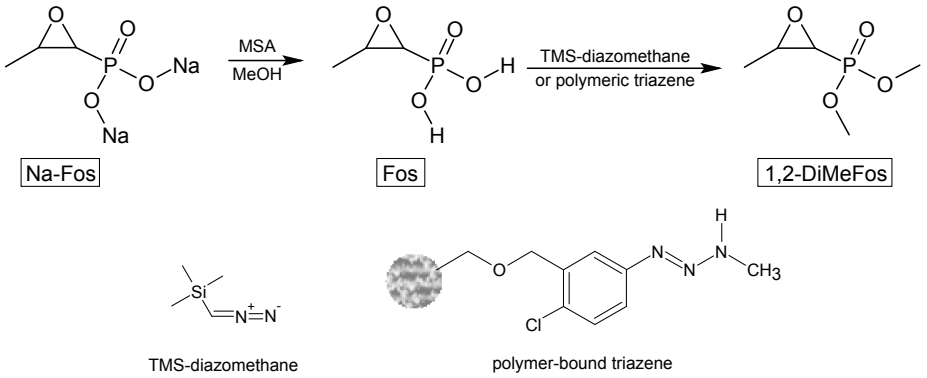

Figure 4.20: Esterification of Na-Fos with TMS-diazomethane, respectively, methylated triazene resin.

In addition, the implementation of the Steglich esterification **(13)** using dicyclohexylcarbodiimide (DCC) as coupling reagent and 4-(dimethylamino)pyridine (DMAP) as catalyst (Figure 4.21) in dichloromethane (CH_2Cl_2), respectively in a mixture of chloroform ($CHCl_3$) and acetonitrile, showed no conversion to the dimethyl- nor diethylesters of fosfomycin. NMR measurements reveal the preservation of the epoxy ring, however no conformation to the esters.

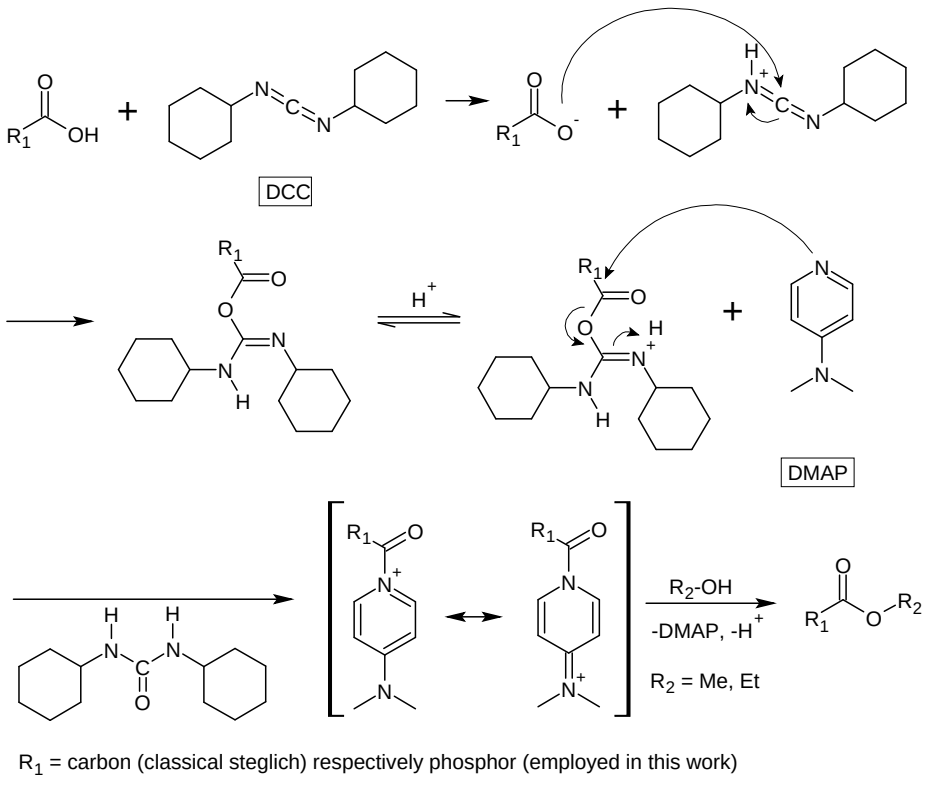

Figure 4.21: Reaction scheme of the esterification via the Steglich esterification.

Therefore, in later approaches conversion of the fosfomycin salt to the corresponding dimethylester (1,2-DiMe-Fos) respectively diethylester (1,2-DiEt-Fos) via the phosphonic acid dichloride (Figure 4.22) was investigated. In this process, the influence of different chlorination agents and solvents was examined. Firstly, the esterification was carried out under mild conditions, using an exchange resin in the form of a previously prepared chlorinated silica gel (SiO_2-Cl) **(14)**. However, no conversion to the corresponding diesters using acetonitrile respectively chloroform as solvents could be detected via NMR measurements.

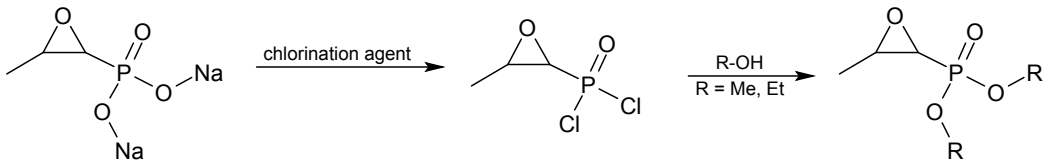

Figure 4.22: Esterification of Na-Fos via phosphonic acid dichloride.

In later approaches, common chlorination agents such as thionylchloride ($SOCl_3$) and phosphorylchloride ($POCl_3$) were evaluated. Since these chlorination agents decompose in aqueous solutions, only anhydrous solvents could be used. Therefore, aprotic pyridine became the solvent of choice, because it is slightly alkaline and forms a crystalline hydrochloride with the evolving hydrochloric acid, which can be removed by filtration from the reaction solution.
Following the synthesis of carboxylic esters via carboxylic acid chloride, it was first examined whether the acid dichloride of the fosfomycin can be synthesized using thionylchloride ($SOCl_2$) **(15)**. Since the phosphonic acid dichloride is unstable in solution, it must be directly converted to 1,2-DiMe-Fos, respectively 1,2-DiEt-Fos, without isolation of the intermediate stage. The short-chain primary alcohols methanol (MeOH) and ethanol (EtOH) as well as sodium methanolate (NaOMe) were used. However, the analytical evaluation showed very high proportion of side products and only traces of the epoxy ring. A clear conversion to the diesters could not be observed. Therefore, the reaction with $SOCl_2$ was discarded and replaced by the more reactive phosphorylchloride ($POCl_3$) **(16)**. Using the short-chain primary alcohols MeOH and EtOH as alkylating agents, conversion of the fosfomycin disodium salt to both corresponding fosfomycin diesters could be evidenced via NMR spectroscopy, however with very low yields (< 6 %). The amount of difficult to remove by-products, was considerable (Figure 4.23). The integrals of the characteristic resonances of the epoxy ring system (proton 1 to 3) were consistent with the expected values in all three ^{1}H NMR spectra (see Figure 4.23). Resonances 4 and 5, which can be assigned to the ester groups, were not in accordance with the expected

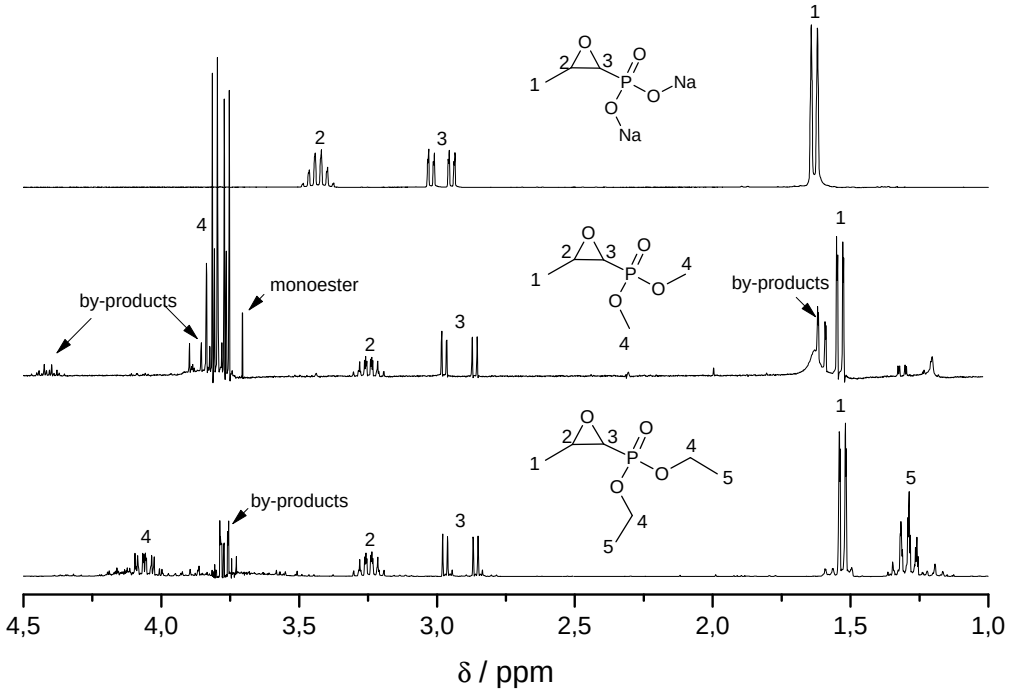

Figure 4.23: Comparision of ^{1}H NMR measurements of the esterification of Na-Fos (upper line) via phosphoric acid chloride using $POCl_3$ and MeOH (middle line), respectively, EtOH (lower line). Resonances are assigned to the respective structure. Na-Fos measured in D_2O, 1,2-DiMe-Fos and 1,2-DiEt-Fos measured in $CDCl_3$ due to solubility properties. There is a shift to higher field for Na-Fos due to the change in the solvent system. ***Na-Fos***: 3.43 ppm (m, 1H, CH = proton 2) = 1, 2.98 ppm (dd, 1H, CH, $^2J_{H-H}$ = 5.2 *Hz*, $^2J_{P-H}$ = 13.4 *Hz* = proton 3) = 0.98, 1.59 ppm (d, 3H, CH_3, ^2J = 5.6 *Hz* = proton 1) = 2.93; ***1,2-DiMe-Fos***: 3.84 ppm (m, 6H, CH_3 = proton 4) = 8.28, 3.28 ppm (m, 1H, CH = proton 2) = 1, 2.88 ppm (dd, 1H, CH, $^2J_{H-H}$ = 4.6 *Hz*, $^2J_{P-H}$ = 27.3 *Hz* = proton 3) = 1.01, 1.63 ppm (d, 3H, CH_3, $^2J_{H-H}$ = 5.5 *Hz* = proton 1) = 3.28; ***1,2-DiEt-Fos***: 4.06 ppm (m, 4H, CH_2, proton 4) = 1.54, 3.30 ppm (m, 1H, CH = proton 2) = 1, 2.88 ppm (dd, 1H, CH, $^2J_{H-H}$ = 4.3 *Hz*, $^2J_{P-H}$ = 27.3 *Hz* = proton 3) = 0.99, 1.59 ppm (d, 3H, CH_3, $^2J_{H-H}$ = 5.8 *Hz* = proton 1) = 2.96, 1.30 ppm (m, 6H, CH_3, proton 5) = 2.46.

values of six protons for the methyl groups in 1,2-DiEt-Fos (resonance 4) respectively four protons for the CH_2 and six protons for the CH_3 groups of 1,2-DiEt-Fos (resonance 4 + 5). Using sodium methanolate as the alkylating agent, the ratio shifted even further in the direction of by-products. Hence, no further experiments were carried out with alkoxides.

As $POCl_3$ is highly hygroscopic and hydrolysis sensitive, the by-products may be due to hydrolysis of the components or reaction of phosphorester groups with traces of water. To reduce the amount of by-products, $POCl_3$ was generated in situ using phosphorus pentachloride (PCl_5) in combination with oxalyl chloride in pure pyri-

dine **(17a)**. Via such an experimental approach and after multiple purification steps (neutralization with $NaHCO_3$, repeatedly extraction with $CHCl_3$ and evaporation in vacuo), the NMR data indicated a conversion to the corresponding diesters of fosfomycin. The yields were very low (9 % for 1,2-DiMe-Fos, respectively 10 % for 1,2-DiEt-Fos) and a monoester/diester ratio of at least 4/25 was determined. For clearity, only the ^1H NMR spectrum of 1,2-DiMe-Fos is shown in Figure 4.24 with an enlargement of the splitting of the ester resonances. As shown in Figure 4.24, the diester resonances split into a doublet of doublets (dd) due to the proximity to the phosphorus atom. Next to the two doublets of the diester, an additional doublet of the monoester is seen, which superimpose with one of the diester doublets. The coupling constants show that this is not a by-product, but the monoester. In addition, the signals of the H-2 are shifted to higher field compared to H-3. Due to the electron-withdrawing effect of the phosphoryl group the contrary was expected. Such an effect may be due to an anisotropic shielding effect caused by the phosphoryl group as described for thiophosphoryl groups by Chesnut.[190]
Due to the fact that there is an increase in hydrophobicity from Na-Fos to the monoester and finally diester, different solvent mixtures and buffers were tested, to reach full conversion to the diesters (Table 4.1). Furthermore, a reduction of the amount of pyridine or even complete substitution of the noxious pyridine, which is difficult to separate from the reaction medium, was attempted. The solvent substitutes show comparable polarity compared to pyridine, but have no buffer effects. Therefore, triethylamine or imidazole were added as buffers. It could be shown that the amount of pyridine can be reduced, yet not substituted completely. Without pyridine no conversion could be obtained. Therefore, a two solvent system is neccessary for the formation of diesters, with preservation of the epoxy ring.

solvent	**buffer**	**preservation of oxirane/formation of diester**
pyridine	/	+ / +
$CHCl_3$	/	- / -
DMF	imidazole	- / -
DMSO	imidazole	work up not possible
acetonitrile	imidazole	- / -
$CHCl_3$	imidazole	- / -
$CHCl_3$	triethylamine	- / -
acetonitrile	triethylamine	- / -
$CHCl_3$	pyridine	+ / +

Table 4.1: Influence of solvent/buffer combinations on epoxy ring preservation and esterification.

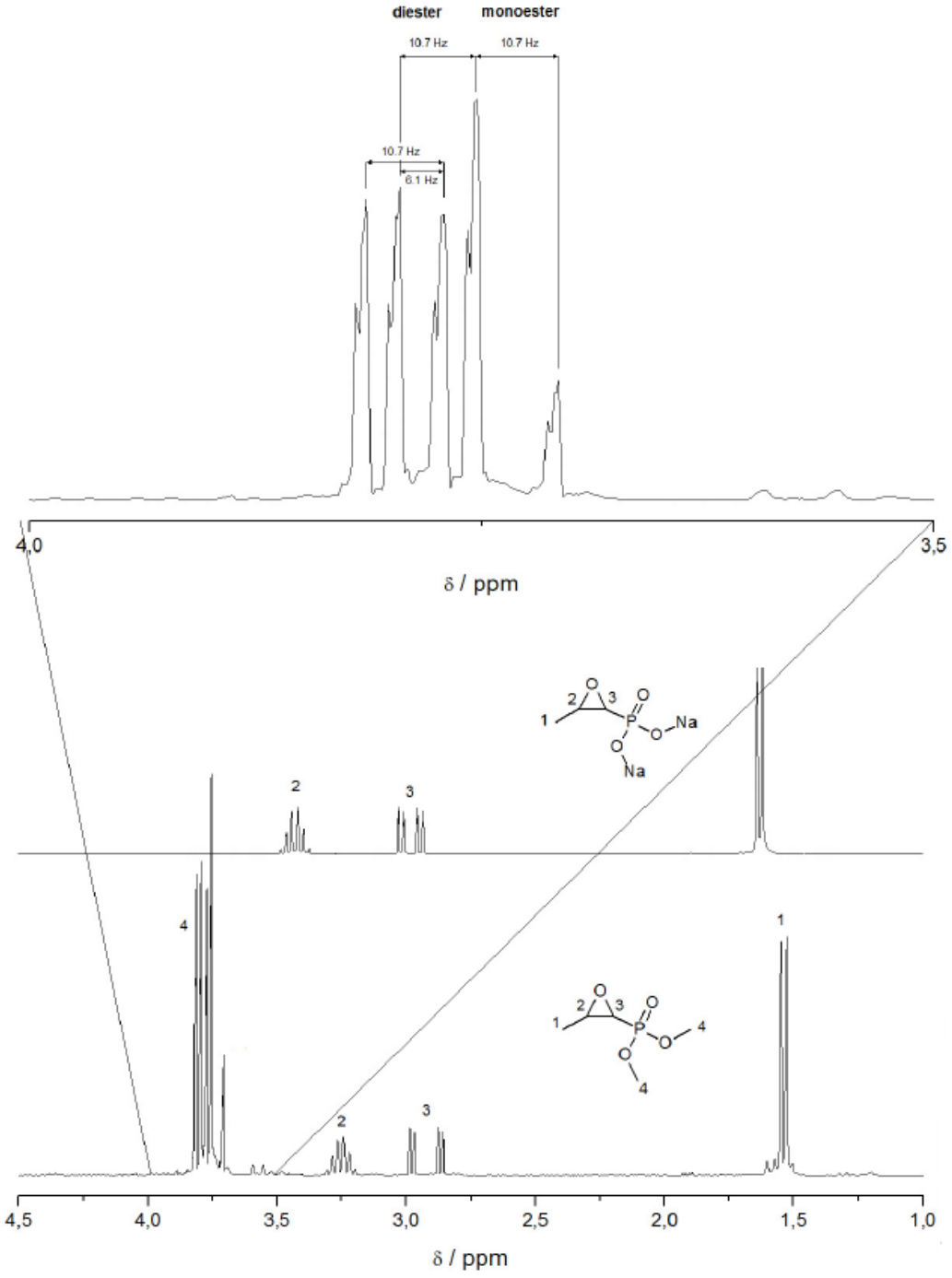

Figure 4.24: Comparision of ^{1}H NMR measurements of the esterification of Na-Fos (upper line) via phosphonic acid dichloride using PCl_5/oxalyl chloride and MeOH (lower line). Characteristic resonances are assigned to the respective structure. Na-Fos measured in D_2O, 1,2-DiMe-Fos measured in $CDCl_3$ due to solubility properties. There is a shift to higher field for Na-Fos due to the change in the solvent system. Coupling constants are shown for the ester resonances close to 3.8 ppm.

By selection of a suitable second phase system, it was attempted to reduce the pyridine content and to reach a product increase while shifting the reaction balance at the same time. Chloroform ($CHCl_3$) was chosen as the second phase, due to the lower hydrophilicity of the evolving diesters compared to the fosfomycin salt. The yields could be increased up to 25 % by the use of a 1 : 2 mixture of $CHCl_3$/pyridine. The reduction of the pyridine content leads not only to raised yields, yet also has economic advantages ($CHCl_3$: 54 EUR/liter; pyridine: 141 EUR/liter). Moreover, the reaction process is strongly shortened due to less extraction steps.
By further lowering and holding the reaction temperature close to -10 °C during addition of the solid PCl_5 and increase of total reaction time of up to 20 h **(17b)**, a further optimization of up to 97 % (1,2-DiMe-Fos) and 99 % (1,2-DiEt-Fos) could be observed via NMR spectroscopy. Both diester spectra are shown in Figure 4.25 with assignment of the resonances and integration values.

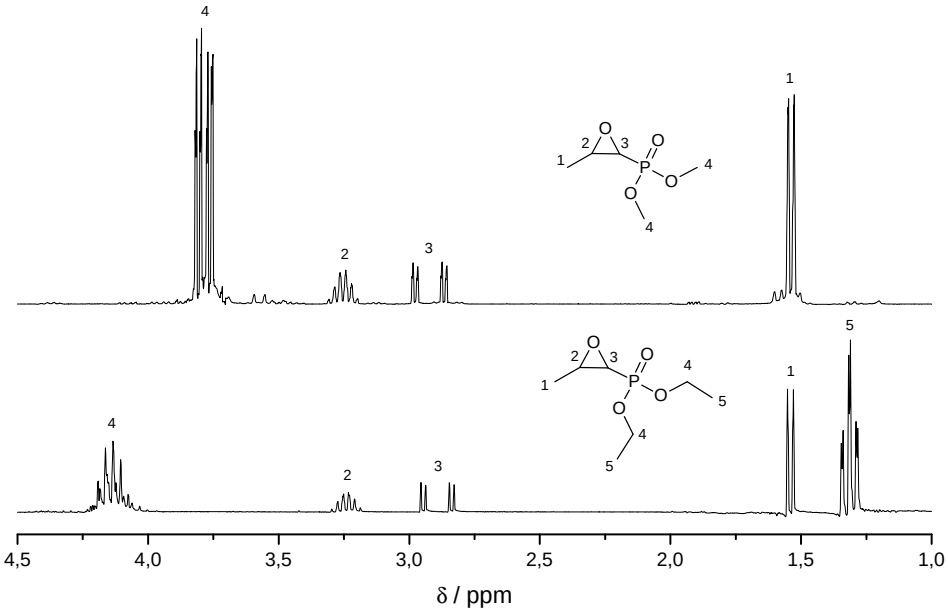

Figure 4.25: ^{1}H NMR spectra of 1,2-DiMe-Fos (upper line) and 1,2-DiEt-Fos (lower line) after optimization of the reaction conditions: 1 : 2 ratio $CHCl_3$ / pyridine, $T <$ -10 °C. The resonances are assigned to the respective structure. Both spectra are recorded in $CDCl_3$. ***1,2-DiMe-Fos***: 3.80 ppm (m, 6H, CH_3 = proton 4) = 6.04, 3.26 ppm (m, 1H, CH = proton 2) = 1, 2.86 ppm (dd, 1H, CH, $^2J_{H-H}$ = 4.6 *Hz*, $^2J_{P-H}$ = 27.3 *Hz* = proton 3) = 1.02, 1.53 ppm (d, 3H, CH_3, $^2J_{H-H}$ = 5.5 *Hz* = proton 1) = 3.16; ***1,2-DiEt-Fos***: 4.16 ppm (m, 4H, CH_2, proton 4) = 4.06, 3.24 ppm (m, 1H, CH = proton 2) = 1, 2.83 ppm (dd, 1H, CH, $^2J_{H-H}$ = 4.3 *Hz*, $^2J_{P-H}$ = 27.3 *Hz* = proton 3) = 1.01, 1.54 ppm (d, 3H, CH_3, $^2J_{H-H}$ = 5.8 *Hz* = proton 1) = 3.01, 1.30 ppm (m, 6H, CH_3, proton 5) = 5.98.

As described in Chapter 2.1.2., a purity of $\leq$ 99 % is not sufficient for living anionic ring-opening polymerization, since even traces of the respective phosphonic monoester or phosphonic acid cause chain termination. In addition, as indicated by the brown color of the product solution (see middle picture in Figure 4.26), phosphorus salts were still present in the solution, which cannot be detected via NMR analysis. Further purification strategies were therefore explored.

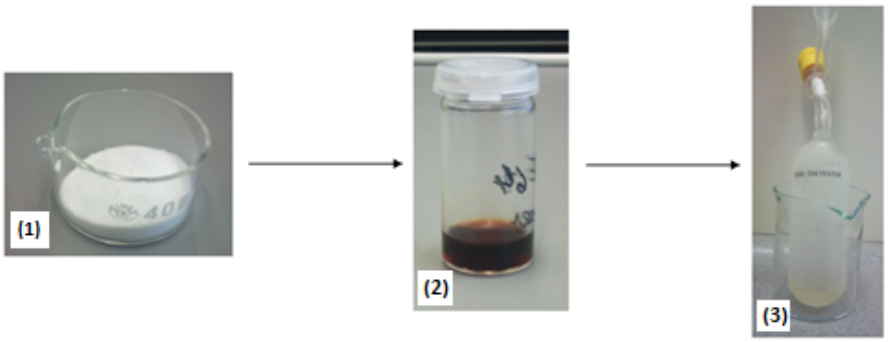

Figure 4.26: Pictorial representation of Na-Fos (1) and 1,2-DiEt-Fos before (2) and after (3) distillation.

After purification over a standard silica column, NMR and infrared (IR) spectra showed almost exclusively the previously observed characteristic resonances of the by-products and no resonances of the epoxy ring, suggesting that by interaction with the column, an opening of the epoxy ring was initiated. Purification using a standard silica column was thus not possible. Due to high costs for other commercially seldom used column materials, purification by column chromatography was not pursued further. The procedure described in the literature by means of purification of phosphorus esters via vigreux distillation under reduced pressure (p) and slightly elevated temperature (T) [191], did not work under the selected conditions ($T \leq 60$ °C, $p \geq 10^{-2}$ bar), since the synthesized diesters have a very high vapor pressure. Therefore the conditions were exchanged. It could be shown that two distillation steps are necessary to achieve a separation of the desired diesters from side products in the required purity **(18)**. For both distillations a pressure of $\leq 3 \cdot 10^{-3}$ bar and a temperature of $T \geq 90$ °C (1,2-DiMe-Fos) respectively $T \geq 110$ °C (1,2-DiEt-Fos) was applied. As drying agent calcium hydride (CaH_2) was used in the first distillation, wherein in the second distillation *iso*-butylaluminum ($^{i}Bu_3Al$) was employed. Pictorial representation of the fosfomycin disodium salt, the diester solution before and after distillation are shown in Figure 4.26. The pure fosfomycin diesters were slightly yellowish and were stored in a refrigerator under argon until further use. An overview about all reactions performed in the context of the synthesis of dialkyl fosfomycin esters are shown in **Appendix A1**.

4.3 Anionic Polymerization of Fosfomycin Esters and Derivatives

As part of the current work, different influences (substituents on the epoxy ring, concentration ratios, temperature, reaction time) where examined for the living anionic ring-opening polymerization of different fosfomycin esters and derivatives. As a first step, the required apparatus for the living anionic polymerization was designed, custom-made and built. All components fulfilled the special requirements, such as high vacuum and chemical resistance. A picture of the apparatus with assignment of the relevant parts is shown in Figure 4.27.

Figure 4.27: Apparatus for the living, anionic polymerization containing (from left to right) two cold traps and Dewar flasks, a 2-liter storage glas vessel for extra dry toluene, several flanges with Young taps and the reaction vessel with one connection to the Schlenk line and four access points for the connection of compound vessels.

In general, the epoxy monomers for the anionic polymerization used in the literature have a terminal epoxy ring with little steric hindrance, such as alkylene oxides. To determine the influence of the substituents on the ring, both mono- and disubstituted phosphorus epoxy monomers where employed. As monosubstituted epoxy monomers, commercially available methylated, respectively ethylated, terminal fos-

fomycin derivatives were applied (bottom row in Figure 4.28). As disubstituted epoxy monomers, the fosfomycin diesters synthesized in Chapter 4.2 were used (top row in Figure 4.28).

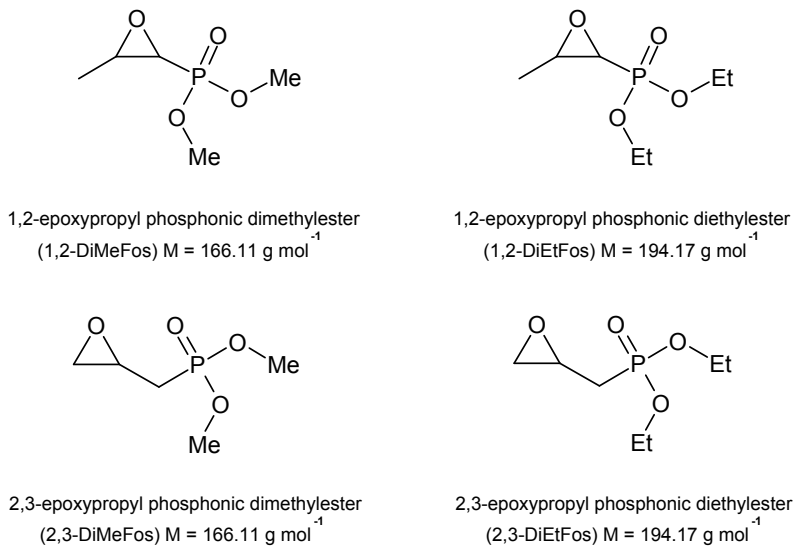

Figure 4.28: Structural formulas of the employed fosfomycin diester and derivatives.

Polymers with structures, as shown in Figure 4.29 can be potentially formed using the two fosfomycin diesters and two corresponding derivatives thereof. Therefore, the influence of the connection to the polymer backbone (comparison of mono- and disubstituted monomers to each other) can be investigated with regard to the polymerization behavior. In addition, the influence of the phosphorus ratio (comparision of methyl to ethyl monomers) on the flame retardancy of the obtained polymers can be evaluated.

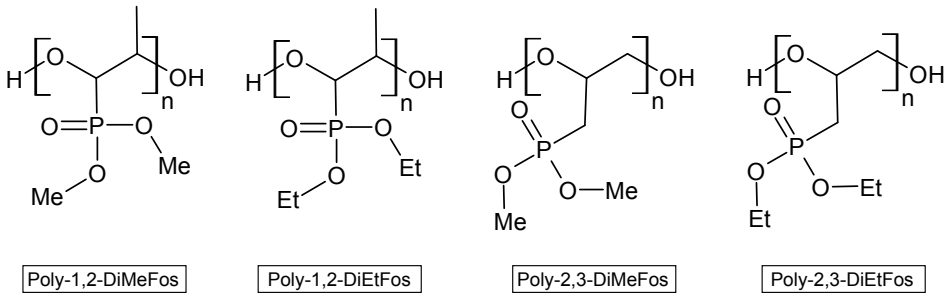

Figure 4.29: Structures of phosphorus-containing polyols via anionic ring-opening polymerization of fosfomycin diesters prepared in the current work and commercially available fosfomycin derivatives.

Preliminary tests for the synthesis of phosphorus-containing polyols were carried out with epichlorohydrin as reference monomer. Epichlorohydrin shows similar structural characteristics and also exhibits an electron-withdrawing group (Cl) as the fosfomycin ester derivatives (phosphonic ester) and was polymerized by Carlotti *et al.* via an anionic ring-opening polymerization mechanism as shown in Figure 4.30. In the study of Carlotti, epichlorohydrin was reacted with an ammonium/aluminum complex in a living anionic ring-opening polymerization. [31]

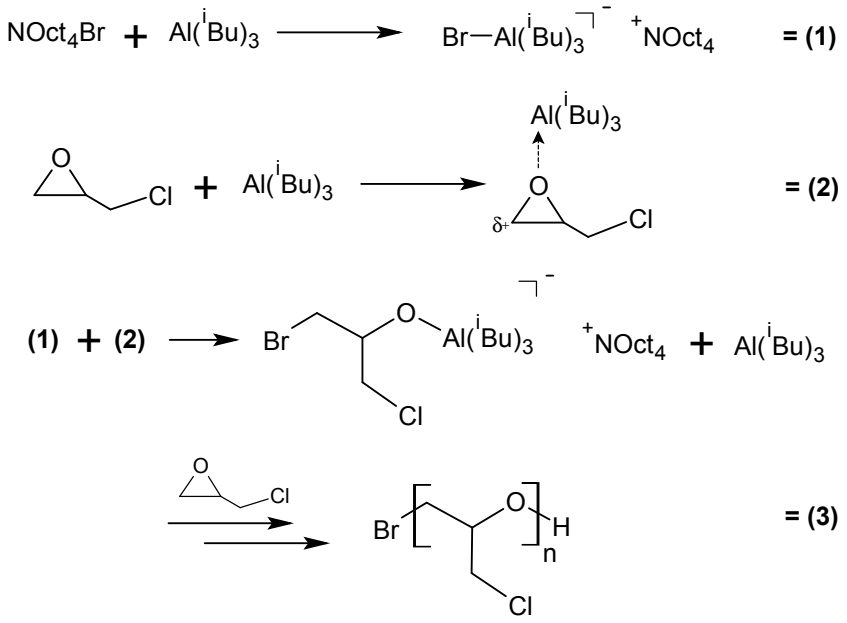

Figure 4.30: Adapted reaction scheme for the anionic ring-opening polymerization mechanism described by Carlotti *et al.*[31] 1) formation of the initiation complex; 2) activation of the monomer; 3) initiation, propagation and termination of the polymerization.

Following the reaction conditions by Carlotti *et al.*, polyepichlorohydrin (PEPI) could be synthesized with molecular weights from 15 900 to 41 500 g·mol^{-1} and polydispersities (PDI) of 1.13 to 1.32. As an example, the SEC measurements of one polyepichlorohydrin dissolved in tetrahydrofuran (THF) with M_n = 15 900 and PDI = 1.13 is shown in Figure 4.31.

In first attempts, implementation of the previously synthesized fosfomycin diesters and their derivatives using the reaction conditions of Carlotti *et al.* were performed **(19)**. However, no polymerization was observed. Even by variation of the initiator/catalyst concentration and increase of the reaction temperature from -18 °C to ≤ 40 °C (see **Appendix A2**), no polymerization could be achieved.

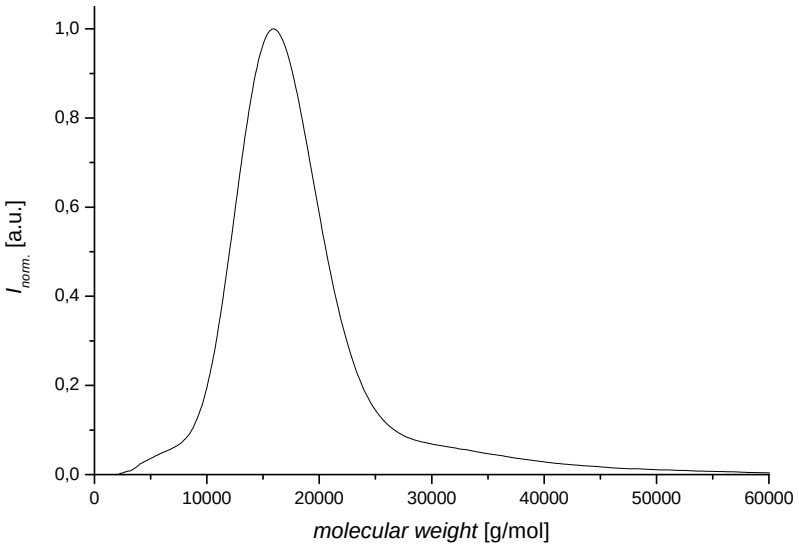

Figure 4.31: Polyepichlorohydrin dissolved in THF with M_n = 15 900 g · mol^{-1} and PDI = 1.13 prepared via anionic ring-opening polymerization using the reaction conditions described by Carlotti *et al.*[31]

In order to exclude low temperatures as the reason for the lack in initiation of the examined fosfomycin diester derivatives in the anionic polymerization, DSC measurements were carried out. With these measurements, both the optimum temperature range of the initiation of the phosphorus-containing monomers as well as the optimum catalyst/initiator ratio in the anionic polymerization were investigated. In addition, the thermal stability of the fosfomycin diesters and derivatives were examined. The DSC curves of 2,3-DiEt-Fos reacted with different catalyst/initiator ratios are shown in Figure 4.32 and are representative for all fosfomycin diesters and derivatives. Therefore, the following analyses are conducted only with 2,3-DiEt-Fos. The DSC studies were carried out directly in the DSC sample containers. In order to ensure approximately the same experimental conditions as in the vessel of the anionic polymerization apparatus, the monomers, the pre-dried toluene (see Chapter 6.3. synthesis **(19)**), the catalyst solution (25 w% $^{i}Bu_3Al$ in toluene) and the initiator (pre-dried) were transferred into a glove box, filled in the DSC sample containers and sealed airtight with exclusion of oxygen and water. Figure 4.32 shows an overview of the DSC measurements as a function of the catalyst/initiator ratio. A doubling of the concentration of catalyst ($^{i}Bu_3Al$) is shown in the horizonal column (graphics A to B, respectively, graphics C to D). In the vertical, the samples were applied with the same concentration of catalyst, however, higher initiator ($NOct_4Br$) quantities (A to C, respectively, B to D) were used. As shown in the DSC graphs, with increasing catalyst ratio (B and D) an exothermic peak around 200 °C appears.

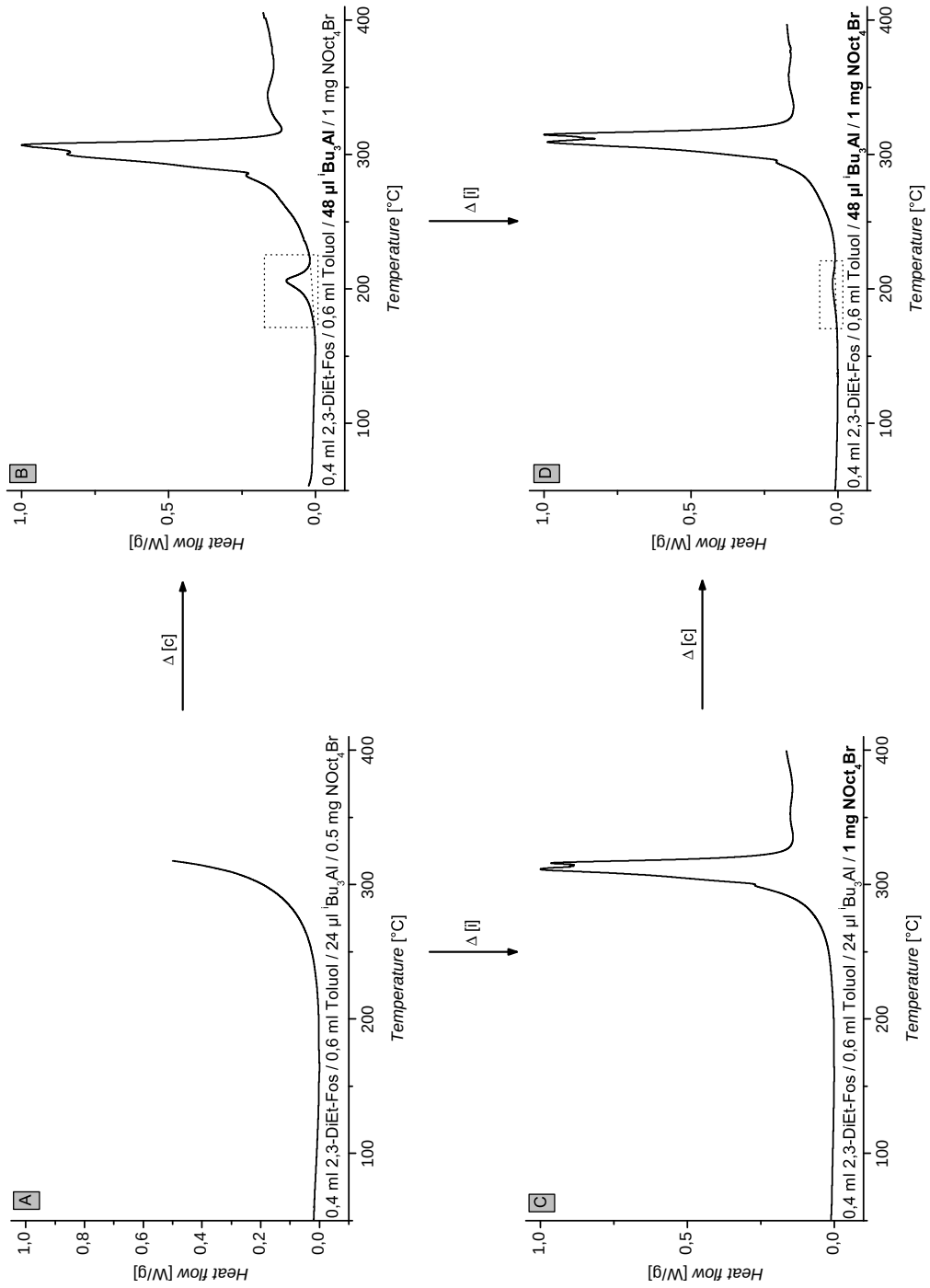

Figure 4.32: DSC experiments of 2,3-epoxypropyl phosphonic diethylester (2,3-DiEt-Fos) reacted with different catalyst/initiator ratios to determine the polymerization ability, as well as the thermal behavior, of the examined fosfomycin diesters.

It was also shown that the exothermic reaction decreases again with increasing initiator concentration (graphics D). The exothermic peaks in the DSC measurements could not be unambiguously assigned to polymerization or decomposition of the examined phosphorus diester. Assuming that the exothermic peak at 205 °C (graphics B) is due to polymerization, a hindered activation of the anionic polymerization must be assumed. In addition it can be observed that the fosfomycin diesters and derivatives thereof are thermally very stable since up to a temperature of around 307 °C, no exothermic or endothermic peaks are visible that would indicate a decomposition.

In view of the probably high activating energy neccessary for the initiation of the investigated phosphorus-containing monomers and at the same time high thermal stability, different sets of experiments were undertaken with the ethylated fosfomycin derivative 2,3-DiEt-Fos. 2,3-DiEt-Fos should exhibit a higher activity towards ring-opening due to its terminal epoxy ring compared to the fosfomycin diesters prepared in Chapter 4.2. Based on the DSC measurements (Figure 4.32), the ratio of 0.4 mL 2,3-DiEt-Fos, 0.6 mL toluene, 48 μL $^{i}Bu_3Al$ and 0.5 mg $NOct_4Br$ was used for the following test series. Both the temperature (25 to 160 °C) and the reaction time (2 h to 2 weeks) were increased. The anionic apparatus mentioned above could not be used for reaction temperature of up to 160 °C. On the one hand, the glas wall of the reaction vessel is too thick in order to ensure a quick and uniform temperature distribution during heating. On the other hand, a very high solvent pressure builds up above 110 °C (boiling point of toluene). Therefore, these reactions were accomplished in a glove box using a high pressure tube. In additional experiments 1,4,7,10,13,16-hexaoxacyclooctadecane (= Crown ether [18]-crown-6) was added to improve the ion complexation. Nevertheless, no polymerization could be obtained. A full overview about the applied reaction conditions is shown in **Appendix A2**.

Since even at high temperatures and increased reaction times, no polymerization was observed, other causes for the unreactivity of the fosfomycin esters had to be considered. Due to the high affinity of aluminum to oxygen [192], a coordinative ligation of the aluminum to the P=O double bond was envisioned. Two potential ligations are shown in Figure 4.33 in addition to the assumption of Carlotti *et al.*

The coordinative access to both the oxygen of the epoxy ring, as well as to the oxygen of the P=O double bond (see right structure in Figure 4.33), is sterically favored, through the formation of a 6-membered structure. With the assumption of coordinative ligation of the aluminum to both the oxygen and the epoxy ring, an anionic ring-opening polymerization should be possible under comparable conditions as described by Carlotti *et. al.* However, as described before, even at high temperatures no polymerization is observed. Therefore, the assumption of the coordination

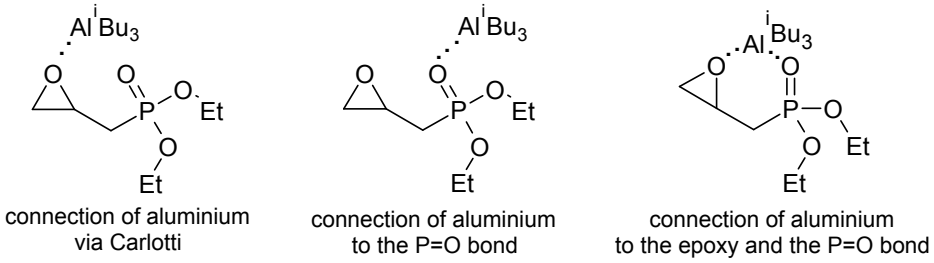

Figure 4.33: Possible connections of aluminium to the 1) epoxy (Carlotti); 2) the P=O bond of the phosphorus diester; 3) the epoxy and P=O bond.

of aluminum only to the P=O double bond is more likely (see middle structure in Figure 4.33). Given the assumption of the coordinative ligation of the aluminum only to the P=O double bond, the use of a "catalytic amount" of more than one equivalent would be necessary, to catalyze the polymerization, because the vast majority of the catalyst is connected to the P=O double bond and therefore no longer available for the ring-opening reaction. In order to prove the assumption of the coordinative ligation of the aluminum only to the P=O double bond, further experiments were carried out with the addition of a catalyst/initiator excess (1.1 eq). Nevertheless, only by heating to $\geq$50 °C for at least a few minutes and reaction times of at least 3.5 h (refer to bold lines in **Appendix A2**), an insoluble white solid precipitated. Due to insolubility of the product, neither SEC nor NMR analysis could be performed. Instead, IR spectroscopy was applied to analyze the structure of the powder. As seen in Table 4.2 and Figure 4.34 the characteristic P-O-C resonances (802, 950 and 1016 cm^{-1}) are both recognizable in the starting material (2,3-DiEt-

sample	**wavenumer [cm^{-1}]**	**bond allocation**	**vibration type**
2,3-DiEt-Fos	802	P-O-C	symetrically stretching
	950	P-O-C	asymetrically stretching
	1016	P-O-C	symetrically deformation
	1250	P=O	stretching vibration
Poly-Fos	803	P-O-C	symetrically stretching
	957	P-O-C	asymetrically stretching
	1019	P-O-C	symetrically deformation
	≈3000	C-O-H (backbone)	symetrically deformation

Table 4.2: Overview of the characteristic wavenumbers of 2,3-DiEt-Fos and Poly-Fos measured by IR spectroscopy.[164]

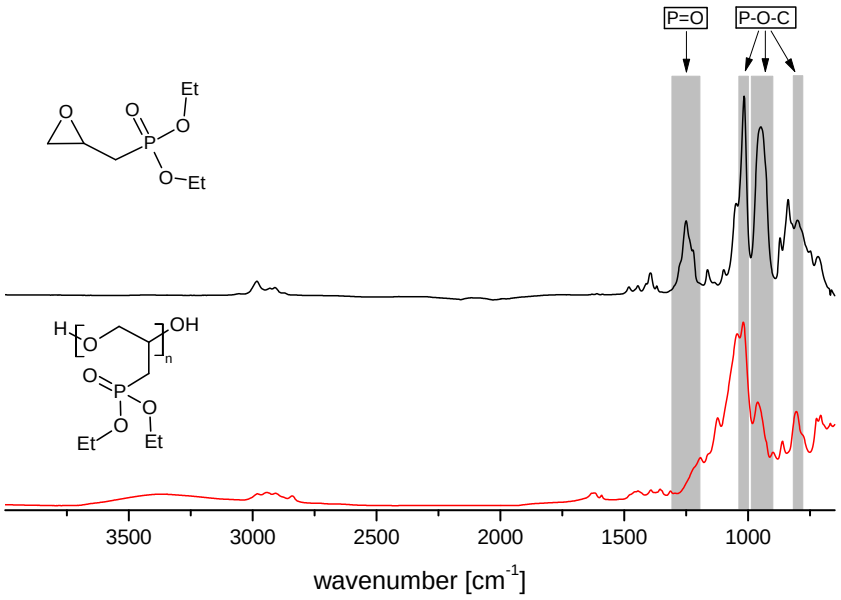

Figure 4.34: IR analysis of 2,3-DiEt-Fos and the polymeric fosfomycin with assignment of characteristic resonances of the phosphoric group. No characteristic P=O resonance in the spectra of Poly-Fos due to linkage of aluminium (P-O-Al) is present.

Fos) and in the product (Poly-Fos) spectra. Therefore, the white powder could be determined as an organic, phosphorus-containing compound. However, the P=O signal at 1250 cm^{-1} has disappeared in the product spectrum. The disappearance of the P=O double bond in the product spectrum in turn, indicates once more a connection of aluminum to the P=O double bond. Since even a coordinative bond of the aluminum to the P=O double bond could be strong enough to shift or eliminate the characteristic IR resonance at 1250 cm^{-1}, further evaluations had to be performed. If the catalyst ($^{i}Bu_3Al$) would only be bonded by a coordinative bond to the double bond of phosphorus, it would be possible to washed it away with an organic solvent, such as toluene. After washing several times with toluene, SEM/EDX and inductively coupled plasma (ICP) mass spectroscopy measurements were performed to determine the ratio of phosphorus to aluminum in the white powder. Both measurements exhibit an approximate 1:1 ratio of phosphorus to aluminum ($\approx$ 2.1 to 2.3 at%), as shown in Figure 4.35 for the SEM/EDX measurement. The almost identical at% values of aluminum and phosphorus indicate that the aluminum catalyst ($^{i}Bu_3Al$) has irreversibly attached to the P=O double bond and was thus consumed in the reaction, explaining the low yield of the anionic polymerization reaction of only $\approx$ 8 % when using 1.1 eq of $^{i}Bu_3Al$.

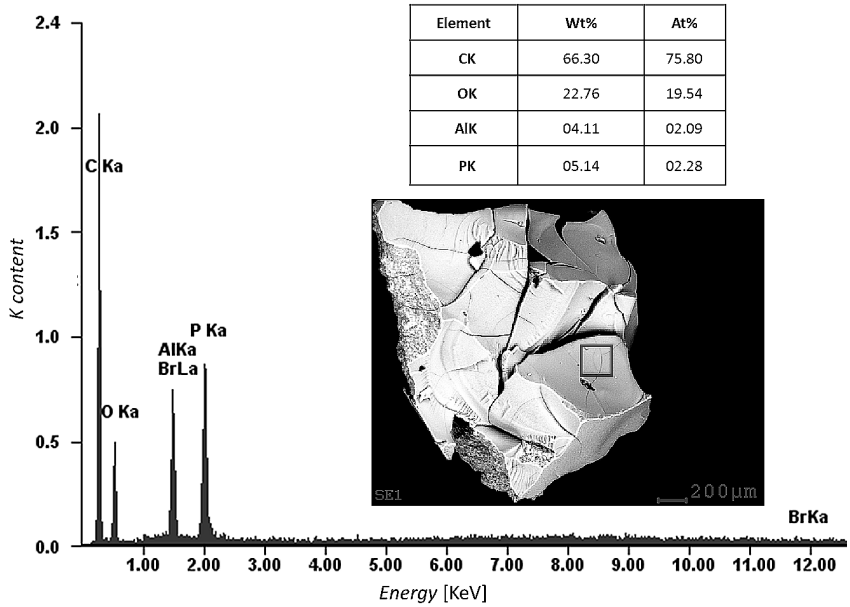

Figure 4.35: SEM/EDX measurement of poly(2,3-DiEt-Fos) showing the equimolar ratio of phosphorus and aluminum.

In the literature AlR_3 compounds were used as catalysts, for example, $AlCl_3$ in Friedel-Crafts-alkylation and -acetylation or Fries rearrangement. In the case illustrated in the current work, a variation of the Meerwein-Ponndorf-Verley reduction (Figure 4.36) can be assumed.[193]

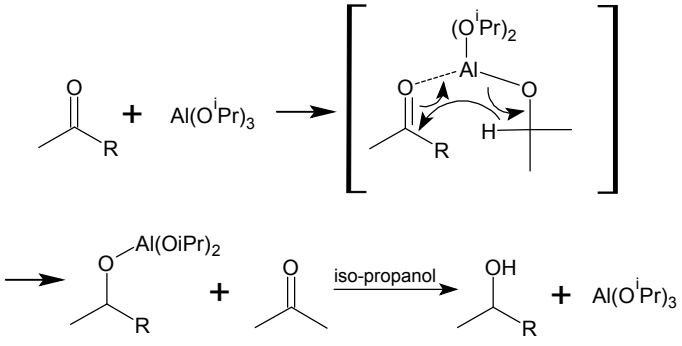

Figure 4.36: Reaction mechanism of the Meerwein-Ponndorf-Verley rearrangement between ketones/aldehydes and alcohols via a cyclic 6-membered transition state.

When transmitted to the epoxy phosphonate ester 2,3-DiEt-Fos and triisobutylaluminum (^{i}Bu$_3$Al) employed as a catalyst in the present work, the following reaction mechanism is assumed:

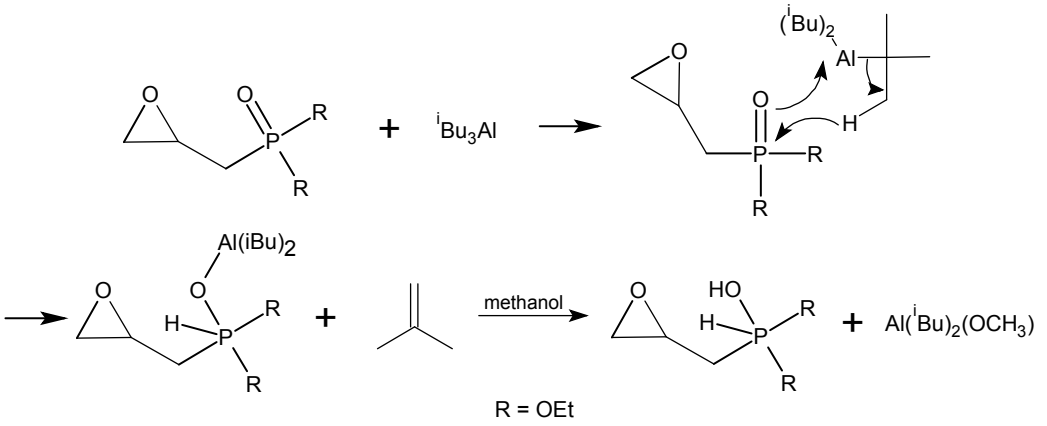

Figure 4.37: Schematic presentation of the assumed mechanism of the binding of aluminum to the P=O double bond with formation of a covalent binding between aluminum and oxygen and shift of one hydride.

Since no hydroxide ions are present in the solution during the anionic ring-opening polymerization, the aluminum catalyst may not be cleaved. Only after completion of the reaction by addition of methanol or water, the aluminum catalyst should be detached from the P=O double bond. Obviously, however, the affinity of aluminum towards the oxygen is strong enough to obtain even after repeated precipitation in methanol, a 1:1 ratio of aluminum to phosphorus in the white solid.
The polymer thus obtained would have the structure shown in Figure 4.38 with both aluminum covalently bound to the new P-O single bond and one transfered hydride.

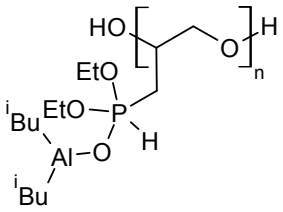

Figure 4.38: Assumed structure of polymerized 2,3-DiEt-Fos obtained by anionic ring-opening using $^{i}Bu_3Al$ as catalyst assuming a covalent Al-O-P bond and a rearrangement of one hydride.

Since the IR, SEM/EDX and ICP measurements cannot reveal the polymeric structure of the powder, matrix-assisted laser desorption/ionization in combination with a time-of-flight mass spectrometry (MALDI-TOF) was used (Figure 4.39). It could be shown that the white powder is an organic oligomer with a mass of approximately 1 600 g $\cdot$ mol $^{-1}$. Despite the assumption that aluminum is covalently

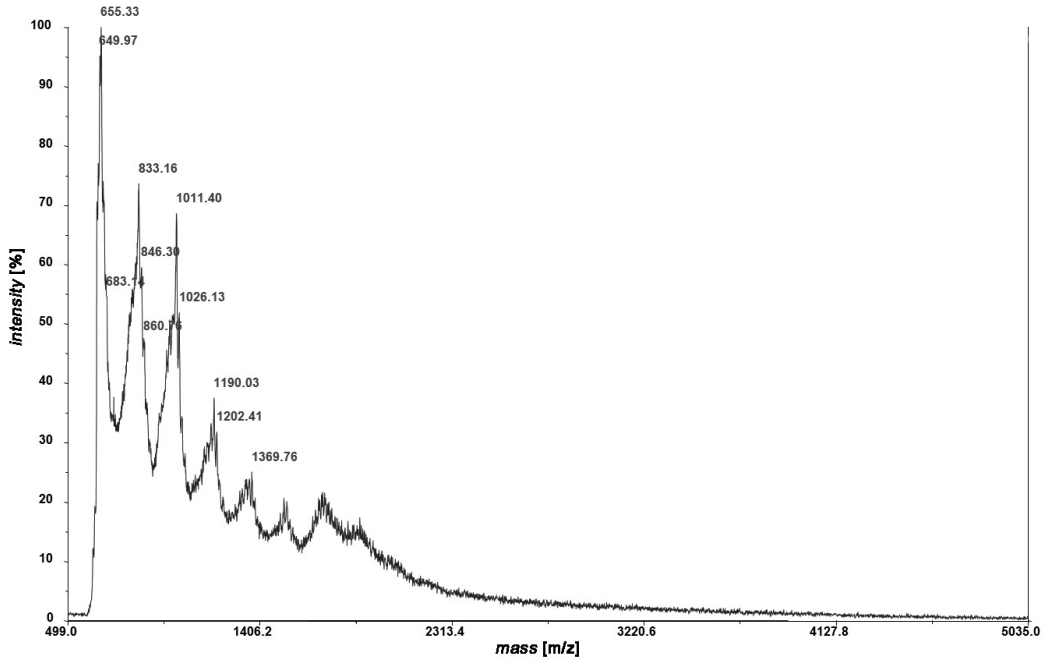

Figure 4.39: MALDI-TOF analysis of the poly(2,3-DiEt-Fos) measured in linear mode and by use of positive ions. The sample (10 mg $\cdot$ L^{-1}) was diluted in acetonitrile with 1 % trifluoroacetic acid (TFA) and mixed with 25 eq. of 2,5-dihydroxybenzoic acid (DHB).

bound to the polymer, the oligomer contains approximately four monomer units (one unit = 377.46 g $\cdot$ mol $^{-1}$). In addition, as can been seen in Figure 4.39, broad lines are observed in the MALDI-TOF spectrum. The broadening may be due to the ligation of aluminum to the P-O bond. This assumption is supported by the high laser intensity of 5200 (normally $\leq$ 4000) which had to be used to ionize the fragments.
To evaluate if even other metals bind to the P=O double bond, also experiments with a change of the catalyst/initiator system were performed employing butyllithium (BuLi), respectively $BF_3{\cdot}Et_2O$ and tin(II)-2-ethylhexanoate ($SnOct_2$) in combination with butanol (refer to **Appendix A3**). Employing butyllithium (BuLi) in dimethyl sulfoxide (DMSO), respectively toluene as solvents, no polymerization could be achieved. With the use of $BF_3{\cdot}Et_2O$ in THF, polymers could be obtained in several approaches. However, NMR and IR measurements reveal that it were not the expected phosphorus polymers, but rather the polymerized solvent tetrahydrofuran (poly-THF). In toluene no polymerization could be achieved. The reaction with $SnOct_2$/butanol finally resulted in a phosphorylated polymer, nevertheless consisting of two polymer blocks with different chain length (Figure 4.40).
Due to time constraints and because it is not a controlled/living system, with this initiator no further tests were carried out.

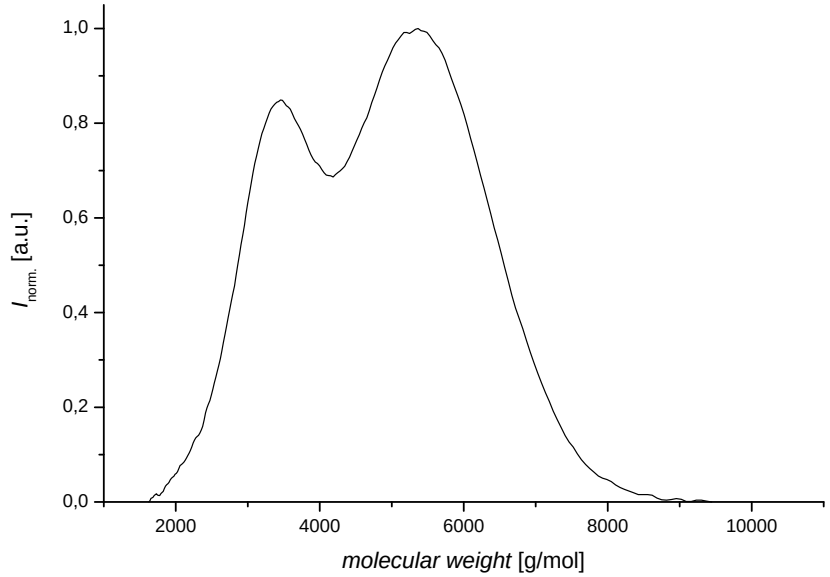

Figure 4.40: Polymerized 2,3-DiEt-Fos dissolved in THF with M_n = 4 100 g · mol^{-1} and PDI = 1.09 prepared via ring-opening polymerization using tin(II)-2-ethylhexanoate ($SnOct_2$) and butanol.

However, to use a controlled system and the fact that for other systems, such as 4-vinylbenzyl chloride (VBC), no homopolymerization, yet copolymerization, can be achieved [160], additional copolymerization experiments were performed (**Appendix A4**). Based on the successful polymerizations of epichlorohydrin, attempts were made to copolymerize 2,3-DiEt-Fos with epichlorohydrin by the mechanism described by Carlotti *et al.* (Figure 4.41).

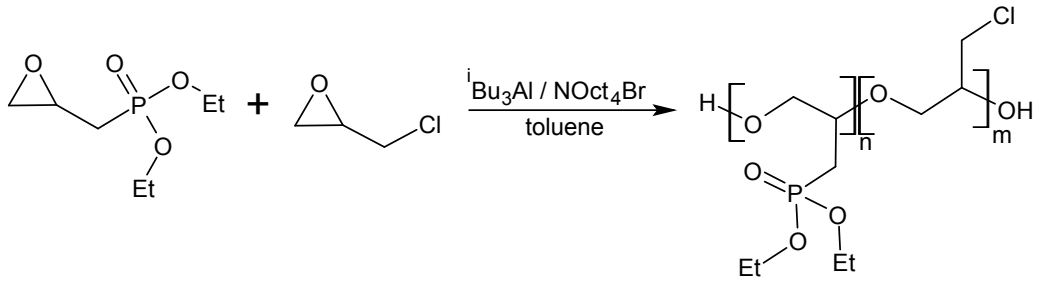

Figure 4.41: Reaction scheme of the copolymerization of 2,3-DiEt-Fos with epichlorohydrin.

The expected copolymers of epichlorohydrin and 2,3-DiEt-Fos would exhibit a lower phosphorus content than the homopolymer of 2,3-DiEt-Fos, however with the same polymer backbone. However, in the performed copolymerization reactions, variations of comonomer ratio, catalyst/initiator ratio and reaction time, showed no success in

terms of copolymerization. The polymers obtained (Figure 4.42), showed no characteristic resonances of the phosphorus ester groups in IR and NMR measurements. It must therefore be assumed that a homopolymerization of epichlorohydrin had take place. In addition, the obtained polymers exhibit high PDI (>2.3). Therefore, it could be shown that under the chosen conditions neither copolymerization of the fosfomycin ester and epichlorohydrin nor a living anionic polymerization could be achieved.

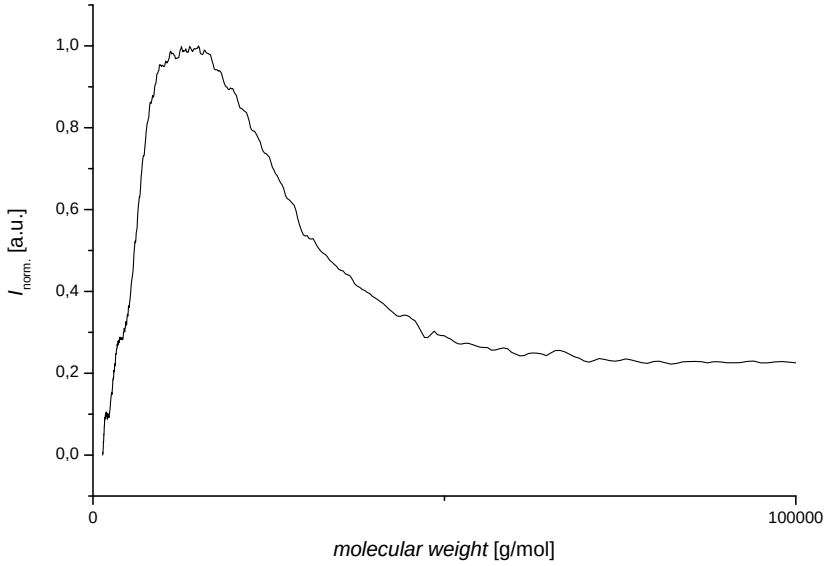

Figure 4.42: Copolymerized 2,3-DiEt-Fos with epichlorohydrin dissolved in THF with M_n = 10 000 g · mol^{-1} and PDI = 3.08 prepared via anionic ring-opening polymerization using the reaction conditions described by Carlotti *et al.*[31]

Due to all mentioned results, the living anionic polymerization was discarded as possible polymerization technique to obtain polymers with narrow molecular weight and well-defined functionalities. Tests on the effect of the double substitution on the ring using the fosfomycin diesters 1,2-DiMe-Fos and 1,2-DiEt-Fos prepared in Chapter 4.2 were not carried out due to the low polymerization ability of the investigated higher reactive phosphorus-containing monomer 2,3-DiEt-Fos.

4.4 Summary of Chapter 4

Different phosphorus esters (methyl, ethyl) of fosfomycin could be prepared starting with fosfomycin disodium salt without opening of the epoxy ring. After optimization of the reaction conditions (very slow addition of PCl_5, reaction temperature decrease, longer reaction times) and several purification steps (including repeated work up and

two times vacuum destillation), the dimethyl- and diethyl esters of fosfomycin were obtained in high purity.

In the subsection of the living anionic ring-opening polymerization of the obtained fosfomycin esters and commercially available derivatives therof, the reaction conditions chosen in the current work did not lead to a living anionic polymerization. This observation is attributed to the assumed irreversible connection of aluminum from the catalyst to the P=O double bond. The assumed hydride shift should have no effect on the low polymerization activity, since lithium aluminum hydride is often used in anionic polymerizations.[194] Since only $SnOct_2$ resulted in phosphorylated polymers, yet with low molecular weight and no living behavior, it is assumed that a living anionic polymerization of such phosphonic ester monomers is not possible using aluminum containing catalysts. Further experiments have to be performed using metal-free catalyst/initiator systems or even other tin compounds. Therefore, the objective to examine the different influences (substituents on the oxirane ring, concentration ratios, temperature, reaction time) on the polymerization behavior could not be achieved. In addition, the influence of the substituents on the ring (mono- respectively disubstituted) and the phosphonic ester groups (methyl or ethyl) on the thermal behavior and the flame retardancy of the synthesized (co)polymers could not be examined in the current work due to time constraints.

Chapter 5

Investigation of Flame Retardant Properties of Phosphorylated Polymers

The current chapter, describes the influences on a polymeric phosphorylated flame retardant prepared in the present study using the processing methods extrusion/molding and stirring. In addition, subsequent flame retardancy tests with the polymeric phosphorylated flame retardant incorporated into various polymer systems were examined.

As polymeric phosphorylated flame retardant, a powdered phosphorylated polystyrene copolymer was employed. The flame retardant PS-DPPP, shown in Figure 5.1, contains a polystyrene (PS) backbone wherein 73 % of the side chains are phosphory-

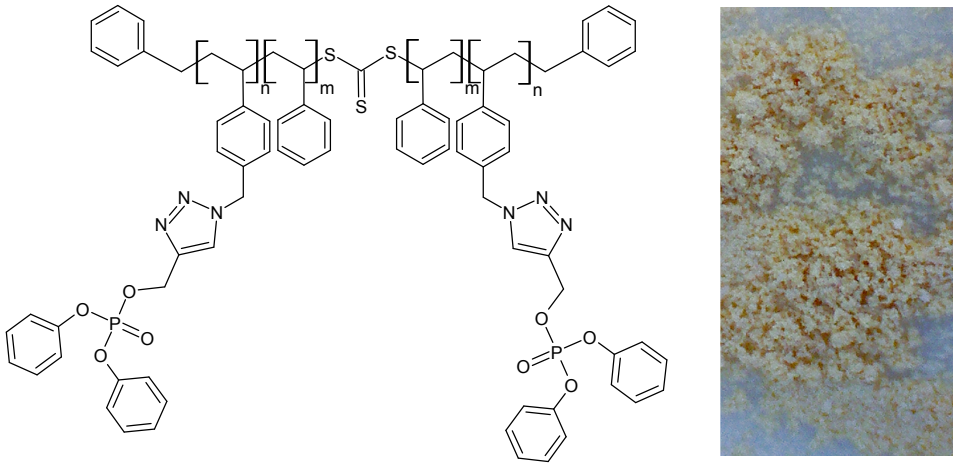

Figure 5.1: Chemical structure and light microscopic representation with 200x magnification of the polymeric flame retardant PS-DPPP used in the current chapter.

lated with DPPP (see Chapter 3.), yielding in a phosphorus content of ≈ 5 % in the flame retardant PS-DPPP. PS-DPPP, which contains phenyl ester groups who can encourage flame retardancy (refer to Chapter 2.4.) [168], was chosen as polymeric phosphorylated flame retardant in the processing studies, since it showed the highest charring in TGA measurements (refers to Chapter 3.3). Therefore, the highest flame retardancy of all prepared polymeric flame retardant samples was expected. The flame retardant PS-DPPP was prepared as described in Chapter 3.

As polymer systems, both inactive (pre-polymerized) and reactive (during processing polymerizing) systems were used. As inactive system, polystyrene "Styrolution PS 156F" obtained by BASF was used due to the comparable styrene backbone of the polymeric flame retardant PS-DPPP, which should favor an incorporation of the polymeric flame retardant PS-DPPP into the inactive polymer system polystyrene. To investigate the flame retardancy in common reactive polymer systems, commercially available and already initiator containing polymer systems were used. Therefore, a detailed description of all components of the compositions is not possible due to corporate secrets. Since both oxygen and nitrogen incorporated into the polymer backbone or in the side chains of the polymer system to be protected, can facilitate the formation of char layers when burned with organic phosphorus-containing compounds [195, 196], ACRIFIX 192 (methylmethacrylate (MMA) composition), Translux D180 (epoxy resin composition) and PUR 765 + PUR 980 (urethane + isocyanate composition) were therefore used as reactive polymer systems with oxygen in the polymer backbone (epoxy resin and polyurethane), respectively, in the side chains (MMA). Nitrogen-containing monomers, such as amides can theoretically be used, yet polymerization of amides mixed with PS-DPPP did not proceed in test approaches. Therefore, polyamides were excluded from the following studies.

The flame retardancy of the phosphorylated polystyrene PS-DPPP incorporated in the protected polymer systems was investigated via LOI measurements. To obtain a LOI value, the oxygen level is detected in the air, which is needed to retain a flame for 3 minutes after ingnition. Moreover, the sample is not allowed to burn down more than 50 mm (LOI condition according to *ISO* 4589-2 norm [197]). It has to take into consideration that it is not permitted to directly describe the fire risk of a material by means of the results obtained. The assessment must always be carried out in the context of a risk analysis taking into account all boundary conditions (e.g. geometry of specimen, fire scenario).[197] Nevertheless, the results can be used to assess the effectiveness of flame retardants. Another fact which also needs to be highlighted for the data obtained in this chapter is the fact that on laboratory scale, only small amounts of flame retardant (up to approximately 20 g) can be prepared per batch. Hence, with the amount available for the incorporation studies, not more than 5 spec-

imens per flame retardant ratio could be produced. According to the *ISO* standard, at least 15 test specimens (ideally even 15 to 30) should be measured [197], since the measured LOI values can vary significantly (refers to Chapter 2.4.2.). The values obtained in the current chapter are therefore to be regarded as the first attempts to determine the applicability in different polymer systems and the optimal incorporation process. Due to the small amounts of PS-DPPP only a few concentration variations are possible for each test series.

5.1 Incorporation using Extrusion and Molding

First, the incorporation of PS-DPPP in the inactive polymer system Styrolution PS 156F (polystyrene with M_n = 53 000 g · mol^{-1}; PDI = 2.88) via extrusion processing (description see Chapter 6.1.) was examined. To determine the lowest temperature, wherein an extrusion process of the phosphorylated flame retardant PS-DPPP is still possible, TGA and evolved gas analysis (EGA) measurements were performed with the pure PS-DPPP. The TGA measurement (Figure 5.2) indicates a cleavage of the phosphorus side chains close to 257 °C, whereas the EGA mea-

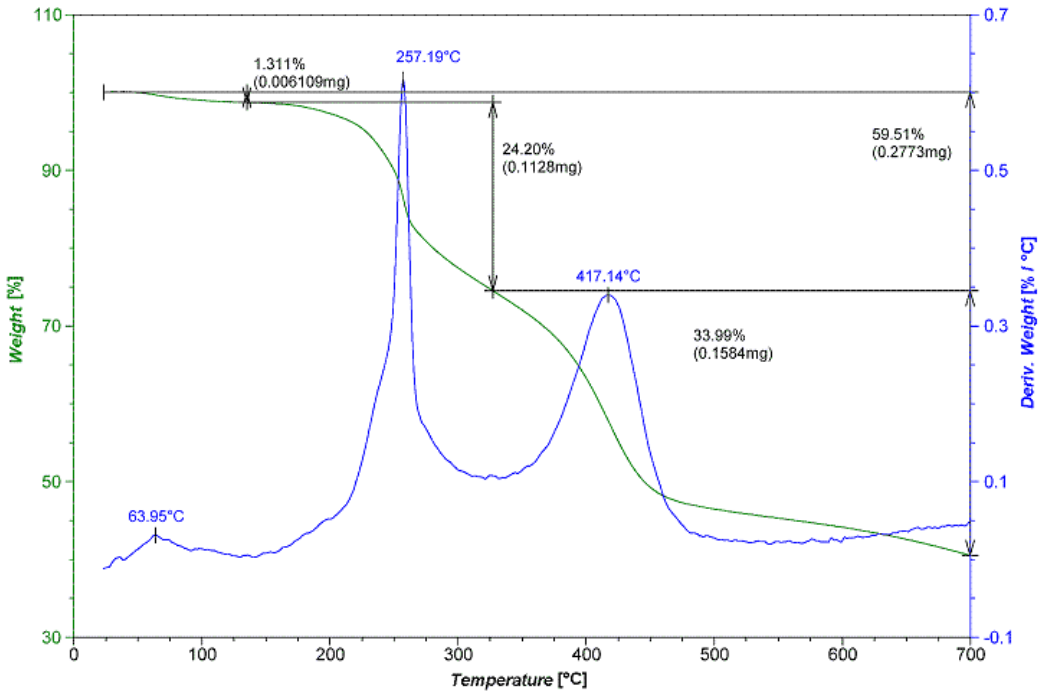

Figure 5.2: Thermogravimetric measurement (original data) of the phosphorylated polystyrene copolymer (PS-DPPP) used as flame retardant showing two decomposition steps around 257.2 °C (cleavage of the phosphorus ester) and 417.1 °C (decomposition of the polymer backbone.

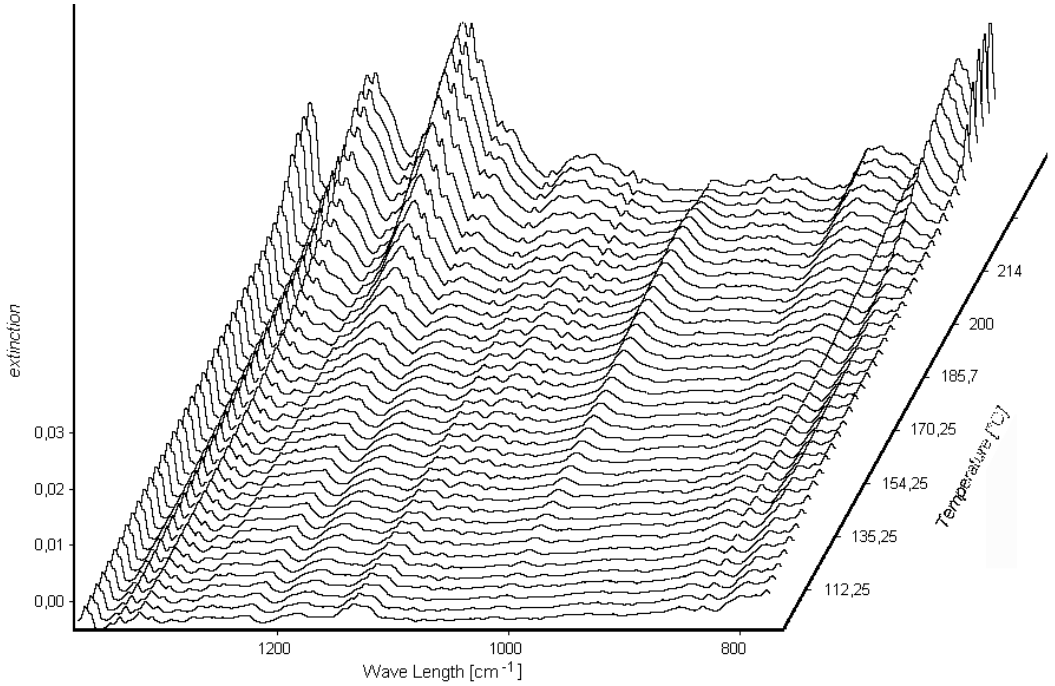

Figure 5.3: Evolved gas analysis (EGA) measurements (original data) of the phosphorylated polystyrene copolymer (PS-DPPP) measured in the temperature range of 50 - 370 °C (shown 114 - 234 °C), 5 K/min heating rate, under nitrogen atmosphere.

surements (Figure 5.3) indicate an increase in the characteristic P-O-C peaks at around 800 cm^{-1} and 1000 cm^{-1}, as well as an increase in the characteristic P=O peak at 1250 cm^{-1}, already at a temperature around 200 °C or even lower (peak at 1000 cm^{-1}). The weight loss in TGA at around 64 °C can be assigned to traces of DMF, which was used as solvent for the modular ligation reaction between the azide functionalized polystyrene copolymer and the alkyne phosphoric ester (refer to Chapter 3.3).

Based on the TGA result (Figure 5.2), the powdered polymeric flame retardant PS-DPPP was dried prior to use in a vacuum oven at 80 °C for 3 days to remove any DMF residue. First of all, the commercially available transparent polystyrene Styrolution PS 156F was tested for its minimum temperature for processing in a mini extruder. Since the minimal temperature for ready processing was close to 170 °C and based on the EGA measurements (Figure 5.3), 180 °C was selected as extrusion temperature to prevent decomposition of the flame retardant during processing. The temperature of 180 °C was just high enough to prepare the flame retardant-polystyrene (PS-DPPP)-PS samples via extrusion.

The dried finely ground polymeric flame retardant and the previously dried and milled polystyrene were mixed in a small extrusion apparatus (Haake MiniLab from

Thermo Scientific) at $T = 180$ °C and $p = 2$ to 3 bar. The duration of the thermal stress from the beginning of the heating to the end of discharging from the extrusion apparatus was about 15 min.

To measure the influence of the flame retardant content, samples with ratios of flame retardant to polystyrene between 18.5 % and 41.2 % were prepared. After extrusion in the mini-extrusion apparatus, a brownish plastic melt (Figure 5.4) was discharged through the nozzle as a strand. As shown in Figure 5.4, the flame retardant PS-DPPP has been homogeneously distributed within the polymer strand. However, the interspersed structure caused by bubbles, points to the formation of gases, which can evolved due to decomposition or cleavage of the flame retardant. Traces of water in the used polystyrene or flame retardant can also cause formation of water vapor bubbles, resulting in bubble-like structures. Since a clear reason for the bubble formation could not be identified, the obtained (PS-DPPP)-PS strands were further used for processing in a mini-injection molding system (Haake MiniJet II from Thermo Scientific) to prepare test specimens with dimensions of 7 x 1 x 0.4 cm, based on the *ISO* 4589-2 norm for LOI measurements of rigid materials.[197]

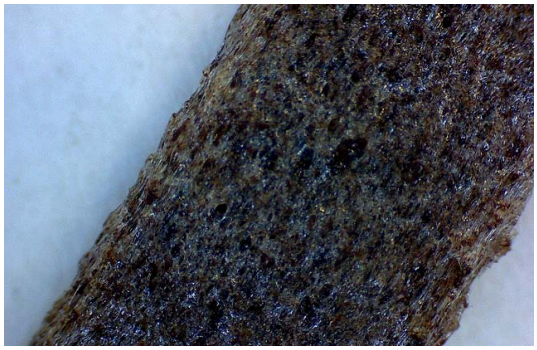

Figure 5.4: Light microscopic representation with 200x magnification of the polymeric flame retardant PS-DPPP incorporated in polystyrene via extrusion.

To prepare one molded flame retardant-polystyrene sample, approximately 5 g of the extrusion strand has to be placed in the mini-molding machine. Heating the sample up to 180 °C at $p = 400$ bar for 6 s to compress and $p = 350$ bar for 12 s to press the samples out of the injection-molding mold were neccessary to mold the samples. Regardless of the flame retardant ratio, all molded samples shared an ebony color (Figure 5.5) and a smooth surface with no visible bubbles.

The molded test samples were subsequently evaluated for flame retardancy using LOI measurements. Firstly, the reference value of the required oxygen concentration was determined, using the polystyrene specimens. The polystyrene used in the

Figure 5.5: Pictorial representation of the molded pure polystyrene (1) and the molded flame retardant-polystyrene samples (PS-DPPP)-PS with flame retardant contents of 18.5 % (2), 37.3 % (3) and 41.2 % (4).

current work showed an oxygen index of 18.75 % (refer to Figure 5.6). As can be seen in Figure 5.6, the LOI values of all molded (PS-DPPP)-PS specimens did not differ a lot, yet were slightly lower than the reference, which unfortunately indicates

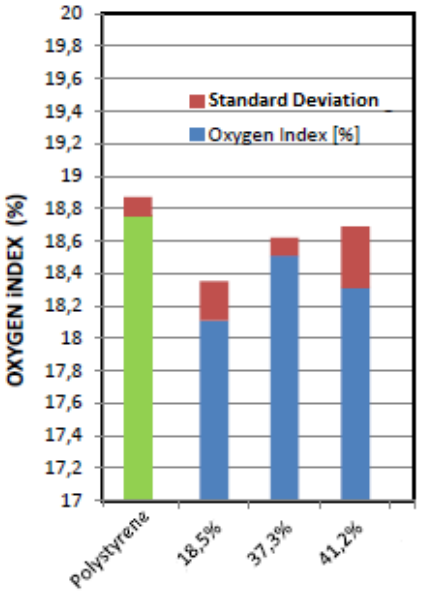

sample	P-content [%]	oxygen index [%]	standard deviation
Polystyrene	0	18.75	0.12
18.5%	0.93	18.11	0.24
37.3%	1.88	18.51	0.11
41.2%	2.08	18.31	0.38

Figure 5.6: Graphical and tabular presentation of the results of the LOI measurements of the extrusion/molding (PS-DPPP)-PS samples compared to the polystyrene reference. "P-content" announce the overal P-content in the (PS-DPPP)-PS sample.

a slightly increased flammability of the molded (PS-DPPP)-PS samples compared to the pure PS to be protected. Nevertheless, an increase in the LOI value with increasing flame retardant ratio can be identified, taking the standard deviation into account. The standard deviation was very high in all measurements, which can be assigned to the small amount of test specimens (maximum 5 per PS-DPPP content). Taking the dark color into account, it must be assumed that the flame retardant was at least partially cleaved during the extrusion process or even decomposed. As a possible reason for the potential decomposition, locally increased temperatures in the extrusion mass higher than 180 °C can be considered. This temperature peaks can be caused by the high shear forces in the mini-extruder generated by the higher ratio of surface area to processed material compared to a conventional extruder. Therefore, maybe by upscaling the extrusion method, a more gentle incorporation using extrusion is possible due to less shear forces.
In addition, the LOI values of the flame retardant-polystyrene (PS-DPPP)-PS specimens are quite low. Although an increase in the LOI values was observed with increasing ratio of flame retardant, the increase is less than 1 %. In addition, all values were lower than the reference value. Therefore, it must be assumed that even a reinforcement of fire, which may be caused by the so-called wicking action at a low content of flame retardant, has occurred.[198] The so-called wick effect describes a capillary action caused by the formation of carbonaceous fibers, comparable to the wick of a candle. Such a capillary action locally increases the vapor pressure and thus lowers the flash point of the molten polymer so that an ignitable mixture is formed. Only at higher levels of flame retardant, the effect can be overcome, since then a sufficiently thick char layer can be formed, which preserves the polymer from further decomposition. However, it is not possible to increase the content of the flame retardant used in the current study, as the flame retardant itself does not melt and thus only a limited amount of flame retardant can be incorporated into the polystyrene using extrusion. Extrusion experiments with higher PS-DPPP content were carried out, yet with inhomogeneous incorporation and stucking in the extrusion apparatus. A proportion of around 43 % PS-DPPP still represents the largest ratio of extrudable flame retardant under the chosen conditions of 180 °C and polystyrene as polymer system. It may be possible to overcome the wick effect even at lower contents of flame retardant in the polymer by a different specimen geometry. The altered geometry can cause an improvement of the measured flame retardancy, due to potentially smaller attack surface for the flame. An alternative approch could be the incorporation of a highly functionalized polymeric flame retardant with additional higher phosphorus content due to smaller ester groups. Such a phosphorylated flame retardant for example can be prepared using the methylated phosphorus-containing flame retardant DMPP

prepared in Chapter 3.3. The polymeric flame retardant PS-DMPP, originated from the modular ligation between an azide functional PS and the alkyne phosphoric ester DMPP, would comprise a phosphorus content of 6.96 % compared to 5.04 % of PS-DPPP at a functionalization of 73 % as used in the flame retardant investigations of the current chapter. As part of the current work, this incorporation was not possible due to time constraints. However, further investigations should be carried out.

5.2 Incorporation using Stirring

In the following section, the incorporation of the polymeric phosphorylated flame retardant PS-DPPP via mixing with different inactive and reactive polymer systems is described. All mixed polymer-flame retardant samples were cured in the custom-made silicone mold shown in Figure 5.7. The form of the stripes corresponds to the requirements of LOI tests.[197] The different samples were cut into stripes of 1 cm width (for rigid materials), respectively pieces with width of 4.5 cm (for rubberlike and thin materials) and heights of at least 5 cm for subsequent flame retardancy testing via LOI measurements.

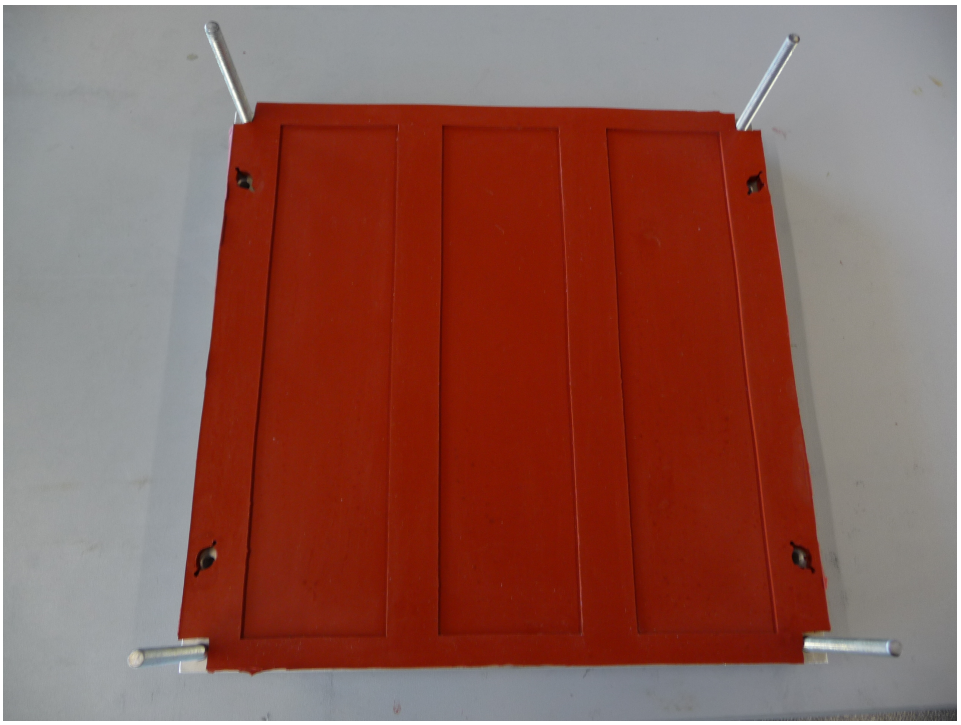

Figure 5.7: Picture of the custom-made silicone mold for the preparation of polymer-flame retardant samples used for flame retardant tests.

As described in the previous extrusion/molding section, incorporation of the phosphorus-containing flame retardant PS-DPPP into polystyrene by extrusion has some disadvantages. Therefore, in order to investigate the influence of the incorporation process on phosphorus-containing flame retardants, PS-DPPP was incorporated at ambient temperature once more in polystyrene by means of stirring in a series of experiments.
For this incorporation, the polystyrene Styrolution PS 156F in granular form was first solubilized in acetone at ambient temperature for 7 hours. The very viscous and partially only swollen polystyrene was subsequently mixed with the previously in a pestle finely ground flame retardant PS-DPPP in the ratio of 10:1. The finally (PS-DPPP)-PS polymer exhibits a phosphorus content of only 0.46 %. Nevertheless, despite vigorous stirring, a homogeneous distribution of the flame retardant PS-DPPP in the highly viscous polystyrene could not be obtained. Regardless, the inhomogenity of PS-DPPP in PS, the solvent acetone was evaporated at room temperature over several days. Unfortunately, the very brittle sample was destroyed upon removal from the silicone mold, thus only a schematic representation of the side view of the sample is shown in Figure 5.8. As seen in Figure 5.8, a concave surface has formed during the evaporation of the solvent. In addition, the flame retardant has sunk to the bottom of the sample during evaporation, thereby forming a non-homogeneous distribution in the polymer sample (see right picture in Figure 5.8). Because of the formation of this non-uniform film thickness, this method is not suitable for the production of reproducible test specimens of (PS-DPPP)-PS for flame retardant measurements. Therefore, this approach was not pursued further and no further tests with polystyrene as protected material were carried out.

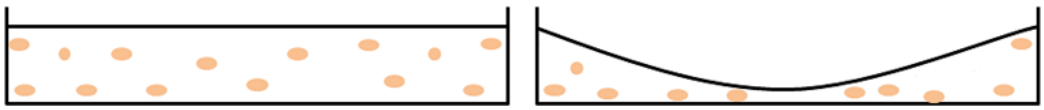

Figure 5.8: Schematic representation of the structure of the flame-retardant-polystyrene sample before (left) and after (right) evaporation of the solvent.

To examine the incorporation behavior of PS-DPPP into reactive oxygen containing polymer systems (see introduction of the current chapter), three commercially available and already initiator-containing monomer systems (MMA, epoxy resin respectively urethane composition) were employed for processing investigations via stirring. Firstly, PS-DPPP was incorporated into a UV light curable molding methylmethacrylate (MMA) composition (ACRIFIX 192 recieved by Degussa) in the ratio MMA to flame retardant of 10:1. The flame retardant was finely grounded in a pestle prior to use. The mixed (PS-DPPP)-MMA bulk was placed in the silicone mold and ir-

radiated due to the not known initiator system with both 254 and 365 nm wave length with a UV lamp for 6 h until full polymerization. As seen in picture (2) of Figure 5.9, the flame retardant could be almost homogeneously distributed within the polymer. However, a slightly concave surface and a very brittle material was formed during polymerization of MMA. Moreover, during polymerization of MMA air entrapments were formed. The test samples of PMMA and flame retardant incorporated in PMMA ((PS-DPPP)-PMMA) were cut into stripes. Due to the slightly concave surface and the high brittleness of the (PS-DPPP)-PMMA sample, the cutting of the initial test sample into reproducable stripes was very difficult. Based on the *ISO* 4589-2 norm for LOI testing of rigid materials [197], the strips had an approximate height of 0.4 cm, length of at least 5 cm and a width of about 1 cm.

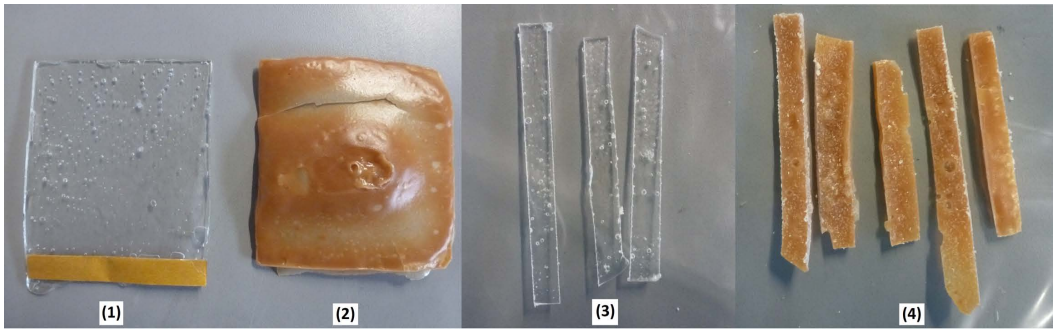

Figure 5.9: Pictorial representation of the reference pure polymethylmethacrylate composition (PMMA) sample (1), the flame retardant (PS-DPPP)-PMMA sample (2), the cut PMMA samples (3) and the cut (PS-DPPP)-PMMA samples (4) used for flame retardant tests.

Attemps have been made with the obtained very brittle specimens to carry out LOI measurements. However, it was not possible to clamp the strips into the apparatus without breaking the specimens. Therefore, the LOI measurements for these samples were discarded.

Secondly, PS-DPPP was mixed with an epoxy resin (Translux D180 received by AXSON) under vigorous stirring. The bulk of PS-DPPP and epoxy resin was placed in the silicone mold and polymerized in a drying oven for 18 h. As shown in picture (2) of Figure 5.10, the finely grounded flame retardant was homogeneously distributed in the epoxy resin without inclusion of air. The test samples of the polymerized epoxy resin (PEpo) and the flame retardant PS-DPPP incorporated in the polymerized epoxy resin (PS-DPPP)-PEpo were cut into stripes. The strips had a height of 0.4 cm, a length of approximately 7.5 cm and a width of close to 1 cm.

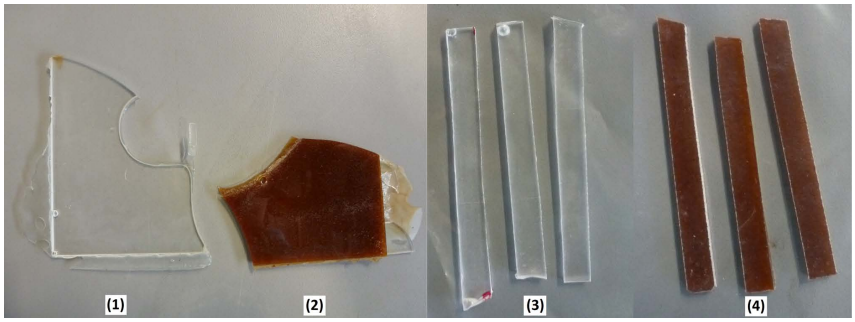

Figure 5.10: Pictorial representation of the polymerized epoxy resin (PEpo) (1), the flame retardant (PS-DPPP)-PEpo (2), the cut PEpo (3) and the cut (PS-DPPP)-PEpo (4) samples used for LOI tests.

The obtained (PS-DPPP)-PEpo samples were investigated using LOI measurements (Figure 5.11). The pure epoxy resin and the epoxy resin mixed with PS-DPPP yielded the same LOI value of 23.2 and comparable char layers. The coincidence of the measured values suggests that the flame retardant PS-DPPP does not interact with the epoxy resin, for example in form of dehydrogenation of the polymer backbone. No flame retardancy effect of the used flame retardant could be determined for the epoxy resin polymer system. Therefore, the epoxy resin was not considered further as polymer system for the incorporation of PS-DPPP.

Figure 5.11: Pictorial representation of the polymerized epoxy resin (PEpo) (left & middle) and the flame retardant (PS-DPPP)-PEpo sample (right) after LOI mesurements.

Thirdly, PS-DPPP was incorporated in a polyurethane (PUR) formulation (PUR 765 recieved from company Rühl). The PUR formulation was composed of 100 parts of polyol, which contains additives that bind water to prevent foaming (see second line in Figure 5.12), and 33 parts of a methylenediphenyldiisocyanate prepolymer (MDI prepolymer PUR 980 recieved from company Rühl Puromer GmbH). Prior to use, the polyol was mixed with 10, respectively 40 parts of the phosphorylated flame retardant PS-DPPP under vigorous stirring. To the mixture of polyol and flame re-

tardant (100 + 10 respectively 40 parts), the MDI prepolymer (33 parts) was added, whereby the polyurethane formation started. A schematic representation of the desired reaction between isocyanate and alcohol and possible side reactions are shown in Figure 5.12.

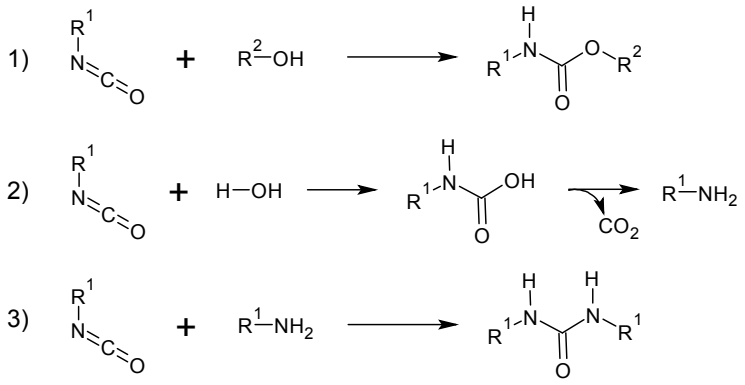

Figure 5.12: Schematic representation of the urethane formation starting from an isocyanate and an alcohol (1), the reaction of isocyanate and water (2) leading to the formation of foam and the reaction to bisubstituted urea (3) caused by reaction products of reaction 2.

The final mixture was stirred for 2 minutes before placing the viscous formulation into the custom-made silicone mold. After one day at ambient temperature, the flame retardant-polyurethane samples (PS-DPPP)-PUR were completely reacted and tack-free. As seen in picture (2) of Figure 5.13, the flame retardant is very homogeneously dispersed in the polymer. The resulting 6 test specimens have a rubbery consistency. Thus, the specimens were cut in the dimensions of 7.5 x 4.5 x 0.2 cm, based on the *ISO* 4589-2 norm for thin and rubber-like samples, and placed in a sample holder as shown in picture (3) of Figure 5.13.

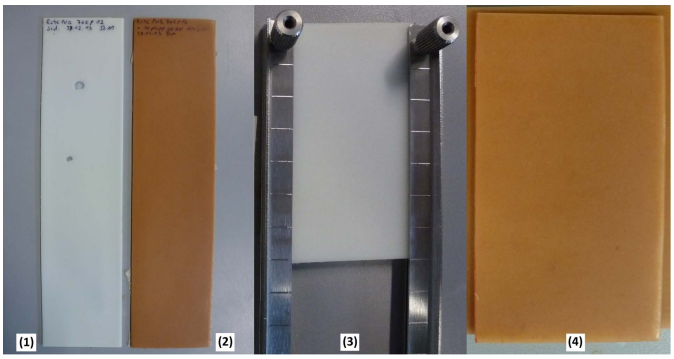

Figure 5.13: Pictorial representation of the pure polyurethane (PUR) (1), the flame retardant (PS-DPPP)-PUR (2), the cut PUR clamped in the LOI measurement holder (3) and the cut (PS-DPPP)-PUR (4) samples used for LOI.

As described for the other flame retardant-polymer samples, LOI measurements were carried out with the flame retardant-polyurethane (PS-DPPP)-PUR samples. It was shown that at incorporation levels of only 10 parts of the flame retardant PS-DPPP (corresponds to a phosphorus content of 0.35 %) no increase in the limiting oxygen index could be observed. By incorporation of 40 parts of PS-DPPP (corresponds to a phosphorus content of 1.17 %), a slightly increase in the LOI value from 19.2 (pure polyurethane) to 19.3 for the (PS-DPPP)-PUR samples could be achieved, which is within the error of the LOI measurement. However, a very strong charring, less visible smoke emission and less burn down was observed with the (PS-DPPP)-PUR samples, which can be very well seen in Figure 5.14.

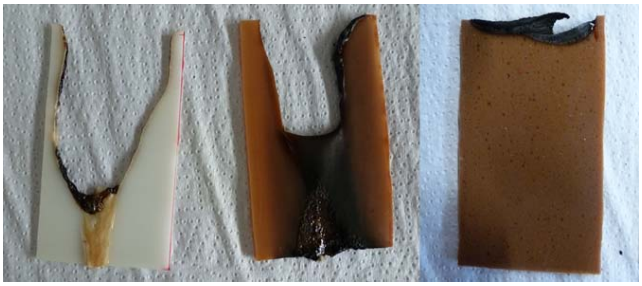

Figure 5.14: Pictorial representation of the reference pure polyurethane (PUR) sample (left) and the flame retardant (PS-DPPP)-PUR samples (middle = 10 parts PS-DPPP; right = 40 parts PS-DPPP) after LOI measurements at 19.2.

The observed lower burning and the formation of a thick char layer, even at a very low phosphorus content of only 1,17 % at incorporation of 40 parts PS-DPPP with a phosphorus content of 5.04 % suggest that just as during incorporation of the flame retardant PS-DPPP in polystyrene by extrusion/molding (see section 5.1.), a flame retardant with a higher proportion of phosphorus could possibly lead to a higher value in the oxygen index. Previous work has shown that at least a proportion of 5 % of phosphorus in the polymer is necessary to achieve a flame retardancy effect at all.[196] Therefore, further experiments should be carried out with polyurethane polymer systems, especially since polyurethanes also allow the possibility of a reactive connection onto the functionalized chain ends of the urethane polymer. Reactive flame retardant polymers with phosphorus-containing side chains can be synthesized for example by controlled/living polymerizations such as ATRP or RAFT of a poly(methyl)methacrylate with azide groups in the side chains, which can be subsequently converted via alkyne/azide modular conjugation reaction with alkyne phosphoric esters, such as DMPP. These reactive phosphorylated polymers can subsequently be incorporated into the polyurethane main chain via a reactive approach. Such an approach may even lead to improvements in the limiting oxygen index (LOI) even at lower levels of flame retardant respectively phosphorus content.

5.3 Summary and Discussion of Chapter 5

In summary, it could be shown that flame retardancy of a given flame retardant incorporated into a polymer system is a very complex task and subject to numerous influences, such as temperature during processing (extruding/molding respectively stirring) and the nature of the investigated polymer system.
In general, it can be said that the incorporation of the phosphorus-containing flame retardant PS-DPPP in different polymeric systems exhibits some exceptional challenges. The incorporation difficulties are associated with the powder-like consistency and non-existent melting point of the phosphorylated styrene-based flame retardant. In addition, PS-DPPP decomposes close to 180 °C, which makes incorporation into various polymer systems via extrusion challenging. However, a slight increase in the limiting oxygen index (LOI) could be measured for the extruded/molded flame retardant-polystyrene samples with increasing flame retardant content. Therefore, further experiments should be carried out with phosphorus-containing flame retardants based on the alkyne phosphoric esters DMPP and DEPP (refer to Chapter 3) prepared in the current work. Both phosphoric esters with shorter side chains (for example, methyl groups), as well as phosphorus-containing polymers with other polymer backbones, such as ethylene oxide instead of styrene, should be examined in further extrusion approaches. By connecting the phosphoric esters to such backbones, the resulting polymers might exhibit a melting point. If the thus synthesized phosphorus-containing polymers would comprise a lower melting point than the polymer to be protected an incorporation without cleavage of the phosphorus ester, or even the degradation of the flame retardant could be possible via extrusion processes. In addition, higher flame retardant contents could be obtained, leading to higher flame retardancy.
The flame retardancy of PS-DPPP incorporated into polystyrene via stirring could not be determined further due to the highly brittle polystyrene and flame retardant-polystyrene (PS-DPPP)-PS samples. Nevertheless, the extrusion/molding experiments give reason to assume that PS-DPPP and derivatives with shorter phosphoric ester groups are applicable in polystyrene system. When using a copolymer of styrene such as styrene-butadiene block copolymer resins, the problem of brittleness may be reduced and further stirring experiments may be performed to prohibit thermal decomposition of the flame retardant during processing.
In the case of the studied epoxy system, no difference between the pure and the epoxy resin mixed with the phosphorylated flame retardant could be determined. The phosphorus-containing styrene-based flame retardant PS-DPPP used in the current work, is therefore not suitable for epoxy systems.

When the phosphorylated flame retardant was incorporated into a polyurethane system, reduced smoke emission and an increased tendency to charring could be determined, in addition to a slight increase in the limiting oxygen index (LOI). Since these effects occurred at very low phosphorus content (1.17 %), it seems likely that the effects increase with the increase of the phosphorus content and therefore the flame retardancy. In order to obtain an increase in the phosphorus content of the phosphorylated polymeric flame retardants, additional tests using flame retardants with shorter ester groups as well as other phosphorylated polymers types, should be performed. By connecting the phosphorus ester to other backbones such as ethylene oxide, the consistency of the phosphorylated flame retardants may possibly change to a more viscous mass, in addition to the increased phosphorus content. It is very likely that the incorporation via stirring is very much improved with a non-powdered flame retardant.

In general, no gas phase mechanism was observed in the experiments carried out. An indication of a condensed phase mechanism in terms of the formation of a strong char layer could only be determined for the polyurethane mixed with the flame retardant. Since only LOI tests were carried out to determine a potential flame retardancy in the current study and in addition with only small amounts of test specimens, however, no definitive statement can be made about the presence of a gas-phase mechanism on the basis of the results obtained. Only with the help of other flame retardancy tests, such as the cone calorimeter test and the UL94 test (see Chapter 2.4.2.), more precise statements about the potential flame retardancy and the place of action of the phosphorylated flame retardant incorporated in various polymers systems can be made. However, higher material quantities are required for these flame retardancy measurements, which could not be generated in the current work.

It can be assumed that further tests with phosphorus-containing flame retardants of the type described in Chapter 3, can lead to an improvement in terms of the flame retardancy of important polymer systems such as polyurethane or even polystyrene. Both polymer systems are widely used in some very distinctive fields, such as in automobiles or furnitures, which require high flame retardancy. Therefore, the flame retardants described in the current work, despite only limited evidence of a condensed phase mechanism, represent potential flame retardants and should be further investigated.

Chapter 6

Concluding Remarks and Outlook

Controlled/living anionic and radical polymerizations (RAFT, NMP, ATRP) are certainly the most efficient methods for the precise construction of polymers with narrow molecular weight and low PDI.

In the current work two approaches to obtain phosphorylated polymers for the use in flame retardant applications were investigated. Via the controlled/living radical copolymerization of styrene and 4-vinylbenzyl chloride and the subsequent introduction of modular ligation points in form of azide groups, copolymers with pre-determined chain length and functionalities were synthesized. Various alkyne phosphoric esters could be synthesized via a novel-metal free approach as matching counterparts. By using modular ligation based on the copper catalyzed alkyne/azide 1,3-dipolar cycloaddition, phosphorylated copolymers were prepared which feature high char residues in thermogravimetric measurements. In addition, the modular ligation approach can be used for the individual adjustment of the flame retardant ratio of various alkyne phosphoric esters or even other flame retardant compounds which contain an alkyne group. The decomposition fragments of the prepared polymeric phosphorylated flame retardants were determined and assigned to the various stages of decomposition. The current study describes for the first time a modular ligation approach in the sector of fire protection. In addition, the approach was patented for the preparation of flame retardants.

To evaluate the flame retardant potential, one polymeric flame retardant was incorporated in various polymer systems via extrusion/molding, respectively, stirring. The flame retardant-polymer specimen were tested on a laboratory scale. LOI and TGA measurements reveal a flame retardant potential of the polymeric phosphorylated flame retardants incorporated in polystyrene and polyurethane systems. In contrast, an application of the polymeric phosphorous-containing flame retardants prepared in the current work in epoxy resins can be excluded after initial incorporation processes and assessments.

In Chapter 4, an anionic polymerization approach was investigated to evaluate the polymerization behavior of phosphorylated epoxy monomers initiated by a tetraoctylammonium bromide/triisobutylaluminum system. In this context, a novel synthesis route for the preparation of phosphorylated epoxy monomers was developed. Since anionic polymerization requires high purities of the monomers, solvents and an ultra clean polymerization apparatus, a multi-step purification was utilized to obtain monomers, which can be employed in anionic polymerizations. It could be shown that a controlled/living polymerization via such an approach is not feasible, due to irreversible connection of the catalyst based aluminum to the P=O double bond of the phosphonic ester. Models for the ligation of aluminum onto the P=O double bond were proposed.

In the current work, the successful synthesis of phosphorus-containing styrene copolymers via RAFT polymerization in combination with a modular ligation reaction was demonstrated. Since the prepared polymeric flame retardants exhibit a powderous structure and no melting point, further studies with polymers containing other functionalized lateral chains have to be performed. Initial experimental studies have shown that the phosphorus-containing polymers prepared in the current study exhibit good flame retardant potential via the formation of a strong char layer. It can be envisaged that the demand for non-halogenated flame retardants will be rising in the coming years. Therefore, further comparative studies on the influence of the polymer backbone of the flame retardant, the ester groups of the flame retardant as well as the protected polymer system are necessary to reveal an encompassing picture of the range of applications for the flame retardants prepared via the synthesis strategies described in the present thesis.
With respect to the anionic polymerization of phosphorylated epoxy monomers, further studies are not recommended, since, although metal-free initiators are available for anionic polymerization (such as the tetraalkylammonium salt employed in the current work), only metal-containing catalysts are currently described, which can form a ring-opening initiator/catalyst system. Only by using a metal-free approach, a controlled/living anionic polymerization of phosphorylated monomers is envisaged. However, the development of such an approach represents a highly synthesis- and time-consuming endeavour.

Chapter 7

Experimental Section

7.1 Materials

Styrene (Sigma-Aldrich, $\geq$ 99 %) was destabilized by passing through a basic alumina column, 4-vinylbenzyl chloride (4-VBC, Sigma-Aldrich, 90 %), epichlorohydrin (EPI, Merck, 98 %) and chloroform ($CHCl_3$, Acros, 95 %) were vacuum distilled prior to use. Toluene (Acros, 99.5 %) was distilled first from CaH_2, then from sodium benzophenone and stored over sodium benzophenone in a storage vessel on the vacuum line prior to use. 1,2-epoxypropylphosphonic acid (Fosfomycin disodium salt, Chemos, 99 %); 18-crown-6 (Acros, 98 %); acetonitrile (ACN, Acros, 99 % extra pure); aluminum trichloride ($AlCl_3$, Sigma-Aldrich; 98 %); ammonium chloride (NH_4Cl, Acros, 98 %); 2,2'-azobisisobutyronitrile (AIBN, Sigma-Aldrich, 98 %); 1,10-azobis-(cyclohexane carbonitrile) (VAZO-88, Sigma-Aldrich, 98%); $BF_3{\cdot}Et_2O$ (Acros, 48 w% in diethylether)); butyllithium (BuLi, Sigma-Aldrich, 1.6M in cyclohexane); butanol (BuOH, Sigma-Aldrich, 99 %); calcium hydride (Acros, 93 %); tetrachloromethane (CCl_4, Fischer, 99 %); copper(II) sulfate pentahydrate (Merck, >99 %); dichloromethane (CH_2Cl_2, Sigma-Aldrich, 98 %); dimethyl phosphoryl chloride (Sigma-Aldrich, 99 %); diethyl phosphoryl chloride (Sigma-Aldrich, 99 %); diphenyl phosphoryl chloride (Sigma-Aldrich, 99 %); dicyclohexylcarbodiimide (DCC, Acros, 97 %); dimethylsulfoxide (DMSO, Sigma-Aldrich, 98 %); ethylenediaminetetraacetic acid (EDTA, Acros, 96 %); ethanol (EtOH, Sigma-Aldrich, 99 % extra pure); potassium hydroxide (KOH, Acros, 99 % pellets); methanol (Roth, > 99,9 %); methane sulfonic acid (MSA, Acros, 98 %); sodium hydride (NaH, Sigma-Aldrich, 60 % in mineral oil); 4-(dimethylamino)pyridine (DMAP, Sigma-Aldrich, 98 %); N,N'-dimethylformamide (DMF, Acros, 99,8 %, extra dry over molecular sieves); phosphorus trichloride (PCl_3, Sigma-Aldrich, 99 %); phosphorus pentachloride (PCl_5, Sigma-Aldrich, 98 %); phosphorylchloride ($POCl_3$, Sigma-Aldrich, 98 %); propargyl alcohol (Sigma-Aldrich, 99 %); pyridine (Acros, 99 %); L-(+)-sodium ascorbate

(Fluka, > 99 %); sodium hydrogen sulfate (Sigma-Aldrich, technical grade); sodium methanolate (NaOMe, Sigma-Aldrich, 98 %); sodium sulfate ($NaSO_4$, Merck, 99 %); sodium azide (Acros, 99 % extra pure); tetraoctylammonium bromide ($NOct_4Br$, Acros; 99 %); tin(II)-2-ethylhexanoate ($SnOct_2$, Acros, 98 %); tetrahydrofuran (THF, Acros, 99,5 %, extra dry over molecular sieves); triethylamine (Et_3N, Sigma-Aldrich, >99 % stored over molecular sieves); triisobutylaluminum ($^iBu_3Al$, Sigma-Aldrich, 25 w% in toluene) and dibenzyltrithiocarbonate (DBTTC, obtained from Orica Pty Ltd., Melbourne, Australia, as a donation) were used as received.

7.2 Characterization Methods

Differential Scanning Calorimetry (DSC)

By using differential scanning calorimetry measurements the difference between the amount of heat required to increase the temperature of a sample and a reference is measured as a function of time or temperature. In the current work, DSC was used to determine the temperature profile at the release of the flame retardant compound.
DSC measurements were recorded with a device from TA Instruments, Model Q 1000. The heating rate was 5 K $\cdot$ min^{-1} in the temperature range of 25 to 600 °C. All samples were measured under a nitrogen atmosphere by Mrs. H. Schuppler at the Fraunhofer ICT.

Evolved Gas Analysis (EGA)

To evaluate the decomposition temperatures of the various fragments of the polymeric flame retardants prepared in the current work, evolved gas analysis was applied. The measurement of the IR spectra was in the range of 600 to 4000 cm^{-1} using the IR spectroscope Nexus recieved from Thermo Nicolet. The heating rate was 5 K $\cdot$ min^{-1} in the range from 50 to 370 °C and were processed by Mrs. W. Schweikert at the Fraunhofer ICT.

Extruding and Injection Molding

In the current work, the polymer to be protected (polystyrene) was melted and mixed with an additive, in the case of the present work a polymeric flame retardant, using an extrusion process. The extrussion process alters the physical and thermal (conductivity, flame retardance) behavior of the polymer to be

protected. The resulting composite material was subsequently injection molded for flame retardancy tests with assistance of Mrs. M. Klemenz at the Fraunhofer ICT.
The polymeric carrier material was pre-dried in a vacuum oven at 60 °C for 2 days and then milled. The extruding was carried out at 180 °C and injection molding at 180 °C at a pressure of 400 bar for 6 s to compress and subsequently 350 bar for 12 s to press the samples from the injection-molding mold.

Infrared (IR) and Raman spectroscopy (Raman)

For IR measurements, a FT-IR-spectrometer Nicolet 510A equipped with a Dura-Scope as diamond ATR accessory was used. The spectra were recorded in the range of 400 to 4000 cm^{-1} by Mrs. W. Schweikert at the Fraunhofer ICT. The intensities are giving as: w (weak), m (medium) and s (strong).

Limiting Oxygen Index (LOI)

Through the determination of the minimum concentration of oxygen in the atmosphere required to maintain burning of a vertically disposed small specimen, the flame retardancy properties of one pepared polymeric flame retardant (PS-DPPP) incorporated in different polymeric materials was investigated. The limiting oxygen index LOI was determined using a Dynisco Analyzer Model
LOI 230b and taking into account the requirements of the *ISO* 4589-2 norm (e.g. geometry of the specimen). The test specimens were burned in a carefully controlled atmosphere of nitrogen and oxygen by Mrs. A. Daniliuc at the Fraunhofer WKI.
Prior to the measurement, the test specimens were conditioned at a temperature of 23 °C ± 2 °C and a relative humidity of 50 % ± 5 % for 88 h. To define a start-oxygen concentration for the LOI test, a specimen was ignited in air:
→ sample burns quickly - 18 %
→ sample burns slowly/flickering - 21 %
→ sample does not burn - 25 %
Before each measurement, the cylinder was purged with pure oxygen for 30 s. After ignition of the sample at the top narrow area, the sample burn 180 s and/or burn down up to 50 mm to determine the LOI value.

Due to the only few specimens obtained per flame retardant content in the current work, the burned tip was removed after each measurement and the remaining specimens were used for further experiments. This procedure is non-compliant with the *ISO* 4589-2 norm.

Matrix-Assisted Laser Desorption/Ionization Time-of-Flight Mass Spectrometry (MALDI-ToF)

The MALDI-ToF measurements were carried out at the Institute for Functional Interfaces (IFG) at the Karlsruhe Institute of Technology (KIT) by Mr. B. Kuehl on a 4800 Plus MALDI TOF/TOF^{TM} Analyzer (AB SCIEX) and evaluated on a Voyager-DE^{TM} STR Workstation (AB Applied Biosystems). The samples were measured in linear mode and by use of positive ions. The sample was diluted in acetonitrile (10 mg $\cdot$ L^{-1}) with 1 % trifluoroacetic acid (TFA) and mixed with 25 eq of 2,5-dihydroxybenzoic acid (DHB) prior to the measurement.

Nuclear Magnetic Resonance (NMR)

Nuclear magnetic resonance (NMR) spectra were recorded in DMSO-d^6 and $CDCl_3$ at ambient temperature using tetramethylsilane as the internal reference on a Bruker Advance 400 NMR spectrometer. The spectra were recorded at 400 M*Hz* (^{1}H), 100 M*Hz* (^{13}C) respectively at 120 M*Hz* (^{31}P). Solid state NMR spectra were recorded on a Bruker Avance spectrometer (BrukerBioSpin, Germany) by Dr. R. Graf at the MPI Mainz. All measurements were performed at 25 k*Hz* MAS with 100 k*Hz* RF field strength on all channels. The ^{1}H MAS measurements were stimulated directly, while - for signal amplification - the ^{31}P and ^{13}C measurements were taken with the cross-polarization method and can therefore not be integrated. The contact time was 1 ms for ^{31}P respectively 2 ms for ^{13}C, while disruptive ^{1}H couplings were decoupled during the acquisition with 100 k*Hz* RF using the SPINAL64 sequence.

Scanning Electron Microscopy combined with Energy Dispersive X-ray Analysis (SEM/EDX)

The SEM images of the phosphorylated polymers were recorded with a scanning electron microscope (Zeiss Supra 55 VP) with an Everhard Thornley

secondary electron detector and in addition a backscattered electron detector by Dr. M. Juez-Lorenzo at the Fraunhofer ICT. For the EDX spectra the microanalysis system type Genesis 4000 (EDAX) was used.

Size Exclusion Chromatography (SEC)

Molecular weight distributions of the prepared polymers and copolymers were determined via size exclusion chromatography (SEC) at 20 °C on a Polymer Laboratories/Varian PL-GPC 50 Plus system comprising a Polymer Laboratories 5.0 μm bead-size guard column (50 x 7.5 mm^2), followed by three PL columns and a differential refractive index detector. The eluent was tetrahydrofuran (THF) at 35 °C with a flow rate of 1 mL $\cdot$ min^{-1}. The SEC system was calibrated using linear polystyrene standards ranging from 2000 g$\cdot$mol^{-1} to $2 \cdot 10^6$ g $\cdot$ mol^{-1} and the Mark-Houwink relationship for polystyrene ($\alpha = 0.7$; $K = 14.1 \cdot 10^{-5}$ dL $\cdot$ g^{-1}).[199] The measurements were carried out by the author.

Thermogravimetry (TGA)

Via thermal thermogravimetry analysis (TGA) the thermal stability of the prepared polymers, phosphoric ester and polymeric flame retardants was determined by monitoring the loss of mass with increasing temperature under controlled conditions. The temperature at which significant mass loss occurs during decomposition in air gives an indication of the ignition temperature. Once ignition has occurred, the mass loss in nitrogen is more representative since the oxygen concentration under a flame is close to 0 %. In the discussion of the temperature range of the expected flame retardancy of the polymeric flame retardant, the temperature range is assumed where the phosphorus components are released according to TGA measurements. In addition, the ability of flame retardancy is related to the amount of char, measured by TGA.
Thermogravimetric measurements (TGA) were carried out using the Model Q 5000 from TA Instruments by Mrs. Y. Galus at the Fraunhofer ICT. The heating rate was 5 K $\cdot$ min^{-1}, sample weights ranged from 1 to 2 mg, measuring the decomposition in the range from 40 to 600 °C under a nitrogen atmosphere. The mass and temperature reproducibility of the instrument are assumed to be 2.5 % and 1 %, respectively, at the given sample weight and heating rate.

Thermal Desorption Mass Spectroscopy (TG-MS)

Combined thermogravimetry with mass spectroscopy was used to observe the volatile decomposition products of polymers when exposed to a heat flux. The obtained data provide insights in the flame retardant mechanism. During the experiment, a small amount of the polymeric flame retardant is place into a stainless steel crucible. The crucible is then heated under high vacuum using a thermal element and the molecular weight of volatile decomposition products are monitored by a mass spectrometer.
The TG-MS measurements were carried out at a 209 F1 Iris from QMS C Aeolos by Mrs. Y. Galus at the Fraunhofer ICT and, in addition, by Dr. K. Emmerich and Mrs. A. Steudel at the Institute for Functional Interfaces (IFG) at the Karlsruhe Institute of Technology (KIT). The heating rate was 5 $K \cdot min^{-1}$, measuring the decomposition in the range from 50 to 800 °C under a nitrogen respectively air atmosphere.

X-ray Photoelectronspectroscopy (XPS)

The conversion of azide-functionalized polymer to phosphorylated polymer was determined by X-ray photoelectron spectroscopy (XPS) at the Institute for Applied Materials (IAM-ESS) and the Karlsruhe Nano MicroFacility (KNMF) at the Karlsruhe Institute of Technology (KIT) by Dr. Michael Bruns.
XPS measurements were performed on a K-Alpha spectrometer (Thermo Fisher Scientific, East Grinstead, UK) using a microfocused, monochromated Al K_α X-ray source (200 $\mu\ m$ spot size). The kinetic energy of the electrons was measured by a 180° hemispherical energy analyzer operated in the constant analyzer energy mode (CAE) at 50 eV pass energy for elemental spectra. The photoelectrons were detected at an emission angle of 0° with respect to the normal of the sample surface. The K-Alpha charge compensation system was employed during analysis, using electrons of 8 eV energy and low energy argon ions to prevent any localized charge build-up. Data acquisition and processing using the Thermo Avantage software is described elsewhere.[200] The spectra were fitted with one or more Voigt profiles (BE uncertainty: 0.2 eV). The analyzer transmission function, Scofield sensitivity factors,[201] and effective attenuation lengths (EALs) for photoelectrons were applied for quantification. EALs were calculated using the standard TPP-2M formalism.[202] All spectra were referenced to the C1s peak of hydrocarbon at 285.0 eV binding energy

controlled by means of the well-known photoelectron peaks of metallic Cu, Ag, and Au, respectively.

7.3 Syntheses

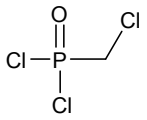

Chloromethylphosphonic dichloride (1)

Equimolar concentrations of PCl_3, $AlCl_3$ and CH_2Cl_2 are placed in a high pressure tube and the mixture is heated for 24 h at 100 °C. After cooling to ambient temperature, the mixture is diluted with CH_2Cl_2 and cooled to -20 °C by an isopropanol/N_2 bath. Under prolonge cooling and stirring with a KPG stirrer, 1.3 equivalents of water are added very slow. The white precipitate is seperated from the supernatant solution in the cold. After evaporation of CH_2Cl_2 in vacuo, the product is obtained as an almost colorless liquid.
Yield: $\leq$ 39 %
^{1}H NMR ($CDCl_3$, δ, ppm): 4.17 (d, CH_2)

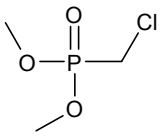

Chloromethylphosphonic dimethylester (2)

Chloromethylphosphonic dichloride **(1)** is dissolved in THF and cooled to at least -15 °C using an isopropanol/N_2 bath. To the cold solution, 2.1 equivalents of triethylamine are added dropwise, followed by dropwise addition of 2.1 equivalents methanol. At this point, it must be ensured that the temperature remains $<$ 10 °C. The mixture is stirred for an additional 30 min at this temperature and then further stirred for 1 h at ambient temperature. The precipitated solid is filtered off. By mixing the filtrate with diethyl ether additional white solid precipitate and has to be filtered. The filtrate is washed several times with saturated NH_4Cl solution and finally extracted 3 times with water. The organic phase is dried over Na_2SO_4 and the exess of diethyl ether is removed under vacuum. As a result a very slightly yellowish oil is obtained.
Yield: 68 %
^{1}H NMR ($CDCl_3$, δ, ppm): 3.51 (d, CH_2), 3.72 (t, CH_2)

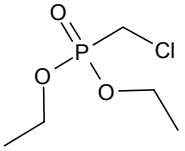

Chloromethylphosphonic diethylester (3)

Chloromethylphosphonic dichloride **(1)** is dissolved in THF and cooled to at least -15 °C using an isopropanol/N_2 bath. To the cold solution, 2.1 equivalents of triethylamine are added dropwise, followed by dropwise addition of 2.1 equivalents methanol. At this point, it must be ensured that the temperature remains < 10 °C. The mixture is stirred for an additional 30 min at this temperature and then further stirred for 1 h at ambient temperature. The precipitated solid is filtered off. By mixing the filtrate with diethyl ether additional white solid precipitate and has to be filtered. The filtrate is washed several times with saturated NH_4Cl solution and finally extracted 3 times with water. The organic phase is dried over Na_2SO_4 and the exess of diethyl ether is removed under vacuum. As a result a very slightly yellowish oil is obtained.
Yield: 74 %
^{1}H NMR ($CDCl_3$, δ, ppm): 4.19-4.07 (m, CH_2), 3.47 (d, CH_2), 1.28 (t, CH_3)

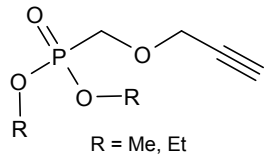

Dialkyl prop-2-yn-1-yl phosphate (4)

First, 1.2 equivalent NaH are suspended in a 50 times the amount of THF **(a)**, respectively, PEG-400 **(b)** and cooled down to 0 °C using an ice bath. Subsequently, 1.2 equivalents propargyl alcohol in 20 times the amount of THF **(a)**, respectively PEG-400 **(b)** are slowly added dropwise. The temperature is not allowed to rise above 5 °C. After completion of the gaseous reaction and recooling to 0 °C, the diethyl ester **(2)** / **(3)** is dissolved in 10 times the amount of THF and slowly added dropwise to the solution. The slightly yellow solution is stirred for 16 h at ambient temperature and finally quenched with saturated NH_4Cl solution. A white precipitate is formed, which is filtered off. The aqueous phase is extracted several times with ethylacetate. The organic phases are combined and dried over $NaSO_4$ and the exess of solvent is removed under reduced pressure. The resulting oils show only partially conversion to the alkyne.

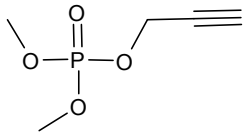

Dimethyl prop-2-ynyl phosphoric ester (DMPP) (5)

Dimethyl prop-2-ynyl phosphoric ester is prepared according to a modified procedure described by Jones et al.[157] Under a nitrogen atmosphere, dimethyl phosphoryl chloride (1 equivalent) dissolved in 20 times the amount of dry THF is cooled to -5 °C in an isopropanol/nitrogen bath. Under continuous stirring triethylamine (1 equivalent) is added drop wise. The isopropanol/nitrogen bath is removed and the mixture is stirred for additional 1.5 h at ambient temperature. After cooling to -10 °C, propargyl alcohol (2.2 equivalents) is added drop wise under continuous stirring. The mixture is stirred at -10 °C for an additional 30 min followed by 2 h at ambient temperature. The obtained slightly yellow mixture is separated from triethylamine hydrochloride by filtration and washed with saturated sodium hydrogen sulfate solution. The aqueous layers are additionally extracted with THF. The combined organic phases are dried over $NaSO_4$. The solvent is removed in vacuo. The residual slightly yellow oil can be stored under argon in the fridge for further reactions.
^{1}H NMR (DMSO-d6, δ, ppm): 4.65 (dd, CH_2), 3.78 (d, CH_3), 2.60 (t, CH)
Raman (ν, cm^{-1}): 2961 (s), 2859 (s), 2128 (s), 1455 (w), 1266 (w), 754 (w), 313 (m)

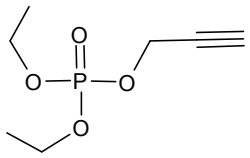

Diethyl prop-2-ynyl phosphoric ester (DEPP) (6)

Diethyl prop-2-ynyl phosphoric ester is prepared according to a modified procedure described by Jones et al.[157] Under a nitrogen atmosphere, diethyl phosphoryl chloride (1 equivalent) dissolved in 20 times the amount of dry THF is cooled to -5 °C in an isopropanol/nitrogen bath. Under continuous stirring triethylamine (1 equivalent) is added drop wise. The isopropanol/nitrogen bath is removed and the mixture is stirred for additional 1.5 h at ambient temperature. After cooling to -10 °C, propargyl alcohol (2.2 equivalents) is added drop wise under continuous stirring. The mixture is stirred at -10 °C for an addi-

tional 30 min followed by 2 h at ambient temperature. The obtained slightly yellow mixture is separated from triethylamine hydrochloride by filtration and washed with saturated sodium hydrogen sulfate solution. The aqueous layers are additionally extracted with THF. The combined organic phases are dried over $NaSO_4$. The solvent is removed in vacuo. The residual slightly yellow oil can be stored under argon in the fridge for further reactions.
^{1}H-NMR ($CDCl_3$, δ, ppm): 4.62 (d, CH_2), 4.09 (q, CH_2), 2.54 (t, CH), 1.30 (t, CH_3)
Raman (ν, cm^{-1}): 2978 (s), 2936 (s), 2729 (w), 2129 (s), 1457 (m), 1269 (m), 1102 (m), 743 (m), 313 (m)

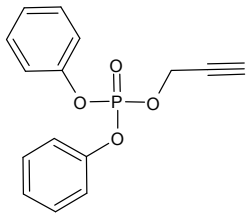

Diphenyl prop-2-ynyl phosphoric ester (DPPP) (7)

Diphenyl prop-2-ynyl phosphoric ester is prepared according to a modified procedure described by Jones et al.[157] Under a nitrogen atmosphere, diphenyl phosphoryl chloride (1 equivalent) dissolved in 20 times the amount of dry THF is cooled to -5 °C in an isopropanol/nitrogen bath. Under continuous stirring triethylamine (1 equivalent) is added drop wise. The isopropanol/nitrogen bath is removed and the mixture is stirred for an additional 1.5 h at ambient temperature. After cooling to -10 °C, propargyl alcohol (2.2 equivalents) is added drop wise under continuous stirring. The mixture is stirred at -10 °C for an additional 30 min followed by 2 h at ambient temperature. The obtained slightly yellow mixture is separated from triethylamine hydrochloride by filtration and washed with saturated sodium hydrogen sulfate solution. The aqueous layers are additionally extracted with THF. The combined organic phases are dried over $NaSO_4$. The solvent is removed in vacuo. The residual slightly yellow oil can be stored under argon in the fridge for further reactions.
^{1}H NMR (DMSO-d6, δ, ppm): 7.42 - 7.46 (m, Ph-H), 7.28 - 7.26 (m, Ph-H), 5.08 (d, CH_2), 3.73 (s, CH)
^{13}C NMR ($CDCl_3$, δ, ppm): 150, 130, 126, 120, 80, 57;
^{31}P NMR ($CDCl_3$, δ, ppm): 12.6.
IR (ν, cm^{-1}): 1589 (m), 1486 (m), 1456 (w), 1285 (m), 1183 (s), 1160 (s), 1024 (s), 939 (s), 752 (s), 685 (s)

Raman (ν, cm^{-1}): 3072 (s), 2950 (w), 2130 (s), 1594 (m), 1220 (w), 1165 (w), 1007 (s), 729 (m)

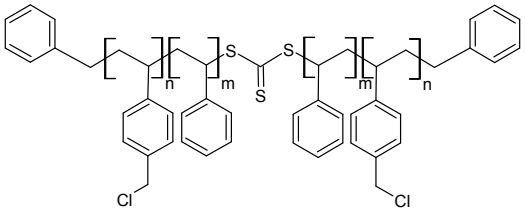

Linear P(S-VBC) Copolymer (8)

Copolymers with various contents of chloride functionalities are prepared according to a procedure described by Lang et al.[161] A mixture of styrene, 4-vinylbenzyl chloride (VBC), dibenzyltrithiocarbonate (DBTTC) and 1,10-azobis-(cyclohexane carbonitrile) (VAZO-88) is cooled in an ice bath and percolated with argon for 1 h. The polymerization proceeds at 80 °C for 20 h. After cooling to 0 °C, the mixture is diluted with THF and precipitated from methanol. The polymer is precipitated twice and finally dried in vacuo at 40 °C. Conversion is determined via SEC and the content of chloride in the polymer can be calculated via ^{1}H NMR analysis.
^{1}H NMR ($CDCl_3$, δ, ppm): 7.47-6.24 (m, Ph-H), 4.54 (s, CH_2-Cl), 2.47-1.13 (m, CH_2 backbone)
XPS (eV): 200.4 (Cl2p3), 201.9 (Cl2p1)
IR (ν, cm^{-1}): 3024 (w), 2920 (m), 2089 (s), 1662 (m), 1625 (m), 1601 (m), 1493 (s), 1451 (m), 1421 (m), 1249 (s), 1213 (m), 1187 (m), 1094 (m), 1011 (m), 815 (m), 760 (s), 698 (s)

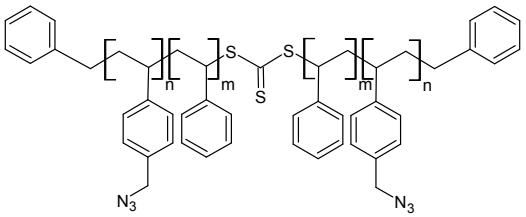

Linear P(S-VBA) Copolymer (9)

A mixture of chloride functionalized copolymer **(8)** and 1.2 equivalents sodium azide (relative to the ratio of -CH2Cl groups) in dry DMF is stirred at ambient temperature for 60 h. After precipitation from water, the azide functionalized copolymer is precipitated from methanol and dried in vacuo at 40 °C.
^{1}H NMR ($CDCl_3$, δ, ppm): 7.38-6.22 (m, Ph-H), 4.24 (s, CH_2-N_3), 2.43-1,16 (m, CH, CH_2 backbone)

XPS (eV): 399.3, 401.0, 404.7 (N1s = azide)
IR (ν, cm^{-1}): 3024 (w), 2920 (m), 2089 (s), 1601 (m), 1493 (s), 1451 (s), 1421 (m), 1340 (m), 1243 (s), 1203 (m), 1019 (w), 805 (s), 758 (s), 698 (s)

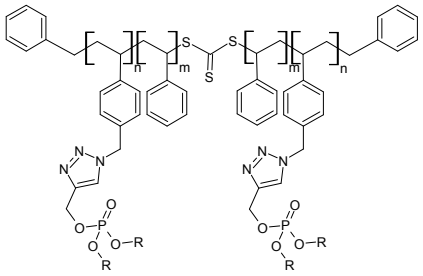

Phosphorylated P(S-VBA) Copolymer (10)

A mixture of azide functionalized styrene copolymer **(9)** (1 equivalent), alkyne functionalized ester **(5),(6)** or **(7)** (2 equivalents), copper (II) sulfate pentahydrate (0.2 equivalents) and sodium ascorbate (0.2 equivalents) in DMF is stirred at ambient temperature for 39 h. All quantities are relative to the CH_2-N_3 groups in the copolymer. After precipitation from water, the phosphorylated copolymer is suspended in DMF. After precipitation from methanol, it is dried in vacuo at 40 °C.
Solid state NMR (δ, ppm): ^{1}H NMR = 2, 4, 7 ; ^{13}C NMR = 40, 130, 148; ^{31}P NMR = -11
XPS (eV): 134.3 (P2p1/P2p3), 400.3, 402.6 (N1s = triazol)

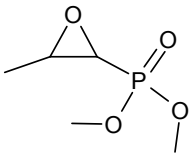

1,2-DiMe-Fos via the free acid using TMS-diazomethane (11)

1 equivalent of the disodium salt of fosfomycin is added to 40 times the amount of methanol and cooled to 0 °C using an ice bath. Via a syringe, 2 equivalents of methanesulfonic acid are applied and subsequently stirred for 1 h at 0 °C. After addition of 2.5 equivalent trimethylsilyl (TMS) diazomethane, the clear solution stirred an additional hour at ambient temperature. The resulting white precipitate was filtered off and the filtrate is neutralized with 0.5 M KOH solution, which in turn precipitates a white precipitate, which is filtered off again. After addition of saturated NaCl solution, the mixture is extracted several times with chloroform. The organic phase is dried over

$NaSO_4$ and concentrated under vacuum. The resulting yellow oil is purified by fractional distillation (40 °C, 0.21 bar). A colorless oil is obtained, which, however, does not contain the characteristic resonances of the dimethyl ester.

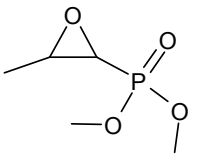

1,2-DiMe-Fos via the free acid using a polymer-bound triazene (12)

1 equivalent of the disodium salt of fosfomycin is added to 15 times the amount of methanol in a flask purged with nitrogen and cooled to 0 °C using an ice bath. Via a syringe, 2 equivalents of methanesulfonic acid are applied and subsequently stirred for 1 h at 0 °C. After addition of 2 equivalents of the methylated polymer bound triazene resin (loading: 0.001 $g \cdot mol^{-1}$) (structure shown in Chapter 4.2), the mixture is stirred an additional hour at ambient temperature. The solid parts of the mixture are filtered off. After addition of saturated $NaHCO_3$ solution, the mixture is extracted several times with chloroform. The organic phase is dried over $NaSO_4$ and concentrated under vacuum. The resulting colorless oil does not contain the characteristic resonances of the dimethyl ester.

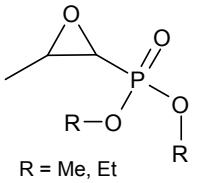

1,2-DiMe-Fos/1,2-DiEt-Fos via Steglich esterification (13)

1 equivalent of the disodium salt of fosfomycin is added to 30 times the amount of dichloromethane (CH_2Cl_2). 0.1 equivalents of 4-(dimethylamino)pyridine (DMAP) and 2 equivalents of methanol, respectively, ethanol are added and the mixture is cooled to 0 °C. Via a syringe, 1.1 equivalents dicyclohexylcarbodiimide (DCC) dissolved in 2 times of the amount CH_2Cl_2 are applied and the final mixture is stirred at 0 °C for 30 min. Subsequently the clear solution is stirred at ambient temperature over night. The white precipitate is filtered off using a pore 4 frit. NMR measurements reveal no conversion to the diesters.

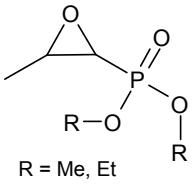

1,2-DiMe-Fos/1,2-DiEt-Fos using SiO_2-Cl (14)

Firstly, the chlorinating agent SiO_2-Cl is prepared by the following procedure: 1 equivalent of silica gel (60 Å) is suspended in 2.5 times of the amount dichloromethane (CH_2Cl_2) under nitrogen atmosphere. To the suspension, 60 w% thionylchloride is added dropwise via a syringe at ambient temperature. After completion of the gas evolution, the mixture is stirred for an additional 1 h. The solution turns slightly red during the reaction. After evaporation of the solvent, the slightly reddish powderous material is stored under argon atmosphere until further use.
For the esterification reaction, 1 equivalent of the disodium salt of fosfomycin is added to 20 times the amount of acetonitrile, respectively, chloroform. After addition of 1 equivalent of the previously prepared chlorinated silica gel (SiO_2-Cl) under nitrogen atmosphere, the mixture is cooled down to 0 °C. Via a syringe, 4 equivalents of methanol/ethanol are added dropwise. Subsequently the colorless soulution is stirred for 20 min at ambient temperature. The white silica gel and precipitate are filtered off and the solvent was evaporated under reduced pressure. NMR measurements reveal no conversion to the diesters.

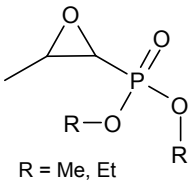

1,2-DiMe-Fos/1,2-DiEt-Fos using $SOCl_2$ (15)

1 equivalent of the disodium salt of fosfomycin is added to 30 times the amount of pyridine and cooled to 0 °C. Via a syringe 2.25 equivalents of thionylchloride ($SOCl_2$) are added dropwise and the mixture is stirred at 0 °C for 1 h. Subsequently, 3 equivalents of MeOH/EtOH, respectively, NaOMe are added to the cooled mixture and stirred at ambient temperature over night. The solution turns black. The solvent is evaporated under reduced pressure. The black oil is diluted in saturated $NaHCO_3$ and extracted with chloroform. The organic

phase is dried over $NaSO_4$ and concentrated under reduced pressure. NMR measurements reveal no conversion to the diesters.

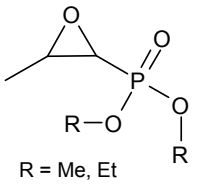

1,2-DiMe-Fos/1,2-DiEt-Fos using $POCl_3$ (16)

1 equivalent of the disodium salt of fosfomycin is added to a 25 times amount of a 5:1 mixture of chloroform and pyridine, which is subsequently cooled to 0°C. Via a syringe 2 equivalents of propargylchloride ($POCl_3$) are added dropwise and the mixture is stirred at 0 °C for 1 h and an additional 2 h at ambient temperature. Despite slow addition of MeOH/EtOH, the solution turns to a brown, yet clear solution. The mixture is stirred at ambient temperature over night. After addition of saturated $NaHCO_3$ solution and after completion of the gas evolution, the solution is extracted with chloroform. The bright yellow solution is concentrated under reduced pressure. NMR measurements reveal partial conversion to the diesters, however, with the formation of many side products. A separation of the one and disubstituted alkyl esters of fosfomycin is not possible, since the fosfomycin ester degenerates on a silica gel column and a fractionated destillation results in a mixture of mono- and dialkylated ester products, yet without side products.

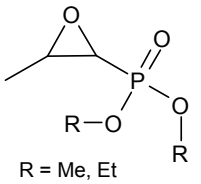

1,2-DiMe-Fos/1,2-DiEt-Fos using PCl_5/oxalyl chloride (17)

First, experiments without application of oxalic acid were performed leading to no conversion. With the addition of carbon tetrachloride (CCl_4) instead of oxalic acid, a conversion could be observed, however, with many by-products. Due to the high health risks, this approach was not pursued and instead performed with oxalic acid to reach an *in-situ* conversion of PCl_5 to $POCl_3$.
1 equivalent of the disodium salt of fosfomycin is added to a 25 times amount of pure pyridine **(a)**, respectively, a 2:1 mixture of pyridine and chloroform **(b)**

and other solvent/buffer systems. The mixture is subsequently cooled to 0 °C. Firstly, 1.5 equivalents of oxylic acid are added under stirring, secondly phosphorus pentachloride (PCl_5) is added in small portions via a solids metering device. The mixture is stirred at 0 °C for 1 h and additional 4 h at ambient temperature. The alcohol (MeOH, respectively, EtOH) is added slowly via a syringe and the resulting clear solution is stirred at ambient temperature over night. After addition of saturated $NaHCO_3$ solution and after completion of the gas evolution, the solution is extracted with chloroform. The slightly yellowish solution is concentrated under reduced pressure. NMR measurements of the reaction in pure pyridine **(a)** show only partially conversion. The NMR measurements in a 2:1 mixture of pyridine/chloroform **(b)** reveal full conversion to the diesters. A purification of the dialkyl esters is carried out by twofold destillation (see number **(18)**).
1,2-DiMe-Fos:
yield: 24.5 %
^{1}H NMR ($CDCl_3$, δ, ppm): 3.80 (m, CH_3), 3.26 (m, CH), 2.86 (dd, CH), 1.53 (d, CH_3)
IR (ν, cm^{-1}): 2956 (m), 1625 (w), 1487 (w), 1403 (w), 1251 (m), 1189 (m), 1010 (s), 817 (s), 783 (m), 762 (m)

1,2-DiEt-Fos:
Yield: 24.8 %
^{1}H NMR ($CDCl_3$, δ, ppm): 4.16 (m, CH_2), 3.24 (m, CH), 2.83 (dd, CH), 1.54 (d, CH_3), 1.30 (m, CH_3)
IR (ν, cm^{-1}): 2956 (m), 1487 (w), 1453 (m), 1402 (w), 1351 (m), 1188 (m), 1012 (s), 815 (s), 781 (m), 762 (m)

Purification of 1,2-DiMe-Fos/1,2-DiEt-Fos (18)

All dialkyl fosfomycin esters were purified by distillation at reduced pressure (at least $1{\cdot}10^{-3}$ bar) and elevated temperatures (1,2-DiMe-Fos $\geq$ 90 °C; 1,2-DiEt-Fos $\geq$ 110 °C; 2,3-DiMe-Fos $\geq$ 135 °C; 2,3-DiEt-Fos $\geq$ 155 °C) after stirring over calcium hydride (CaH_2) overnight. After stirring over iso-butyl aluminum (Aldrich, 1 M in toluene) for 1 h the dialkyl fosfomycin esters were destilled a second time at the same reduced pressure and temperature as in the first destillation procedure. The slightly yellowish liquids filled in precalibrated ampoules, which were sealed by Young taps, were degassed afterwards

by three successive freezing-evacuation-thawing cycles using extra dry argon and stored for further use in a freezer at -20 °C (maximum 3 days).

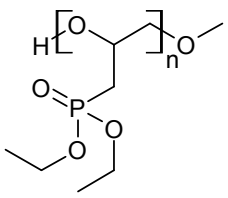

Polymerization of 2,3-DiEt-Fos via anionic ROP (19)

To obtain the extra dry toluene, the toluene is distilled out of the storage container under vacuum in a nitrogen cooled glass vessel via the anionic system. The methanol, respectively, destilled water to quench the polymerization are degassed using the cryo-thraw-methode. Prior to use of the anionic reactor, the toluene, degassed methanol/water and monomer vessels all sealed by Young taps must be placed before annealing at the anionic apparatus (see picture of the apparatus in Chapter 4.3.). The reactor and the transition pieces to the vessels are heated with a heat gun under vacuum (at least $1{\cdot}10^{-3}$ bar) and cooled down under pre-dried argon atmosphere for three times. The powderous initiator $NOct_4Br$ was dried prior to use in the anionic reactor by dissolving $NOct_4Br$ in extra dry toluene and evaporation of toluene under high vacuum for three times. Then 3 times the amount of the employed monomer volume is poured in the reaction vessel from the toluene vessel. The reactor vessel is cooled down by a $CaCl_2{\cdot}6\ H_2O$ ice bath to -20 °C. The monomer is employed from the pre-calibrated monomer vessel, followed by the application of the $^{i}Bu_3Al$ dissolved in toluene (25 w% in toluene) via a syringe, which was connected to the reaction vessel via a PTFE plug before annealing. The syringe was protected from the heat and vaccum during annealing by a Young tap. In subsequent experiments, the reaction time was increased from 2 h to 2 weeks. Beyond, also the reaction temperature was increased to up to 70 °C. At higher temperatures, the pre-dried reagents were initially introduced into a glove box. There, all reagents were placed in a high-pressure tube, and reacted in it up to a temperature of 160 °C. To quench the polymerization reaction, a small amount of degassed methanol, respectively, degased water is added. The final solution is precipitated in cold methanol. The white precipitate is filtered off and dried under vacuum at 40 °C.

Appendix A

The chapter "Appendix" provides an overview of the syntheses carried out for the conversion of fosfomycin disodium salt to the methylated, respectively, ethylated fosfomycin diester (**Appendix A1**) and the subsequently polymerization approches to polymerize fosfomycin diesters and derivatives thereof (**Appendix A2 to A4**). Only the employed reagents are specified.

In the case of the conversion reactions (**Appendix A1**), the syntheses were carried out according to the reaction conditions **(11)** to **(17)** described in Chapter 7.3. Table A1 gives an overview of the conversions of Na-Fos to dialkyl fosfomycin esters regarding the preservation of the epoxy ring and the conversion to dialkyl esters measured by NMR. Bold lines show the syntheses with good conversion to the diester and preservation of the epoxy ring.

Appendix A2 - A4 give an overview about the polymerization approaches to polymerize fosfomycin diesters and derivatives thereof. Table A2 gives an overview about the polymerization approaches based on the ammonium/aluminum initiator/catalyst complex by Carlotti et al., employing epichlorohydrin (EPI) as reference monomer, the prepared fosfomycin ester 1,2-DiEt-Fos and in addition, the commercial available 2,3-DiEt-Fos, due to the terminal epoxy ring and the therefore assumed higher reaction ability. The syntheses were carried out according to the reaction condition **(19)** described in Chapter 7.3. Table A3 shows approaches in which unlike the ammonium/aluminum complex employed by Carlotti et al., different catalyst/initiator systems were used.

A.1 Syntheses of Fosfomycin Diesters

solvent	**reagents**	**epoxy**	**ester**	conditions	**comments**
MeOH	Na-Fos; MSA; TMS-diazomethane	+	-	(11)	
MeOH	Na-Fos; MSA; polymeric triazene resin	+	-	(12)	
CH_2Cl_2	Na-Fos; DCC; DMAP; MeOH	+	-	(13)	
acetonitrile/$CHCl_3$	Na-Fos; DCC; DMAP	+	-	(13)	
acetonitrile	Na-Fos; SiO_2-Cl; MeOH	-	-	(14)	
$CHCl_3$	Na-Fos; SiO_2-Cl; MeOH	-	-	(14)	
pyridine	Na-Fos; $SOCl_2$; MeOH	+	-	(15)	
pyridine	**Na-Fos; $POCl_3$; MeOH**	+	+	(16)	**by-products**
pyridine	**Na-Fos; PCl_5; CCl_4; MeOH**	+	+	(17)	**ratio by-products T dependent**
pyridine	Na-Fos; PCl_5; NaOMe respectively MeOH	-	-	(17)	
DMSO respectively THF	Na-Fos; PCl_5; MeOH ; pyridine	-	-	(17)	
$CHCl_3$	Na-Fos; PCl_5; NaOMe	-	+	(17)	
pyridine	**Na-Fos; PCl_5; oxalic acid; MeOH**	+	+	(17)	**by-products**
DMF/imidazol	Na-Fos; PCl_5; oxalic acid; MeOH	-	-	(17)	
$CHCl_3$/NEt_3	Na-Fos; PCl_5; oxalic acid; MeOH	-	-	(17)	
$CHCl_3$/imidazol	Na-Fos; PCl_5; oxalic acid; MeOH	-	-	(17)	
DMSO/imidazol	Na-Fos; PCl_5; oxalic acid; MeOH	-	-	(17)	
acetonitrile/NEt_3	Na-Fos; PCl_5; oxalic acid; MeOH	-	-	(17)	
acetonitrile/imidazol	Na-Fos; PCl_5; oxalic acid; MeOH	-	-	(17)	
$CHCl_3$/pyridine	**Na-Fos; PCl_5; oxalic acid; MeOH/EtOH**	+	+	(17)	**by-products solvent ratio dependent**

Table A.1: Syntheses of Na-Fos to dialkyl fosfomycin esters regarding preservation of the epoxy ring and conversion.

A.2 Homopolymerization of fosfomycin diesters via Carlotti et al.

monomer	**monomer : ^{i}Bu$_3$Al : NOct$_4$Br [mol]**	**comments; reaction time (RT); pressure tube (HPT)**	polymer
1,2-DiEt-Fos	1 : 0.0182 : 0.0090	NOct$_4$Br stock solution; RT = 2:00 h	-
1,2-DiEt-Fos	1 : 0.0089 : 0.0088	NOct$_4$Br stock solution; RT = 2:13 h	-
EPI	1 : 0.0057 : 0.0014	NOct$_4$Br stock solution; RT = 2:00 h	-
EPI	1 : 0.0023 : 0.0019	NOct$_4$Br stock solution; RT = 2:00 h	-
EPI	1 : 0.0071 : 0.0003	RT = 2:00 h	M_n = 15900 g · mol^{-1}; PDI = 1.13 (THF)
2,3-DiEt-Fos	1 : 0.0137 : 0.0004	RT = 5:00 h	-
2,3-DiEt-Fos	**1 : 0.0340 : 0.0009**	**70 °C for 5 min; RT = 5:00 h**	**$M_n \approx$ 1600 g · mol^{-1} (MALDI)**
2,3-DiEt-Fos	1 : 0.0068 : 0.0004	Glove box; HPT; 157 °C for 30 min; RT = 2:15 h	-
EPI	1 : 0.0068 : 0.0022	HPT; RT = 2:00 h	M_n = 41600 g · mol^{-1}; PDI = 2.08 (THF)
EPI	1 : 0.0071 : 0.0035	RT = 2:00 h	M_n = 16000 g · mol^{-1}; PDI = 1.18 (THF)
2,3-DiEt-Fos	1 : 1.1340 : 0.0008	RT = 3:00 h	-
2,3-DiEt-Fos	1 : 0.5670 : 0.0008	RT = 2:00 h	-
2,3-DiEt-Fos	1 : 0.5670 : 0.0016	RT = 3:00 h	-
2,3-DiEt-Fos	1 : 0.5670 : 0.0016	Glove box; PT; 157 °C for 30 min; RT = 2:15 h	-
2,3-DiEt-Fos	1 : 0.0340 : 0.0003	Glove box; RT = 2 days	-
2,3-DiEt-Fos	1 : 0.0177 : 0.0087 + 0.0008 (crown ether)	RT = 8:00 h	-
2,3-DiEt-Fos	1 : 0.0181 : 0.0087 + 0.0002 (crown ether)	Glove box; RT = 2 weeks	-
2,3-DiEt-Fos	1 : 0.0181 : 0.0087	Glove box; RT = 2 weeks	M_n = 10000 g · mol^{-1}; PDI = 2.47 (THF)
2,3-DiEt-Fos	**1 : 0.0340 : 0.0004**	**Glove box; RT = 70 °C for 3.5 h; HPT**	**white unsoluble powder**
2,3-DiEt-Fos	**1 : 0.0170 : 0.0087**	**Glove box; RT = 50 °C over night**	**white unsoluble powder**

Table A.2: Homopolymerization approaches for the anionic ROP of dialkyl fosfomycin esters via Carlotti et.al.

A.3 Homopolymerization of fosfomycin diesters via different initiator systems

reagents	**ratios [mol]**	**conditions; reaction time (RT)**	polymer
2,3-DiEt-Fos : BuLi	1 : 0.0272	in toluene; RT = 2 h	-
2,3-DiEt-Fos : BuLi	1 : 0.0272	in DMSO; RT = 2 h	-
2,3-DiEt-Fos : butanol : $Sn(Oct)_2$	1 : 0.0007 : 0.0003	in toluene; Glove box; RT = 100 °C for 20 h	M_n = 4100 g · mol^{-1}; PDI = 1.09 (THF)
2,3-DiEt-Fos : butanol : TBD	1 : 0.0002 : 0.0115	in toluene; RT = 21 h	-
2,3-DiEt-Fos : $BF_3{\cdot}Et_2O$	1 : 0.0008	in THF; RT = 1 h	poly-THF
2,3-DiEt-Fos : $BF_3{\cdot}Et_2O$: H_2O	1 : 0.0008 : 0.0056	in THF; RT = 1 h	poly-THF
2,3-DiEt-Fos : $BF_3{\cdot}Et_2O$	1 : 0.0008	in THF; under air; RT = 1 h	poly-THF
2,3-DiEt-Fos : $BF_3{\cdot}Et_2O$	1 : 0.0008	in toluene; RT = 15 h	poly-THF

Table A.3: Polymerization approaches with various initiator systems unlike the ammonium/aluminum complex of Carlotti et al.

A.4 Copolymerization of fosfomycin diesters via Carlotti et al.

monomer	**monomer : $^{i}Bu_3Al$: $NOct_4Br$ [mol]**	**comments reaction time (RT); high pressure tube (HPT)**	polymer
2,3-DiEt-Fos/EPI	1+9 : 0.0076 : 0.0037	RT = 2:00 h	-
2,3-DiEt-Fos/EPI	1+5 : 0.0132 : 0.0007	RT = 3:00 h	M_n = 10000 g · mol^{-1}; PDI = 3.08 (THF)
2,3-DiEt-Fos/EPI	1+9 : 0.0485 : 0.0003	RT = 3:00 h	M_n = 34000 g · mol^{-1}; PDI = 2.36 (DMSO)

Table A.4: Copolymerization approaches for the anionic ROP of dialkyl fosfomycin esters via Carlotti et.al.

Bibliography

[1] Hellerich, Harsch, and Haenle. *Werkstoff-Führer Kunststoffe*. Hanser, Munich, Germany, 1996.

[2] H.-G. Elias. *An introduction to plastics*. Wiley-VCH, Weinheim, Germany, 2003.

[3] J.M.J. Fréchet. Functional polymers: From plastic electronics to polymer-assisted therapeutics. *Progress in Polymer Science*, 30:844–857, 2005.

[4] A. Akelah and A. Moet. *Functionalized polymers and their application*. Chapman and Hall, New York, USA, 1990.

[5] X. Wang, Y. Hu, L. Song, W. Xing, and H. Lu. Preparation, mechanical properties, and thermal degradation of flame retarded epoxy resins with an organophosphorus oligomer. *Polymer Bulletin*, 67:859–873, 2011.

[6] R. Yang, L. Chen, W.Q. Zhang, H.B. Chen, and Y.Z. Wang. In situ reinforced and flame-retarded polycarbonate by a novel phosphorus containing thermotropic liquid crystalline copolyester. *Polymer*, 52:4150–4157, 2011.

[7] M. Lewin and E.D. Weil. Mechanism and modes of action in flame retardancy of polymers. In A.R. Horrocks and D. Price, editors, *Fire Retardant Materials*. Woodhead Publishing, UK, 2001.

[8] S. Bourbigot and M. Le Bras. Flame retardants. In J. Troitzsch, editor, *Plastics Flammability Handbook*. Hanser, Munich, Germany, 3rd edition, 2004.

[9] R.V. Petrella. Factors affecting the combustion of polystyrene and styrene. In M. Lewin, S.M. Atlas, and E.M. Pearce, editors, *Flame*

Retardant Polymeric Materials. Plenum Press, New York, 2nd edition, 1978.

[10] C.A. Wilkie. An introduction to the use of fillers and nanocomposites in fire retardancy. In *Fire Retardancy of Polymers*. Royal Society of Chemistry - Special Publication, New York, USA, 2005.

[11] C. Barner-Kowollik. *Handbook of RAFT Polymerization*. Wiley-VCH, 2008.

[12] A. Gregory and M. H. Stenzel. Complex polymer architectures via RAFT polymerization: From fundamental process to extending the scope using click chemistry and nature's building blocks. *Progress in Polymer Science*, 37:38–105, 2012.

[13] C. Barner-Kowollik, F.E. Du Prez, P. Espeel, C.J. Hawker, T. Junkers, H. Schlaad, and W. Van Camp. "Clicking" polymers or just efficient linking: What is the difference? *Angewandte Chemie International Edition*, 50:60–62, 2011.

[14] A. Echte. *Handbuch der technischen Polymerchemie*. VCH, Weinheim, Germany, 1st edition, 1993.

[15] H. Fischer and L. Radom. Factors controlling the addition of carbon-centered radicals to alkenes - an experimental and theoretical perspective. *Angewandte Chemie International Edition*, 40:1340–1371, 2001.

[16] M. Buback, R.G. Gilbert, R.A. Hutchinson, B. Klumperman, F.-D. Kuchta, B.G. Manders, K.F. O'Driscoll, G.T. Russell, and J. Schweer. Critically evaluated rate coefficients for free-radical polymerization. *Macromolecular Chemistry and Physics*, 196:3267–3280, 1995.

[17] H.-G. Elias. *Makromoleküle 1. Chemische Struktur und Synthesen*. Wiley-VCH, Weinheim, Germany, 2000.

[18] K. Matyjaszewski and T.P. Davis. *Handbook of Radical Polymerization*. Wiley and Sons, Ldt., 1 edition, 2002.

[19] B. Tieke. *Makromolekulare Chemie*. Wiley-VCH, Weinheim, Germany, 3th edition, 2005.

[20] A. Brandrup, E.H. Immergut, and E.A. Grulke. *Polymer Handbook*. Wiley and Sons, 4th edition, 1999.

[21] F.R. Mayo. Chain transfer in the polymerization of styrene: The reaction of solvents with free radicals. *Journal of the American Chemical Society*, 65:2324–2329, 1943.

[22] D.I. Christie and R.G. Gilbert. Transfer constants from complete molecular weight distributions. *Macromolecular Chemistry and Physics*, 198:663, 1997.

[23] J.P.A. Heuts, T.P. Davis, and G.T. Russell. Comparison of the Mayo and chain length distribution procedures for the measurement of chain transfer constants. *Macromolecules*, 32:6019–6030, 1999.

[24] B. Vollmert. *Grundriß der makromolekularen Chemie*. Vollmert Verlag, Karlsruhe, Germany, 3th edition, 1988.

[25] J.E. McGrath. *Anionic Polymerization: Kinetics, Mechanism and Synthesis*. ACS Symposium Series, St. Louis, USA, 166th edition, 1981.

[26] M. Szwarc. *Living Polymers and Electron Transfer Process*. Wiley Interscience, New York, USA, 1968.

[27] R.P. Quirk and W.-C. Chen. Functionalization of polymeric organolithium compounds. Carbonation. *Macromolecular Chemistry*, 183:2071–2076, 1982.

[28] H.L. Hsieh and R.P. Quirk. *Plastics engineering: Anionic polymerization - principles and practical applications*. Marcel Dekker, Inc., New York, USA, 1996.

[29] Odian. G. *Principles of polymerization*. Wiley-Interscience, Hoboken, NJ, 4th edition, 2004.

[30] A. Hirao and M. Hayashi. Recent advance in syntheses and applications of well-defined end-functionalized polymers by means of anionic living polymerization. *Acta Polymerica*, 50:219–231, 1999.

[31] S. Carlotti, A. Labbé, V. Rejsek, S. Doutaz, M. Gervais, and A. Deffieux. Living/controlled anionic polymerization and copolymerization of epichlorohydrin with tetraoctylammonium bromide - triisobutylaluminum initiating systems. *Macromolecules*, 41:7058–7062, 2008.

[32] P. Kubisa. Cationic polymerization of heterocycles. In K. Matyjaszewski, editor, *Cationic Polymerizations: Mechanisms, Synthesis and Applications*. Marcel Dekker, Inc., New York, USA, 1996.

[33] K. Matyjaszewski. *Controlled/Living Radical Polymerization – Progress in ATRP, NMP and RAFT*. ACS Symposium Series, Washington, USA, 768 edition, 2000.

[34] E. Rizzardo and D.H. Solomon. A new method for investigating the mechanism of initiation of radical polymerization. *Polymer Bulletin*, 1:529–534, 1979.

[35] J.-S. Wang and K. Matyjaszewski. Controlled/"living" radical polymerization. Atom transfer radical polymerization in the presence of transition-metal complexes. *Journal of the American Chemical Society*, 117:5614–5615, 1995.

[36] M. Kato, M. Kamigaito, M. Sawamoto, and T. Higashimura. Polymerization of methyl methacrylate with the carbon tetrachloride/dichlorotris-(triphenylphosphine)ruthenium-(II)-methylaluminum bis(2,6-di-tert-butylphenoxide) initiating system: Possibility of living radical polymerization. *Macromolecules*, 28:1721–1723, 1995.

[37] J. Chiefari, Y.K.B. Chong, F. Ercole, J. Krstina, J. Jeffery, T.P.T. Le, R.T.A. Mayadunne, G.F. Meijs, C.L. Moad, G. Moad, E. Rizzardo, and S.H. Thang. Living free-radical polymerization by reversible addition fragmentation chain transfer: The RAFT process. *Macromolecules*, 31:5559–5562, 1998.

[38] W. Tang, N.V. Tsarevsky, and K. Matyjaszewski. Determination of equilibrium constants for atom transfer radical polymerization. *Journal of the American Chemical Society*, 128:1598–1604, 2006.

[39] P. Corpart, D Charmot, T. Biadatti, S. Zard, and D. Michelet. *Method for block polymer synthesis by controlled radical polymerization.* WO9858974 A1, 1998.

[40] C. Barner-Kowollik, M. Buback, B. Charleux, M.L. Coote, M. Drache, T. Fukuda, A. Goto, B. Klumpermann, A.B. Lowe, J. McLeary, G. Moad, M.J. Monteiro, R.D. Sanderson, M.P. Tonge, and P. Vana. Mechanism and kinetics of dithiobenzoate-mediated RAFT polymerization, 1: The current situation. *Journal of Polymer Science Part A: Polymer Chemistry*, 44:5809–5831, 2006.

[41] W. Kern, R.C. Schulz, and D. Braun. Macromolecules with groups of high reactivity. *Journal of Polymer Science*, 48:91–100, 1960.

[42] H. Staudinger. Die Chemie der hochmolekularen organischen Stoffe im Sinne der kekuléschen Strukturlehre. *Berichte der deutschen chemischen Gesellschaft*, 59:3019–3043, 1926.

[43] H.C. Kolb, M.G. Finn, and K.B. Sharpless. Click chemistry: Diverse chemical functions from a few good reactions. *Angewandte Chemie - International Edition*, 40:2004–2021, 2001.

[44] Wikipedia. Click-chemie.

[45] F. Himo, T. Lovell, R. Hilgraf, V.V. Rostovtsev, L. Noodleman, K.B. Sharpless, and V.V. Fokin. Copper(I)-catalyzed synthesis of azoles. DFT study predicts unprecedented reactivity and intermediates. *Journal of the American Chemical Society*, 127:210–216, 2005.

[46] D.D. Díaz, S. Punna, P. Holzer, A.K. McPherson, K.B. Sharpless, V.V. Fokin, and M.G. Finn. Click chemistry in materials synthesis. 1. Adhesive polymers from copper-catalyzed azide-alkyne cycloaddition. *Journal of Polymer Science Part A: Polymer Chemistry*, 42:4392–4403, 2004.

[47] B. Helms, J.L. Mynar, C.L. Hawker, and J.M.J. Fréchet. Dendronized linear polymers via "click chemistry". *Journal of the American Chemical Society*, 126:15020–15021, 2004.

[48] P. Wu, A.K. Feldman, A.K. Nugent, C.J. Hawker, A. Scheel, B. Voit, J. Pyun, J.M.J. Fréchet, K.B. Sharpless, and V.V. Fokin. Efficiency and fidelity in a click-chemistry route to triazole dendrimers by the copper(I)-catalyzed ligation of azides and alkynes. *Angewandte Chemie International Edition*, 43:3928–3932, 2004.

[49] L. Macarie and G. Ilia. Poly(vinylphosphonic acid) and its derivatives. *Progress in Polymer Science*, 35:1078–1092, 2010.

[50] S. Gottesfeld and T.A. Zawodzinski. Polymer electrolyte fuell cells. In R.C. Alkire, H. Gerischer, D.M. Kolb, and C.W. Tobias, editors, *Advances in electrochemical science and engineering*. Wiley-VCH, New York, USA, 1997.

[51] M. Yamada and I. Honma. Anhydrous proton conducting polymer electrolytes based on poly(vinylphosphonic acid)-heterocycle composite material. *Polymer*, 46:2986–2992, 2005.

[52] B.T. Dahiyat, M. Richards, and K.W. Leong. Controlled release from poly(phosphoester) matrices. *Journal of Controlled Release*, 33:13–21, 1995.

[53] L.W. Becker. *Poly(alenyl)phosphonic acid and methods of use thereof.* US 4446046, 1984.

[54] M. Anbar, G.A. St John, and A.C. Scott. Organic polymeric polyphosphonates as potential preventive agents of dental caries: In vitro experiments. *Journal of Dental Research*, 53:867–878, 1974.

[55] Y. Tang, T.J. Su, J. Armstrong, A.L. Lu, J.R. Lewis, T.A. Vick, P.W. Stratford, R.K. Heenan, and J. Penfold. Interfacial structure of phosphorylcholine incorporated biocompatible polymer films. *Macromolecules*, 36:8440–8448, 2003.

[56] J. Tan, R.A. Gemeinhart, M. Ma, and M.W. Saltzman. Improved cell adhesion and proliferation on synthetic phosphonic acid-containing hydrogels. *Biomaterials*, 26:3663–3671, 2005.

[57] M.L. Renier and D.H. Kohn. Development and characterization of a biodegradable polyphosphate. *Journal of Biomedical Materials Research*, pages 95–104, 1997.

[58] J.R. Lu, E.F. Murphy, T.J. Su, A.L. Lewis, and S.K. Stratford, P.W. Satija. Reduced protein adsorption on the surface of a chemically grafted phospholipid monolayer. *Langmuir*, 17:3382–3389, 2001.

[59] G.T. Eom, S.Y. Oh, and T.G. Park. In situ thermal gelation of water-soluble poly(n-isopropylacrylamide-co-vinylphosphonic acid). *Journal of Applied Polymer Science*, 70:1947–1953, 1998.

[60] V. Deluchat, S. Lacour, B. Serpaud, and J.C. Bollinger. Washing powders and the environment: has TAED any influence on the complexing behaviour of phosphonic acids? *Water Research*, 36:4301–4306, 2002.

[61] B. Nowack. Environmental chemistry of phosphonates. *Water Research*, 37:2533–2546, 2003.

[62] T. Nonaka, Y. Hanada, T. Watanabe, T. Ogata, and S. Kurihara. Formation of thermosensitive water-soluble copolymers with phosphinic acid groups and the thermosensitivity of the copolymers and copolymer/metal complexes. *Journal of Applied Polymer Science*, 92:116–125, 2004.

[63] S.J. Paddison and R. Paul. The nature of proton transport in fully hydrated Nafion(R). *Physical Chemistry, Chemical Physics*, 4:1158–1163, 2002.

[64] S.U. Celik, U. Akbey, R. Graf, A. Bozkurt, and W. Spiess. Anhydrous proton-conducting properties of triazole-phosphonic acid copolymers: A combined study with MAS and NMR. *Physical Chemistry Chemical Physics*, 10:6058–6066, 2008.

[65] K.S. Annakutty and K. Kishore. A novel approach to structure - flammability correlation in polyphosphate esters. *Polymer*, 29:1273–1276, 1988.

[66] S.H. Kim, J.Y. Kim, H.S. Kim, and H.N. Cho. Ionic conductivity of polymer electrolytes based on phosphate and polyether copolymers. *Solid State Ionics*, 116:63–71, 1999.

[67] S.R. Morris and B.G. Dixon. A novel approach for development of improved polymer electrolytes for lithium batteries. *Journal of Power Sources*, 119-121:487–491, 2003.

[68] B.G. Dixon, R.S. Morris, and S. Dallek. Non-flammable polyphosphonate electrolytes. *Journal of Power Sources*, 138:274–276, 2004.

[69] P. Kannan and K. Kishore. New flame retardant polyarylazo phosphate and phosphoramide esters. *European Polymer Journal*, 27:1017–1021, 1991.

[70] T. Saito. *Cyclic organophosphorus compounds and process for making them.* US3702878, 1972.

[71] C.H. Lin. Synthesis of novel phosphorus-containing cyanate esters and their curing reaction with epoxy resin. *Polymer*, 45:7911–7926, 2004.

[72] X. Wang, Y. Hu, L. Song, H. Xang, W. Xing, and H. Lu. Synthesis and characterization of a dopo-substitued organophosphorus oligomer and its application in flame retardant epoxy resins. *Progress in Organic Coatings*, 71:72–82, 2011.

[73] P. Wyman, V. Crook, J. Ebdon, B. Hunt, and P. Joseph. Flame-retarding effects of dialkyl-p-vinylbenzyl phosphonates in copolymers with acrylonitrile. *Polymer International*, 55:764–771, 2006.

[74] D. Price, K. Pyrah, T.R. Hull, G.J. Milnes, J.R. Ebdon, B.J. Hunt, P. Joseph, and C.S. Konkel. Flame retarding poly(methyl methacrylate) with phosphorus-containing compounds: Comparison of an additive with a reactive approach. *Polymer Degradation and Stability*, 74:441–447, 2001.

[75] E.L. Grefter. Organophosphorus monomers and polymers. In D.H.R. Barton and W. Doering, editors, *International Series of Monographs on Organic Chemistry*. Pergamon Press, Oxford, UK, 1962.

[76] J. Pretula and S. Penczek. Poly(ethylene glycol) ionomers with phosphate diester linkage. *Makromolekulare Chemie, Rapid Communications*, 9:731–737, 1988.

[77] J. Baran, P. Klosinski, and S. Penczek. Poly(alkylene phosphate)s by polycondensation of phosphonic diamides with diols. *Makromolekulare Chemie*, 190:1903–1917, 1989.

[78] S. Iliesu, E. Avram, A. Visa, N. Plesu, A. Popa, and G. Ilia. New technique for the synthesis of polyphosphoesters. *Macromolecular Research*, 19:1186–1191, 2011.

[79] S. Iliescu, G. Ilia, N. Plesu, A. Popa, and A. Pascariu. Solvent and catalyst-free synthesis of polyphosphates. *Green Chemistry*, 8:727–732, 2006.

[80] S. Iliescu, G. Ilia, and A. Pascariu. Novel synthesis of phosphorus containing polymers under inverse phase transfer catalysis. *Polymer*, 47:6509–6512, 2006.

[81] K. Kaluzinski, J. Libiszowski, and S. Penczek. A new class of synthetic polyelectrolytes. acidic polyesters of phosphoric acid (poly(hydroxyalkylene phosphates)). *Macromolecules*, 9:365–367, 1976.

[82] J.B. Pretula, K. Kaluzynski, and S. Penczek. Living reversible anonic polymerization of N,N´-diethylamine-1,3,2-dioxaphosphorinan. *Journal of Polymer Science: Polymer Chemistry Edition*, 22:1251–1258, 1984.

[83] S. Penczek, J.B. Pretula, K. Kaluzynski, and G. Lapienis. Polymers with esters of phosphoric acid units: From synthesis, models of biopolymers to polymer-inorganic hybrids. *Israel Journal of Chemistry*, 52:306–319, 2012.

[84] S. Iliesu, L. Zubizarreta, N. Plesu, L. Macarie, A. Popa, and G. Ilia. Polymers containing phosphorus groups and polyethers: From synthesis to application. *Chemistry Central Journal*, 6:132–145, 2012.

[85] N. Moszner, U. Salz, and J. Zimmermann. Chemical aspects of self-etching enamel–dentin adhesives: A systematic review. *Dental Materials*, 21:895–910, 2005.

[86] A.E. Arbuzov and N.P. Kushkova. Action of dihalo hydrocarbons on ethyl phosphite and the salts of diethyl phosphite. *Chemical Abstracts*, 30:4813–4814, 1936.

[87] P. Coutrot and C. Grison. *Encyclopedia of Reagents for Organic Synthesis*. Wiley and Sons, Ltd., New Jersey, USA, 2001.

[88] Z. El Asri, K. Chougrani, C. Negrell-Guirao, G. David, B. Boutevin, and C. Loubat. An efficient process for synthesizing and hydrolyzing a phosphonated methacrylate: Investigation of the adhesive and anticorrosive properties. *Journal of Polymer Science Part A: Polymer Chemistry*, 46:4794–4803, 2008.

[89] C. Negrell-Guirao, G. David, B. Boutevin, and K. Chougrani. Synthesis of novel copolymers obtained from acceptor/donor radical copolymerization of phosphonated allyl monomers and maleic anhydride. *Journal of Polymer Science Part A: Polymer Chemistry*, 49:3905–3910, 2011.

[90] R.J. Cohen, D.L. Fox, J.F. Eubank, and R.N. Salvatore. Mild and efficient Cs_2CO_3-promoted synthesis of phosphonates. *Tetrahedron Letters*, 44:8617–8621, 2003.

[91] G. David, C. Negrell-Guirao, F. Iftene, B. Boutevin, and K. Chougrani. Recent progress on phosphonate vinyl monomers and polymers therefore obtained by radical (co)polymerization. *Polymer Chemistry*, 3:265–274, 2012.

[92] M.I. Kabachnik and T. Medved. Vinylphosphonic acid and some of its derivatives. *Russian Chemical Bulletin*, 8:2043–2045, 1959.

[93] F. Rochlitz and H. Vilcsek. beta-chloroethylphosphonic dichloride: Its synthesis and use. *Angewandte Chemie International Edition*, 1:652–656, 1962.

[94] H.-J. Kleiner and G. Roscher. *Process for preparing vinylphosphonic acids*. US5811575, 1998.

[95] H.-J. Kleiner and W. Dursch. *Process for the preparation of vinylphosphonic acid diesters and vinylphosphonic acid*. US4493803, 1985.

[96] P. Tavs and H. Weitkamp. Herstellung und KMR-Spektren einiger α,β-ungesättigter Phosphonsäureester: Nickelsalzkatalysierte Reaktion von Vinylhalogeniden mit Trialkylphosphiten. *Tetrahedron*, 26:5529–5534, 1970.

[97] B. Bingöl, G. Hart-Smith, C. Barner-Kowollik, and G. Wegner. Characterization of oligo(vinyl phosphonate)s by high-resolution electrospray ionization mass spectrometry: Implications for the mechanism of polymerization. *Macromolecules*, 41:1634–1639, 2008.

[98] S. Jin and K.E. Gonsalves. Synthesis and characterization of functionalized poly(ϵ-caprolactone) copolymers by free-radical polymerization. *Macromolecules*, 31:1010–1015, 1998.

[99] Q. Wu and R.A. Weiss. Synthesis and characterization of poly (styrene-co-vinyl phosphonate) ionomers. *Journal of Polymer Science Part B: Polymer Physics*, 42:3628–3641, 2004.

[100] J. Muzart. Palladium-catalysed reactions of alcohols. Part C: Formation of ether linkages. *Tetrahedron*, 61:5955–6008, 2005.

[101] F. Iftene, G. David, B. Boutevin, R. Auvergne, A. Alaaeddine, and R. Meghabar. Novel dialkyl vinyl ether phosphonate monomers: Their synthesis and alternated radical copolymerizations with electron-accepting monomers. *Journal of Polymer Science Part A: Polymer Chemistry*, 50:2432–2443, 2012.

[102] F. D´Agosto, M.-T. Charreyre, F. Delolme, G. Dessalces, H. Cramail, A. Deffieux, and C. Pichot. Kinetic study of the "living" cationic polymerization of a galactose carrying vinyl ether. MALDI-TOF MS analysis of the resulting glycopolymers. *Macromolecules*, 35:7911–7918, 2002.

[103] R. Auvergne, L.R. Saint, C. Joly-Duhamel, J.J. Robin, and B. Boutevin. UV curing of a novel resin derived from poly(ethylene terephthalate). *Journal of Polymer Science Part A: Polymer Chemistry*, 45:1324–1335, 2007.

[104] R. Tayouo, G. David, and B. Ameduri. New fluorinated polymers bearing pendant phosphonic groups for fuel cell membranes. Part 1: Synthesis and characterizations of the fluorinated polymeric backbone. *European Polymer Journal*, 46:1110–118, 2010.

[105] K.G. Olson and G.B. Bulter. Stereochemical evidence for participation of a donor-acceptor complex in alternating copolymerization. 1. Model compound synthesis. *Macromolecules*, 17:2480–2486, 1984.

[106] X. Zhang, L. Zi-Chen, L. Kai-Bo, L. Song, D. Fu-Sheng, and L. Fu-Mian. Donor/acceptor vinyl monomers and their polymers: Synthesis, photochemical and photophysical behavior. *Progress in Polymer Science*, 31:893–948, 2006.

[107] P. Kohli and G.J. Blanchard. Design and growth of robust layered polymer assemblies with molecular thickness control. *Langmuir*, 15:1418–1422, 1999.

[108] P. Kohli, M.C. Rini, J.S. Major, and G.J. Blanchard. Elucidating the balance between metal ion complexation and polymer conformation in maleimide vinyl ether polymer multilayer structures. *Journal of Materials Chemistry*, 11:2996–3001, 2001.

[109] S.R. Sandler and W. Karo. *Polymer Syntheses*. Academic Press, 1992.

[110] C. Carbonneau, R. Frantz, J.O. Durant, G.F. Lanneau, and R.J.P. Corriu. Efficient syntheses of new phosphonate terminated trialcoxysilane derived oligoarylenevinylene fluorophores. *Tetrahedron Letters*, 40:5855–5858, 1999.

[111] B. Boutevin, Y. Hervaud, A. Boulahna, and M. El-Asri. Free-radical polymerization of dimethyl vinylbenzylphosphonate controlled by Tempo. *Macromolecules*, 35:6511–6516, 2002.

[112] I. Cabasso, J. Jaguar-Grodzinski, and D. Vofsi. Synthesis and characterization of polymers with pendent phosphonate groups. *The Journal of Organic Chemistry*, 18:1969–1986, 1974.

[113] Z. Yu, W.X. Zhu, and I. Cabasso. Synthesis and polymerization of vinylbenzylphosphonate diethyl ester. *Journal of Polymer Science Part A: Polymer Chemistry*, 28:227–230, 1990.

[114] F. Jiang, A. Kaltbeitzel, W.H. Meyer, H. Pu, and G. Wegner. Proton-conducting polymers via atom transfer radical polymerization of diisopropyl-p-vinylbenzyl phosphonate and 4-vinylpyridine. *Macromolecules*, 41:3081–3085, 2008.

[115] H. Pu, Y. Qin, D. Wan, and Z. Yang. Proton-conducting polymers via free radical polymerization of diisopropyl-p-vinylbenzyl phosphonate and 1-vinylimidazole. *Macromolecules*, 42:3000–3004, 2009.

[116] M. Gaboyard, T. Jeanmaire, C. Pichot, Y. Hervaud, and B. Boutevin. Seeded semicontinuous emulsion copolymerization of methyl methacrylate, butyl acrylate, and phosphonated methacrylates: Kinetics and morphology. *Journal of Polymer Science Part A: Polymer Chemistry*, 41:2469–2480, 2003.

[117] B. Rixens, G. Boutevin, A. Boulahna, Y. Hervaud, and B. Boutevin. Synthesis of new phosphonated monomers. *Phosphorus, Sulfur, and Silicon and the Related Elements*, 179:2617–2626, 2004.

[118] G. David, B. Boutevin, and Y. Hervaud. Synthesis of a new phosphonate methacrylate monomer. *Phosphorus, Sulfur, and Silicon and the Related Elements*, 180:2201–2209, 2005.

[119] Y. Catel, M. Degrange, L. Le Pluart, P.-J. Madec, T.-N. Pham, F. Chen, and W.D. Cook. Synthesis, photopolymerization, and adhesive properties of new bisphosphonic acid monomers for dental application. *Journal of Polymer Science Part A: Polymer Chemistry*, 47:5258–5271, 2009.

[120] D. Avci and A.Z. Albayrak. Synthesis and copolymerization of new phosphorus-containing acrylates. *Journal of Polymer Science Part A: Polymer Chemistry*, 41:2207–2217, 2003.

[121] S. Salman, A.Z. Albayrak, D. Avci, and V. Aviyente. Synthesis and modeling of new phosphorus-containing acrylates. *Journal of Polymer Science Part A: Polymer Chemistry*, 43:2574–2583, 2005.

[122] G. Sahin, A.Z. Albayrak, Z. Sarayli, and D. Avci. Synthesis and photopolymerization of new dental monomers from o-hydroxyaryl phosphonates. *Journal of Polymer Science Part A: Polymer Chemistry*, 44:6775–6781, 2006.

[123] S. Edizer, G. Sahin, and D. Avci. Development of reactive phosphonated methacrylates. *Journal of Polymer Science Part A: Polymer Chemistry*, 47:5737–5746, 2009.

[124] J. Sun and I. Cabasso. Impact of degree of phosphorylation on intrinsic and thermal properties of poly(styrenephosphonate diethyl ester)s. *Journal of Polymer Science Part A: Polymer Chemistry*, 27:3985–3999, 1989.

[125] W. Vogt. Polymere ester von säuren des phosphors. *Makromolekulare Chemie*, 178:3179–3190, 1977.

[126] K.D. Belfield and J. Wang. Modified horner–emmons reaction of polymeric phosphonates: Versatile synthesis of pendant stilbene-containing polymers. *Journal of Polymer Science Part A: Polymer Chemistry*, 33:1235–1242, 1995.

[127] C.F. Cullis and M.M. Hirschler. *The Combustion of Organic Polymers*. Clarendon Press, Oxford, UK, 1981.

[128] J. Troitzsch. *Plastics Flammability Handbook*. Hanser, Munich, Germany, 3th edition, 2004.

[129] Flammschutz-online. Fire initiation.

[130] G. Camino, L. Costa, and M.P. Luda di Cortemiglia. Overview of fire retardant mechanisms. *Polymer Degradation and Stability*, 33:131–154, 1991.

[131] G. Camino and R. Delobel. Intumescence. In A.F. Grand and C.A. Wilkie, editors, *Fire Retardancy of Polymeric Materials*. Marcel Dekker Inc., New York, USA, 2000.

[132] S. Bourbigot, M. Le Bras, S. Duquesne, and M. Rochery. Recent advances for intumescent polymers. *Macromolecular Materials and Engineering*, 289:499–511, 2004.

[133] S.V. Levchik, G.F. Levchik, A.I. Balabanovich, E.D. Weil, and M. Klatt. Phosphorus oxynitride - a termally stable fire retardant additive for polyamide 6 and poly(butylene terephtalate. *Angewandte Makromolekulare Chemie*, 264:48–55, 1999.

[134] J. Green. Phosphorus-containing fire-retardant compounds. In A.F. Grand and C.A. Wilkie, editors, *Fire Retardancy of Polymeric Materials*. Marcel Dekker Inc., New York, USA, 2000.

[135] Ceresana. *Market Study: Flame Retardants (2nd Edition)*. Ceresana Research, 2011.

[136] S. Bourbigot, M. Le Bras, R. Leeuwendal, K.K. Shen, and D. Schubert. Recent advances in the use of zinc borates in fame retardancy of EVA. *Polymer Degradation and Stability*, 64:419–425, 1999.

[137] M. Lewin. Physical and chemical mechanisms of flame retarding polymers. In *Fire Retardancy of Polymers*. Royal Society of Chemistry - Special Publication, New York, USA, 1998.

[138] J. Funt and J.H. Magill. Estimation of the fire behavior of polymers. *Journal of Fire and Flammability*, 6:28–36, 1975.

[139] A.M. Aaronson. *Phosphorus Chemistry*. ACS Symposium Series, 1992.

[140] J.R. Ebdon and M.S. Jones. Flame retardants (overview). In J.C. Salomone, editor, *Polymeric Materials Encyclopedia*. CRC Press, Boca Raton, USA, 12th edition, 1986.

[141] T. Kashiwagi, J.W. Gilman, M.R. Nyden, and S.M. Lomakin. The use of intumescence. In M. Le Bras, G. Camino, S. Bourbigot, and R. Delobel, editors, *Fire Retardancy of Polymers*. Royal Society of Chemistry, Cambridge, UK, 1998.

[142] Y. Wheeler, J.W. andZhang and J.C. Tebby. The use of intumescence. In M. Le Bras, G. Camino, S. Bourbigot, and R. Delobel, editors, *Fire Retardancy of Polymers*. Royal Society of Chemistry, Cambridge, UK, 1998.

[143] J.H. Troitzsch. Methods for the fire protection of plastics and coatings by flame retardant and intumescent systems. *Progress in Organic Coatings*, 11:41–69, 1983.

[144] A. Granzow, R.G. Ferrillo, and A. Wilson. The effect of elemental red phosphorus on the thermal degradation of poly(ethylene terephthalate). *Journal of Applied Polymer Science*, 21:1687–1697, 1977.

[145] C.A. Wilkie, J.W. Pettegrew, and C.E. Brown. Pyrolysis reactions of poly(methyl methacrylate) and red phosphorus: An investigation with cross-polarization, magic angle NMR spectroscopy. *Journal of Polymer Science Part C: Polymer Letters*, 19:409–414, 1981.

[146] S.V. Levchik, L. Costa, and G. Camino. Effect of the fire-retardant, ammonium polyphosphate, on the thermal decomposition of aliphatic polyamides: Part II - Polyamide 6. *Polymer Degradation and Stability*, 36:229–237, 1992.

[147] J.W. Hastie and D.W. Bonnel. *Molecular Chemistry of Inhibited Combustion Systems*. National Bureau of Standard Report NBSIR 80-2169, Washington, USA, 1980.

[148] P. Joseph and S. Tretsiakova-Mcnally. Reactive modifications of some chain- and step-growth polymers with phosphorus-containing compounds: Effects on flame retardancy. *Polymers for Advanced Technologies*, 22:395–406, 2011.

[149] I. van der Veen and J. de Boer. Phosphorus flame retardants: Properties, production, environmental occurrence, toxicity and analysis. *Chemosphere*, 88:1119–1153, 2012.

[150] U. Einsele. Über Wirkungsweise und synergistische Effekte bei Flammschutzmitteln für Chemiefasern. *Lenzinger Berichte*, 40:102–116, 1976.

[151] P. Kannan and K. Kishore. Novel flame retardant polyphosphoramide esters. *Polymer*, 33:418–422, 1992.

[152] T.F. Montezin, J.-M. Lopez Cuesta1, A. Crespy, and P. Georlette. Flame retardant and mechanical properties of a copolymer PP/PE containing brominated compounds/antimony trioxide blends and magnesium hydroxide or talc. *Fire and Materials*, 6:245–252, 1997.

[153] C. Huggett. Estimation of rate of heat release by means of oxygen consumption measurements. *Fire and Materials*, 4:61–65, 1980.

[154] J. Eisenblaetter, M. Bruns, U. Fehrenbacher, L. Barner, and C. Barner-Kowollik. Synthesis of polymers with phosphorus containing side chains via modular conjugation. *Polymer Chemistry*, 4:2406–2413, 2013.

[155] R.S. Edmundson. Phosphoric acid derivatives. In D. Barton and W.D. Ollis, editors, *Comprehensive Organic Chemistry*. Pergamon Press Ltd., Oxford, UK, 2nd edition, 1979.

[156] T.N. Mitchell and B. Costisella. *NMR - From Spectra to Structure*. Springer, Heidelberg, Germany, 2007.

[157] S. Jones, Selitsianos D., and K.J. Thomp. An improved method for lewis acid catalyzed phosphoryl transfer with Ti(t-BuO)$_4$. *Journal of Organic Chemistry*, 68:5211–5216, 2003.

[158] C.Y. Liu, V.D. Pawar, and J.Q. Kao. Substitution- and elimination-free phosphorylation of functionalized alcohols catalyzed by oxidomolybdenum tetrachloride. *Advanced Synthesis and Catalysis*, 352:188–194, 2010.

[159] B.C. Boren, S. Narayan, L.K. Rasmussen, L. Zhang, H. Zhao, Z. Lin, G. Jia, and V.V. Fokin. Ruthenium-catalyzed azide-alkyne cycloaddition: Scope and mechanism. *Journal of the American Chemical Society*, 130:8923–8930, 2008.

[160] M. Kamigaito, T. Ando, and M. Sawamoto. Metal-catalyzed living radical polymerization. *Chemical reviews*, 101:3689–3746, 2001.

[161] C. Lang, C. Kiefer, E. Lejeune, A.S. Goldmann, F. Breher, P.W. Roesky, and C. Barner-Kowollik. Palladium-containing polymers via a combination of RAFT and triazole chemistry. *Polymer Chemistry*, 3:2413–2420, 2012.

[162] S. Kondo, T. Ohtsuka, K. Ogura, and K. Tsuda. Convenient synthesis and free-radical copolymerization of p-chloromethylstyrene. *Journal of Macromolecular Science. Part A*, 13:767–775, 1979.

[163] Y. Sun, Z. Chen, E. Puodziukynaite, D.M. Jenkins, J.R. Reynolds, and K.S. Schanze. Light harvesting arrays of polypyridine ruthenium-(II)-chromophores prepared by reversible addition–fragmentation chain transfer polymerization. *Macromolecules*, 45:2632–2642, 2012.

[164] G. Socrates. *Infrared and Raman Characteristic Group Frequencies*. Wiley and Sons, LTD., Chichester, UK, 2001.

[165] S. Ciampi, M. James, and J.J. Michaels, P. andGooding. Tandem "click" reactions at acetylene-terminated Si(100) monolayers. *Langmuir*, 27:6940–6949, 2011.

[166] M. Es-Sounia, H. Fischer-Brandiesa, and V. Zaporojshenkoc. On the interaction of polyacrylic acid as a conditioning. *Biomaterials*, 23:2871–2878, 2002.

[167] A. Basch and M. Lewin. Influence of fine structure on the pyrolysis of cellulose. III: the influence of orientation. *Journal of Polymer Science Part A: Polymer Chemistry*, 12:2053–2063, 1974.

[168] L.S. Birnbaum and D. F. Staskal. Brominated flame retardants: Cause for concern? *Environmental Health Perspectives*, 112:9–17, 2004.

[169] L. Costa, R. Di Montelera, E.D. Camino, G.and Weil, and E.M. Pearce. Flame-retardant properties of phenolformaldehyde-type resins and triphenyl phosphate in styrene-acrylonitrile copolymers. *Journal of Applied Polymer Science*, 68:1067–1076, 1998.

[170] M. Banks, J.R. Ebdon, and M. Johnson. Influence of covalently bound phosphorus-containing groups on the flammability of poly(vinyl alcohol), poly(ethylene-co-vinyl alcohol) and low-density polyethylene. *Polymer*, 34:4547–4556, 1993.

[171] D. Hendlin, E.O. Stapley, M. Jackson, H. Wallick, A.K. Miller, F.J. Wolf, T.W. Miller, L. Chaiet, F.M. Kahan, E.L. Foltz, H.B. Woodruff, J.M. Mata, S. Hernandez, and S. Mochales. Phosphonomycin, a new antibiotic produced by strains of streptomyces. *Science*, 166:122–123, 1969.

[172] F.M. Kahan, J.S. Kahan, P.J. cassidy, and H. Kropp. The mechanism of action of fosfomycin (phosphonomycin). *Annals of the New York Academy of Science*, 235:364–386, 1974.

[173] L.J. Higgins, F. Yan, P. Liu, H.-W. Liu, and C.L. Drenn. Structural insight into antibiotic fosfomycin biosynthesis by a mononuclear iron enzyme. *Nature*, 437:838–844, 2005.

[174] B. Iorga, F. Eymery, and P. Savignac. The syntheses and properties of 1,2-epoxyalkylphosphonates. *Synthesis*, 2:207–224, 1998.

[175] E.J. Glamkowski, G. Gal, R. Purick, A.J. Davidson, and M. Sletzinger. A new synthesis of the antibiotic phosphonomycin. *Journal of Organic Chemistry*, 35:3510–3512, 1970.

[176] C. Giordano and G. Castaldi. First asymmetric synthesis of enantiomerically pure (lR,2S)-(-)-(1,2-epoxypropyl)phosphonic acid (fosfomycin). *Journal of Organic Chemistry*, 54:1470–1473, 1989.

[177] Z. Zhang, J. Tang, X. Wang, and H. Shi. Chiral ketone- or chiral amine-catalyzed asymmetric epoxidation of cis-1-propenylphosphonic acid using hydrogen peroxide as oxidant. *Journal of Molecular Catalysis A: Chemical*, 285:68–71, 2008.

[178] J.J. Li. *Name Reactions - A Collection of Detailed Mechanisms and Synthetic Applications*. Springer, Heidelberg, Germany, 4th edition, 2009.

[179] P. Coutrot and P. Savignac. A one-step synthesis of diethyl 1,2-epoxyalkanephosphonates. *Synthesis*, 1:34–36, 1978.

[180] B.G. Christensen, P. Scotch, R. Firestone, and F. Armond. *Synthese von Epoxyphosphonaten*. DE1924135, 1969.

[181] N.N. Girotra and N.L. Wendler. Synthesis and transformations in the phosphonomycin series. *Tetrahedron Letters*, 53:4647–4650, 1969.

[182] G.H. Jones, E.K. Hamamura, and J.G. Moffatt. A new stable Wittig reagent suitable for the synthesis of α,β-unsaturated phosphonates. *Tetrahedron Letters*, 55:5731–5734, 1968.

[183] R.H. Churi and C.E. Griffin. 1,2-shifts of dialkoxyphosphono groups in skeletal rearrangements of α,β-epoxyvinylphosphonates. *Journal of the American Chemical Society*, 88:1824–1825, 1966.

[184] M. Sprecher and D. Kost. The rearrangement of dialkyl α,β-epoxyphosphonates. *Tetrahedron Letters*, 10:703–706, 1969.

[185] C.E. Griffin and S.K. Kundu. Phosphonic acids and esters. XX: Preparation and ring opening reactions of α,β- and β,γ-epoxyalkylphosphonates. The proton magnetic resonance spectra of vicinally substituted ethyl- and propylphosphonates. *The Journal of Organic Chemistry*, 34:1532–1539, 1969.

[186] D. Redmore. Heterocyclic systems bearing phosphorus substituents. synthesis and chemistry. *Chemical Reviews*, 71:315–337, 1971.

[187] C.E. Burgos-Lepley, R.A. Mizsak, S.A. Nugent, and R.A. Johnson. Tetraalkyl oxiranylidenebis(phosphonates). Synthesis and reactions with nucleophiles. *The Journal of Organic Chemistry*, 58:4159–4161, 1993.

[188] F. Hammerschmidt and H. Kählig. Biosynthesis of natural products with a phosphorus-carbon bond. 7: Synthesis of [1,1-2H2]-, [2,2-2H2]- (R)- and (S)-[1-2H1](2-hydroxyethyl)phosphonic acid and (R,S)-[1-2H1](1,2-dihydroxyethyl)phosphonic acid and incorporation studies into fosfomycin in streptomyces fradiae. *The Journal of Organic Chemistry*, 56:2364–2370, 1991.

[189] N. Jung, M. Wiehn, and S. Bräse. Multifunctional linkers for combinatorial solid phase synthesis. In S. Bräse, editor, *Combinatorial Chemistry on Solid Supports*. Springer Verlag, Heidelberg, Germany, 2007.

[190] D.B. Chesnut, L.D. Quin, and P.J. Seaton. Bonding and 33S NMR chemical shielding in the thiophosphoryl group. *Magnetic Resonance in Chemistry*, 42:S20–S25, 2004.

[191] B.C. Saunders and P. Simpson. Esters containing phosphorus. Part XVIII: Esters of ethynylphosphonic acid. *Journal of the Chemical Society*, pages 3351–3360, 1963.

[192] H. Römpp, J. Falbe, and M. Regitz. *Römpp Chemie Lexikon*. Thieme Verlag, 1992.

[193] H. Meerwein and R. Schmidt. Ein neues Verfahren zur Reduktion von Aldehyden und Ketonen. *Justus Liebigs Annalen der Chemie*, 444:221–238, 1925.

[194] O. Solomon and C. Oprescu. Anionic polymerization of ϵ-caprolactam with lithium aluminum hydride and with N-acetyl-caprolactam and phenyl isocyanate activators. *Macromolecular Chemistry and Physics*, 126:197–205, 1969.

[195] G.F. Levchik, S.V. Levchik, G. Camino, and E.D. Weil. Fire retardant action of red phosphorus in nylon 6. In M. Le Bras, G. Camino, S. Bourbigot, and R. Delobel, editors, *Fire Retardancy of Polymers-The Use of Intumescence*. Royal Society of Chemistry, London, UK, 1998.

[196] B.J. Sutker. Flame retardants. In F. Ullmann, editor, *Ullmanns Encyclopedia of Industrial Chemistry*. Wiley-VCH, Electronic Release, 6th edition, 2000.

[197] *Plastics - determination of burning behaviour by oxygen index - Part2: Ambient-temperature test*. ISO 4589-2, Beuth, Germany, 1996.

[198] Y. Xu, Y. Liu, and Q. Wang. Melamine polyphosphate/silicon-modified phenolic resin flame retardant glass fiber reinforced polyamide-6. *Journal of Applied Polymer Science*, 129:2171–2176, 2013.

[199] H.L. Wagner. The Mark-Houwink-Sakurada equation for the viscosity of atactic polystyrene. *Journal of Physical and Chemical Reference Data (JPCRD)*, 14:1101–1106, 1985.

[200] K.L. Parry, A.G. Shard, R.D. Short, R.G. White, J.D. Whittle, and A. Wright. ARXPS characterisation of plasma polymerised surface chemical gradients. *Surface Interface Analysis*, 38:1497–1504, 2006.

[201] J.H. Scofield. Hartree-slater subshell photoionization cross-sections at 1254 and 1487 eV. *Journal of Electron Spectroscopy and Related Phenomena*, 8:129–137, 1976.

[202] S. Tanuma, C.J. Powell, and D.R. Penn. Calculations of electron inelastic mean free paths. V: Data for 14 organic compounds over the 50–2000 eV range. *Surface Interface Analysis*, 21:165–176, 1994.

List of Figures

List of Tables

List of Abbreviations

Δ	delta; supplying temperature
°C	degree Celsius
(1) - (19)	molecule synthesized in the current work (see Chapter 6.3)
1,2-DiEt-Fos	1,2-epoxypropyl phosphonic diethylester
1,2-DiMe-Fos	1,2-epoxypropyl phosphonic dimethylester
2,3-DiEt-Fos	2,3-epoxypropyl phosphonic diethylester
2,3-DiMe-Fos	2,3-epoxypropyl phosphonic dimethylester
Ag	silver / argentum
AGET ATRP	activator generated by electron transfer ATRP
AIBN	2,2'-azodi(isobutyronitrile)
$AlCl_3$	aluminum chloride
$Al_2O_3 \cdot 3\ H_2O$	aluminum oxide trihydrate
APP	ammonium polyphosphate
APPA	acryloyloxypropyl phosphinic acid
ARGET ATRP	activator re-generated by electron transfer ATRP
at%	atom percentage
ATR	attenuated total reflection (IR spectroscopy)
ATRP	atom transfer radical polymerization
Au	gold / aurum
azabutane	tert-butyl[(4-"X"phenyl)(phenyl)methyl]aminooxidane (X=Cl,Br,OMe)
$BaCl_2$	barium chloride
$BF_3 \cdot Et_2O$	boron trifluoride diethyl etherate
BPO	divinylbenzoyl peroxide
Br_2	bromine

$^{i}Bu_3Al$	triisobutylaluminum
BuLi	n-butyl lithium
BuOH	butanol
C	carbon
C_2H_5	ethylene group
$^{i}C_3H_7$	iso-propyl group
n-C_3H_7	n-propyl group
n-C_4H_9	n-butyl group
Ca	calcium
CAE	constant analyzer energy (XPS)
CaH_2	calcium hydride
$Ca_5(PO_4)_3(OH)$	hydroxyapatite
CCl_4	tetrachloromethane
$CDCl_3$	deuterated chloroform
CH_3	methyl group
CH_3CHO	formaldehyde
$CHCl_3$	chloroform
CH_2Cl_2	dichloromethane
CH_3CN	acetonitrile
CHI_3	triiodomethane
CH_2I_2	diiodomethane
CH_3I	iodomethane
CH_3OH	methanol
Cl	chloride
Cl_2	chlorine
Co	cobalt
CO	carbon monoxide
CO_2	carbon dioxide
$CsCO_3$	cesium carbonate
Cu	copper
$CuSO_4$	copper sulfate
Da	Dalton
DBTTC	dibenzyl trithiocarbonate

DCC	dicyclohexylcarbodiimide
DCU	dicyclohexylurea
Deca-BDE	decabromodiphenylether
DHB	2,5-dihydroxybenzoic acid
D_2O	deuterated water
DEBP	diethylbenzyl phosphonate
DEPN	N-tert-butyl-N-(1-diethylphosphono-2,2-dimethylpropyl) nitroxide
DEPP	diethyl prop-2-ynyl phosphoric ester
diglyme	bis(2-methoxyethyl)ether
DMAP	4-(dimethylamino)pyridine
DMF	N,N‘-dimethylformamide
DMHP	dimethyl hydroxyethyl phosphonate alcohol
DMPP	dimethyl prop-2-ynyl phosphoric ester
DMSO	dimethylsulfoxide
DMSO-d_6	deuterated dimethylsulfoxide
DNA	deoxyribonucleic acid
DOPO	9,10-dihydro-9-oxa-phosphaphenthrene-10-oxide
DPPP	diphenyl prop-2-ynyl phosphoric ester
DSC	differential scanning calorimetry
EA	elemental analysis
EAL	effective attenuation length (XPS)
EDTA	ethylenediaminetetraacetic acid
EDX	energy dispersive X-ray analysis
e.g.	for example
EGA	evolved gas analysis
EPI	epichlorohydrin
Et-Fos	diethylester of fosfomycin
Et_2O	diethylester
EtOH	ethanol
eV	electron volt
Fos	fosfomycin
fosfomycin	1,2-epoxypropylphosphonic acid

FR	flame retardant
FRP	free radical polymerization
FT-IR	fourier-transformated infrared
h	hour
$H^{\bullet}$	hydrogen radical
H_2	hydrogen
HBCDD	hexabromocyclododecane
HBr	hydrobromic acid
HCl	hydrochloric acid
HCN	hydrocyanic acid
Hz	Hertz
H_2O	water
H_2O_2	hydrogen peroxide
HOMO	highest occupied molecule orbital
H_2SO_4	sulfuric acid
$[I]_0$	initiator concentration at t = 0
ICP	inductively coupled plasma (mass specroscopy)
i.e.	id est (*lat.*) = that is
IEM	isocyanatoethyl methacrylate
IR	infrared
ISO	International Organization for Standardization
K	Kelvin
K_a	activation rate constant
k_d	rate cofficient of initiator fragmentation
K_{da}	de-activation rate constant
K_e	equilibrium constant
k_i	rate cofficient of initiation
k_p	rate cofficient of propagation
k_t	rate cofficient of termination reactions
k_{tc}	rate cofficient of termination reactions (combination)
k_{td}	rate cofficient of termination reactions (disproportionation)
k_{tr}	rate cofficient of transfer reactions
K_2CO_3	potassium carbonate

KOH	potassium hydroxide
KO^{t}Bu	potassium tert-butoxide
KPG	core drawn precision glass unit
La	lanthanum
LCST	lower critical solution temperature
LDA	lithium diisopropylamide
LOI	limiting oxygen index
LUMO	lowest unoccupied molecule orbital
L x W x H	length x width x height
M	molar mass
$[M]$	molecular weight
$[M]_0$	molecular weight at t = 0
M_n	number average molecular weight
M_w	weight average molecular weight
MA	methacrylate
MADIX	macromolecular design by interchange of xanthates
MALDI-TOF	matrix-assisted laser desorption/ionization - time-of-flight (mass spectroscopy)
MAS	magic angle spinning (NMR)
MAUPHOS	3-methoxy-3-oxido-7-oxo-2,6-dioxa-8-aza-3λ^5-phosphadecan-10-yl 2-methylprop-2-enoate
MDI	methylenediphenyldiisocyanate
Me-Fos	dimethylester of fosfomycin
MEK	methyl ethyl ketone
melamine	2,4,6-triamino-1,3,5-triazine
MeOH	methanol
Mg	magnesium
$Mg(OH)_2$	magnesium hydroxide
min	minute
MMA	methylmethacrylate
$MoOCl_4$	molybdenum(VI) tetrachloride oxide
MPC	2-methacryloyloxyethyl phosphorylcholine
MSA	methane sulfonic acid

N	nitrogen
N_2	nitrogen atmosphere gas
Na	sodium
NaClO	sodium hypochlorite
Na-Fos	disodium salt of fosfomycin
NAG	N-acetylmuramic acid
NaH	sodium hydride
$NaHCO_3$	sodium hydrogen carbonate
NAM	N-acetylglucosamic acid
NaN_3	sodium azide
NaOH	sodium hydroxide
NaOMe	sodium methanolate
Na-P(O)$(OR)_2$	sodium dialkyl phosphite
$NaSO_4$	sodium sulfate
Na_2WO_4	sodium tungstate dihydrate
NBA	N-bromoacetamide
Nd	neodymium
NEt_3	triethylamine
NH_2	amine
NH_3	ammonia
NH_4Cl	ammonium chloride
Ni	nickel
N^iPAAM	*N*-isopropylacrylamide
NMP	nitroxide mediated polymerization
NMR	nuclear magnetic resonance
$NOct_4BrO_2$	tetraoctylammonium bromide
O_2	oxygen
OH	hydroxide
$OH^\bullet$	hydroxide radical
OMe	methoxide
p	pressure
P	phosphorus
P_n	degree of polymerization

PA	polyamide
PCl_3	phosphorus trichloride
PCl_5	phosphorus pentachloride
PDI	polydispersity index
$Pd(OAc)_2$	paladium acetate
PE	polyethylene
PEG	polyethylene glycol
PEP	phosphoenolpyruvate
PEPI	poly(epichlorohydrin)
PEpo	poly(epoxy resin)
PET	polyethylenetherephtalate
pH	potentia hydrogenii (*lat.*)
PMMA	poly(methylmethacrylate)
PnAA	phosphonoacetaldehyde
P(N^iPAAM)	poly(*N*-isopropylacrylamide)
PnPy	phosphonopyruvate
PO_4^{-3}	phosphate ion
PO_x	phosphorus oxide
$POCl_3$	phosphoryl chloride
Poly-Fos	polymerized fosfomycin
$P(OR)_3$	trialkyl phosphite
PP	polypropylene
PS	polystyrene
PS-DPPP	polystyrene copolymer phosphorylated with DPPP
Pt	platinum
PUR	polyurethane
PVC	poly(vinylchloride)
PVPA	poly(vinylphosphonic acid)
$R^\bullet$	initiator radical
RAFT	reversible addition-fragmentation chain transfer
R-Br	allyl bromide
R-CHO	aldehyde
REM	scanning electron microscopy

RF	radio frequency (NMR)
R-NH_2	alkyl amine
R-OH	alcohol
ROP	ring-opening polymerization
S	sulfur
SEC	size exclusion chromotography
S-HPP	2-hydroxypropylphosphonic acid
SiO_2	silica gel
Sm	samarium
$SnOct_2$	tin(II)-2-ethylhexanoate
$SOCl_2$	thionylchloride
St	styrene
T	temperature
T_g	glass transition temperature
TBBA	tetrabromobisphenol
TBD	triazabicyclodecene
^{t}-BuClO	tert-butyl hypochlorite
^{t}BuI$^-$NH$_4^+$	tert-butyl ammoniumiodide
^{t}-BuOH	tert-butanol
^{t}-BuOK	potassium tert-butoxide
^{t}-C_4H_9	tert-butyl group
TEA	triethyamine
TEMPO	2,2,6,6-tetramethyl-1-oxide
tetraglyme	tetraetyleneglycoldimethylether
TFA	trifluoroacetic acid
TGA	thermogravimetry
TG-MS	thermogravimetry combined with mass specroscopy
THF	tetrahydrofuran
Ti(^{t}-BuO)$_4$	titanium tert-butoxide
TIPNO	2,2,5-tri-methyl-4-phenyl-3-azahexane-3-nitroxide
TMEDA	*N,N,N‘,N‘*-tetramethylethylenediamine
TMS	trimethylsilyl
UL94	Tests for Flammability of Plastic Materials for Parts in Devices and Applications (Underwriters Laboratories)

UV	ultraviolet
v_p	propagation rate
V0	classification of the UL94 test
VAZO-88	1,10-azobis-(cyclohexane carbonitrile)
VBC	4-vinylbenzyl chloride
VC_2	vinylidene chloride
VPA	vinylphosphonic acid
W/g	watt / gram (DSC)
Wt%	weight percentage
X	halogen
XPS	X-ray photoelectron spectroscopy

Acknowledgements

The work included in the present thesis was carried out at the Fraunhofer Institute for Chemical Technology (ICT) under the supervision of Prof. Dr. Christopher Barner-Kowollik at the Karlsruhe Institute of Technology (KIT).

Firstly, I would like to thank Prof. Dr. Christopher Barner-Kowollik, who offered me the possibility to conduct my PhD thesis under his supervision in the field of polymer chemistry. His ideas, tireless motivation and constant support during the entire time were critical for the implementation of the thesis. His enthusiasm for science motivated me during hard times. Many thanks also go to Dr. Leonie Barner, who has not only helped me with fruitful discussions and suggestions, but aided in bridging fundamental and applied research.

Many thanks also go to Dr. Ulrich Fehrenbacher, who has guaranteed the financial support from the Fraunhofer ICT for my studies and always had an open ear for research and personal topics.
I also thanks Rainer Schweppe for his extraordinary efforts enabling me to concentrate on research.

I have to thank all my co-workers at the Fraunhofer ICT for making my days much brighter. Especially my office colleagues, Kristian Kowollik and Thomas Philipps, who in addition to interesting discussions always had a joke on there lips. This amazing atmosphere helped me through days when nothing seemed to work. They have helped me not only through the daily chaos, for which I have to blame at least partly myself, but also helped me through my privately hardest time.

For the tremendous help with XPS measurements and their evaluation I would like to thank Dr. Michael Bruns.
Thanks to Dr. Reinhard Meusinger from TU Darmstadt for measuring and evaluation of my strange fosfomycin NMR data. Without his insights, I would possibly still be puzzled about the coupling patterns.

Thanks also Dr. Robert Graf for the solid NMR measurements at the MPI Mainz and Pia Lang for ^{1}H and ^{13}C measurements at the Karlsruhe Institute of Technology (KIT) .
I have to thank Andreea Daniliuc from the Fraunhofer WKI for the LOI measurements and discussion of the results.
Dr. Katja Emmerich and Annett Steudel helped me with the TG-MS measurements and the explanation for the cause of non-detectable fragments.
Many thanks also to Boris Kühl, who has provide me shortly MALDI-TOF measurements of my insoluble polymers. Thanks also to all employees of the Fraunhofer ICT, who performed the analytical measurements for me: Wenka Schweikert and Manuela Dörich (IR, EGA), Yvonne Galus (TGA, TG-MS), Mar Juez-Lorenzo (SEM/EDX), Heike Schuppler (DSC) and Melanie Klemenz (extrusion/molding).

Many thanks also to my HiWi-student Thomas Hurrle, who helped me extraordinarily during my last practical weeks.
I thank all the members of the macroarc group at the KIT, which made me feel like a fully-fledged member of the group even they saw me just occasionally at group meetings and some social events.

Many thanks go to Dr. Leonie Barner, Kristian Kowollik and Lars Petzold, who were so kind to proof read parts of my thesis.

I am grateful to my family for their support over the past years. Especially to my mum, who always motivated me since I can remember, and more importantly since I can learn. I hope I reached your expectations. Dad, unfortunately this thesis took a little bit too long, so that you are no more able to see it in its final state. Mum and dad, I would not be at this point without you both.

Finally, yet most importantly, I want to thank my fiancé for his constant support during my difficult research and personal times. Without you I would not have accomplished the present thesis. You and the 'kids' have always prepared a place where I was able to gather new strength. Hopefully there are much more happy years to come.

List of Publications, Patents and Conference Contributions

Journal Publications

[1] Synthesis of Polymers with Phosphorus Containing Side Chains via Modular Conjugation
Eisenblaetter, J.; Bruns, M.; Fehrenbacher, U.; Barner, L.; Barner-Kowollik, C.
Polymer Chemistry, 2013, 4, 2406-2413

Patents

[2] Methode zum Aufbau einer kombinatorischen Bibliothek zur Darstellung flammgeschützter Polymere mit individuell einstellbarem Flammschutz auf Basis von phosphorhaltigen Verbindungen in *Click*-Reaktionen
Eisenblaetter, J.; Barner, L.; Barner-Kowollik, C.; Fehrenbacher, U.; Lang, C.
Amtliches Kennzeichen: 10-2012-023-513.5

Conference Contributions

[3] Synthesis of Phosphoric Polyols for Flame Retardant Polyurethane Foams
CRP Meeting on Controlled Radical Polymerizations, Belgium
17.-18. September 2009

[4] Phosphorylated Polymers via RAFT and Click Chemistry
Belgian-German Macromolecular Meeting, Belgium
03.-04. Dezember 2012

[5] Polymers with Phosphor Containing Side Chains via Modular Conjugation as Potential Flame Retardants
JCF Frühjahrssymposium, Germany
06.-09. March 2013